WEST AFRICAN PRECIPITATION AND RELATED ATMOSPHERIC CIRCULATION

by

JOSEPH ADESOLA ADEDOKUN

Department of Physics, (Atmospheric Group)
Imperial College of Science and Technology

A thesis submitted for the Degree
of Doctor of Philosophy in the
University of London

December, 1976

"Neither said they,

'Where is the Lord

that brought us up .....

that led us through the wilderness,

through a land of deserts and of pits

through a land of drought, and of the shadow of death

through a land that no man passed through, and

where no man dwelt?' "

Jeremiah 2.6

ABSTRACT

Climatological latitude-time cross sectional studies of the West African precipitation indicate a strong association between the May to September cycle of precipitation in the Sahel and the January to December cycle in the South.

Aerological thermodynamic analyses show a good agreement between the observed precipitation cross-sections and the thermally allowed regions of convective instability where low level θ_w, typical of the bottom 1 or 2 km of the earth's surface, exceeds the (mid-tropospheric) θ_e minimum aloft. In the face of inadequate data coverage and no prospect of isentropic analysis in the region, an invaluable role is played by stationary (local) analysis in depicting the thermally preferred season of convective instability in the Sahelian area, in agreement with precipitation observed in case studies of a wet and a dry year. This season occurs between the advent and the retreat of the ITD over the station and is typified by $\theta_w \geq 22^{\circ}C$ near the surface. For $\theta_w \leq 20^{\circ}C$ near the surface, no precipitation results.

The roles of the Intertropical Discontinuity (ITD) (as distinct from the ITCZ) and the Zonal Walker Circulation on the region's precipitation are discussed. The Sahel precipitation is ITD controlled. This control, beyond a threshold of about 7° latitude South of the mean ITD surface, declines as the Little Dry Season (LDS) region is reached giving way to a Southern Oscillation (SO) influence.

A mechanism is postulated whereby a decrease in Easterly disturbances and squall line activity - and consequently, precipitation in the Sahel - can result from a decrease in the meridional temperature contrast between the Saharan region in the North and the Guinea region in the South through increased radiative cooling over the former (e.g. by increasing the albedo of the Sahara) or anomalous warming of the latter (e.g. effected by weakening the upwelling process at the Guinea Coast -

itself consequent on a weakening of the strength of the South Westerly (Monsoon) winds - though this phenomenon can increase precipitation in the South as in the dry year case study considered).

An instability index, defined to take account of two layers of the atmosphere crucial in consideration of convection, is used to investigate occasions of convective instability within the ITD environment on various time scales.

A two month lag maximum is found in the cross correlation of Lagos and Niamey precipitation, suggesting some relation between the latter and the former some months previously. This can be of great value in effecting timely agricultural planning in case of drought.

LIST OF CONTENTS

SYMBOLS USED IN THE THESIS

ϕ_I = Latitude (degrees) of the Inter-tropical Discontinuity (ITD)

ϕ = Latitude (degrees)

α = Latitude/time slope of isohyets

R = Precipitation (sometimes R_N, R_L for precipitation over Niamey and Lagos).

T = Temperature (T_d, T_w, T_e for dewpoint, wet bulb and equilibrium temp.)

S = Entropy (specific)

E = Internal Energy

P = Pressure

ρ = Density of air (ρ_v for water vapour)

c = Specific heat (C_p at const. pressure, C_v at const. volume)

e = Water vapour pressure (e_s for saturation)

f = Coriolis parameter, $2\Omega \sin \phi$

g = Apparent gravitational acceleration

$\underset{\sim}{i}, \underset{\sim}{j}, \underset{\sim}{k}$ = Unit vectors in direction of co-ordinate axes x,y,z

q = Specific humidity

r = (Humidity) Mixing ratio (r_s for saturation)

r = Correlation coefficient (r_c for cross correlation, r_a for auto-correlation)

t = Time

u, v, w = Velocity components in x,y,z directions (to the East, North and vertically)

a = Albedo

θ = Potential temperature

θ_w = Wet bulb potential temp.

θ_s = Saturation potential temp.

θ_e = Equivalent potential temp.

C_D = Drag Coefficient

E = Rate of evaporation per unit area

G = Heat flux into the ground

K = Eddy transfer coefficient (K_m, K_H, K_v for momentum, heat and vapour)

L = Latent heat (L_v, for vapourisation)

R = Gas constant for dry air, 2.87×10^6 erg g^{-1} $^oK^{-1}$
R_v for water vapour.

R_i, R_o = Richardson, Rossby Number

S = Solar constant (1400 $Wm^{-2} \approx 2$ cal cm^{-2} min^{-1})

Ω = Angular velocity of earth ($\sim 7.3 \times 10^{-5}$ s^{-1})

σ = Stefan's constant = 5.67×10^{-5} eng cm^{-2} s^{-1} $^oK^{-4}$

τ = Frictional stress (τ_{zx} vertical transfer of x momentum)
τ_{zy} vertical transfer of y momentum)

ν = Coefficient of kinematic viscosity

μ = Coefficient of dynamic viscosity

ϵ = $R/R_v = 0.622$

Q = Static energy (Cal/gm)

I = Instability index (^oC)

W = Precipitable water (W_T for total over an atmospheric column)

CHAPTER I

I N T R O D U C T I O N

I.(i) Drought in the Sahel Region of West Africa

The recent (mainly 1970-73) drought that occurred in the Sahel region of West Africa fig (1.1) subjected about six million people to the danger of starvation and led to the death of many, particularly children and women (Bryson, 1973). But for the timely action of many Christian and other humanitarian relief bodies, a lot more people would have lost their lives in that 'wind of drought that blows no one good'.

Pastoral farming in the Sahel region is highly dependent on the seasonal trends in vegetation growth and the mostly Tuareg and Fulani population occupying the area have developed a nomadic pattern of life, migrating North and South with the region's seasonal (Monsoon) precipitation.

A delay in the on-set of the Monsoon precipitation is disastrous to the welfare of the Nomads' flocks and a prolonged culmination of this can lead to the death of whole herds of cattle as happened in the recent drought. Though there have been droughts in the region in the recent past e.g. 1913, 1940 (fig 9 of Mason, 1976) there has never been any as severe as the 1970-73 one in this century.

The economy of the Sahelian countries is highly dependent on livestock and since, for example, 45% of Mali's and 65% of Upper Volta's total export of merchandise is from livestock (Swift, 1973) an estimated death of 80% of the Sahelian gross cattle population in the drought constitutes no small blow to the region's economy.

In the light of this, a proper understanding of the characteristics of the region's precipitation and the atmospheric mechanisms influencing its distribution, intensity and duration, is essential if a timely forecast of, and an effective response to, such a drought is to be accomplished.

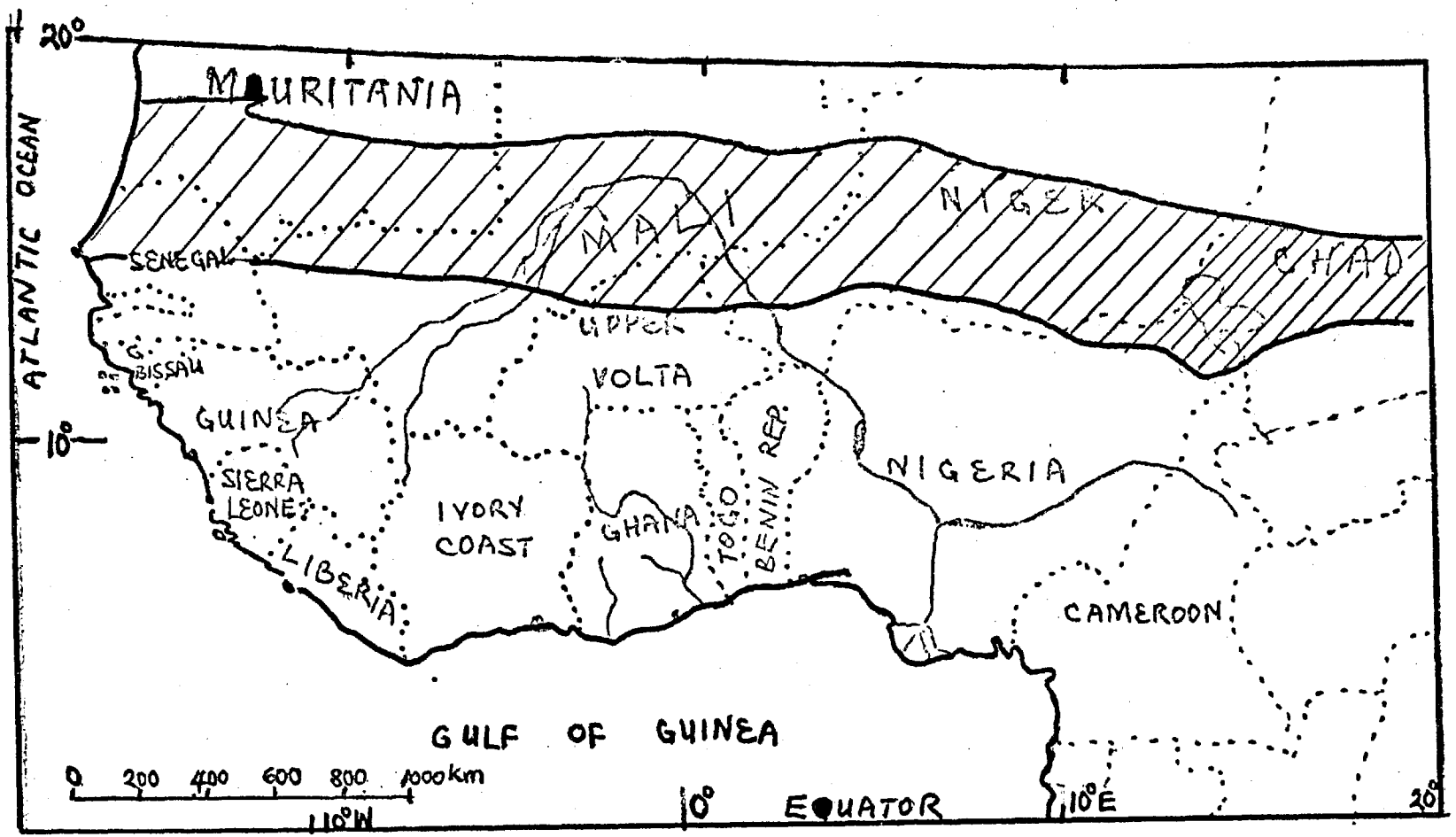

Fig.1.1 West Africa showing the approximate region covered by the 'Sahel Zone' (shaded).

Groups of ten, five, three and two year dry periods exist in the region's precipitation history (e.g. Jenkinson, 1973) but these do not occur at regular intervals capable of being forecast (Bunting et Al, 1976, Mason, 1976). In addition, for them to have any predictive value, historical records must contain "a well established trend whose cause is well understood" or "variations that are demonstrably controlled by some known periodic forcing factor". (Mason, 1976) Hence a study of atmospheric mechanisms behind the observed precipitation cannot be underestimated in the search for possible prediction of the region's precipitation.

Furthermore, surprisingly little or no attention has hitherto been given to the association, in a given year, between the cycle of precipitation in the Sahel and those of the Guinea region further South. This study shows that this association is important in the consideration of useful monthly seasonal and annual forecasts of the Sahel precipitation.

1.(ii) OBJECTIVES OF THE STUDY

This study is aimed at:

1. examining the distribution of monthly precipitation in a South-North direction across West Africa, from the Guinea coast to the Sahel region with a view to understanding its climatology and variability;

2. examining the stratification of the West African atmosphere with a view to investigating the conditions for, and nature of, convective instability occurring within the ITD environ and hence, the preferred regions and season of predominant precipitation;

3. examining some atmospheric circulation systems that affect the West African precipitation. These, due to the fact that the region's climate is not wholly determined by the local atmospheric processes at play there but by various large scale mechanisms set up by the atmospheric 'heat

engine', will include some aspects of the global circulation as deemed appropriate; and,

4. undertaking inter-station correlation of monthly precipitation across the region with a view to investigating the relation between the Sahel precipitation and that observed at the Southern stations previously;

as typical wherever possible, of a wet and a dry year.

1.(iii) DATA SOURCES AND LIMITATION

The sources of the data used in the study are indicated in Appendix I, and the stations over which the data were observed, in Appendix II and fig (1.2)

It need be stressed that some of the upper atmosphere (radiosonde, rawinsonde) stations in the region are 'dummy'. The operating ones, even during the IGY (July 1957 - December 1958) which period is only second to GATE, (1974) in its high density of observations, are so few that an adequate Upper air coverage of the region is lacking.

Conspicuously absent from the upper atmosphere data reported over the few available stations are the upper level winds. This data limitation has exercised some constraint on the approach used in this study. GATE, (1974) has greatly improved the situation providing more data coverage but this study is geared towards the (pre-GATE) drought experienced by the region and commenced before its results began to be released.

1.(iv) TROPICAL CONVECTION AND PRECIPITATION

Most of the precipitation in the tropics results from convection (Riehl, 1954). A lot of the prevailing types of convection in low latitude regions fall into Ludlam's (1963) 'little' and 'deep little' convection manifest in Cumulus (Cu) and Cumulonimbus (Cb) cloud systems. The Cb often organise themselves into the classical 'hot towers' through which latent heat, accumulated by the trades at the Equatorial trough (Inter-tropical convergence zone, ITCZ) is converted

Fig 1.2

Location of the stations used in the study along with the positions of Zones 1, 2 and 3.

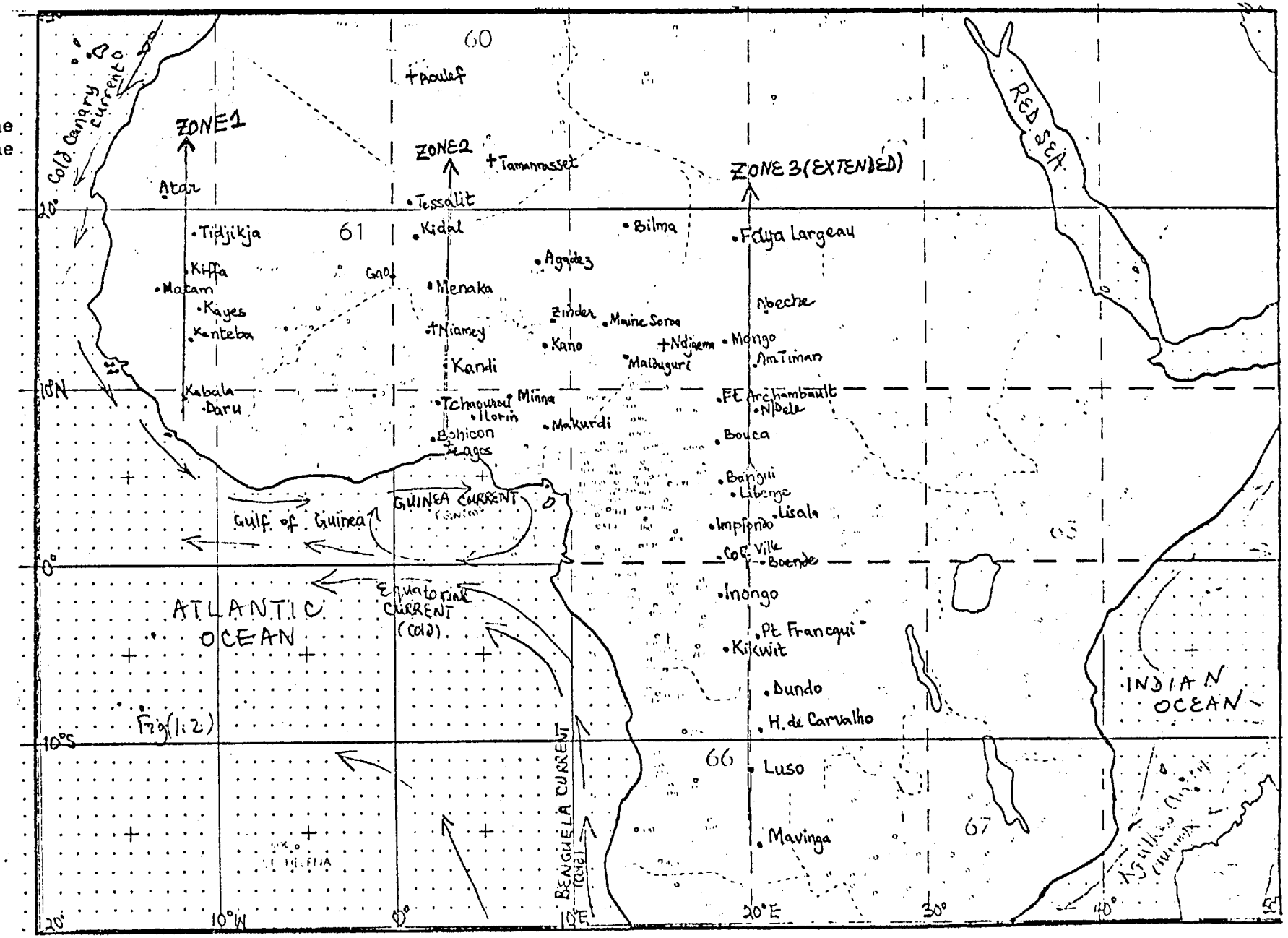

into sensible and potential energy (Riehl and Malkus., 1958) before being transported polewards aloft.

Maximum convective activity and Cb development occur over the ITCZ surface (on the oceans) and maximum precipitation results there. However, the situation over land is remarkably different. Maximum precipitation does not fall at the ITD surface which often is dry, but rather about 700-1000 km South of it.

For an understanding of the nature of precipitation over the West African continent, a study of the stratification of the atmosphere in the ITCZ/ITD environment is necessary. The convection in this environment ranges from:

1. Cu/Cb scale (1-10km): Scale D of GATE (GATE Report No.1,1972)
2. Meso scale: (10-100km): Scale C of GATE (" " " "
3. Squall line and Cloud Clusters (10^2 - 10^3 km) : Scale B of GATE ; to
4. Mid-tropospheric Easterly wave disturbances: (10^3 - 10^4 km) : Scale A of GATE.

These various scales of convection interact considerably, the small scale ones co-operating to form the big scale ones, the whole system consituting a spectral range of complex phenomena.

1.(iv) a) Requirement for strong convective activities

For the initiation of convective storms (and these can range from severe local thunderstorms and squall lines in West Africa to tornadoes in the United States of America), the following conditions need be satisfied:

i) Conditional and Convective Instability

This is the condition that a parcel of air, lifted from the surface, would rise within the environment in order to provide the necessary updraught needed for Cu and Cb cloud formation. It involves the provision of high wet bulb potential temperature, θ_w , averaged

over the first kilometre or two of the earth's surface, which would sufficiently exceed the mid-tropospheric saturation potential temperature, θ_s .

Sufficient moisture has to be available, particularly at lower levels of the atmosphere, in order to facilitate the condensation process required for cloud formation - as the parcel rises to the condensation level.

ii) Favourable wind shear

The role of pronounced wind shear in severe storm situations has been studied by Ludlam (1963) and in Cb systems, by Moncrieff and Green (1972).

The shear is an efficient mechanism for convective overturning necessary for the release of the instability. Furthermore, the structure of the wind shear is important in determining the storm characteristics, for instance, most mid-latitude severe local storms have associated with them, a constant wind shear and hence, a steering level which makes them propagate with the mean flow, whereas, a tropical squall line has, associated with it, a reversal in wind shear between the lower and upper levels and it propagates faster than the mean flow at all levels. (Moncrieff and Miller, 1976).

The strong temperature contrast between the hot Saharan region at the North and the cool Guinea area to the South gives rise to a strong easterly shear which spells an Easterly flow above the low-level South Westerly moist current.

The factors affecting this temperature contrast are crucial to the squall frequency and climatic precipitation input over the Sahel. Such factors are:

1. the heating of the Saharan region via decrease in surface albedo.

2. the cooling of the Gulf of Guinea through upwelling of cold water in summer. This is expected to strengthen

the Zonal Walker Circulation (Flohn, 1971, Wright, 1975)

Hence, apart from the increased large scale descending motion resulting from increased albedo over the Sahara (Charney, 1975), the shortage of rain over the Sahel may be due to the interplay of atmospheric factors (one of which is increased albedo) hindering or decreasing the frequency of squall lines, the major 'tankers' of the region's precipitation. This is hence, another way in which albedo increase can play a role in causing drought in West Africa.

1.(v) A BRIEF OUTLINE OF THE THESIS

In the light of the foregoing, this study begins with an investigation, in chapter II, of the nature of the climatological association between the cycle of precipitation in the Sahel and those of the Guinea region along with the ITD latitude variation. Three longitudinal zones: Zone 1 ($12^{\circ}W$), Zone 2 ($3^{\circ}E$) and Zone 3 ($20^{\circ}E$) are considered in order to ensure a fair coverage of the West African region. Case studies of a wet and a dry Sahel year are carried out. The variability in the precipitation is discussed.

In Chapter III, we seek to explain the peculiar nature of the observed latitude-time cross-sections of precipitation (Chapter II) by studying the stratification of the region's atmosphere and examining the convective instability criterion accounting for the preferred region and seasons of high precipitation around the ITD environment. Stationary thermodynamic analyses of θ_w, θ_s and θ (dry bulb potential temperature) for Niamey are used to compare the atmospheric states in the wet and the dry Sahel year.

In Chapter IV we discuss the ITD, in relation to the ITCZ and important scales of motion associated with it. The Zonal Walker Circulation and its effect on the region's precipitation are discussed. The effect on this circulation, of the upwelling of sea water, and the control of squall line activity, important in determining the summer precipitation over the Sahel, are considered.

The dependence of precipitation on the stations' position relative to the ITD for the IGY, an extension of a problem already considered for some Nigerian stations by Ilesanmi, (1971), indicates a decline in ITD control in the LDS area. The Southern Oscillation (SO) effect is, however, found to be important in that area.

In Chapter V we bring into juxtaposition, the interplay of two factors:

a) the establishment of the convective instability criterion of Chapter III, by defining an instability Index, I, taking account of two layers of the atmosphere that are crucial to the initiation and development of convection, and

b) the position of the station relative to the ITD, by estimating $(\phi_I - \phi)$ in considering the monthly and daily occasions of convective instability studied.

The association between the large scale variation of θ_w(850mb) and the ITD is also studied.

In Chapter VI studies of the inter-station correlation of precipitation along the 3 zones, (specified in ChapterII) are carried out and a 'model' of the various regimes present and their variability in the wet and dry Sahel year case studies presented. Furthermore, cross-correlations of precipitation along zone 2 are carried out to investigate possible tele-connection between the Southern region and the Sahel area.

Finally, in Chapter VII, we summarise the conclusions drawn from the study along with recommendations for further research.

CHAPTER II

SPACE - TIME PRECIPITATION CROSS-SECTIONS IN WEST AFRICA

2.(i) INTRODUCTION

In this chapter, we shall examine the variation of monthly precipitation in a South-North direction across West Africa from the Atlantic coast, through the Sahel to the Sahara border by means of cross-section (latitude-time) analyses. This is being carried out in order to show the precipitation regimes prevalent in the region and in particular, the strong association existing between the May to September cycle of precipitation observed in the Sahel and the January - December precipitation in the Guinea Savannah/Equatorial regions further South. This association is in good agreement with the variation in the latitude of the Inter-tropical Discontinuity (ITD) surface position in a typical year.

For an effective coverage of the region, three zones have been considered: Zone 1 (along longitude $12^{\circ}W$); Zone 2 (longitude $3^{\circ}E$) and Zone 3 (longitude $20^{\circ}E$). A further extension of zone 3 across the Equator was carried out to show the cross-equatorial nature of the precipitation regimes.

Apart from the Normal (long-term : 30 years (1931-60) wherever possible) monthly mean precipitation, two case studies are considered:-

i) a typical wet year in the Sahel: 1958 (after, at least, Bunting et Al, 1974).

ii) A typical dry year in the Sahel, 1970 which is conspicuous as one of the (1970-73) drought years in the region. (Winstanley, 1973a, 1973b).

The variability in the precipitation is estimated by calculating the mean, standard deviation and coefficient of variation in the monthly precipitation considered.

2.(ii) NORMAL PRECIPITATION CROSS-SECTIONS

a) Zone 1 : (longitude 12°W)

The normal precipitation observed along longitude 12°W for eight stations running from latitude 8° to 20.5°N are arranged in a plane depicting the two-dimensional distribution (space-time) of precipitation in the zone (fig.2.1). The isohyets can be questioned particularly where two of the stations are more than two degrees apart : Kabala and Kenteba. However, the strong association between these stations and the others in the zone lends support to the "inverted 'V'" structure of isohyets obtained.

It is remarkable that although Daru and Kabala in the South have rain all the year round while the other (mainly Sahel) stations in the North have rain mainly in the Northern Hemisphere (NH) Summer (May to September, to be precise) a reasonable link exists between the cycle and amount of precipitation in the entire zone. Unlike Zone 2 (fig. 2.3), only one precipitation maximum exists in the climatological Normal for the zone. This maximum occurs in September in the Southern stations and in August in the Northern stations. It varies in value from about 40cm in the South to less than 5cm as one moves Northwards. The marked demarcation between the dry seasons and the rainy season is typical of this and other areas which experience the Monsoon weather.

The importance of this climatological pattern lies in the fact that given the precipitation for January to March for Daru and Kabala, one can achieve a reasonable estimate of the general precipitation tendency throughout the zone till, at least, July/August. This is illustrated in fig. (2.2) where a simple but fairly reasonable prediction of the 5cm isohyet has been made for the entire zone using:-

i) an estimate of the position of the 5cm isohyet from the January to March, 1958 precipitation at Daru and Kabala along with,

ii) the climatological latitude/time slope, $\alpha = \partial\phi/\partial t$ of the 5 - 25cm isohyets.

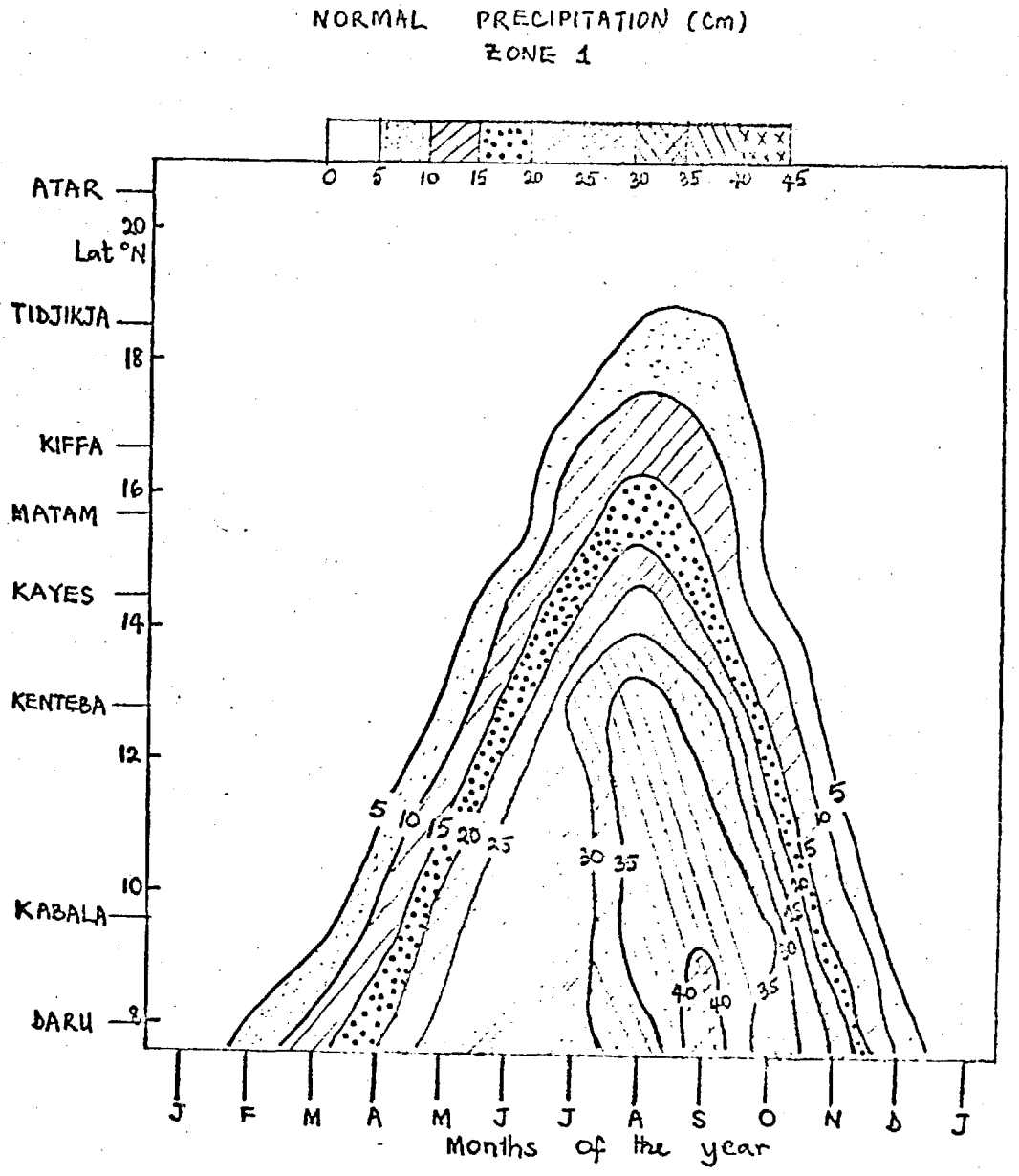

Fig 2.1

Latitude-time cross-section of Normal (1931-60) wherever possible) precipitation (cm) along zone 1. The cycle of precipitation in the South is related to that further inland (i.e. the Sahel) as the North-South variation of the isohyets here indicate.

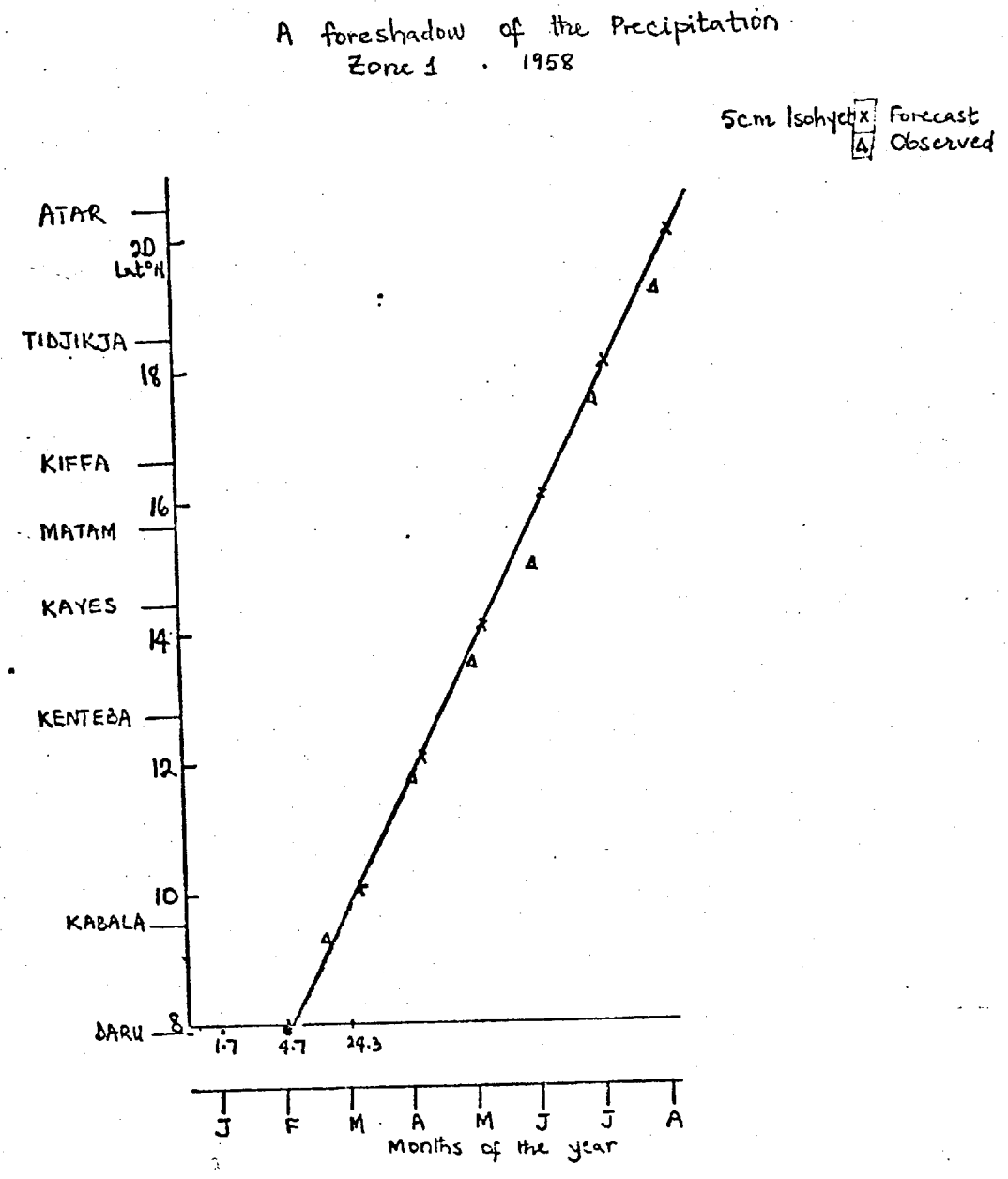

Fig. 2.2

A simple forecast of the time when the precipitation of an inland station will be up to 5cm, given the Jan-March precipitation in a Southern station. See Appendix VIII for a more detailed procedure towards forecasting the April to August precipitation for the region.

b) Zone 2 : (longitude 3°E)

The average course of the seasonal precipitation in this zone - which lies in a central position relative to the entire West African region - ranges from a double (March to June and September to October) peak in the South to a single (August) peak in the Sahel and Sahara border. Fig. (2.3) shows a latitude-time cross-section of the long term (Normal) mean monthly precipitation for the zone running from Lagos/Ikeja near the coast to Tessalit in the Sahara.

It can be observed that even though the Sahel precipitation comes mainly between May and September, its cycle is related to the January to December cycle of precipitation at the coast. A fair semblance to the pattern in fig. (2.1) is depicted by the isohyets particularly from latitude 8° to 20°N.

The mean surface position of the I.T.D. as observed along this longitude (Clackson, 1957) has been plotted along with the isohyets. It is remarkable to note that the isohyets parallel the I.T.D. position. Here then is the explanation for the "inverted 'V'" isohyet patterns of the cross-sections. Hence, using the latitude-time slope of the I.T.D., $\alpha = \partial\phi/\partial t$ can be more accurately estimated and a better forecast of the precipitation tendency several months ahead achieved.

The maximum precipitation of 30cm is obtained in June in Lagos area before the end of July to August 'little dry season' (LDS) observed in the area (Ireland, 1962).

Much of the area, particularly, the Sahel zone, gets its maximum precipitation in August. This occurs some 7-10° South of the I.T.D. position.

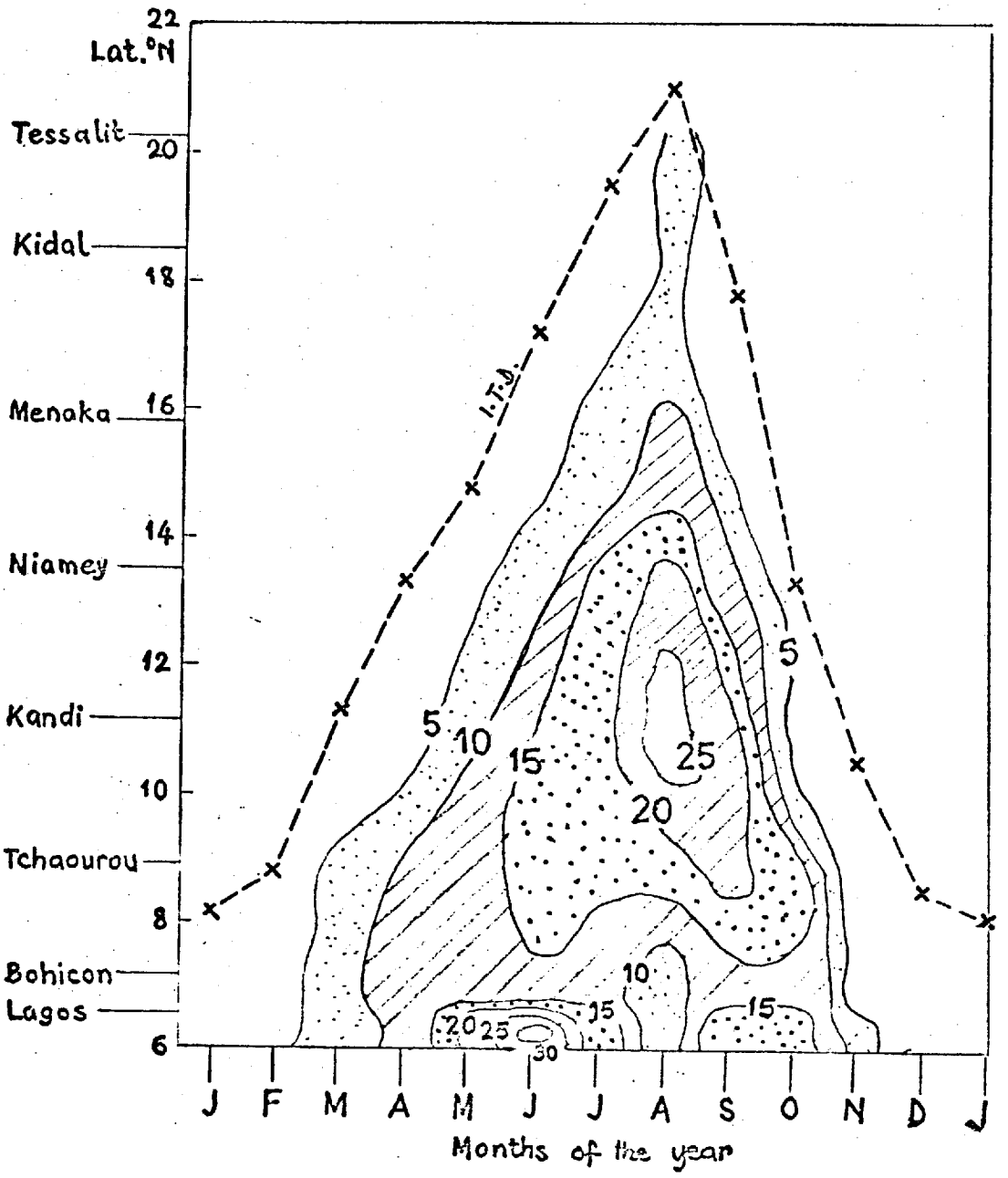

Fig 2.3

Legend as in fig 2.1 but for zone 2. The mean surface ITD position (---) (1956-61) (Clackson, 1957) has been plotted for this zone. It is remarkable to note that the precipitation belt moves North and South with the ITD.

c) Zone 3 : (longitude 20°E)

As shown in fig. (2.4), the general pattern of the isohyets observed in this zone is highly similar to those in Zones 1 and 2.

The stations around 4°N have a double minima in their precipitation cycle, one from June to July and the other, September. On the other hand, stations between 6°N and 18°N have a single (August) maximum. Hence, the L.D.S. is not an established phenomenon in this zone. It is an important feature only around the Southern region of the Zone 2 environ. We shall discuss the L.D.S. and associated atmospheric conditions in some chapters to follow.

Again, as in Zones 1 and 2, it is remarkable that a good association exists between the cycle of precipitation in the South and that to the North of the Zone. The region of maximum precipitation (of 30cm) spans a 5° latitudinal extent in August, during which month the I.T.D. is in its most Northernly position over most of West Africa.

The broad similarity in these Zones (1, 2 and 3) can be explained by the fact of the quasi-zonal uniformity in the I.T.D. location (though strictly speaking, Zone 3 often witnesses a slight WNW - ESE I.T.D. slant-wise displacement).

It is pertinent to ask what becomes of the "inverted 'V'" structure of the 5- , 10- , 15- and 20- cm isohyets as one goes further South across the Equator: do they, for instance, close up in a quasi-concentric manner? As this Zone, unlike Zones 1 and 2, lies near the central African region, where inland precipitation data abound, the Zone has been extended across the Equator to investigate the cross-Equatorial precipitation pattern and the associated seasonal contrast in the NH and Southern Hemisphere (SH) precipitation climatology as discussed below.

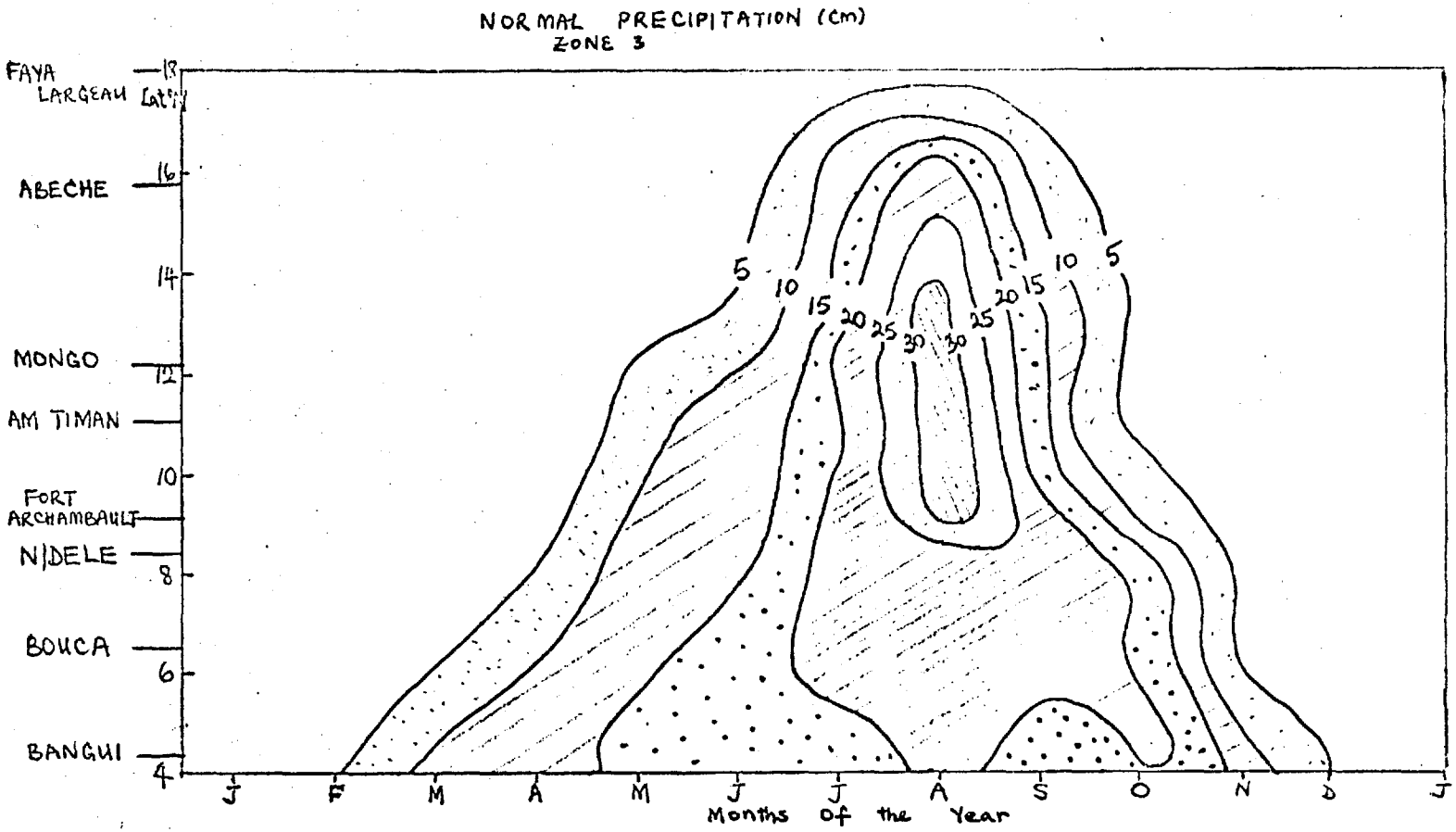

Fig 2.4

Legend as in fig 2.1 but for zone 3.

d) Cross-Equatorial : (Extension of Zone 3 Across the Equator)

We shall, here, consider an extension of Zone 3 across the Equator in order to:-

1. investigate the complete locus of the "inverted 'V'" isohyet patterns observed above, 2.(ii)(a - c) :

2. observe the precipitation regimes associated with the Equatorial environ, and

3. observe the manifestation of the Northern and Southern Hemispheric Seasonal variation over the African Continent, barring orographic and micro-meteorological (mainly local) effects.

To this effect, precipitation data observed over twenty stations situated in a North-South direction across the Equator (along the 20°E longitude) have been analysed (fig. 2.5a). To depict the space-time precipitation pattern on the Equator more clearly, two stations situated very near (North and South respectively), the Equator have been included: Coquilhatville and Boende.

The following significant features are worthy of note:-

a) Contrary to expectation, the 5cm- , 10cm- and 15cm-isohyets do not form a close loop similar to the 30cm, 25 and 20cm isohyets; rather, some of them spread along the South of the Equator.

b) A transition in isohyet structure occurs on the Equator, as a boundary between the Northern "inverted 'V'" precipitation pattern and its Southern counterpart. The regime to the South decreases inwards in a manner inverse to the pattern to the North. This accords with the fact that the SH dry season (Southern Winter) occurs during the NH rainy season (Northern Summer) as expected .

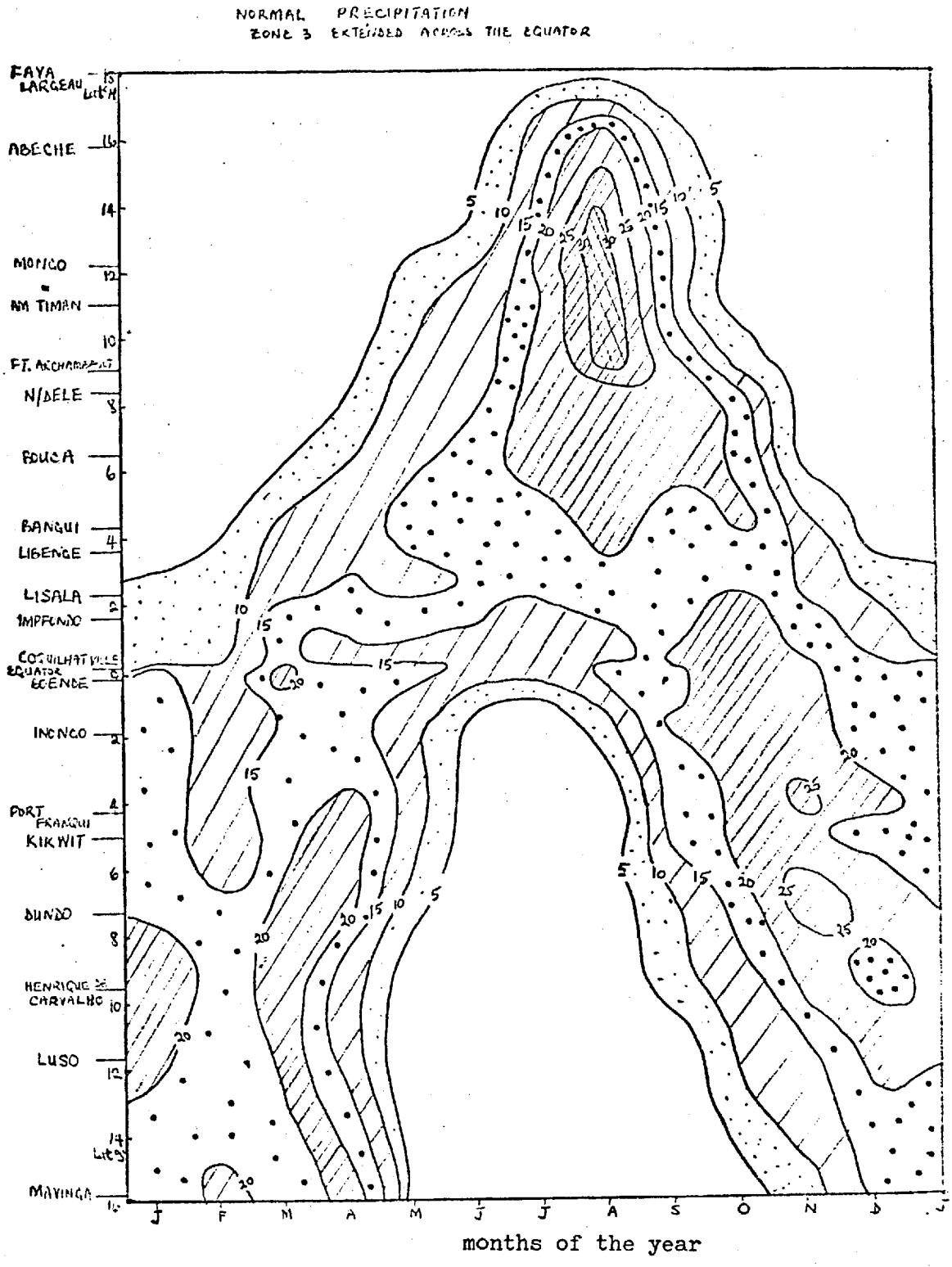

Fig 2.5a

Legend as in fig 2.1 but for the cross-equatorial extension of zone 3.

The isohyets in fig. (2.5a) raise some other questions:-

i) Does the SH Summer rainfall regime resemble an inverse of the Northern Summer case? (ie is there a wave number one pattern to it?)

ii) How does the observed pattern relate to the I.T.D. position over the zone?

The first question is answered by the pattern in fig. (2.5b) obtained by an extension (in a cyclic manner, since normal precipitation is being used) of the observations to the following July. However a more complete pattern would require more data further South of the Equator than presently used.

Regarding the second question, the I.T.D. does not cross the Equator owing to the absence of an Ekman layer pumping of moisture and hence, condensation (Charney, 1969). Also, the Equatorial temperature is the same as that of the I.T.D. and is higher than the radiative equilibrium value, hence sinking motion results to compensate for radiative cooling. This will be treated further with the observed I.T.D. plotted along with the corresponding isohyets later (2.iv)).

Fig 2.5b: A cyclic extension of fig 2.5a to July.

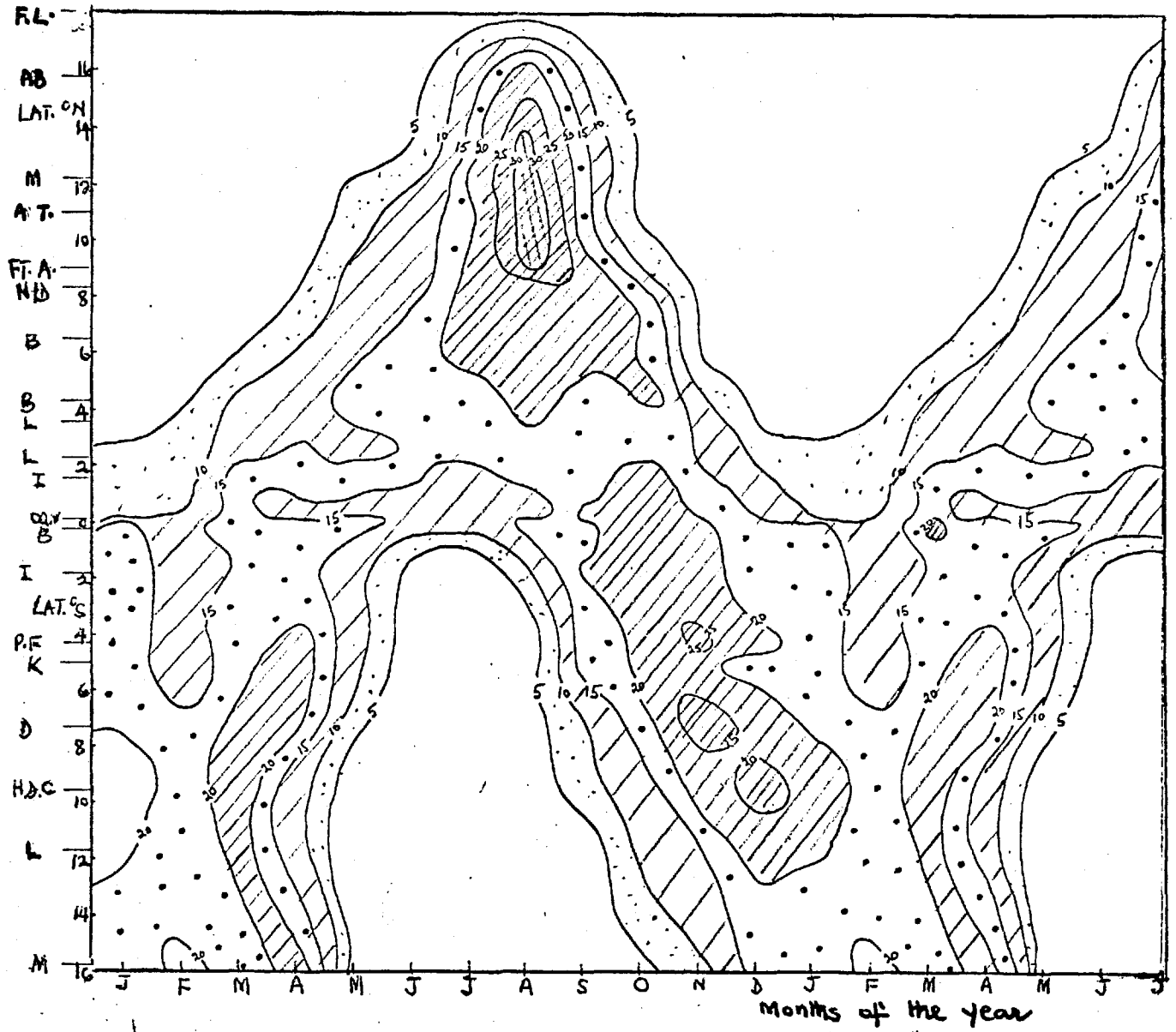

2.(iii) ON THUNDERSTORM OCCURRENCE IN THE REGION

Thunderstorms often develop from strong cumulonimbus (Cb) convection. They are characterized by a longer life time than that of an ordinary Cb owing to the fact that the updraught and downdraught currents are kept separate within the cloud system. Severe local storms, in particular, are often associated with hail, thunder and lightening. Such storms often characterise the first rain (styled 'ojo ipẹbu' in Yoruba) following the dry season in West Africa. This, in a way, is similar to the severe local thunderstorm situation experienced after a long dry spell in Mid-latitude regions.

In such cases, high wet bulb potential temperature, θ_w, occur at the bottom kilometre or two of the earth's surface due to energy fed into the boundary layer over many days of high insolation. This supply of warm air provides the necessary updraught for the storms. We shall treat this further in chapter III.

Orographically induced thunderstorms often occur in the evenings or afternoons in places like the Jos plateau, Futa Jallon Highlands, Adamawa Mountains, the Cameroon Mountains and Oshogbo and Okeiho hills. These often get organized into squall lines oriented between N-S to NE-SW, propagating Westwards across the region (Hamilton and Archbold, 1945; Eldridge, 1957).

The Summer 'widespread rain and thundery activity' experienced in the region are usually associated with organized (850mb) vortices (eg Aina, 1964). Aina's analyses, here emphasized because of its relevance to thunderstorm occurrence in the region, show that the bad weather zone advected from the East to the West across West Africa is often located South or South-East of the vortex region. Above these vortices were found Easterly waves at about 700mb (fig. 2.6). The 850mb level is the approximate cloud base for the inland areas (higher for the arid region) and the cyclonic vortices, depicted here, could enhance strong convergence of winds, capable of initiating strong ascending motion in cumulonimbus clouds. These vortices may well be the source from which the Easterly waves draw their energy.

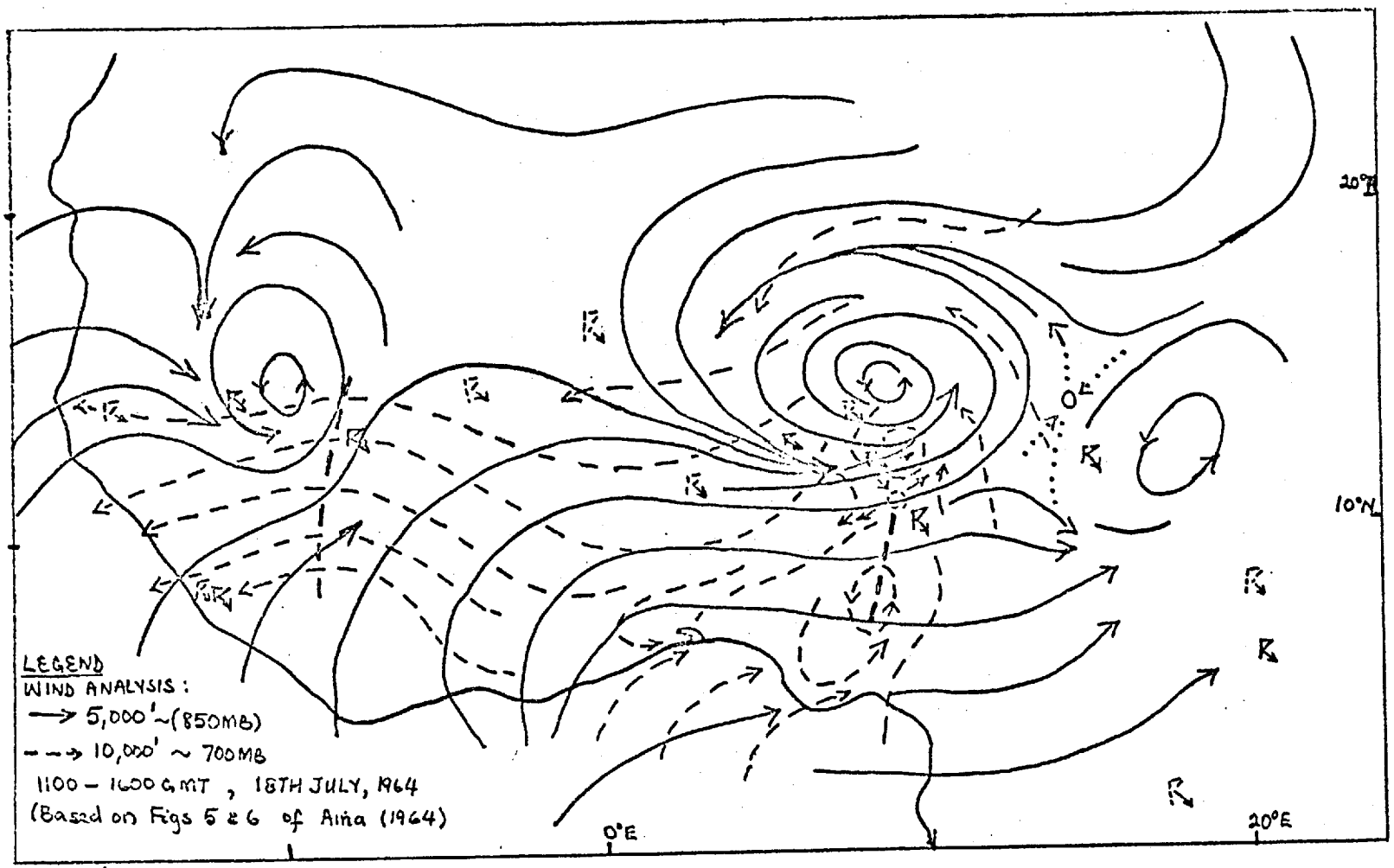

Fig 2.6

A typical example of the Summer circulation (After Aina, 1964) associated with thundery and squally weather, over the region: organized (850mb) vortices overlain by (700mb) Easterly waves.

Thunderstorm days

A thunderstorm day has been defined by the World Meteorological Organisation, WMO (1953) as ' a local calendar day on which thunder is heard'. From the mean data of thunderstorm occurrence over various years collected by the Organisation, the latitude-time cross sections of thunderstorm days for zones 1 and 2 have been constructed as shown in figs. (2.7) and (2.8). Along zone 1 (fig. 2.7) although not all the stations' data were available, a double Southern (near coastal) thunderstorm maxima was experienced, the intervening thunderstorm minimum occurring in July - August. A single inland maximum is experienced corresponding to the precipitation maximum observed there. However, in some stations, maximum precipitation is not experienced at the month of maximum thunderstorm occurrence, as already remarked by Zipzer (private communication). For example, some stations around the Futa Jallon highland experience maximum precipitation during the minimum thunderstorm period, possibly due to the outplay of orographic lifting on the moist Monsoon winds experienced at this time of predominant layer cloud situation.

However, in zone 2, fig. (2.8), a good correspondence exists in the thunderstorm cycle and that of the precipitation : (compared with fig. 2.3) each having a double maxima in the Southern part and a single maximum in the Northern (Sahel) region. Hence, most of the precipitation experienced in zone 2 result from thunderstorm systems. Many zone 3 stations (not shown) also exhibit this behaviour, although some of them have their maximum thunderstorm days in October, November or December depending on their altitude and location within the cross-Equatorial section of that zone.

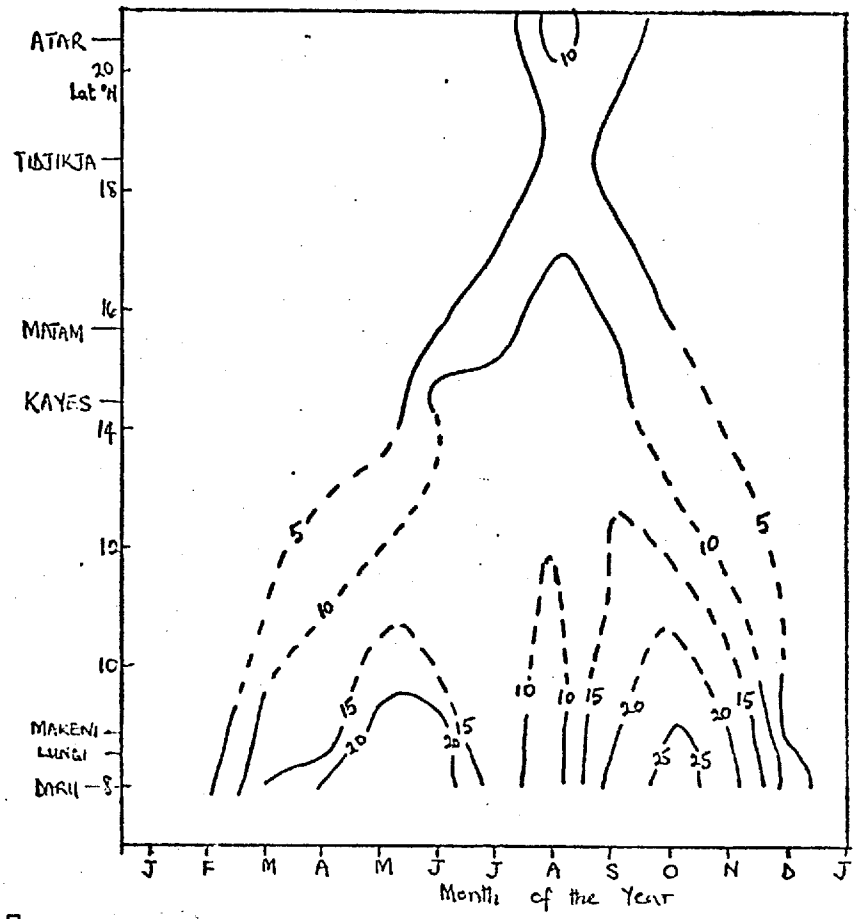

Fig 2.7

Thunderstorm days along zone 1. The July-Aug. minimum does not affect the zone's precipitation.

Fig 2.8 (below)

As in fig 2.7 but for zone 2. A good correspondence exists between thunderstorm days and precipitation.

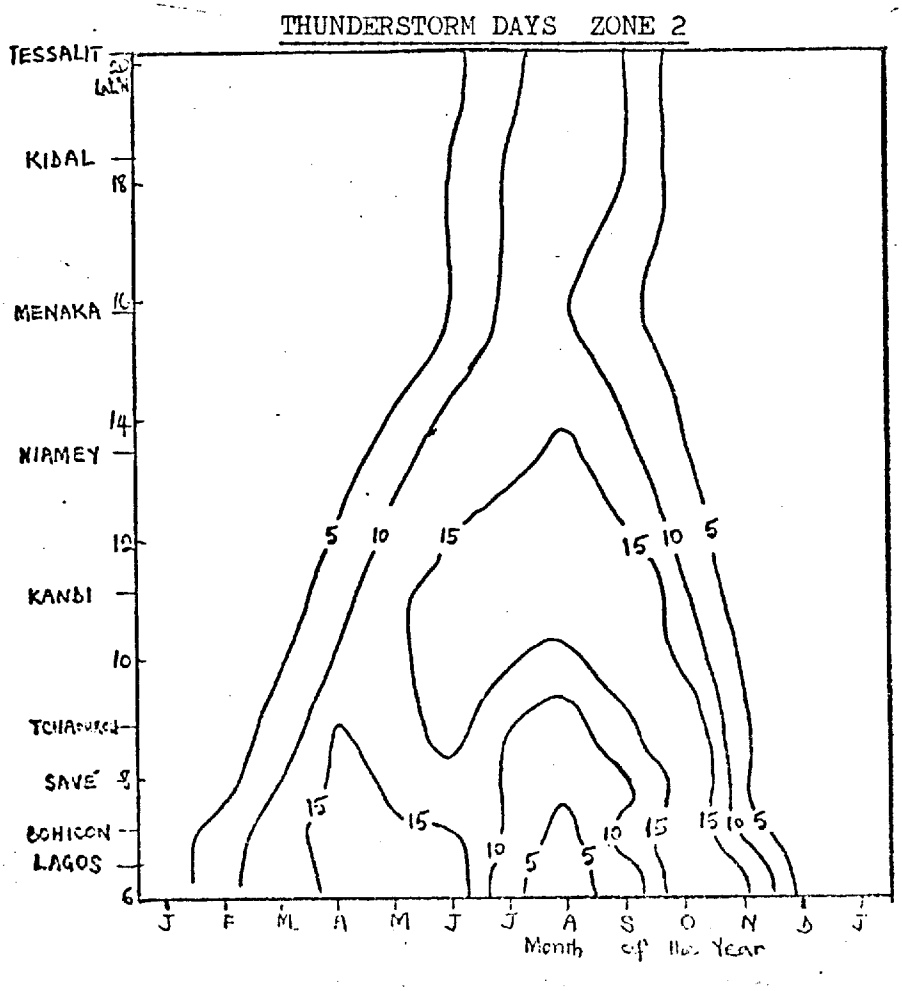

2.(iv) CASE STUDIES OF A TYPICAL WET AND A TYPICAL DRY SAHEL YEAR

Oscillations, though often irregular, of ten, five, three and two dry years have been found in some Sahel stations' precipitation (Jenkinson, 1973; Bunting et Al, 1976). We shall, here, study the precipitation distribution in a typical wet Sahel year, 1958 (after, at least, Bunting et Al, 1974) and that in a dry year, 1970.

Such a study is advantageous in that it affords an opportunity to investigate the steadiness of the cross-sections considered in Section 2.(ii) in wet and dry years and to spot, using aerological analyses (Chapter III) what atmospheric and thermodynamic conditions lead to the lateness or shortage of rains.

a) Wet Sahel Year, 1958

i) Zone 1

As shown by the distribution of the isohyets in fig. (2.9), the Southern station of Daru experiences less precipitation than 'Normal' (compared with fig. (2.1)) but the stations to the North experience higher-than-'Normal' precipitation.

The cycle of precipitation at the South now has a relatively drier (than Normal) July to August period, a mild form of a L.D.S. The other (Northern) stations retain their single precipitation maxima.

Plotted along with the isohyets is the latitude of the I.T.D. for the various months of the year 1958, as observed along the $12^{o}W$ longitude. The zone of maximum precipitation is 8 degrees South of the I.T.D. latitude in August but it is only about 6 to 4 degress South of the phenomenon in September and October.

Though the "inverted 'V'" isohyet structure still remains, the general pattern of zone 1 precipitation tends towards that in zone 2. Broadly speaking, the main change is the higher-than-Normal precipitation experienced in all the stations but the Southernmost, Daru.

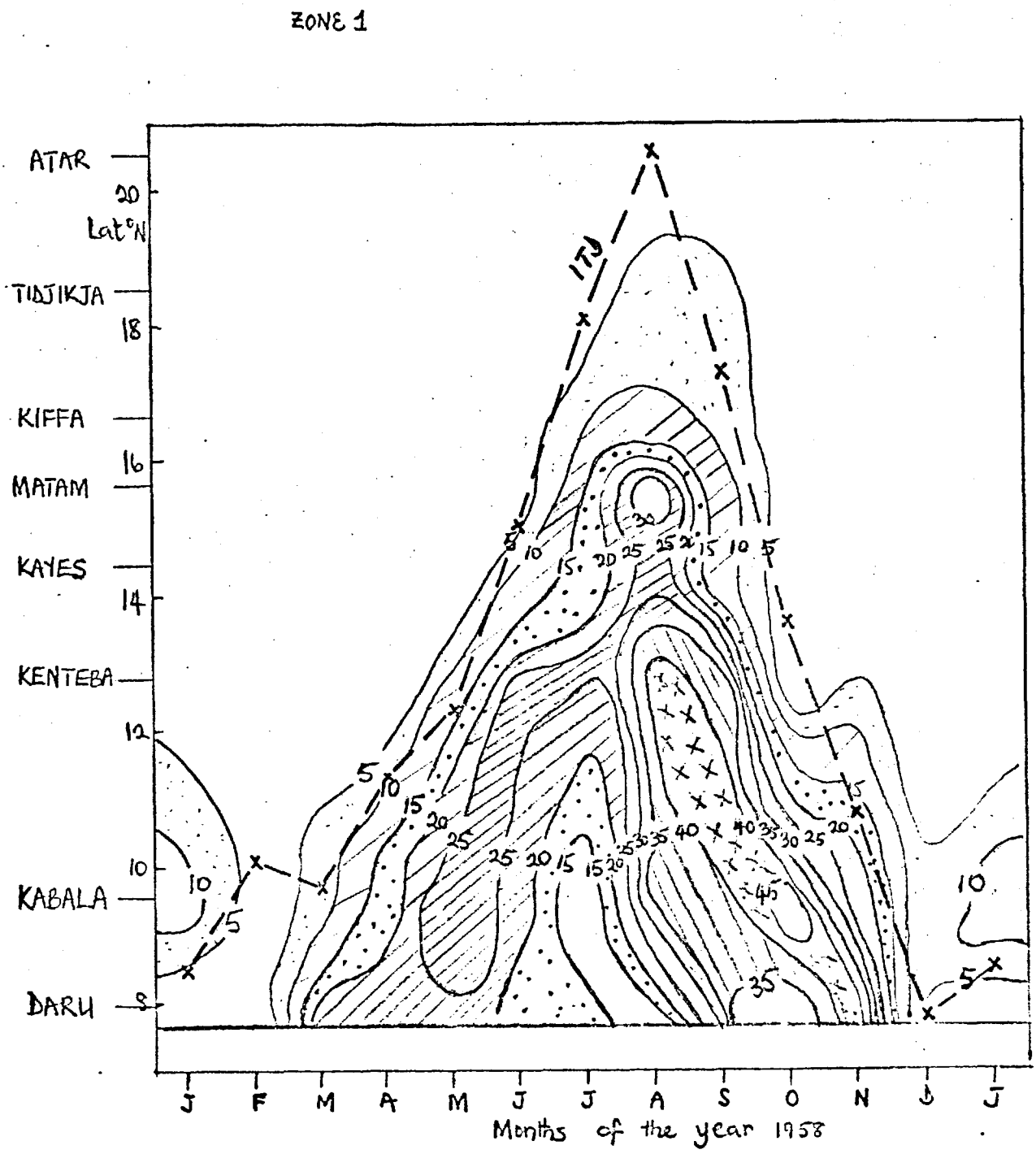

Fig 2.9

A latitude-time corss-section of precipitation (cm) along Zone 1, 1958. The mean monthly ITD positions along the zone are as indicated.

ii) Zone 2

The wet year situation in this zone (fig. 2.10) was that of increased Northward penetration of the July ending - August L.D.S. and considerable less-than-Normal precipitation in the Southern stations. This effect, already noticed in zone 1, is more pronounced here.

In contrast to the situation in the South, the Sahel zone experienced higher-than-Normal precipitation. The region of maximum precipitation was about 8-10° South of the I.T.D., particularly in August, and has also moved Northwards relative to the Normal case. This was associated by a further Northward penetration, by one degree, relative to the Normal situation, of the I.T.D.

iii) Zone 3 and its Cross-Equatorial Extension

Zone 3, occupying the area north of latitude 4°N in fig. (2.11) had experienced more precipitation than in the Normal case. Although a lower than-normal June-July precipitation minimum occurred in the Southern part, there has been little change in the precipitation pattern. It is remarkable that the region of maximum precipitation was just 5° South of the I.T.D. at this zone (in August when over 35cm of rain fell at Mongo).

A Southward extension of this zone across the Equator shows that, in fact, there has been a greater Northward penetration of the SH Winter (dry) season. This may be due to an intensification of the SH Hadley cell. More precipitation has, however, occurred in the SH Summer. It is remarkable that the I.T.D. never crosses the Equator and neither was a second I.T.D. branch (sometimes reported in some part of the globe (Ch.IV))found in the zone .

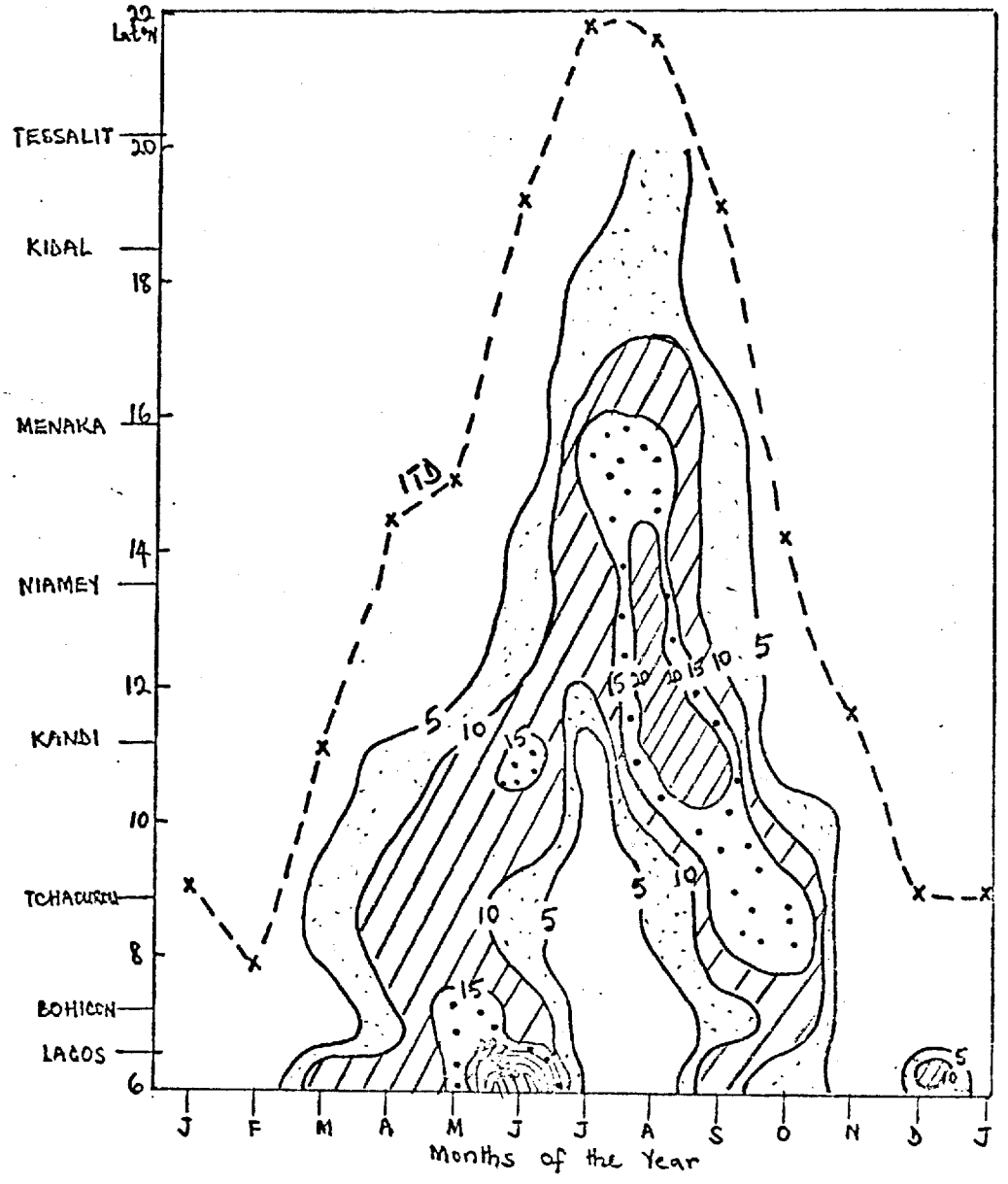

Fig 2.10

Legend as in fig 2.9 but for zone 2, 1958.

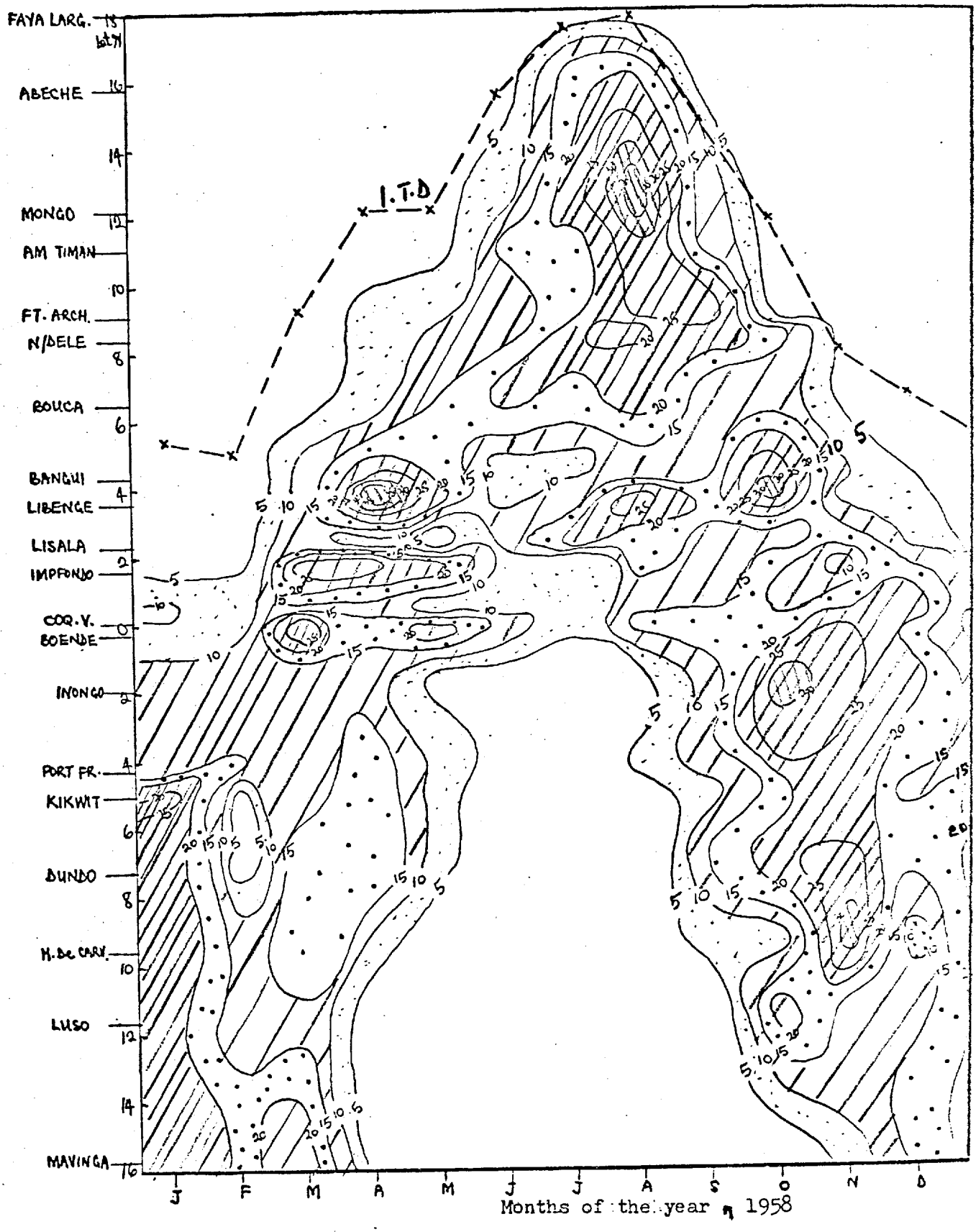

Fig 2.11

Legend as in fig 2.9 but for the cross-equatorial extension of zone 3, 1958. It is noted that the ITD does not cross the equator or move South of it in this zone.

b) Dry Sahel Year, 1970

i) Zone 1

A comparison between the observed precipitation pattern in the dry year fig.(2.12) and the wet year above, fig. (2.9) shows that though a similar general structure results, considerably less (about 15%) precipitation typify the former. A delay in the onset of the Monsoon rain is evidenced in Tidjikja and Atar. Even when the rains did come, they did not last as long as usual (eg only 3 months of rain was experienced at Tidjikja, compared with the usual 7!)

There has been about a degree latitude Southward shift in the isohyets relative to the situation in the wet year.

The L.D.S. effect is hardly noticeable as the Southern station (Daru) now has a higher precipitation than in the wet year. (The reverse of the situation in the Northern stations).

It, therefore, appears that the more intense the L.D.S. is, the less the precipitation in the Southern station but the more the precipitation in the Northern station. When the L.D.S. effect does not penetrate considerably Northwards, however, the converse results. A similar observation can be made in zone 2 below, fig. (2.13).

ii) Zone 2

As shown in fig. (2.13) the L.D.S. did not penetrate inland as in the wet year considered and the Southern area (Lagos, Bohicon etc) enjoyed more precipitation than usual while stations to the North were relatively drier than usual (as was the case in Zone 1). Kandi, 10° South of the I.T.D. position, had an unusually high precipitation.

It is worthy of note that the I.T.D. maximum Northerly position is 21°N, 1° further south than in the wet Sahel year.

The drought period was here marked by an anomaly in the cycle of

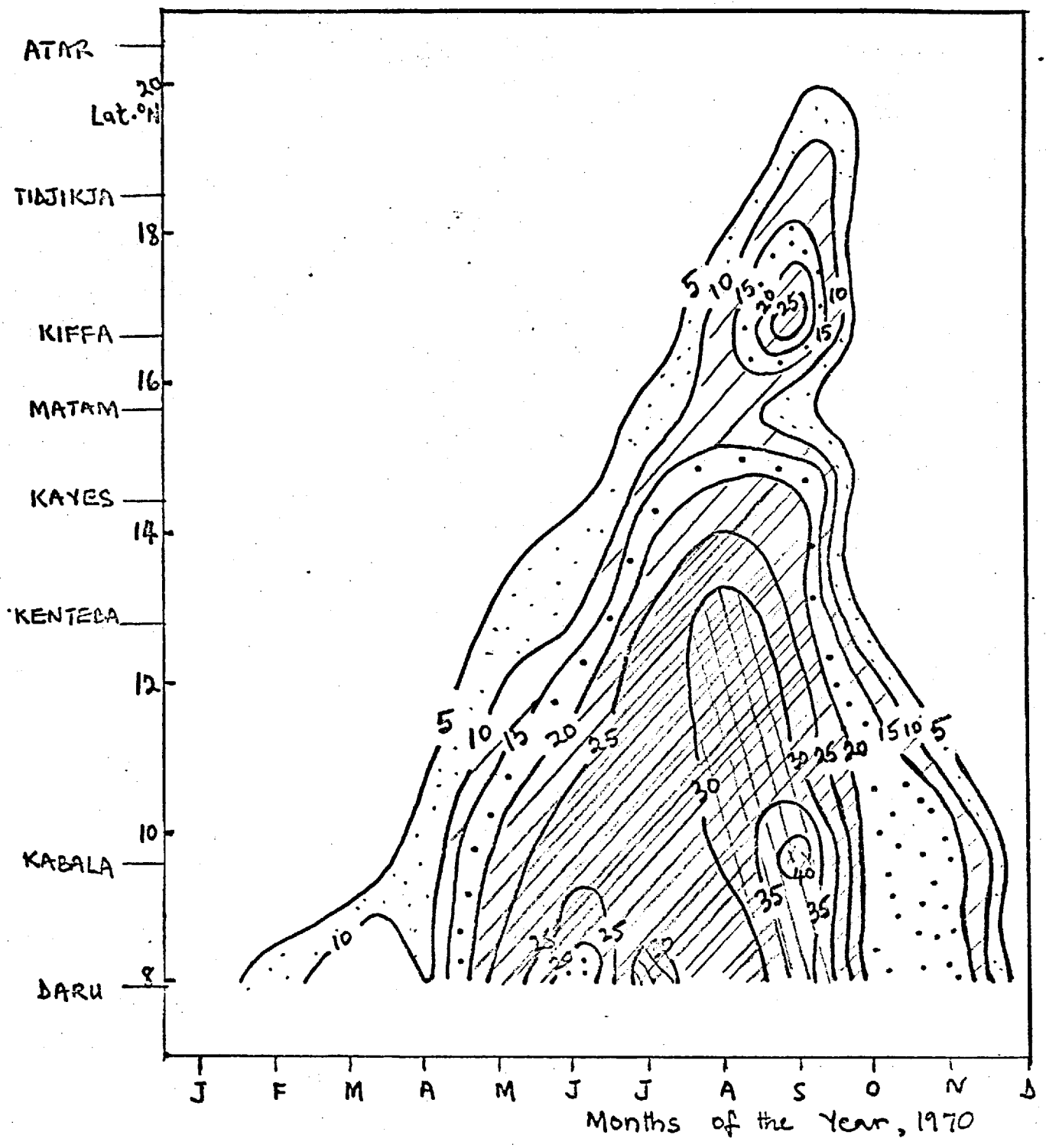

Fig 2.12

Legend as in fig 2.9, but for 1970, a dry year in the Sahel.

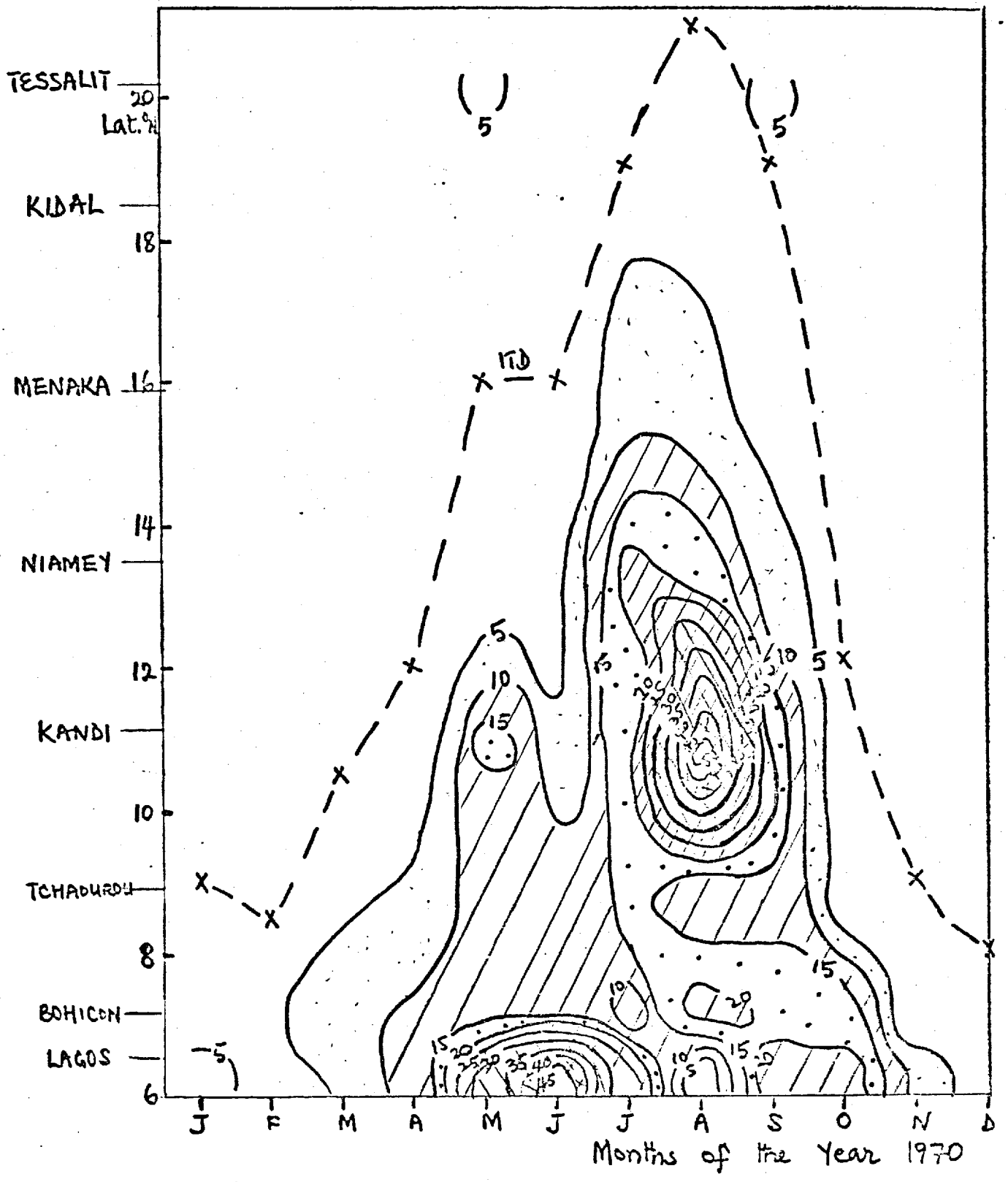

Fig 2.13

Legend as in fig 2.9 but for zone 2, 1970. The ITD positions have been plotted as indicated.

some Sahel stations' precipitation eg Tessalit, where the usual single peak gave way to several peaks.

iii) Zone 3 and its cross-Equatorial Extension

Owing to the gaps in the available data, the complete pattern of this zone cannot be obtained for this year. Faya Largeau's and Bouca's data could not be obtained, for example. Existing data, as analysed in fig. (2.14), shows a fall in the April and October maxima in the precipitation of the Southern station of Bangui (relative to the wet year). However, but for the lateness in the advent of substantial precipitation, there is not much difference between the dry and the normal case.

A place like Mongo even experienced more precipitation in August of the dry year than it had either Normally, or in the wet year. Little or no trace of the L.D.S. occurred North of $4^{o}N$ this year.

An extension of the zone across the Equator shows that there was a failure of the March-May and September to November precipitation.

The SH Winter dry season did not penetrate inlands as it did in the wet year. This suggests that a mild SH Winter is associated with drought in West Africa and vice versa.

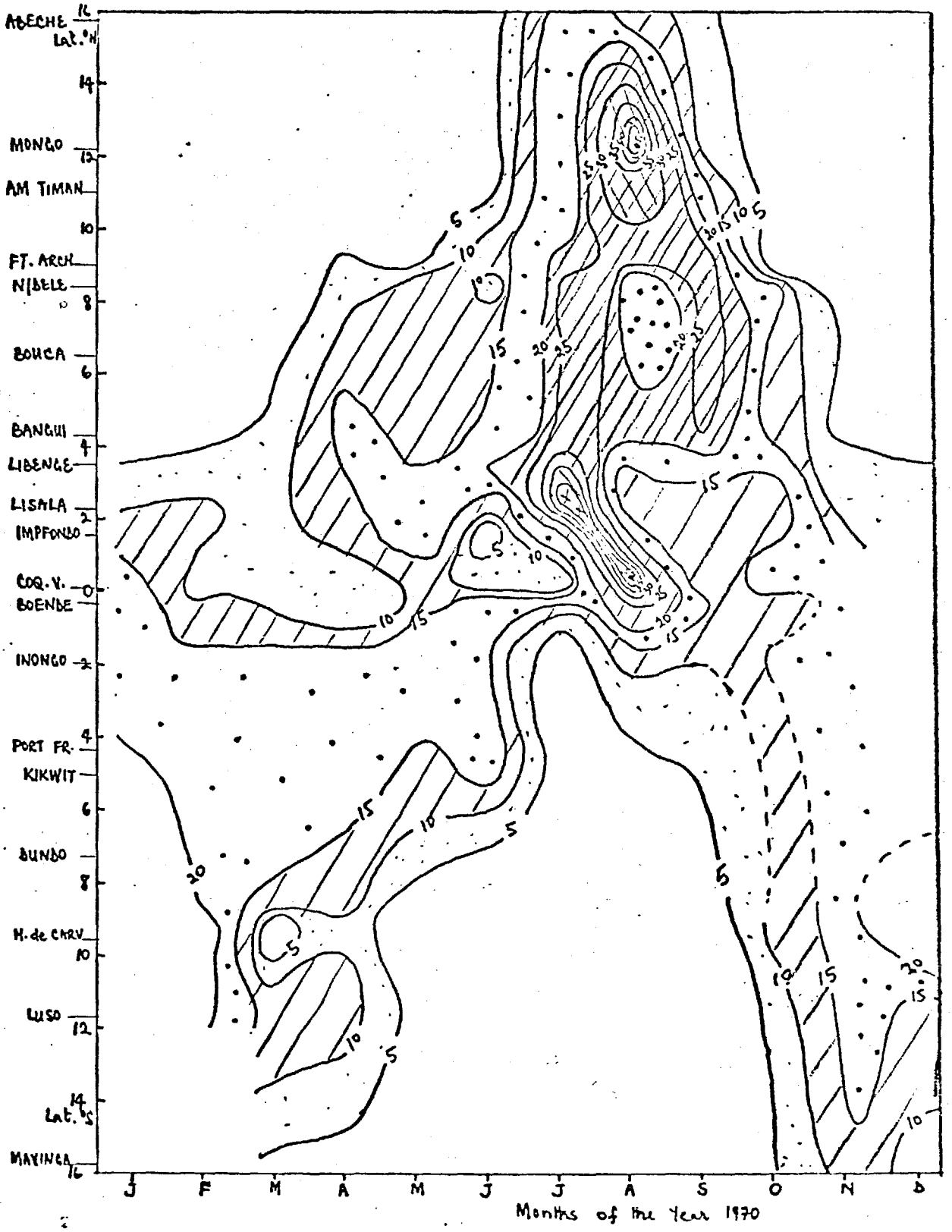

Fig 2.14

Legend as in fig 2.9 but for the cross-equatorial extension of zone 3, 1970.

2.(v) VARIABILITY IN THE REGIONS PRECIPITATION

In as much as averages are not sufficient to characterise a region's precipitation, a method of expressing its dispersion or spread about the average value has to be devised. Methods of measuring the dispersion range from estimating the range, the mean deviation and the standard deviation, to finding the coefficient of variation of the set of observations.

1. The range of the observed set of precipitation is the difference between the maximum and the minimum value in the set over the scale of time being considered.

While the range is a simple quantity to measure, it is highly unstable and practically, not a true measure of the twelve-monthly variability existing across the zones considered in this study. For example, the range in the January - December Normal precipitation for Lagos and Tessalit are 279mm and 55mm respectively. However, it is obvious that the arid environment of Tessalit is typified by a higher variability than the Equatorial climatic environment of Lagos, the L.D.S. here responsible for the high Lagos range, notwithstanding.

2. The Mean Deviation , M.D., is given by

$$M.D. = \frac{\Sigma|R - \bar{R}|}{N} \quad .. \quad .. \quad .. \quad .. \quad .. \quad 2.1$$

where R is the monthly precipitation observed;

$\bar{R}$ is the mean of the monthly precipitation for the time scale considered;

N is the total number of observations in the set.

3. The Standard Deviation , S.D. is given by

$$S.D. = \sqrt{\Sigma(R-\bar{R})^2/N} \quad .. \quad .. \quad .. \quad .. \quad .. \quad 2.2$$

4. The Coefficient of Variation , C.V. is given by

$$C.V. = \frac{S.D.}{\bar{R}} \times 100\% \quad .. \quad .. \quad .. \quad 2.3$$

Although C.V. is less useful when $\bar{R}$ tends to zero, it is dimensionless and popular as a good indicator of relative dispersion, suitable for comparing variability in observations over various places. C.V., estimated for Lagos (Normal, January - December) precipitation is 70% as compared to 170% for Tessalit [Appendix III (Table 2.1b)]. This is consistent with the well known fact that the semi arid/arid areas of the world have higher variability in precipitation than the humid regions. We shall use C.V. as our measure of variablity in the region's precipitation.

a) 12-monthly Variability in Precipitation

The coefficient of variation, C.V., evaluated for zones 1 to 3 on a 12-monthly basis and for the Normal, the wet and the dry years under consideration, has been plotted against the corresponding mean precipitation, $\bar{R}$ fig. (2.15), (2.16) and (2.17).

i) Zone 1

As shown in fig. (2.15), as $\bar{R}$ decreases, C.V. increases, indicating a negative correlation between the two. The Normal and the wet years show a near—asymptotic behaviour as C.V. tends towards a near constant value of 150% for $\bar{R} < 60$mm (Curve 1). In the dry year, however, a second branch developed which increases for $\bar{R} \leq 60$mm (Curve 2). As Table 2.1a further illustrates, C.V. increases gradually as one leaves the Guinea/Savannah area in the South for the Sahel arid area to the North, particularly in the Normal and wet years considered. Matam has the maximum variability observed in the zone in these years and C.V. decreases Northwards again from there. However, in the dry year, Tidjikja had the maximum variability, indicating a shift in the region of maximum drought effect two stations to the North. Also, compared to the Normal and wet year, the dry year is marked by increase in C.V. (and consequent fall in $\bar{R}$) everywhere in the zone.

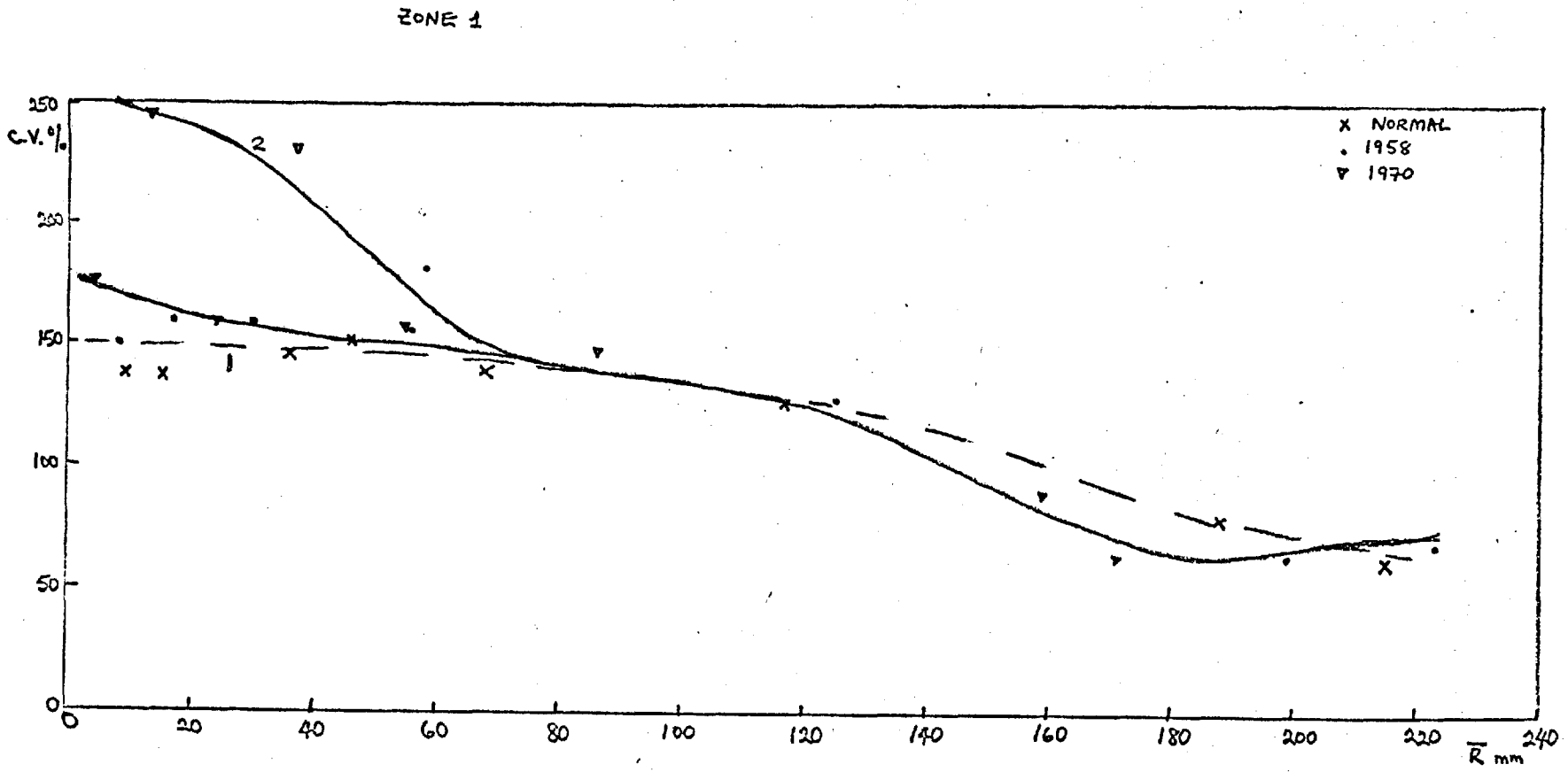

Fig 2.15

The variability in precipitation along zone 1 for the Normal, the 1958 and 1970 precipitation as indicated by a plot of CV(%) against $\overline{R}$(mm). For $\overline{R} < 60$mm, CV tends towards a constant (threshold) value e.g. as in curve 1. However, this threshold was overshot in the dry year, 1970 (solid curve 2).

Variability in the (Jan.-Dec.) precipitation: Zone 1

TABLE 2.1a

PLACE	NORMAL PPTN:			1958			1970		
	MEAN $\overline{R}$ (mm)	S.D. (mm)	C.V.(%)	MEAN $\overline{R}$ (mm)	S.D. (mm)	C.V.(%)	R (mm)	S.D. (mm)	C.V.(%)
1. Daru	215	130	60	199	128	68	171	110	64
2. Kabala	188	147	78	223	150	67	159	141	89
3. Kenteba	117	147	125	125	158	126	86	125.	146
4. Kayes	68	94	138	56	87	155	555	86	156
5. Matam	46	69	150	58	104	180	24	38	158
6. Kiffa	36	52	145	30	46	157	37	87	230
7. Tidjika	15	20	137	17	27	159	13	32	246
8. Atar	9	12	137	8	12	150	4	7	175

ii) Zone 2

A negative correlation exists between C.V. and $\overline{R}$ both in the Normal, wet and dry cases considered fig. (2.16) The range of both C.V. and $\overline{R}$ are much less than in Zone 1. (Range of C.V. $\sim$ 138% here, compared with 186% in Zone 1 while $\overline{R}$ range is 142mm compared with 219mm in 1). Unlike in zone 1, a gradual, consistent rise in variability is not observed in this zone. Lagos, near the coast often has a higher variability than Bohicon and Tchaourou, further inland (Appendix III, Table 2.1b). This is due to the L.D.S.

iii) Zone 3 (extended Southwards across the Equator)

Unlike in zones 1 and 2 where C.V. is nowhere $\leq$ 50%, many cases of C.V. $\leq$ 50% exist, particularly for stations that are close to the Equator, fig. (2.17). The Equatorial region experience rain all the year round, hence, high $\overline{R}$ and, consequently, low C.V. Hence, a gradual fall in variability is observed as one approaches the Equator from North or South. A systematic fall in C.V. exists in the Normal precipitation (Table 2.1C, Appendix III) up to Boende by the Equator from where C.V. starts to rise again as one goes Southwards. The range in C.V. is about 150% as in zone 2 and $\overline{R} \sim$ 170mm — less than in those zones. The negative correlation between C.V. and $\overline{R}$ for the Normal, the wet and the dry years is quite remarkable fig. (2.17).

Except at Faya Largeau in the North where C.V. has a value of 300% in the Normal mean, C.V. is higher than the Normal in the Sahel wet year, 1958, undermining the wetness of 1958 in this zone. However, the variability is higher than the Normal and wet year values during 1970, the dry year.

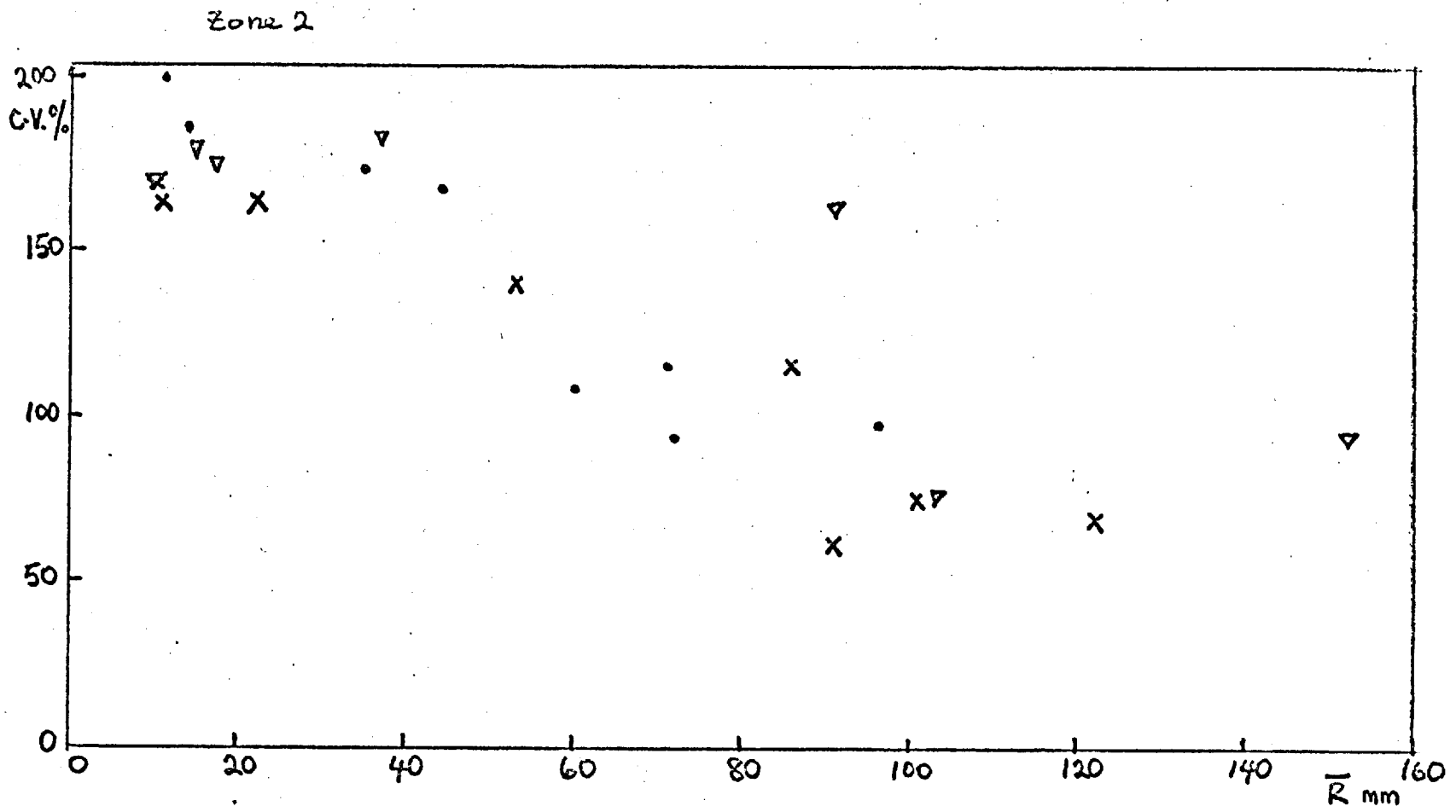

Fig 2.16

Legend as in fig 2.15 but for zone 2. Generally, a negative correlation exists between CV and $\bar{R}$.

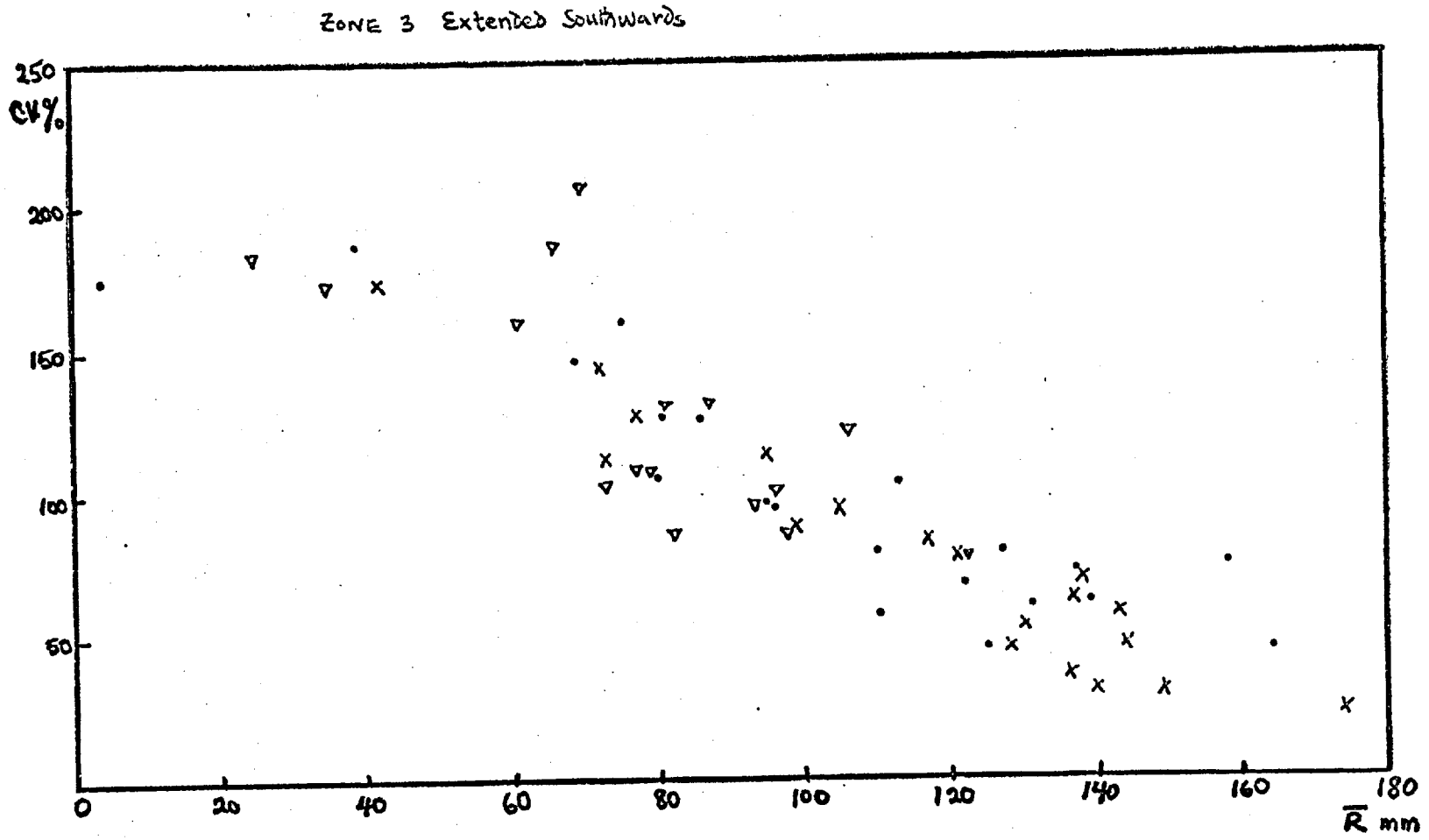

Fig 2.17

Legend as in fig 2.15 but for the cross-Equatorial extension of zone 3.

b) Variability in Seasonal precipitation

The variability in the Monsoon precipitation of May to October is found to be generally lower than that in the annual precipitation, particularly in the Sahel where nearly all of the annual precipitation falls in this period. Table 2.2 shows the seasonal variability in precipitation for Niamey, estimated for each year of 1951-1970.

While the effective variability in the Southern Equatorial/Guinea zones depends on the January - December monthly estimate, that in the Sahel is principally dependent on the Monsoon seasonal estimate. In view of this, the variability of precipitation over a decade (1951-60) with due reference to the Monsoon months, is given a further consideration below.

c) Variability on a decadal scale

The Sahel precipitation is quasi-steady during the 1951-60 decade (eg Bunting et Al, 1976). A study of precipitation variability over this decade has been carried out, as shown in Table (2.3), for the zone 2 stations for the Monsoon (rainy) season of May to October. It is remarkable to note that:-

i) Months of precipitation minima are months of high variability, a consequence of equation 2.3, e.g. as in July and August over Lagos (the LDS). This criterion spots out areas of unusual precipitation shortage although the general trend is that of increased variability as one moves from the Guinea coast inland.

ii) As shown in the graph of C.V. against $\overline{R}$ (fig. 2.18), C.V. is negatively correlated with $\overline{R}$. However, an exponential increase in C.V. occurs as $\overline{R} \longrightarrow 0$

iii) A low C.V. threshold of 20% is observed in the zone.

A comparison of fig. (2.18) with the results of Mooley and Crutchers (1968) on Indian rainfall indicates a faily good agreement in the variation of C.V. with $\overline{R}$ in these two marginal precipitation regions.

TABLE (2.2)

Year to Year variability in May - October Precipitation : NIAMEY

YEAR	MEAN, $\bar{R}$ (mm)	S.D. (mm)	C.V.%
1951	90	58	65
1952	163	162	99
1953	127	92	72
1954	73	62	86
1955	106	75	71
1956	89	85	95
1957	121	101	84
1958	87	87	100
1959	88	81	92
1960	84	71	85
1961	105	89	84
1962	120	139	115
1963	62	56	91
1964	142	106	74
1965	122	86	71
1966	83	55	66
1967	140	110	78
1968	92	68	74
1969	102	92	91
1970	74	83	111

TABLE (2.3)

VARIABILITY OF DECADAL PRECIPITATION: (1951-60) - ZONE 1

	MAY			JUNE			JULY			AUGUST			SEPTEMBER			OCTOBER		
	MEAN (mm)	STD (mm)	C.V. %	M	SM	CV	M	SD	CV	M	SD	CV	M	SD	CV	M	SD	CV
1. Lagos	215	67	31	336	120	36	150	118	79	59	51	86	214	95	44	222	79	36
2. Bohicon	151	58	38	178	49	27	133	82	62	66	66	100	153	75	49	187	53	28
3. Tchaourou	129	39	30	162	68	42	194	115	59	170	94	55	244	65	27	188	76	40
4. Kandi	110	68	62	162	38	23	212	102	48	278	79	28	274	59	22	65	60	92
5. Niamey	45	37	82	78	40	51	171	75	44	203	105	52	100	56	56	21	21	100
6. Menaka	8	7	82	35	32	91	93	43	46	128	60	47	59	39	66	8	12	150
7. Kidal	5	10	200	11	10	91	44	27	61	49	21	43	33	24	73	1	1	100
8. Tessalit	2	3	150	7	9	129	19	18	95	55	44	80	27	22	82	1	2	200

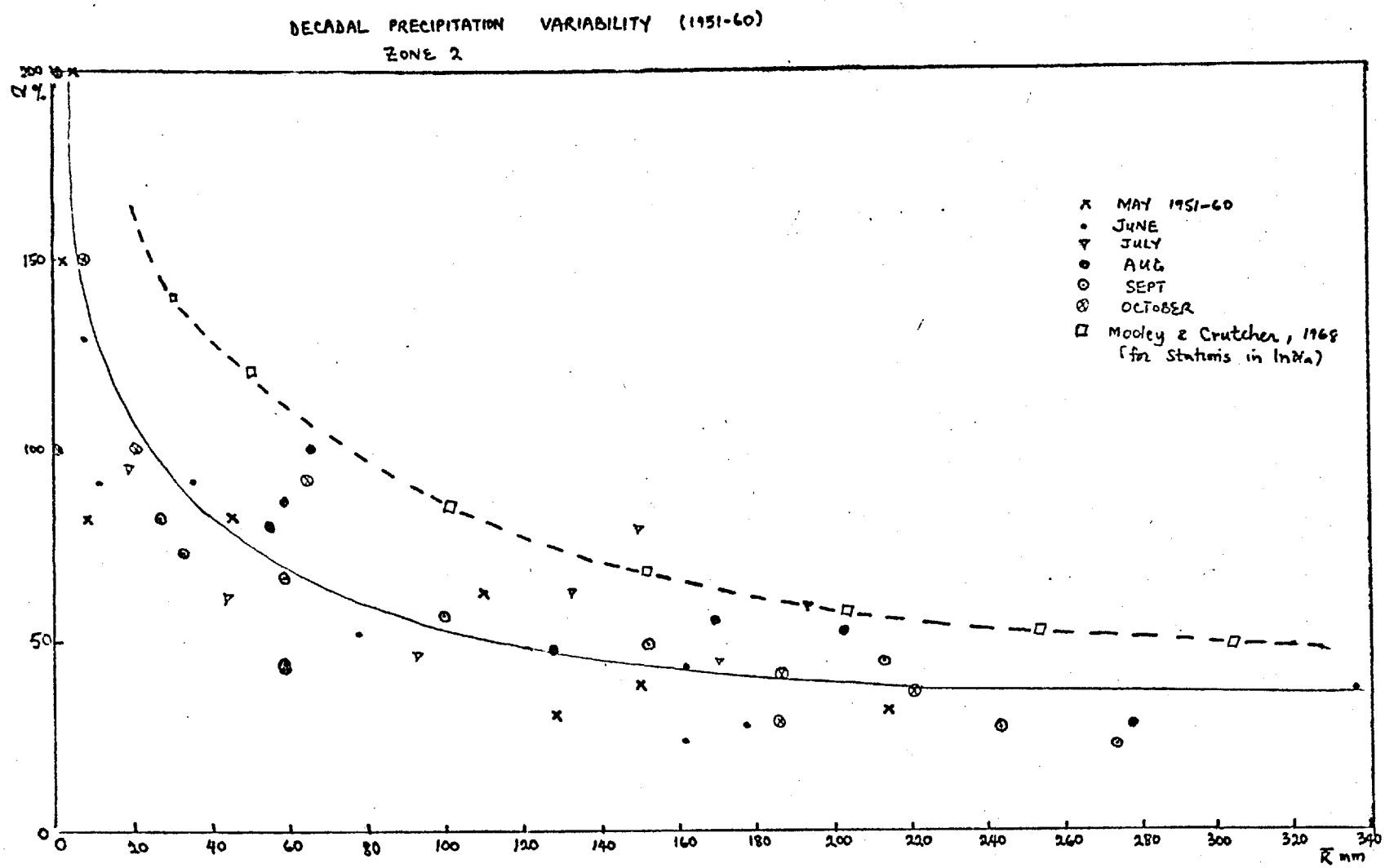

Fig 2.18

The variability in the zone 2 precipitation as estimated for May to October of the decade, 1951 to 1960. This is compared with the results of Mooley and Crutcher (1968) for stations in India.

2.(vi) CONCLUSION

Latitude-time cross-sectional analyses of precipitation across West Africa show that in any one year, the January - December cycle of precipitation in the South and the May - September cycle further North are strongly related. The isohyets, while assuming an "inverted 'V'" latitude-time pattern, parallel the latitudinal variation of the I.T.D. These climatological phenomena can, given the January to March precipitation in the South, be used to forecast (or foreshadow) the Sahel precipitation from May to about August.

The region was divided into three meridional zones for purpose of good coverage. While pretty similar features exist along these three zones, some slight variations can still be pin-pointed, particularly, regarding the I.T.D. climatological behaviour and the zones of precipitation associated with it.

West of the region (zone 1), the I.T.D. attained a mean maximum Northerly position of 20.6°N, in August (1958) while this maximum position was 22°N and occurred towards July ending in the Central of the region (Zone 2) but it was only 17.8°N to the East of the region (Zone 3) at the end of August. This may be due to variability in the pulses (Pedgley, 1972) existing in the opposing airstreams meeting at the I.T.D. These airstreams assume various degrees in complexity and type as one moves from the West to the East of the region eg while these are, mainly, the moist South Westerly and North Westerly currents and the dry Northerly and North Easterly currents in zone 1 where the I.T.D. is more of a semi-continental type (Leroux, 1971), they are principally the moist Southerly to South Westerly and the dry Northerly to North Easterly currents in zones 2 and 3 which are, mainly, of the continental I.T.D. type.

Also, while the zones of precipitation generally lie South of the I.T.D., substantial (at least up to 5cm per month) precipitation starts from the I.T.D. surface (Zone 1) or from less than one to two latitude degrees South of it (Zones 2 and 3).

The precipitation increases with distance South of the I.T.D. to an August maximum 7 to 10 latitude degress (700 to 1000 km) South

of the I.T.D. in zones 1 and 2 and 5 to 7 degrees South in zone 3. A prominent latitude-time August to October slant-wise region of maximum precipitation characterizes the cross-sections particularly in zones 1 and 2. South of the maximum precipitation region, a sharp fall in precipitation is experienced particularly noticeable in the L.D.S. region of zone 2. This is a rich, cocoa growing area in West Africa.

The precipitation zones move North and South with the I.T.D. and when the I.T.D. does not move sufficiently far North, the region of maximum precipitation is restricted to the Southern area and the Sahel region to the North experiences drought. A delay in the on-set of the rains and a decrease in its period characterize the dry year studied.

The variability in the region's precipitation increases Northwards as one goes from the Guinea Coast towards the Sahara except during the L.D.S. in the South when a higher Southern variability results.

The thermodynamic state of the I.T.D. environment from which the observed precipitation fell out shall be studied in chapter III.

CHAPTER III

THE CHARACTERISTICS OF ATMOSPHERIC VERTICAL STRUCTURE IN WEST AFRICA

3(i) INTRODUCTION

An analysis of the vertical structure of the atmosphere can be very instrumental in explaining the preferred regions and seasons of strong convective activities. This, no doubt, will answer the obvious questions raised by the observed features of the West African precipitation (Chapter II). Such questions as :

1. Why is the region of heaviest rainfall 7-10° South of the ITD latitude?

2. What accounts for the LDS in Lagos area at the heart of the Sahel rain period?

3(ii) THERMODYNAMICS

A statement of the second law of thermodynamics as applied to an air parcel is:

$$Tds = dE + p\,d(1/\rho) \qquad \ldots\ \ldots\ \ldots\ 3.1$$

(dE: Internal Energy; $p\,d(1/\rho)$: Work done by pressure field)

Where S = the Entropy of the system, here, consisting of dry air, water vapour and liquid water.

For a mixture of gasses, total Entropy, S is

$\sum$ Entropy of each constituent.

As shown by Brunt (1934),

$$S = [C_p + c(r_L + r_v)]\ln T - R\ln(p-e) + \frac{Lr_v}{T} \quad .. \quad .. \quad 3.2$$

Where C_p = Specific heat of dry air

c = Specific heat of the liquid

e = Partial pressure of water vapour

r_v = Mixing ratio for water vapour = $\frac{\text{mass of vapour}}{\text{total mass of air}}$

$= \frac{\epsilon e}{(p-e)}$

r_L = Mixing ratio for liquid water = $\frac{\text{mass of liquid water}}{\text{mass of dry air}}$

Partial pressures and temperatures are linked by Clausius-Clapeyron's Equation:

$$\frac{de}{e} = \frac{L}{R_v}\frac{dT}{T^2}$$

.. .. .. 3.3

Differentiating eqn 3.2: and multiplying through by T :

$$T\,dS = [C_p + c(r_L + r_v)]\,dT - \frac{TR\,dp/p}{(1-e/p)} + \frac{eR\,de/e}{(p-e)} - Lr_v\frac{dT}{T} + L\,dr_v$$

.. .. .. 3.4

Applying equation 3.3 in 3.4 with the approximations:

$$e/p \text{ small} \sim (1-e/p)^{-1} \sim 1 + e/p + (e/p)^2,$$
$$\sim 1 + e/p \sim 1 + \frac{r_v}{\epsilon}$$

Therefore, for a unit of dry air, r_v unit of water vapour and r_L unit of liquid water,

$$T\,dS = \frac{1}{(1+r_v+r_L)}\left\{[C_p + c(r_L + r_v)]\,dT - RT\left(1 + \frac{r_v}{\epsilon}\right)\frac{dp}{p} + L\,dr_v\right\}$$

.. .. .. 3.5

a) Atmospheric Reference Processes:

Atmospheric processes may be assumed to be generally adiabatic. i.e. $dS = 0$ in equation 3.5. Although this is not always so, it is useful to identify three major adiabatic reference processes:

a) Dry adiabatic, in which air is devoid of moisture or water vapour;

b) moist adiabatic, in which though water vapour exists, it does not attain saturation. Hence, there is no release of latent heat, and

c) Saturated adiabatic, in which latent heat release is available.

i) Dry Adiabatic process :

In addition to the constraint, $dS = 0$, $r_L = r_V = 0$ also, in equation 3.5.

Therefore $$0 = C_p\, dT - RT\,\frac{dp}{p} \qquad \ldots\ \ldots\ \ldots\ \ldots\ 3.6$$

Integrating equation 3.6 ,

$$C_p \ln T = R \ln p + \text{Const}$$

If, at a standard pressure level, $p = 1000\text{mb}$, $T = \theta$,

$$C_p \ln\theta = R \ln 1000 + \text{const}$$

Hence, $$\theta = T\left(\frac{1000}{p}\right)^{R/C_p} \qquad \ldots\ \ldots\ \ldots\ \ldots\ \ldots\ 3.7$$

Where θ = Dry bulb potential temperature
= the temperature an air parcel will have if brought down dry adiabatically to the 1000 mb level.

ii) Moist Adiabatic process:

Neglecting latent heat release and r_l in equation 3.5,

$$0 = \left(\frac{C_p + Cr_v}{1+r_v}\right)dT - \frac{RT(1+r_v/\epsilon)\,dp/p}{(1+r_v)}$$

Therefore, $$RT^*\frac{dp}{p} = (C_p + Cr_v)\,dT \qquad .. \quad .. \quad .. \quad 3.8$$

Where $$T^* = T(1+r_v/\epsilon)$$ = virtual temperature

implying that moist air behaves as if a dry air but with a higher temperature, T*.

iii) Saturated process:

From equation 3.5, neglecting condensed water,

$$TdS = 0$$

$$= \frac{1}{(1+r_v)}\left\{(C_p + Cr_v)dT - RT(1+r_v/\epsilon)\frac{dp}{p} + L\,dr_v\right\}$$

$$(C_p + Cr_v)dT = RT^*\frac{dp}{p} + L\,dr_v \qquad .. \quad .. \quad .. \quad 3.9$$

The saturated adiabatic process is reversible but depends on initial conditions.

We are more interested in a process which is independent of initial conditions. Hence we make re-course to the pseudo-Adiabatic process in which a parcel of air is lifted until saturated, and a volume of water is condensed and instantly removed. The air is then brought down saturated adiabatically to 1000mb. Similarly, in descent, just enough water is added to the air to keep it saturated.

At saturation, $r = r_s$

As the parcel rises from level p with temperature T to level p - dp, temperature T-dT, condensed water is

$$r_s\ (p, T) - r_s\ (p-dp, T-dT)$$

Latent heat release is Ldr_s

Therefore, $C_p dT - RT\frac{dp}{p} + L dr_s = 0$ 3.10

Equation 3.10 is not integerable.

However, assuming hydrostatic conditions and using Clausius-Clapeyron's equation for saturated case,

$$\frac{de_s}{e_s} = \frac{L_v}{R_v}\frac{dT}{T^2}$$

It can be shown that the lapse rate of pseudo-adiabatic process is given by

$$-\frac{dT}{dz} = \frac{g}{C_p}\left\{\frac{1 + L_v/RT\, r_s}{1 + \epsilon L_v^2/RT^2 C_p r_s}\right\}$$

b) <u>The Wet bulb potential temperature, θ_w and saturation potential temperature, θ_s</u>

Equations 3.8 and 3.10 can give us θ_w and θ_s respectively at 1000mb level.

θ_w is the wet bulb potential temperature obtained by lifting a parcel of air dry adiabatically while keeping its mixing ratio constant at the same time. The parcel is lifted until it attains saturation (i.e. $r_s = r$). It is then brought down pseudo saturated adiabatically to the 1000mb level where its resulting temperature is the wet-bulb potential temperature, θ_w .

θ_s is the saturation potential temperature, obtained by bringing down saturated adiabatically to 1000mb level, a parcel of air from any level in the troposphere.

θ_w is a function of dry bulb temperature T of the air and its dew point temperature, T_d. θ_w is an invariant property of a parcel in the atmosphere during adiabatic displacement. Along with θ_e (the equivalent potential temperature, defined as the absolute temperature obtained after lifting the parcel until it has lost all its moisture and is then returned dry adiabatically to the 1000mb level), θ_w can be effectively used as an

identifier of air masses in the atmosphere. (Saucier,1955).

θ_s , on the other hand, is a function of the dry bulb temperature only and can be effectively used to define the environment, in which the parcel of air of interest is rising.

The values of θ_w and θ_s for various levels of the atmosphere were evaluated from soundings of dry bulb temperature, T and dew point temperature T_d, plotted on a tephigram, eg fig (3.1)

3(iii) PREFERRED REGIONS OF STRONG CONVECTIVE ACTIVITY

The months of July, August and September of the Wet Sahel year, 1958, have been selected for study as most of the precipitation experienced in the region fell during these months (Chapter II). Maximum precipitation occurred in August while July and September were months of ascending and descending precipitation tendencies respectively.

Moreover, July - August are months during which the LDS is strong in Lagos and nearby Southern regions. An aerological study of these months would, no doubt, shed some light on the associated stability of the atmosphere.

a) Updraught into Cumulonimbus clouds

The bottom 1 to 2 km layer of the earth's surface is the source region for the energy available to cumulus and cumulonimbus convection. A measure of this energy is given by the difference between the value of θ_w averaged over the 1-2km surface layer and the θ_s minimum in mid-troposphere.

θ_s minimum level is usually the top of the layer containing Cumulus.

When the averaged lower level θ_w value exceeds the minimum mid-tropospheric θ_s value, thermal instability results, giving rise to convection. This is a state of unstable stratification of the atmospheric

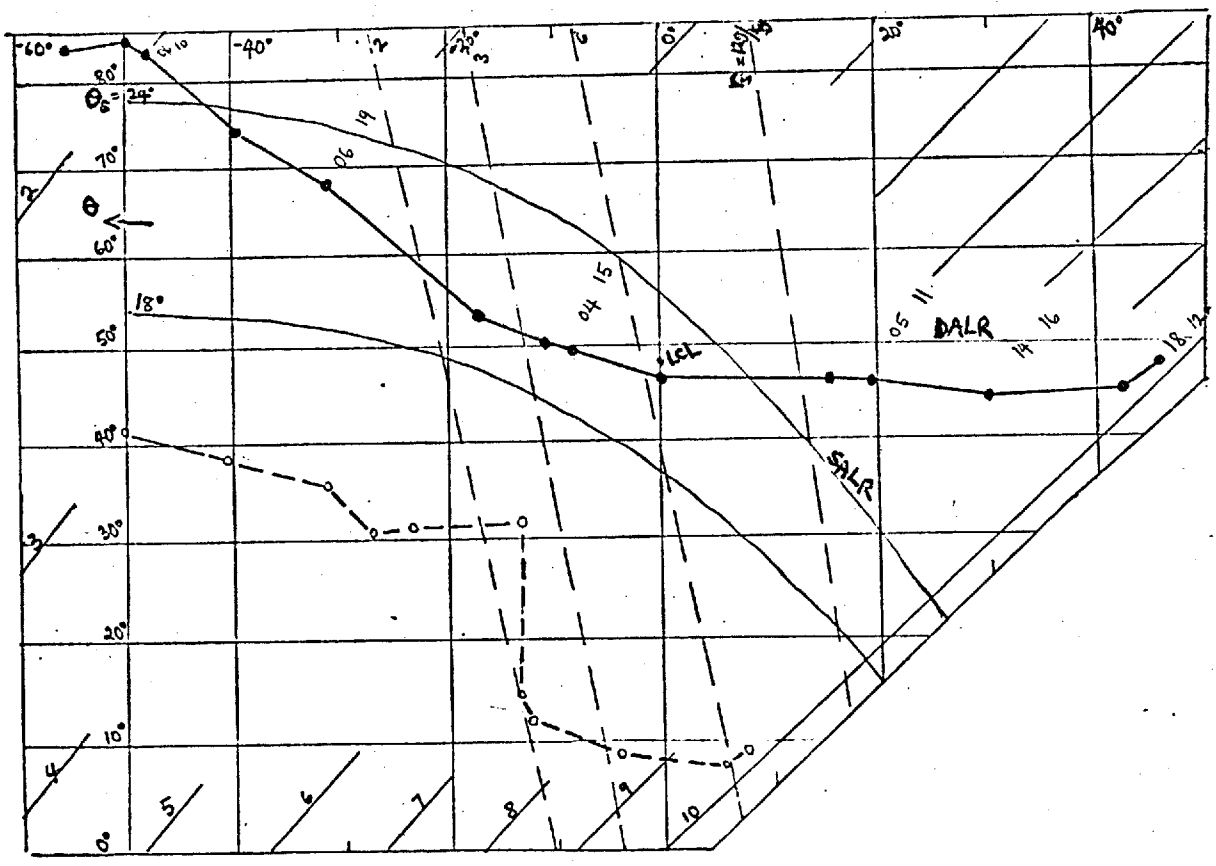

Fig. 3.1:

A typical sounding plotted on a tephigram. In this case, Aoulef, 1100GMT, 16th July, 1958. The solid curve is the dry bulb Temperature T(°C) sounding while the dashed curve is the dew-point, T_d(°C) sounding. The wind direction (in degrees) and speed (in kts) are as indicated for various levels. An air parcel lifted dry adiabatically (i.e. with a dry adiabatic lapse rate (DALR)) from the surface becomes saturated at the lifted condensation level (LCL) where its mixing ratio, r equals the saturation mixing ratio, r_s. This air is then brought down saturated adiabatically along the saturated adiabatic lapse rate (SALR) to the 1000mb surface where the θ_s value obtained gives us θ_w for the parcel.

However the process of lifting a parcel moist adiabatically (along θ_s curves) from any level to 1000mb gives us θ_s .

layer favourable for development of cumulus (Cu) or Cumulonimbus (Cb) clouds.

$\theta_{s\,(\text{midtrop})} > \theta_{w}$ (averaged low-level value) { results in a stable stratification of the atmosphere and a suppression of convective activity.

However, when θ_{w} (averaged low-level value) = θ_{s} (midtrop.), a neutral condition is established.

θ_{w} at the surface can be increased by considerable input of solar radiation into the bottom kilometer or two of the atmosphere. Severe thunderstorms often result from two or three days intense sunshine during which the surface θ_{w} value considerably builds up. Cu and Cb clouds then develop within the boundary layer, often topped by an inversion layer, serving as a lid over the convection. The updraught generated within the dry adiabatic layer (just above the super-adiabatic layer) resulting from the high build up of θ_{w} can be strong enough to break through the inversion layer allowing the growth of deep Cb towers which can pump energy right through the troposphere into the lower stratosphere. Such deep systems give a lot of rain and are often associated by thunderstorms and hail.

In the tropics, scattered severe thunderstorms are common in the evenings, and nights, evidently owing to the increase in θ_{w} experienced from the high insolation of the morning and afternoon hours.

The large-scale circulation influences the value of θ_{s} .

b) Thermodynamic State of the Atmosphere in July

Fig. 3.2 shows the cross-section of θ_w and θ_s for West Africa, running from Lagos on the Atlantic coast to Aoulef by the Saharan border (along the longitude of Lagos). Surface θ_s range from 20.2°C at Lagos to 27°C at Niamey and 38.4°C at Aoulef (not shown). The θ_s values decrease with height up to the 600mb level at Lagos (and 500 mb level in other parts of the region) where a minimum θ_s value of 21°C is observed. Above this level, a general increase in θ_s is observed again until the 150mb level is reached. The θ_s minimum level represents the top of the layer containing Cumulus convective systems. Of great significance is the mid-tropospheric cooling existing above this layer.

The θ_w distribution for this month indicates a maximum value of 23.5°C over Niamey while places to the North and South all experience low θ_w . A minimum θ_w of about 15°C exists over Niamey at the 700mb level. Places North and South of the station generally have higher θ_w at this same level. From 700 mb level upwards, θ_w values increase tending towards the θ_s values.

Areas of considerable thermal instability have been lightly dotted. Here, θ_w at the bottom lower layer exceeds the value of θ_s minimum at mid-troposphere. This region is a likely source of rising thermals that can rise through the troposphere to the condensation level where clouds are formed. The latent energy released as water vapour condenses in these clouds act as the source of energy for further cloud growth. This process can give rise to growth of Cumulonimbus (Cb) clouds as the necessary warm updraught air rise into the clouds from the hot surface.

Usually, this Cu and Cb convection develops under an environment of large scale descending air which gives rise to the formation of an inversion layer acting as a lid supressing the Cu convection. The higher θ_w at lower levels is (over θ_s at the mid-troposphere), the stronger the updraught likely to be generated and the higher the tendency of growing cb clouds which can be so powerful as to break through the inversion layer and grow deep enough to give considerably high precipitation. Cb cloud

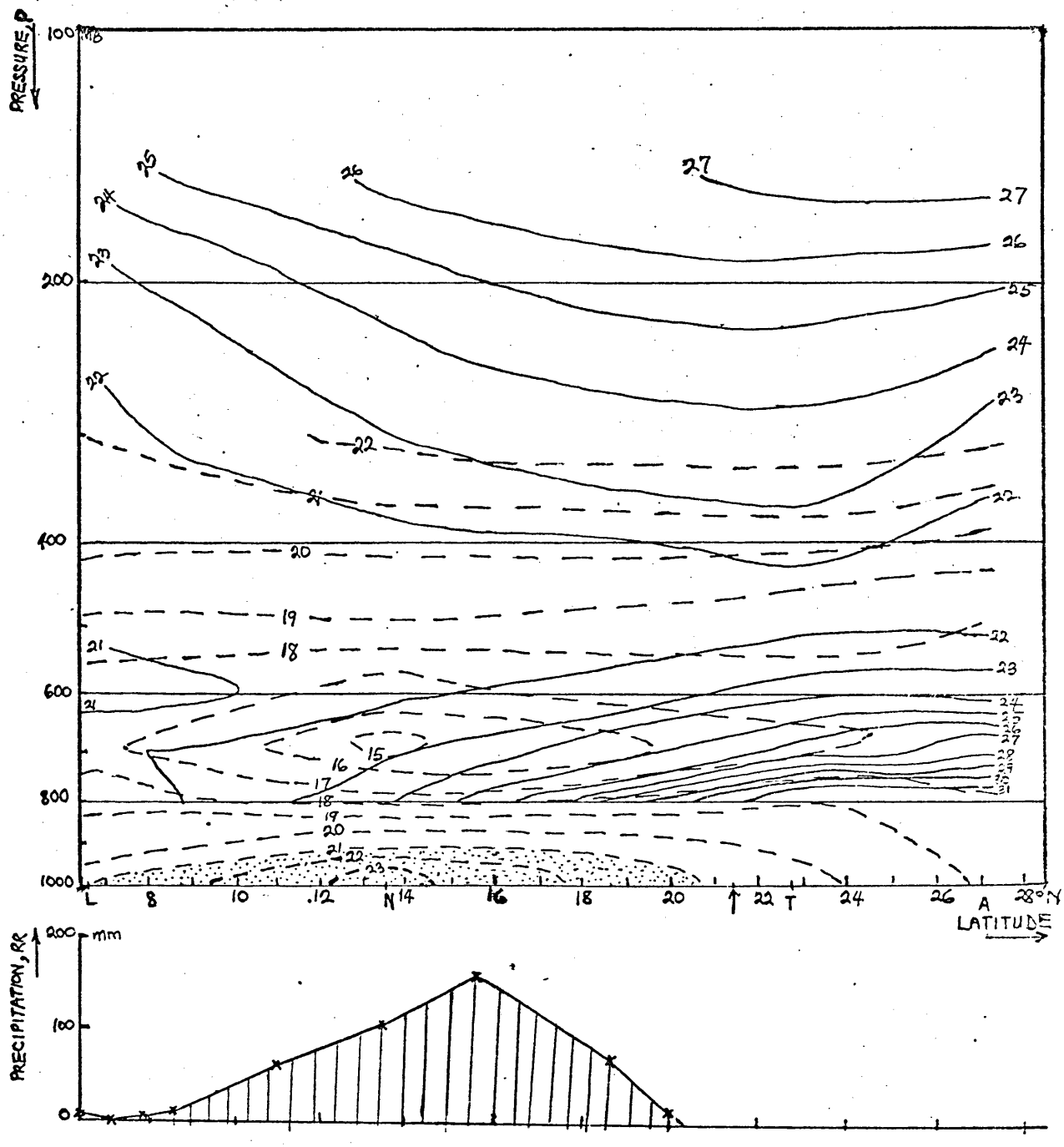

Fig 3.2

A latitude-height (in pressure co-ordinates) cross-section, along the longitude of Lagos (Zone 2), of isopleths of θ_w (pecked) and θ_s (solid) for the month of July, 1958. L,N,T,A stand for Lagos/Ikeja, Niamey, Tamanrasset and Aoulef respectively. The dotted region is the area where θ_w exceeds mid-tropospheric θ_s minimum, a source region for convectively unstable air capable of providing necessary updraughts for Cb convection. The observed precipitation is plotted below the cross-section. The mean ITD position for the month is indicated by an arrow (↑).

[illegible] have been observed to reach the tropopause level, sometimes up to [illegible]km.

The precipitation resulting from the observed thermodynamic structure of the atmosphere is expected to be centred on the predominant [illegible] region of updraught air (dotted). To verify the validity of this hypothesis, the precipitation observed across the zone in July 1958 has been plotted below the thermodynamic cross-section. It can be noted that a striking agreement is established. This indicates that thermal instability generated in the Monsoon air centred over the Niamey area is responsible for the convection and hence, precipitation observed in the region. The cool, though moist, air over Lagos area (experiencing the cooling effect of upwelling of cold water at the Guinea coast which is not influenced by the cold Benguella current) and the hot, dry Saharan air over Aoulef area are rather stably stratified and do not support convection.

It is worthy of note that the observed area of strong convection was some 6-10° South of the surface position of the ITD for this month.

c) The Thermodynamic structure of the Atmosphere at the height of the Sahel precipitation

The month of August witnesses the maximum Northernly penetration of the ITD into the hinterland. Consequently, the South Westerly (Monsoon) air stream penetrates into much of the Sahel region, giving the region its maximum precipitation for the season. It is worthy of note that relative to the July situation there has been a wider area coverage of high lower level θ_w (of 23°C) - figure 3.3. Also, the minimum mid-tropospheric θ_w value has increased from 15°C at 700mb (over Niamey) in July to 18.2°C during this month. About 1°C rise in θ_w has occurred in the North Easterly air stream over Aoulef also.

On the other hand, there has been less than a degree (0.2 - 0.5°C) rise in θ_s in most of the troposphere. Hence, the stability of the troposphere has not changed much between July and August. The mid-tropospheric saturation potential temperature, θ_s is about 21.5°C (500mb).

Hence, compared with the July situation, there is a wider zone (9.5 - 18.5)°N over which the low level averaged θ_w value (over the bottom kilometre or two) exceeds the mid-tropospheric θ_s minimum value. This increased source region of updraught air spells an increased area of deep cb convection activity. Consequently, a broad region of high precipitation is expected. The observed monthly total precipitation distribution plotted below the thermodynamic structure cross-section agrees well with the thermally induced convective activity region. Between 9.6°N and 17.6°N, precipitation observed is $R \geqslant 10$cm. This region is 4-12° south of the ITD position for the month.

A difference of -1.5°C between θ_w at the surface lower layer and θ_s minimum at the mid-troposphere over the Lagos area indicates the stability of the atmosphere, prolonging the LDS effect which started in July.

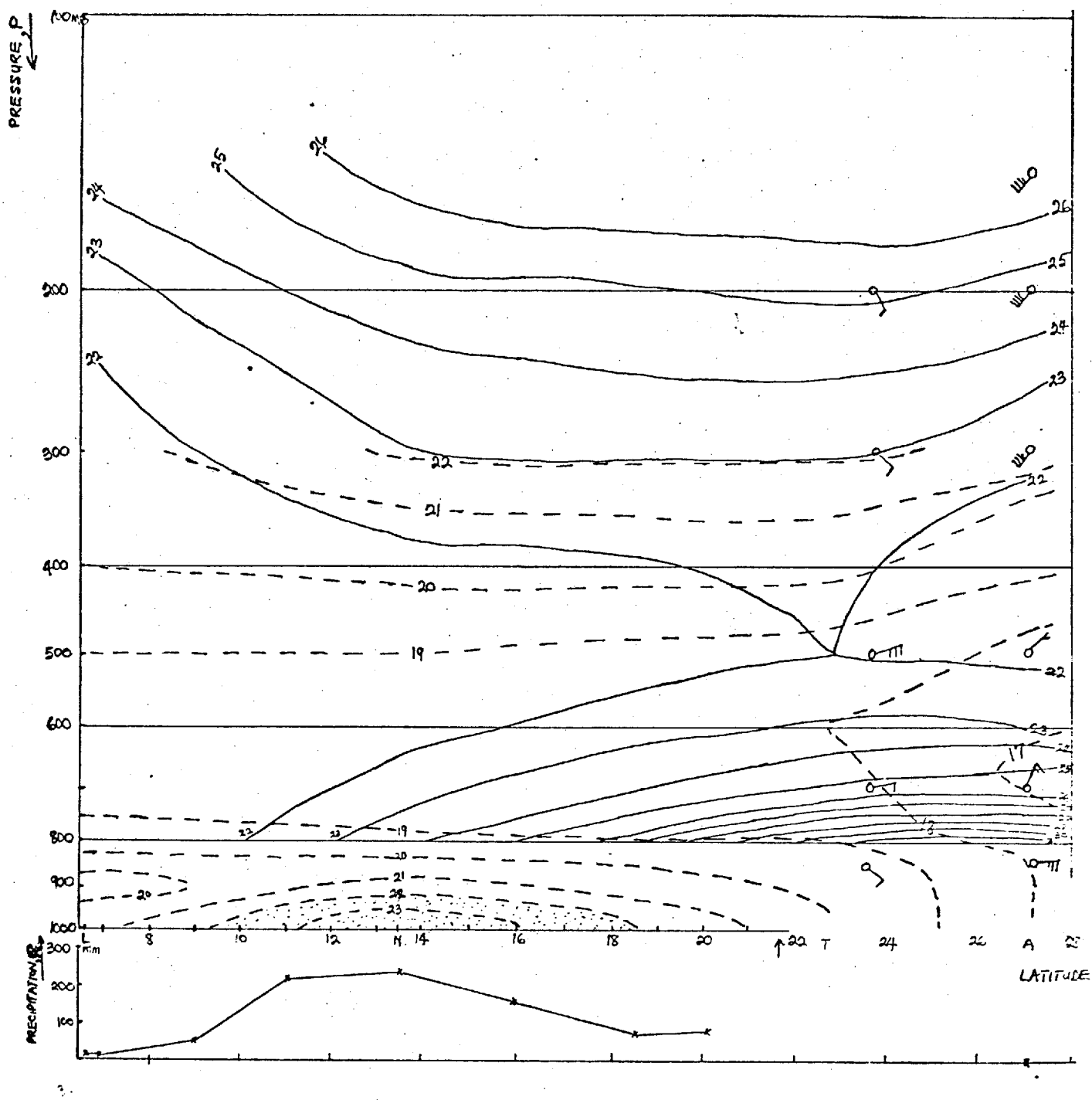

Fig. 3.3

Same as in fig. (3.2) but for August, 1958.

d) Atmospheric structure during the retreating ITD Season

The month of September witnesses the retreat of the ITD Southwards from its most Northernly position and the commencement of a gradual fall in the Sahel region's precipitation.

As shown in fig. 3.4 there has been a general tropospheric θ_s cooling of about 1°C, θ_s = 21°C over the region. This cooling increases to about 2°C at lower levels particularly near the Sahara (Aoulef) environ.

As shown by the θ_w isopleths, a θ_w decrease of about 1°C exists at 700mb over the Sahel region. About a 1°C θ_w increase can be noted over the Lagos area, indicating a cessation of the LDS effect. A noteworthy 2°C increase in θ_w to 25°C over Niamey spells an increased moistening of the Sahel atmosphere in this month relative to the August situation.

This thermodynamic structure suggests the occurrence of considerable convective activity right from the Lagos environ, 6.6°N to the Sahel outskirt, 20°N. High precipitation is, therefore, expected over the region. As indicated by the plot of observed precipitation, the convectively unstable region has some precipitation recorded but the region of maximum precipitation does not match the theoretical spot of maximum thermal instability. This might be due to several factors:

a) The amount of precipitable water in the atmospheric column over Niamey may not be as high as that observed further South where, with the considerable warming of the Gulf of Guinea water, increased moisture flux is now evidenced over the Lagos area.

b) Dynamical mechanisms necessary to cause convective overturning might have moved further South in intensity with the Southward retreat of the ITD. Squall lines produce the necessary wind shear to effect convective over-turning and are important in this respect.

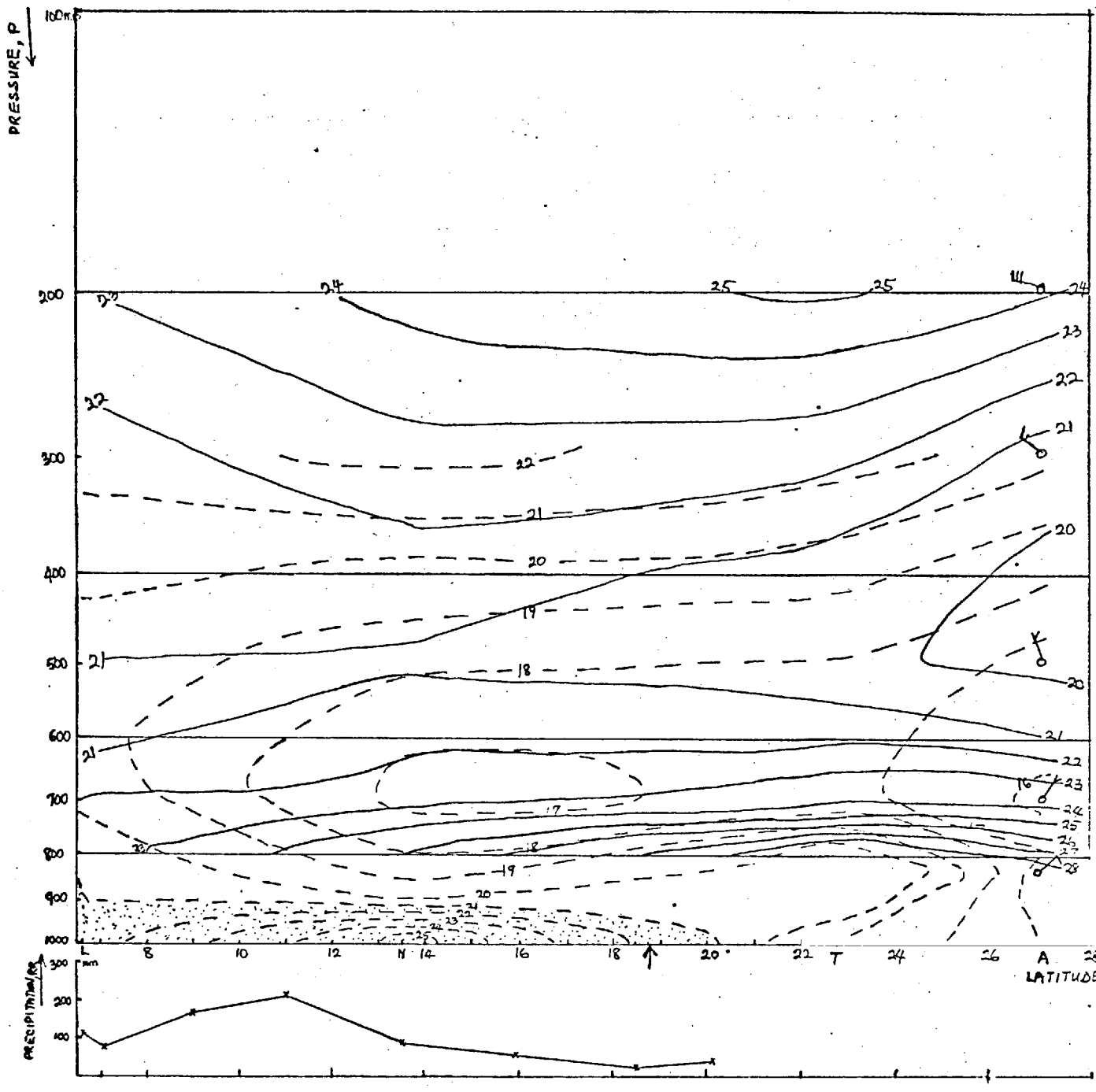

Fig. 3.4

Same as in fig (3.2) but for September, 1958.

We shall consider the precipitable water distribution below, while the role of dynamical mechanisms would be further treated in the next chapter.

3.(iv) THE AMOUNT OF PRECIPITABLE WATER IN A VERTICAL COLUMN OF AIR

In an air column of depth dZ, and unit ($1cm^2$) cross-sectional area, the volume of liquid water equivalent is given by:

$$dW = r\rho dz \qquad \ldots\ \ldots\ \ldots\ 3.11$$

Where r = mixing ratio averaged over the layer.

Using the hydrostatic equation,

$$dp = -\rho g dz \qquad \ldots\ \ldots\ \ldots\ 3.12$$

$$dW = -\frac{r\rho dp}{\rho g} = -\frac{r dp}{g} \qquad \ldots\ \ldots\ \ldots\ 3.13$$

Integrating equation 3.13 from surface (pressure P_s) to any level p,

$$\int_{p_s}^{p} dW = -\int_{p_s}^{p} \frac{r}{g} dp$$

$$W = \frac{1}{g}\int_{p}^{p_s} r dp \qquad \ldots\ \ldots\ \ldots\ 3.14$$

(assuming that g does not vary (much) with p)

Hence, the depth of precipitable water available in a given layer is proportional to the average mixing ratio in the layer.

Obasi (1964) used this procedure to estimate the precipitable water over Ikeja for 1958-1960.

Realistically, W can be effectively estimated for the surface to the 300mb level. Above the 300mb level, dew point or relative humidity values cease to be reliable as the accuracy of radiosonde measurements are questionable aove this level.

For typical Summer tropical conditions, the mixing ratio is about 0.4g/kg at the 300mb level: negligibly small.

Hence,

$$W = \frac{1}{g}\int_{p_s}^{300mb} r\,dp \qquad .. \quad .. \quad .. \quad 3.15$$

It is thought that for an accurate estimation of r, equation 3.15 should be integrated over many pressure layers i.e. the greater the number of pressure layers chosen between the surface and the 300mb level, the greater the accuracy in the estimation of W. e.g. for September 1958, W over Ikeja/Lagos was estimated using monthly mean soundings and was averaged over every 50mb depth thus:

$$W = \frac{1}{g}\left[\int_{1000mb}^{950mb} r\,dp + \int_{950mb}^{900mb} r\,dp + \int_{900mb}^{850mb} r\,dp + \cdots + \int_{350mb}^{300mb} r\,dp\right]$$

$$= 4.85\,cm.$$

However, this value is slightly lower than that obtained by Obasi (1964) for the same month. (W = 4.97cm). Also, a reference to the observed profiles of r obtained over Niamey, as a typical example shows that it is reasonable and in accordance with significant data points to integrate W between 1000 - 850, 850 - 700, 700 - 500 and 500 - 300 mb - figure 3.5. W above, can then be re-estimated as

$$W = \frac{1}{g}\left[\int_{1000mb}^{850mb} r\,dp + \int_{850mb}^{700mb} r\,dp + \int_{700mb}^{500mb} r\,dp + \int_{500mb}^{300mb} r\,dp\right]$$

.. .. .. 3.16

= 4.97cm, agreeing perfectly with Obasi's result.
(2% above the former estimate.)

Fig. 3.5 Profiles of θ, θ_w, θ_s and r Over Niamey Sept. 1958

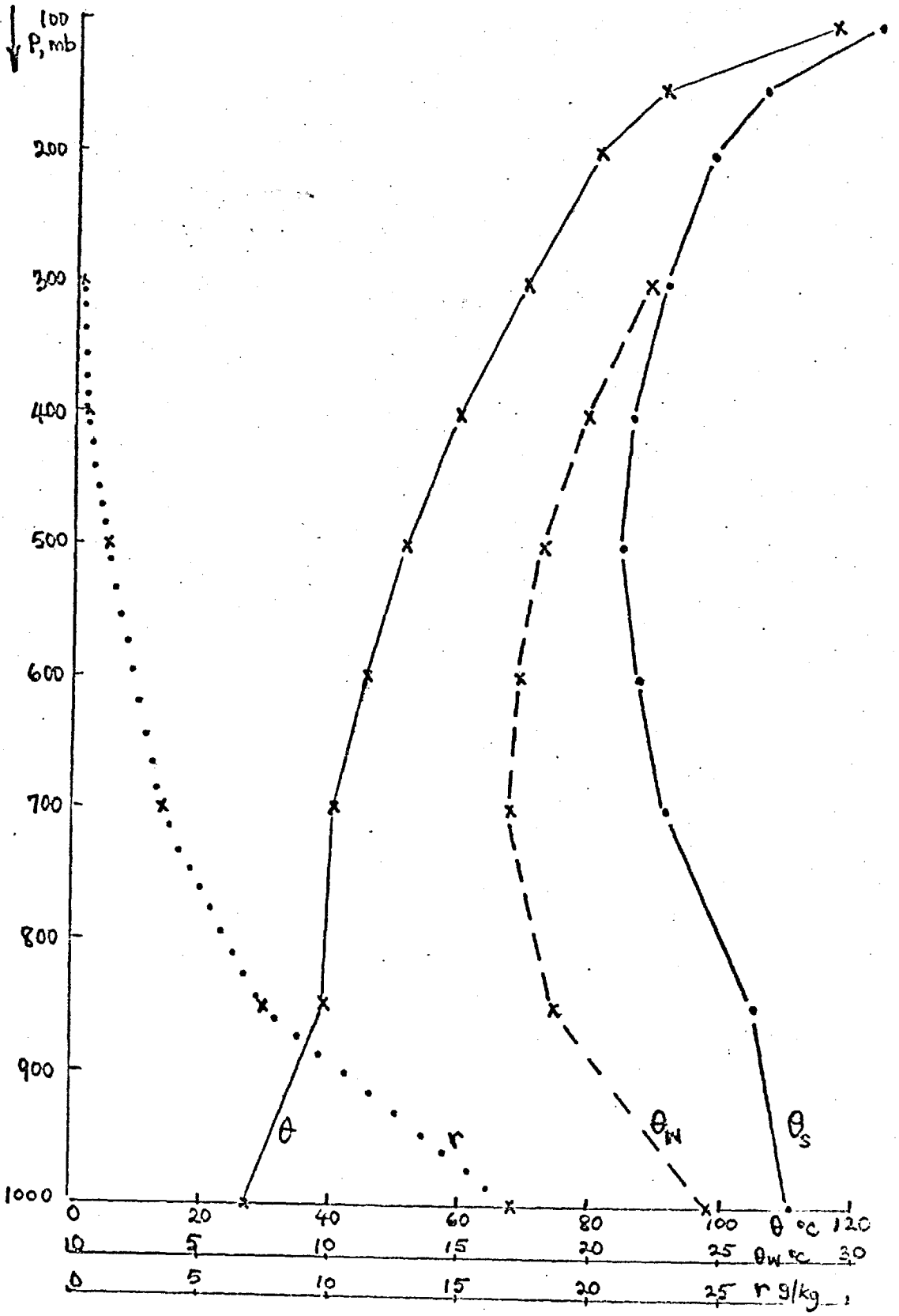

The method in 3.16 was then applied in estimating W.

a) August and September Precitable Water Compared

Fig 3.6 shows a plot of the precipitable water observed over the four operative upper air stations in the Zone 2 of the region, for August 1958. It can be observed that:

a) a good agreement exists between the observed precipitation (plotted below) and the total precipitable water.

b) The Niamey and Lagos W values are approximately equal though Lagos experienced a little precipitation, owing to the LDS effect.

c) As should be expected, the observed precipitable water was much less than the observed precipitation. The difference is made for by the evaporation, E:

$$R - E \approx \frac{1}{g}\int_{p_s}^{300\,mb} r\,dp$$

where R is the observed precipitation.

The results of W computed for September, 1958 indicated a much lower value of W over Niamey than in Lagos/Ikeja, figure 3.7. The precipitation maximum hence consistently shifted towards the direction of increasing W. This accounts for the situation depicted in fig.3.4.

3(v) PREFERRED SEASON OF STRONG CONVECTIVE ACTIVITY

i) Problems in Cross-sectional (latitude-height) Aerological Analyses

The analyses of the last section has been somewhat affected by problems resulting from:

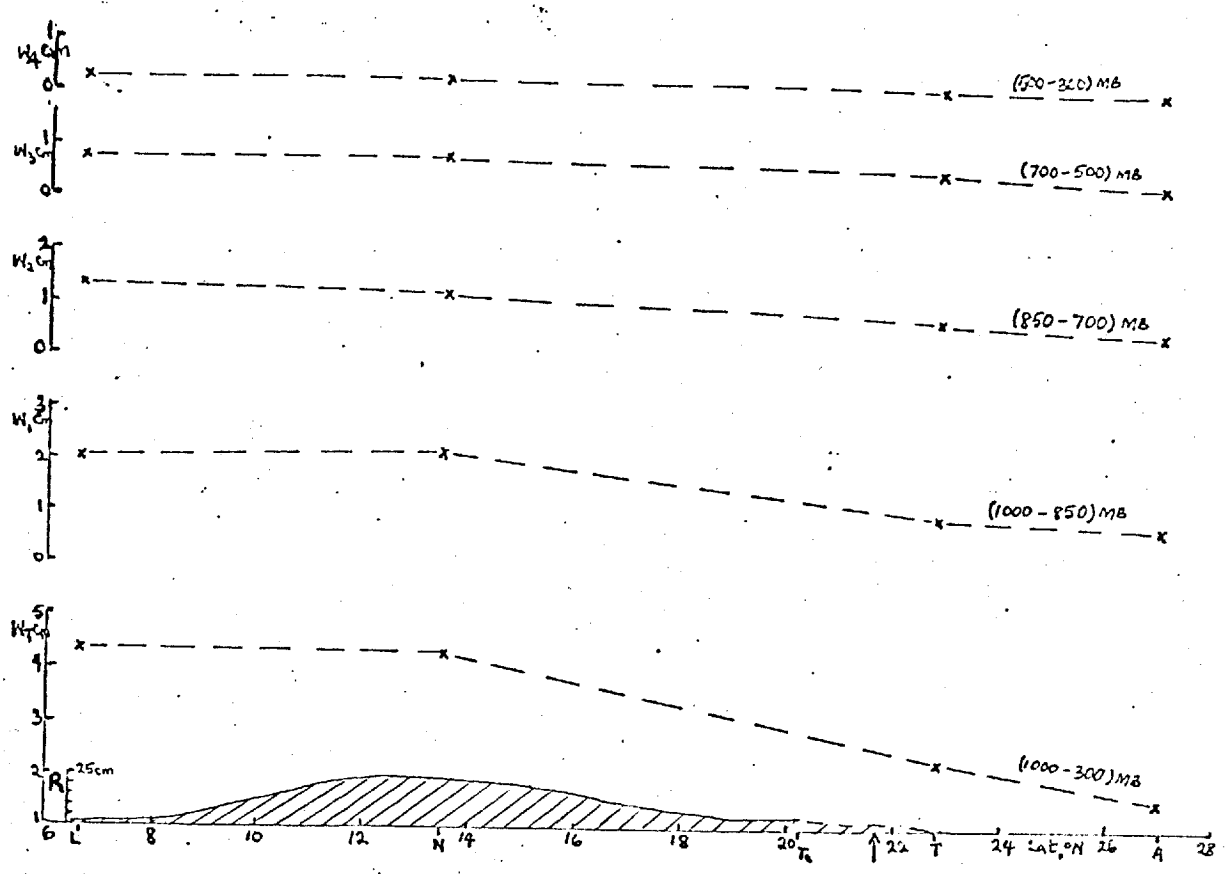

Fig. 3.6

Precipitable water W_1, W_2 ---W_4(cm) obtained over four layers of the atmosphere as specified, for Zone 2, August 1958. W_T is the total value for the atmospheric column and R(cm) is the observed precipitation (hatched).

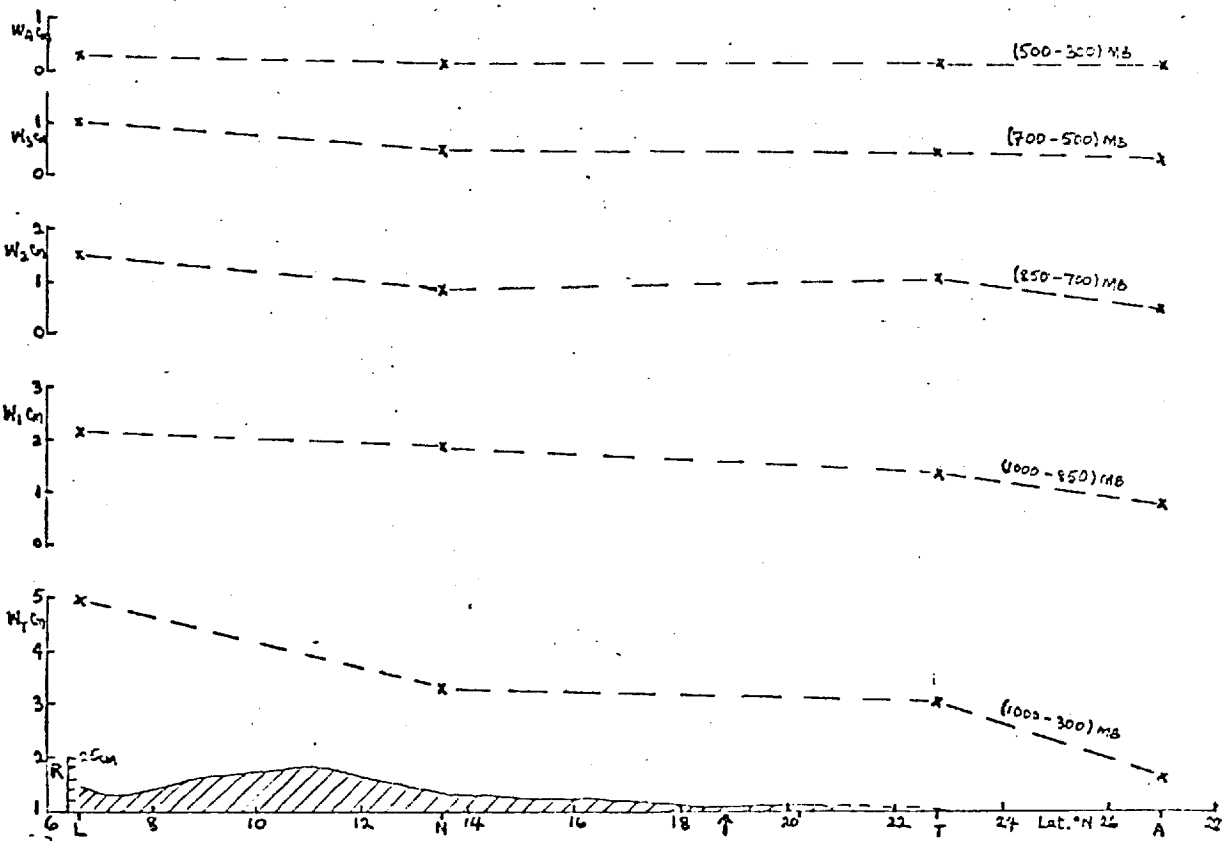

Fig. 3.7

Same as in fig. 3.6 but for September, 1958.

a) Paucity of operating Radiosonde stations

Not all the rawinsonde and radio sonde stations situated in the region operate or are very active. The scanty turn out of data during the famous IGY intensive observation period is a manifestation of this. This hinders effective cross-sectional analysis. The ITD thermal structure could not, for instance, be well portrayed by the latitude-height cross-sections as would a stationary pressure-time analysis (cf Section 3.v(iii) below).

b) Absence of Wind reports:

Many of the few stations that reported radiosonde soundings left out the winds. Pilot balloon observations were often terminated at the lower troposphere $\sim$ 3-4 km in most of the stations considered.

c) Non-synchronization of the observing times:

The daily observations published in 1958 indicated that while some stations made radiosonde soundings at 06 GCT (Greenwich Civil Time) e.g. Lagos/Ikeja and Niamey - at the onset of convection - others (e.g. Aoulef) launched their radiosondes at 11 GCT - at the time of strong convective activity.

These stations only reported their upper atmosphere observations once daily, making the tracking of atmospheric disturbances like squall lines (see Chapter IV) difficult.

d) Surface (screen level) data

For the particular time of making upper troposphere rawinsonde soundings, surface (screen level) data were sometimes missing in some stations although the 12 GCT surface observations might be recorded.

Suggestions for improvement

1. For effective acquisition, processing, dissemination and archiving of the meteorological data observed over the mainly

Francophone and Anglophone countries of West Africa, an adequte regional data management system should be developed to co-ordinate the input of the various national networks.

2. The present rawinsonde and radiosonde stations need be activated and more ones set up to give a closer data coverage. In particular, fixed sea stations are needed for the Gulf of Guinea and possibly the zone of the Scale B array of GATE (see GATE report 7). In addition to aiding the study of air-sea interactions, this will lead to a better understanding of the thermodynamic structure of the semi-continental as compared with the continental Inter-tropical Discontinuity (ITD) over the land (Chapter IV) and the Inter-tropical convergence zone over the sea.

3. A proper observation net-work, yielding a continuous data coverage, would highlight various meso-scale and organized systems of the tropics and benefit agricultural concerns as far as precipitation distribution and frequency are concerned.

This, more than a once-in-a-blue-moon IGY or GATE-type experimental expeditions, encouraging as these are, would enhance the long-term understanding of the Tropical atmosphere and its ways.

To this end, the Meteorological concerns in the region need to utilize the tremendous information collection available from meteorological satellites e.g. Automatic picture transmission (APT) facilities, as in Dakar, for instance. Cloud formations, as well as systems like Easterly Disturbances (organized cloud systems) and squall lines can be tracked across parts of the region with the aid of the daily satellite pictures resulting from these.

ii) Prospect for Isentropic Analysis?

Although the dry bulb potential temperature, θ is not as conserved in atmospheric processes as θ_e , Equivalent potential temperature and θ_w , wet bulb potential temperature, more often than not, atmospheric surfaces tend to be dry adiabatic, giving rise to a greater uniformity in θ surfaces than in those of other thermodynamic properties. This fact has prompted aerological analyses carried out at constant θ

surface, styled, "isentropic analysis" right from about fifty years ago (Sir Napier Shaw, 1926, Rossby 1937 etc) mainly in Mid-latitude and high latitude regions.

A direct indication of vertical motion and of the processes at work in the atmosphere is easily portrayed by an isentropic map. This gives it an advantage over isobaric maps. Observations of the flow relative to a large-scale motion system can usefully be analysed on isentropic charts: an important tool in the study of large scale (slope) convection (Green, Ludlan and McIlveen, 1965).

For the West African region under study, a cross-section of isopleths of θ has been plotted (for the longitude of Lagos) for the month of maximum rain in the Sahel (August, 1958) (figure 3.8). It can be gathered that a dry adiabatic region (with θ constant with height from surface up to 700mb occurred over and around Tamanrasset and Aoulef. This may be due to dry convection.

To the South of this region, a quasi-baroclinic zone can be seen over the Niamey area. This depicts the temperature contrast between the potentially hot Saharan region, $\theta \sim 43^{\circ}C$ and the cooler Southern (Lagos) area, $\theta \sim 21^{\circ}C$. The cooling in Lagos area is due to the upwelling of cold water at the Guinea coast, a cause of the LDS experienced by the area at this time of year. From the thermal wind relation, this temperature contrast determines the easterly flow above the region (aloft) and the consequential frequency of Easterly disturbances arriving at the region as shown more fully in Chapter IV.

However, apart from the surface-to-700mb region, not much can be made of the near isobaric variation in θ portrayed in figure 3.8 . This characteristic is an indication of the little or no prospect that can attend any isentropic analysis carried out in this predominantly barotropic region. This view is buttressed by the results of the earlier efforts made by Carlson (1965) who included much of W. Africa in his isentropic analyses of the NH.

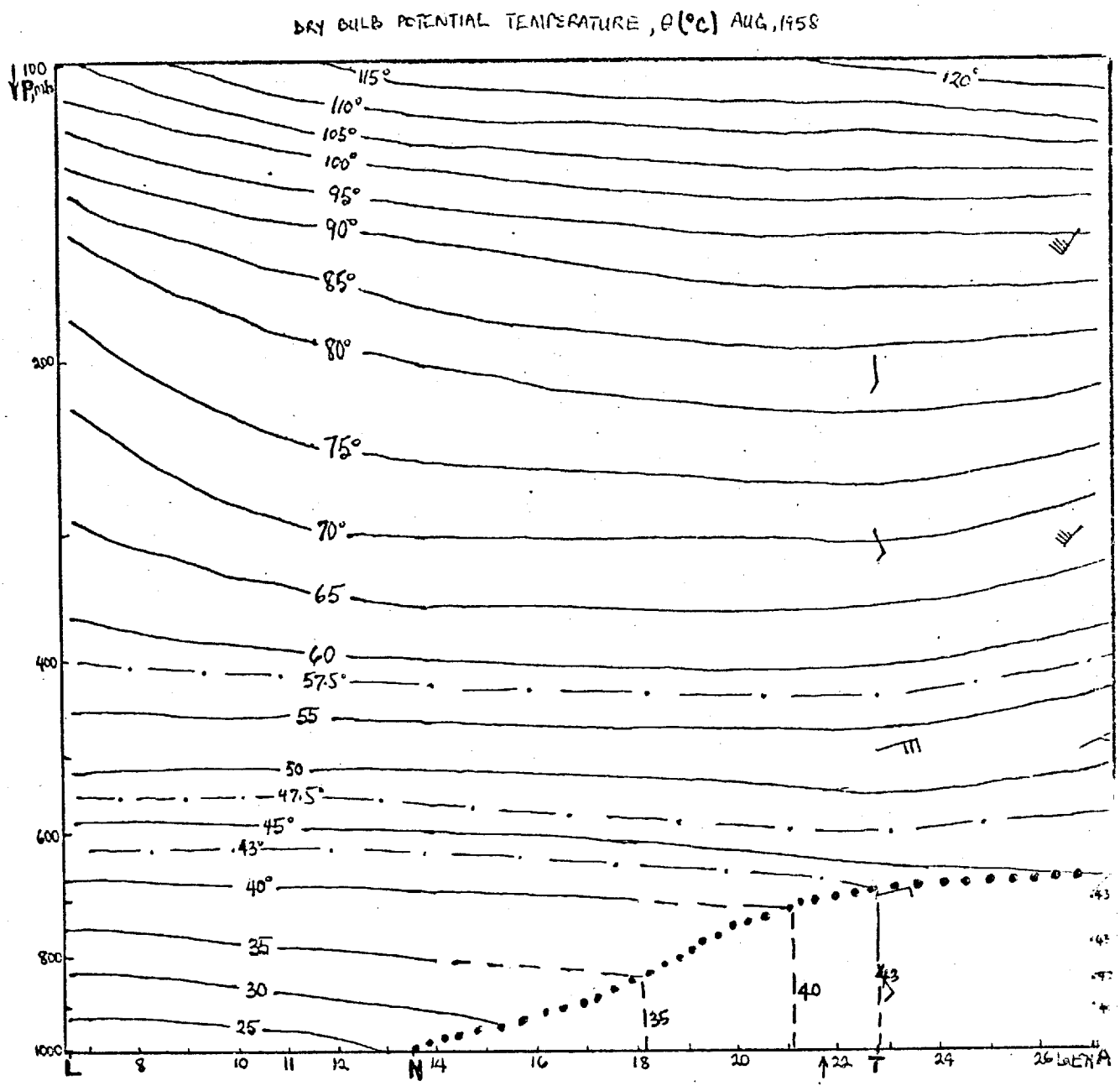

Fig. 3.8

The latitude-height (in p coords) cross-section of θ for August 1958. Dry convection is evident over Tamanrasset and Aoulef environ as shown by the deep dry adiabatic layer (DAL) running from the surface to between 700 and 675mb (marked out with dots). Notice the decline in the depth of this DAL as dry convection gives way to moist convection further south of the ITD (Niamey area) where owing to the presence of some baroclinicity, squall activities are enhanced.

iii) Stationary θ , θ_w and θ_s Cross-Sections for Niamey

A local (Stationary) analysis of the atmospheric theormodynamic structure over Niamey for the IGY period, July 1957 to December 1958, was carried out to indicate:-

1) the stratification associated with the ITD, and

2) the typical atmospheric state that prevails during the Sahel precipitation period and why this season is the preferred period of convective activities.

This stationary analysis has the advantage of being able to portray the features the latitude-time cross-sections could not show properly owing to the sparseness of observation involved in the latter whose analysis rests mainly on four upper air stations across the region.

Fig. 3.9a is a height (in pressure co-ordinates) - time cross-section of the dry bulb potential temperature, θ (^{o}C) and the Wet bulb potential temperature, θ_w (^{o}C). It is worthy of note that as the ITD passes over Niamey between October and November on its Southward journey, it brings with it relative low tropospheric warming with $\theta \gtrsim 30^{o}C$ at bottom kilometre of the surface. The moist monsoon air typified by high $\theta_w \geq 20^{o}C$ below 800mb level which had been over the Station since the Summer (at least July-October shown) is now replaced by the potentially warmer but drier 'harmattan' air ($\theta_w \leq 18^{o}C$) The dry 'harmattan' air occupies the area till April when the ITD moves over the station again on its Northward track and the (SW'ly) Monsoon air with $\theta_w \geq 20^{o}C$ moves in again.

θ_w minimum level is a good indication of the likely top of Cu convective clouds. The Monsoon period is marked by a much higher level of minimum θ_w than the 'harmattan' period indicating that Cu clouds deepen considerably during the former than the latter.

Moreover, the θ_s cross-section (fig.3.9b) shows that high low-level saturation potential temperature ($\theta_s \sim 34^{o}C$ in April) accompany the

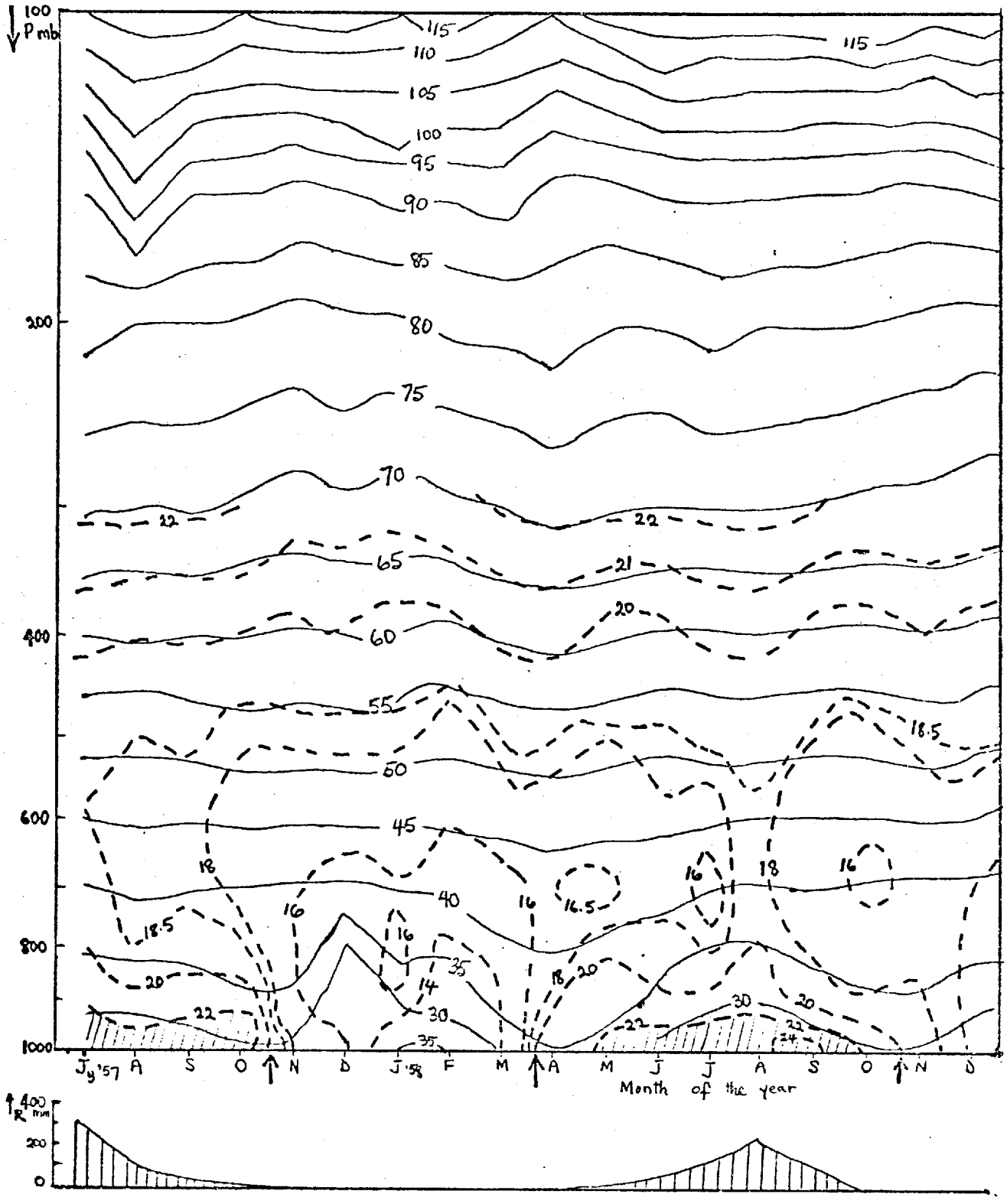

Fig. 3.9a

A stationary (vertical-time) cross section of the atmosphere over Niamey for the IGY (July 1958 - December 1958). θ_w isopleths ($^{\circ}C$) are shown (pecked) and θ ($^{\circ}C$)(solid). The area with low-level $\theta_w \geq$ mid-tropospheric θ_s minimum (fig.3.9b) are shown with diagonal hatching. R(mm) shows the observed precipitation(shown with vertical hatching) below. Notice that R > 0 for $\theta_w \geq 20^{\circ}C$ near the surface.

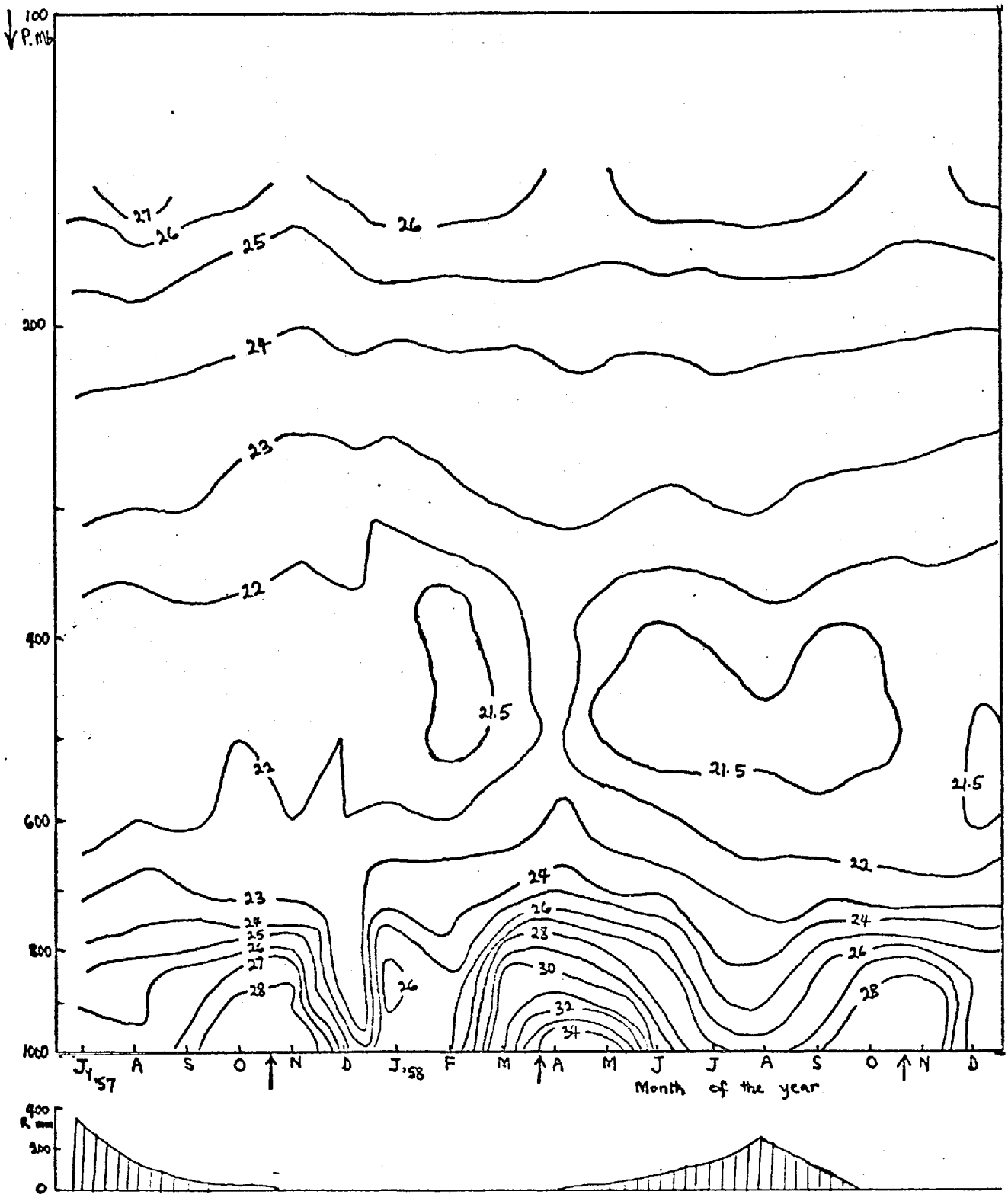

Fig. 3.9b

Same as in 3.9a but for θ_s (°C) isopleths only. This environment is typified by mid-tropospheric cooling between (550-400)mb, a mechanism responsible for its conditionally unstable nature. Notice that $R > 0$ for relatively low surface θ_s values.

ITD, constituting a high potential resistance to the ascent of the potentially warm air advected to the area at the advent of the ITD.

However, as thermal instability is determined mainly by the difference between the averaged θ_w at the bottom kilometre or two of the surface and the mid-tropospheric θ_s minimum, attention shall be focussed on the latter. The 400-500mb layer is marked by considerable tropospheric cooling; the θ_s minimum being between 21.5 - 22°C. Hence, a season of considerable thermal instability shall be that over which low-level averaged $\theta_w \geq 22°C$.

This condition earmarks the Monsoon period, following the passage over the station, from South to North, of the ITD as the season of high thermal (Convective) Instability, and, consequently, high parcel ascent, giving rise to strong Cb cloud updraughts. The atmosphere is convectively stable during the 'harmattan' period as low-level θ_w average is less than 21.5°C, the observed Mid-tropospheric θ_s minimum.

The observed precipitation, plotted below the cross-sections, agree to the fact that the season of rain is that when the condition for thermal instability is satisfied. The precipitation, R, is predominantly greater than zero when θ_w (at bottom kilo-metre of the surface) is $\geq 20°C$. This also corresponds to low-level $\theta_s \leq 27°C$. (except during Dec. '57 - Feb. 1958 when though θ_s was low, thermal instability condition did not hold).

Hence, convective instability and Cu/Cb cloud development takes place in the moist, though cooler Monsoon air while large scale descent of air in the sub-tropical anticyclone characterises the 'harmattan' period between the ITD passage Northward and Southward again, over the region. Maximum precipitation is observed in August, four months after the ITD has passed over Niamey from South to North.

(iv) THE ASSOCIATED PRECIPITABLE WATER

Using the method already discussed in (3.iv), we worked out the amount of precipitable water contained within the atmosphere (essentially between the surface and the 300mb level) as shown in table (3.1) below for four convenient levels of the atmosphere see fig. (3.10).

It can be noticed that:-

1. The precipitable water, W(cm) was maximum at the lower level of the atmosphere and decreases progressively upwards.

2. Very high values of precipitable water were obtained for the months of May to September, the rainy season and, consistent with expectation, maximum precipitable water occurred in August, the month of maximum precipitation, maximum θ_w and maximum Northward ITD penetration.

Also, it is reasonable to expect that at every time of the year, some precipitable water, however small, exists in the atmosphere but no rain falls unless this precipitable water, $W \geq$ 3cm.

TABLE 3.1

PRECIPITABLE WATER OVER NIAMEY, JAN-DEC, 1958 COMPARED WITH THE OBSERVED PRECIPITATION.

MONTHS	PRECIPITATABLE WATER, W (cm)					Observed Precipitation R (cm)	Excess W_T-R (cm)
	Level 1 (1000-850)mb	Level 2 (850-700(mb	Level 3 (700-500)mb	Level 4 (500-300)mb	Total W (10000-300)mb		
JAN.	0.8	0.6	0.3	0.1	1.7	0	1.7
FEB.	0.4	0.3	0.2	0.1	1.0	0	1.0
MARCH	0.6	0.3	0.3	0.2	1.3	0	1.3
APRIL	1.2	0.5	0.3	0.1	2.2	T	2.2
MAY	1.7	0.9	0.3	0.1	3.0	1.2	1.8
JUNE	1.8	0.9	0.5	0.2	3.4	7.7	-4.3
JULY	2.0	0.8	0.3	0.2	3.3	10.8	-7.5
AUG.	2.2	1.2	0.7	0.2	4.3	24.3	-20.0
SEPT	1.9	0.8	0.5	0.1	3.3	8.3	-5.0
OCT.	1.4	0.6	0.3	0.1	2.4	T	2.4
NOV.	1.3	0.8	0.5	0.1	2.7	0	2.6
DEC.	0.7	0.4	0.4	0.1	1.7	T	1.6

PRECIPITABLE WATER OVER NIAMEY . 1958

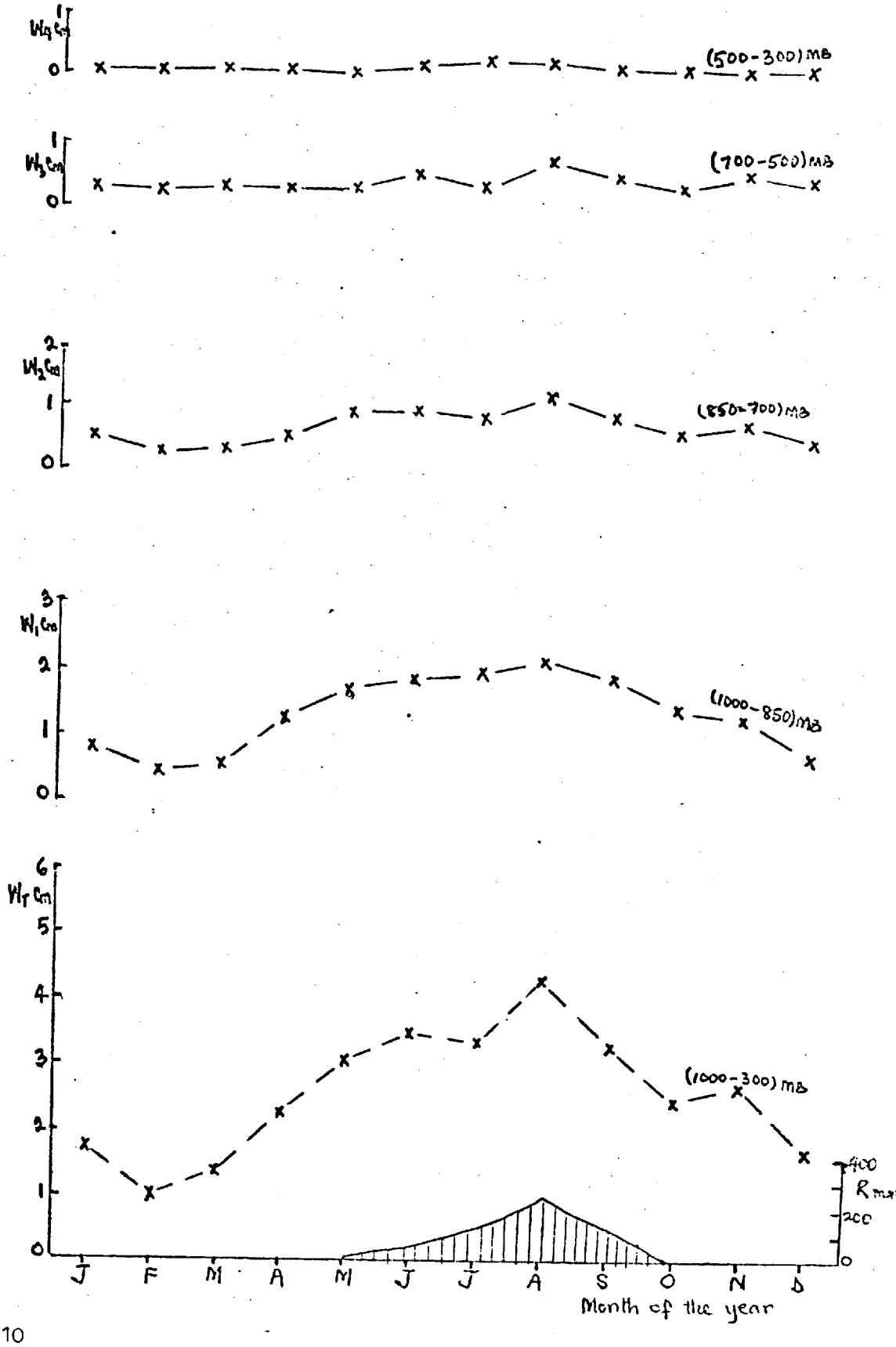

Fig. 3.10

The precipitable water W(cm) present in the atmospheric column over Niamey, January - December, 1958. A good correlation exists between the total precipitable water, W_T and the observed precipitation R(mm) (hatched) below. For R> O, $W_T \geq$ 3cm.

3.(vi) THE THERMODYNAMIC STRUCTURE OF THE ATMOSPHERE IN THE DRY YEAR, 1970

The atmospheric thermodynamic structure for Niamey during the dry year, 1970, has been investigated through Pressure-time cross-sectional analyses of θ , θ_s and θ_w as shown below [figs (3.11, 3.12 and 3.13)].

Certain features worthy of note in the analyses are:-

1. The atmosphere was potentially cooler during the months of June to September at lower levels with $\theta \sim 30^{\circ}C$, about $5^{\circ}C$ cooler than much of the earlier months of the year [fig (3.11)].

   Compared with the situation in the wet year (1958) (fig.(3.9a) the troposphere, even up to the stratosphere, has warmed up by $\sim 5^{\circ}C$. However, the thermal structure of the atmosphere in the two years did not change much.

2. In its advent to the region around May, the ITD effected a considerable warming of the lower troposphere: $\theta \sim 35^{\circ}C$, but unlike in the wet year when the atmosphere cooled down by a few degrees after passage of the ITD, the warming continued until June with $\theta \sim 35^{\circ}C$. May and June were cooler in the Wet year than in the dry case.

3. The θ_s minimum of $22^{\circ}C$ occurred between 600-500mb in June-July and September-October 1970 (fig.3.12a). Apart from these, mid-tropospheric θ_s values were $\sim 22.2^{\circ}C$. Relative to the wet year, there was an increase of between 0.5 to $1^{\circ}C$ in the θ_s warming of the mid-tropospheric environment and of between $1\text{-}4^{\circ}C$ at lower levels - (fig. 3.12b). Unlike in the wet year when, from April to October, Mid-tropospheric (500mb) cooling of the environment (a necessary requirement for tropical convection, Betts 1973) took place, a lesser degree and shorter period of cooling characterized the dry year (θ_s min· June-July and September to Octoher only). From this observation, the drought experienced in the area could be termed a warm , rather than a cool, drought.

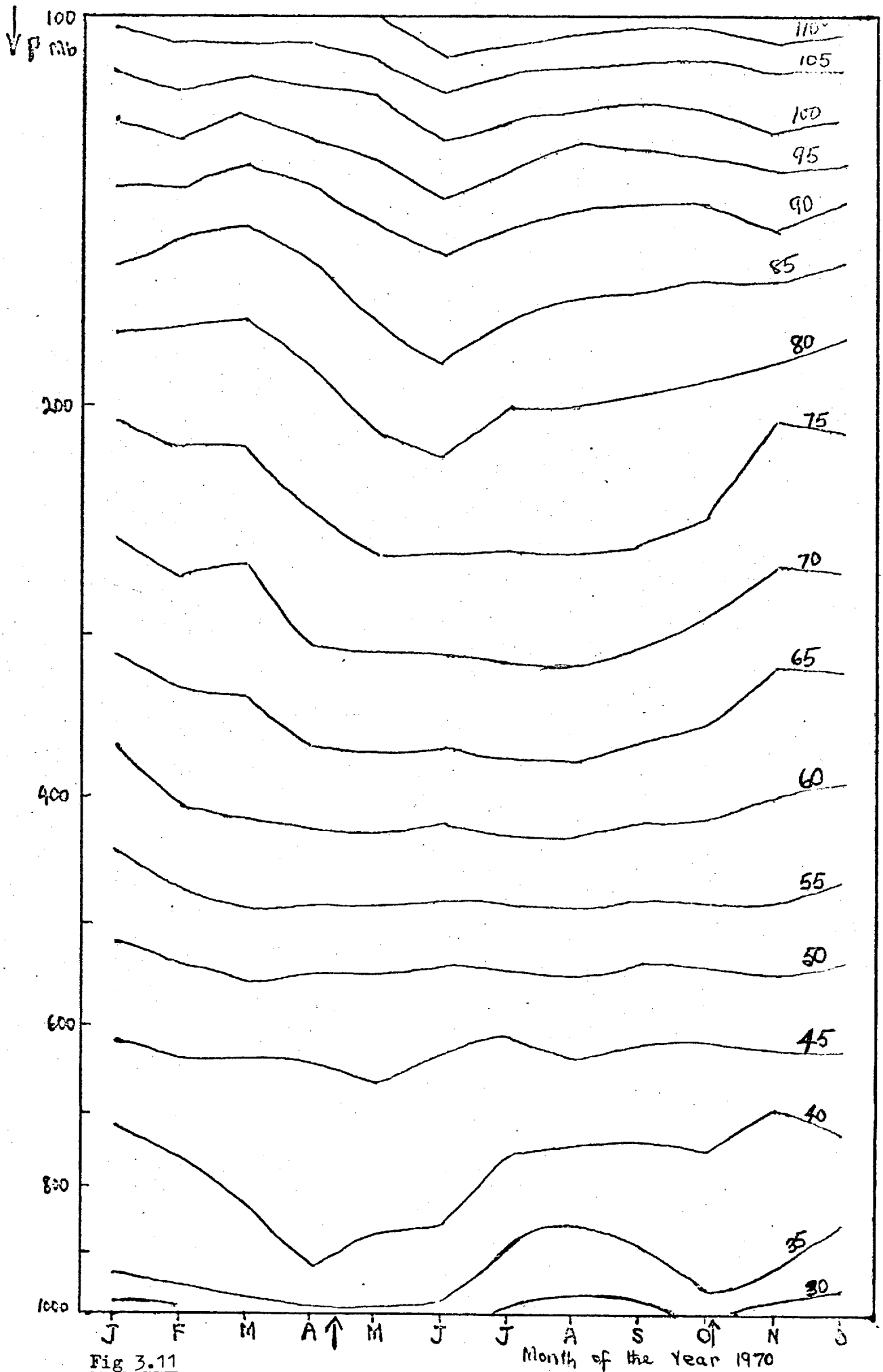

Fig 3.11

A stationary (vertical-time) cross-section of θ over Niamey for January-December of the dry year, 1970. Compared with the isopleths in fig 3.9a, the atmosphere, in the dry year was much warmer (by about $5^{o}C$) than in the wet. It is remarkable to note that potentially warmer air typify the ITD environ.

SATURATION POTENTIAL TEMPERATURE, θ_s (°C)
NIAMEY, 1970

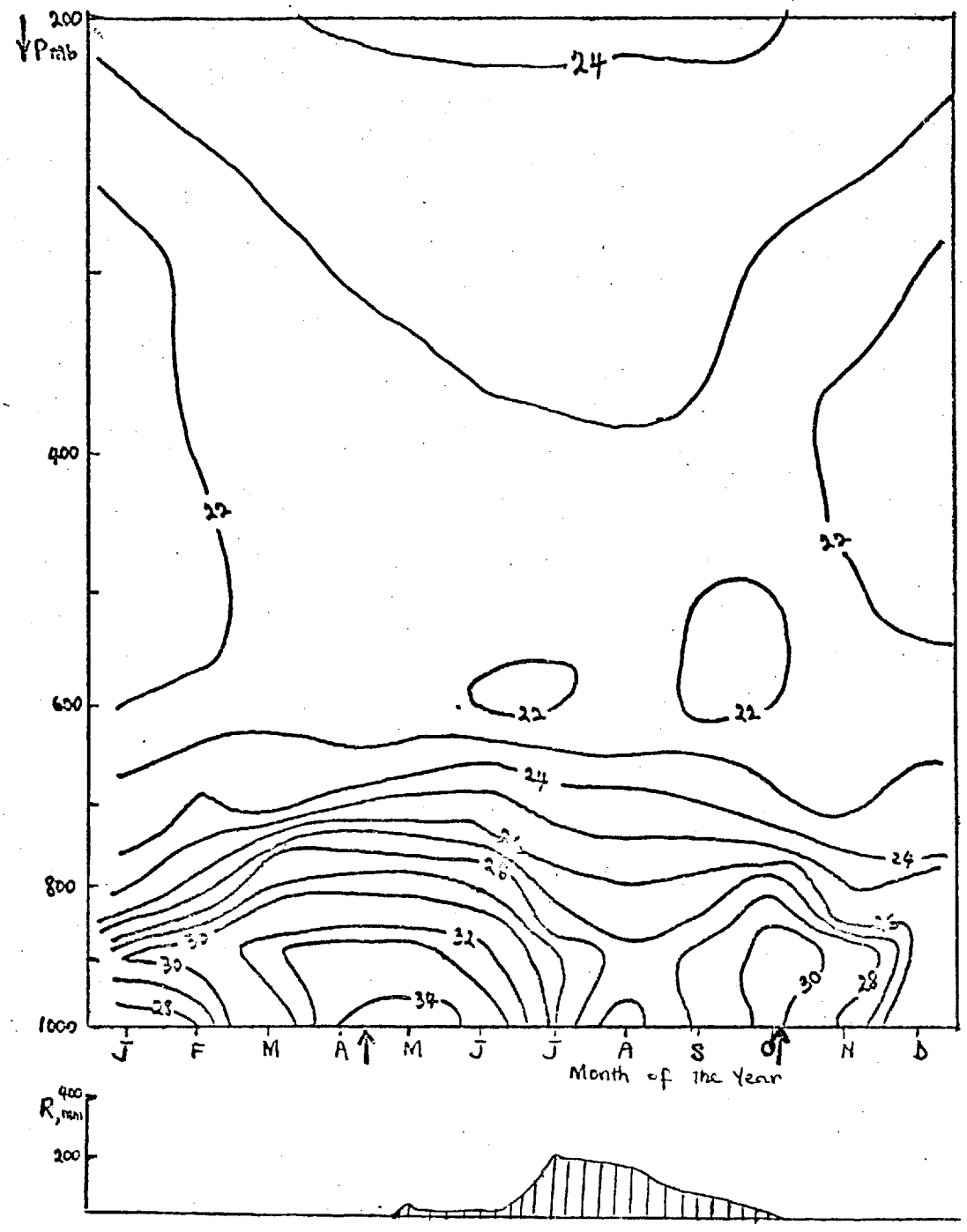

Fig 3.12a

Same as for fig. 3.11 but for θ_s (°C) only. Most of the precipitation observed occurred under low surface θ_s .

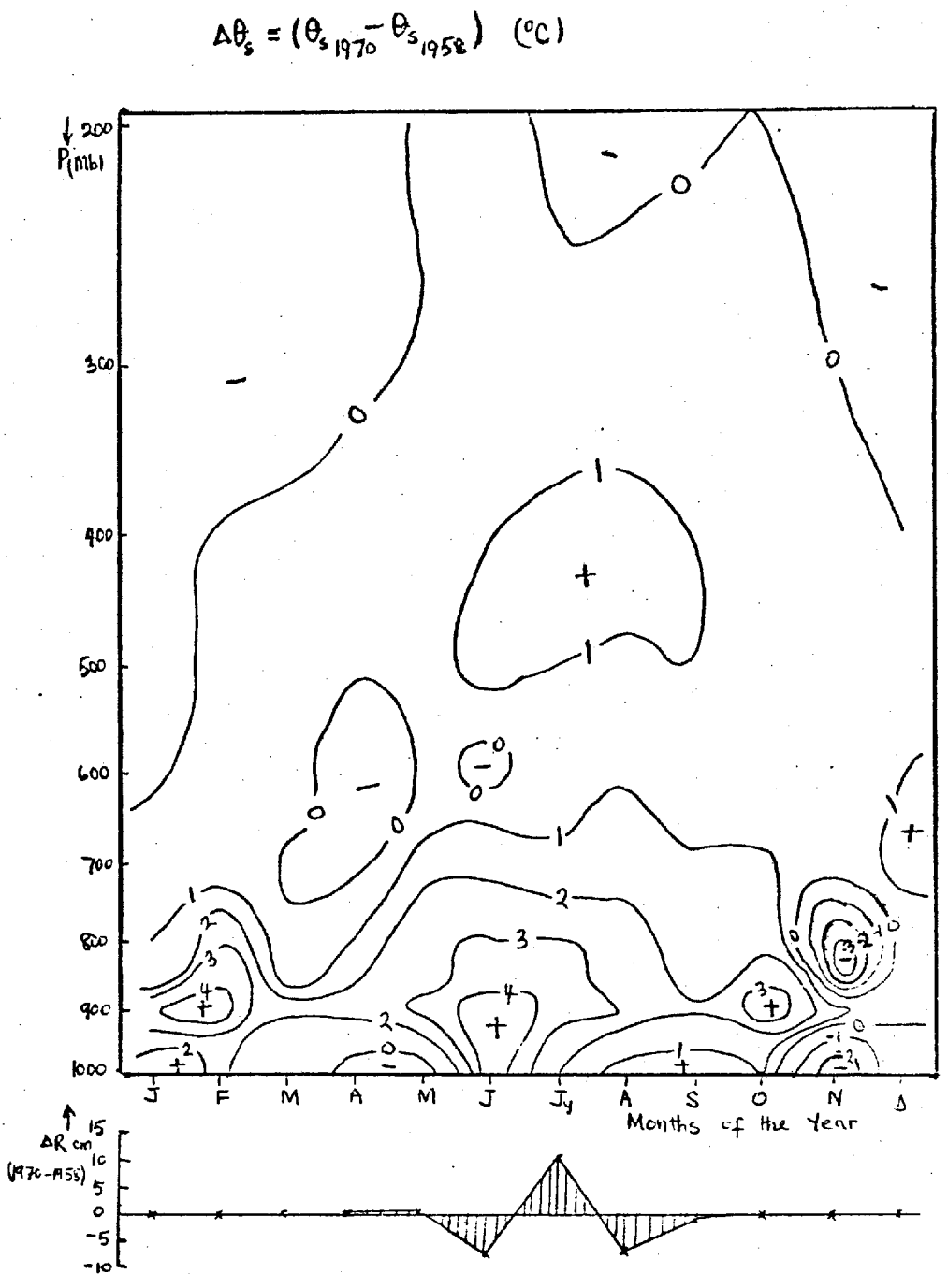

Fig. 3.12b

The stability of the Niamey atmosphere in 1970 relative to the 1958 case as indicated by $\Delta\theta_s$ (1970-1958) °C. A general θ_s 'warming' of the atmosphere has taken place.

The precipitation deficit, plotted below, indicates that the effect, on the precipitation of high positive $\Delta\theta_s$ (+4°C) at the lower levels outweights the effect of the smaller $\Delta\theta_s$ (+1) and the mid-troposphere.

Change in humidity element between 1958 and 1970

4. Regarding availability of moisture, abnormally high mixing ratios were depicted in the observations and as $\theta_w = f(\bar{T}, \bar{T}_d)$, θ_w was unrealistically high for the dry year. On inquiry from Mr C Hawson of the British Meteorological office, (private communication) it was gathered that the French radiosonde humidity element was changed sometime between the late 1950's and early 1970's. Hence, the 1970 humidity measurement, and, hence, θ_w, would not compare effectively with the 1958 one. The said change was later confirmed by the French Meteorological office, Paris.

A further note on this type of change is that as was reported to have happened some years ago in Norway and Portugal the instrument manufacturers may not notify the Meteorological office authorities of any such change. Only scientific investigation of this nature usually brings the change to light ie as one compares various years' measurements.

On account of this, the θ_w distribution of fig (3.13) should be considered on its own merit rather than compared numerically with the wet year situation. Similarly, as shown in the precipitable water estimation below (3.vi), the two years' precipitable water cannot be compared. The current of the NE'lies, typified by θ_w between 15-19°C could be seen over the region (occupying from surface to 600mb) from January to April when this current is replaced by the Monsoon current (typified by $\theta_w \sim$ 20-24°C) between late April and October.

The Monsoon moist current was replaced again by the drier NE'ly current after October. The level of minimum θ_w (20°C) took place between August and October at the 700mb level as well.

The layer over which convection occurrs is typified by $\frac{\partial \theta}{\partial z} < 0$ and

WET BULB POTENTIAL TEMPERATURE, θ_w
NIAMEY, 1970

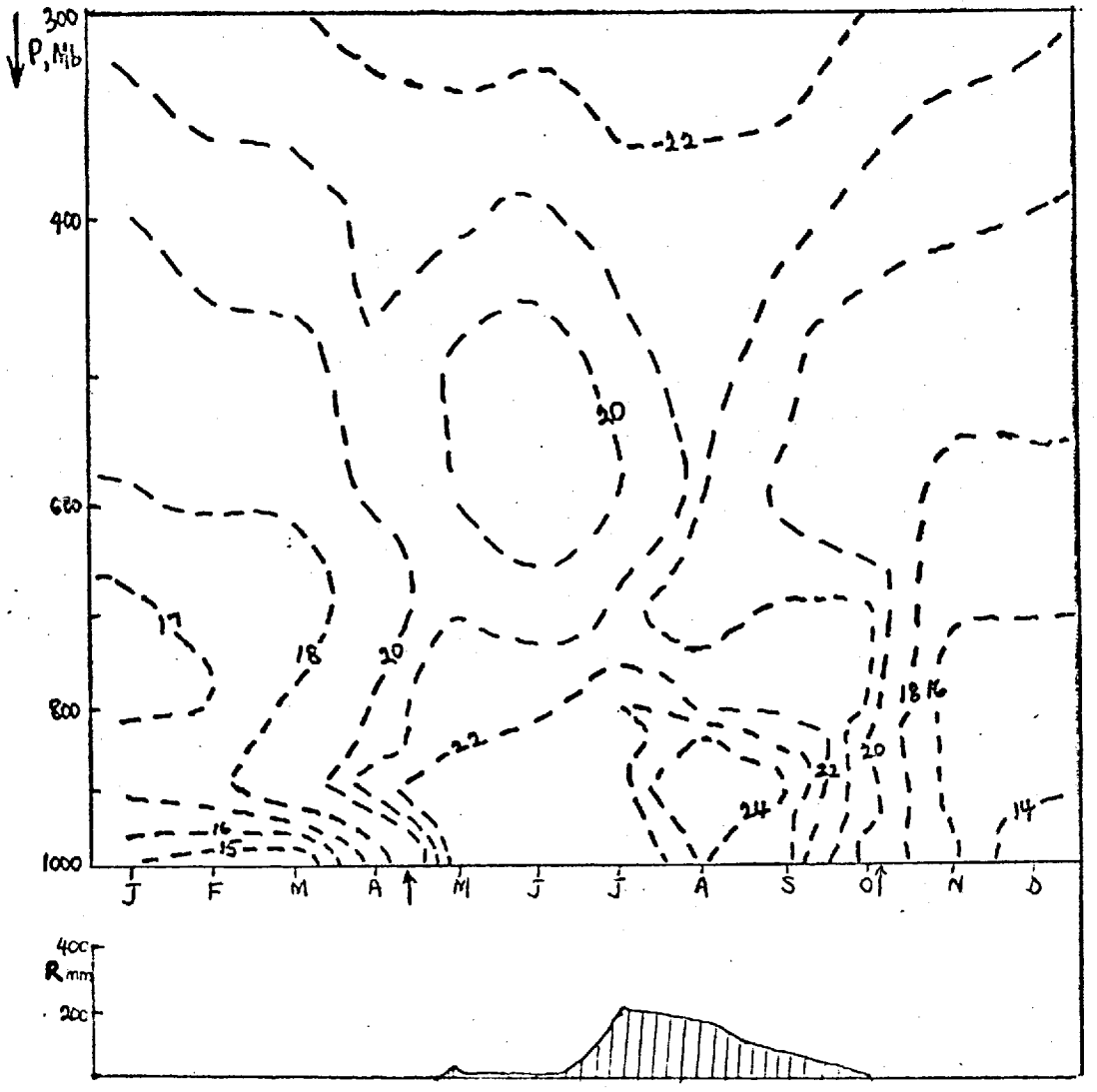

Fig. 3.13

The vertical-time cross-section of θ_w (°C) over Niamey for January - December 1970. Having been measured with a different humidity element, these isopleths should not be compared numerically with the equivalent values for 1958. The deep dry mid-tropospheric (θ_w minimum) layer centred on June is associated with a failure in June precipitation for this year.

the tops of the convective systems are marked by the minimum θ_s . This is, hence, an indication of the depth of penetration of the convection in the atmosphere.

5. The precipitation observed (plotted below the thermodynamic cross-sections) (fig.3.13) show that:

a) As in the wet year, the 1970 rains started in May over Niamey but failed in June. Over the (650-450)mb level a minimum exists in θ_w in the month of June. This marks the presence of dry air acting as a 'lid' to convection. Although a minimum in θ_w exists at about 700mb level in Mid-April, July and October of the wet year, the wet year June was free from such a barrier to the growth of convective systems.

b) The maximum precipitation of 210mm (for 1970) occurred in July instead of August, the usual month of maximum precipitation, maximum ITD Northerly penetration into West Africa and maximum low-level θ_w . August had only 167mm of rain indicating a relatively drier situation than in the wet year. This may be due to the existence of a θ_w minimum ($\sim$ 21°C) at 700mb in the dry year as compared to the wet year when no θ_w minimum exists below 550mb.

Hence, while shallow systems like Cu typify the dry year, strong cb cloud activity was thermodynamically permitted in the wet year.

c) Unlike in the wet year, the ITD arrived at the region later and it returned Southwards just a little earlier than normal. If it is realized that the period between the Northward and Southward passage of the ITD over a station defines the period over which precipitation is allowed, the implication of this will become obvious. Serving as the meteorological Equator, the ITD advects low-tropospheric heating and hence, plays a role in setting the large scale temperature constrast between the hot North (Sahel/Saharan region) and the cooler South (Guinea

region). As shall be demonstrated more clearly in Chapter IV the higher this temperature contrast, the stronger the baroclinicity of the Sahel region and the stronger the easterly flow aloft (according to the thermal wind relation) and, consequently, the higher the frequency and intensity of the Easterly disturbances bearing cloud clusters moving westwards over the region. The westward propagating squall lines can be similarly affected, culminating in rainy conditions. The converse also holds, culminating in drought.

6. PRECIPITABLE WATER

The precipitable water, W, available over Niamey in 1970 has been calculated for each month as shown in fig.(3.14). The values of W so obtained cannot be compared with those of the wet year, 1958, owing to the fact that there has been a change in the humidity element used in-between the two years.

As later explained by the General Director of the French Meteorological Service, R. Mittner (private communication) 'Radiosonde Metox type CT' having, as humidity element, a gold beater's skin 24mm long, 8mm wide, mounted on two supports in plastic material, was used in 1958. However, in January or February of 1970, type FMO 1943 (still being used) was used, having as humidity element, a gold beater's skin, mounted on a revolving drum, whose diameter is 26mm.

The contrast in the calibration of the two radiosondes is more clearly portrayed in fig (3.15) where the total monthly precipitable water, W_T for (May - September) has been plotted aginst the monthly precipitation, R, for the two years.

The shift between the two curves obtained is a measure of the calibration difference between the two humidity elements.

It need be noted, however, that similar W_T variations were experienced in the January - December of the two years (figs. 3.10 and 3.14). The agreement between the variations of W_T and R is striking. However, unlike in the wet year, the 1970 maximum W_T of 5.8cm was in August, although July had the maximum precipitation that year.

PRECIPITABLE WATER OVER NIAMEY 1970

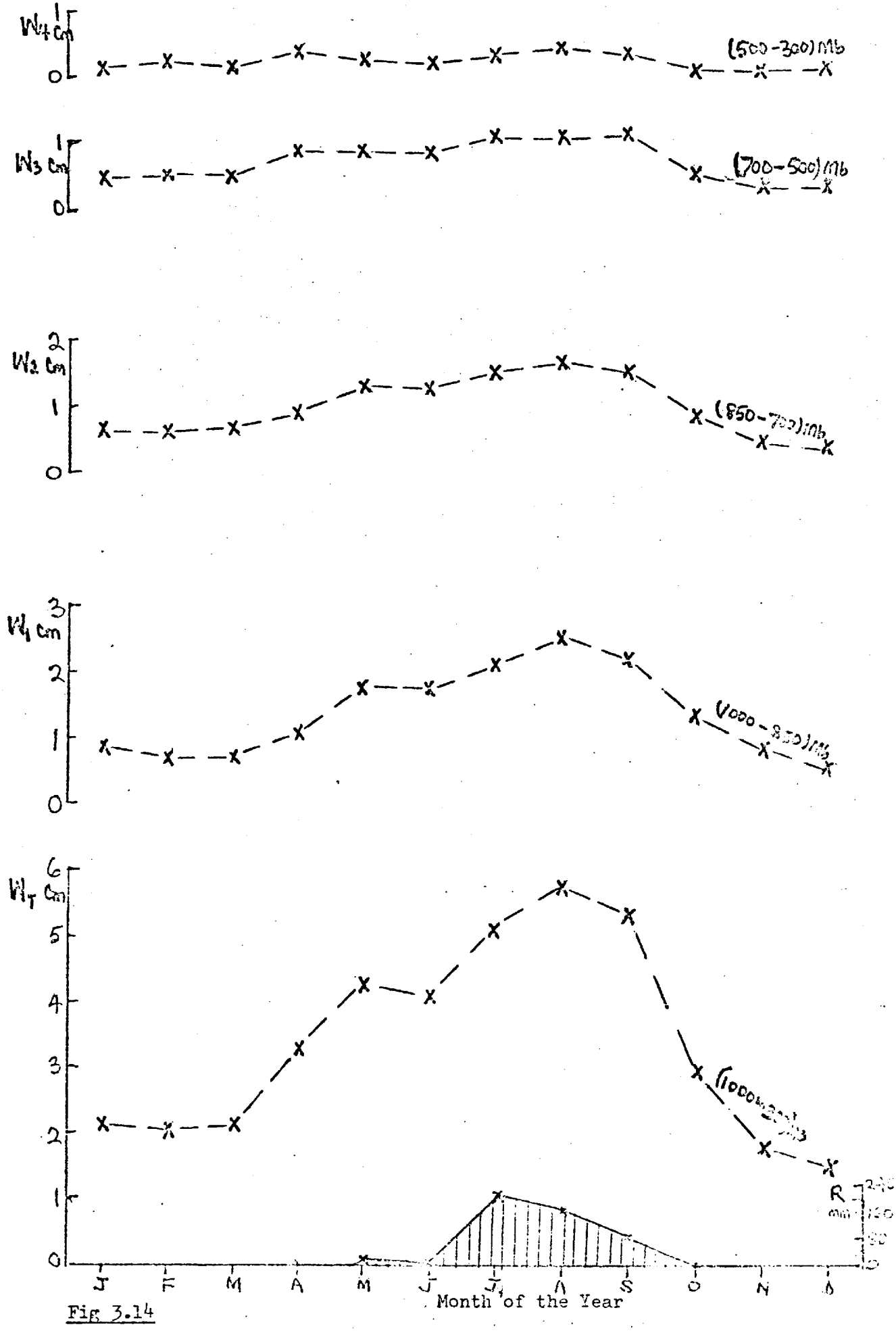

Fig 3.14

The precipitable water obtained over various layers of the atmospheric column, Niamey, 1970.

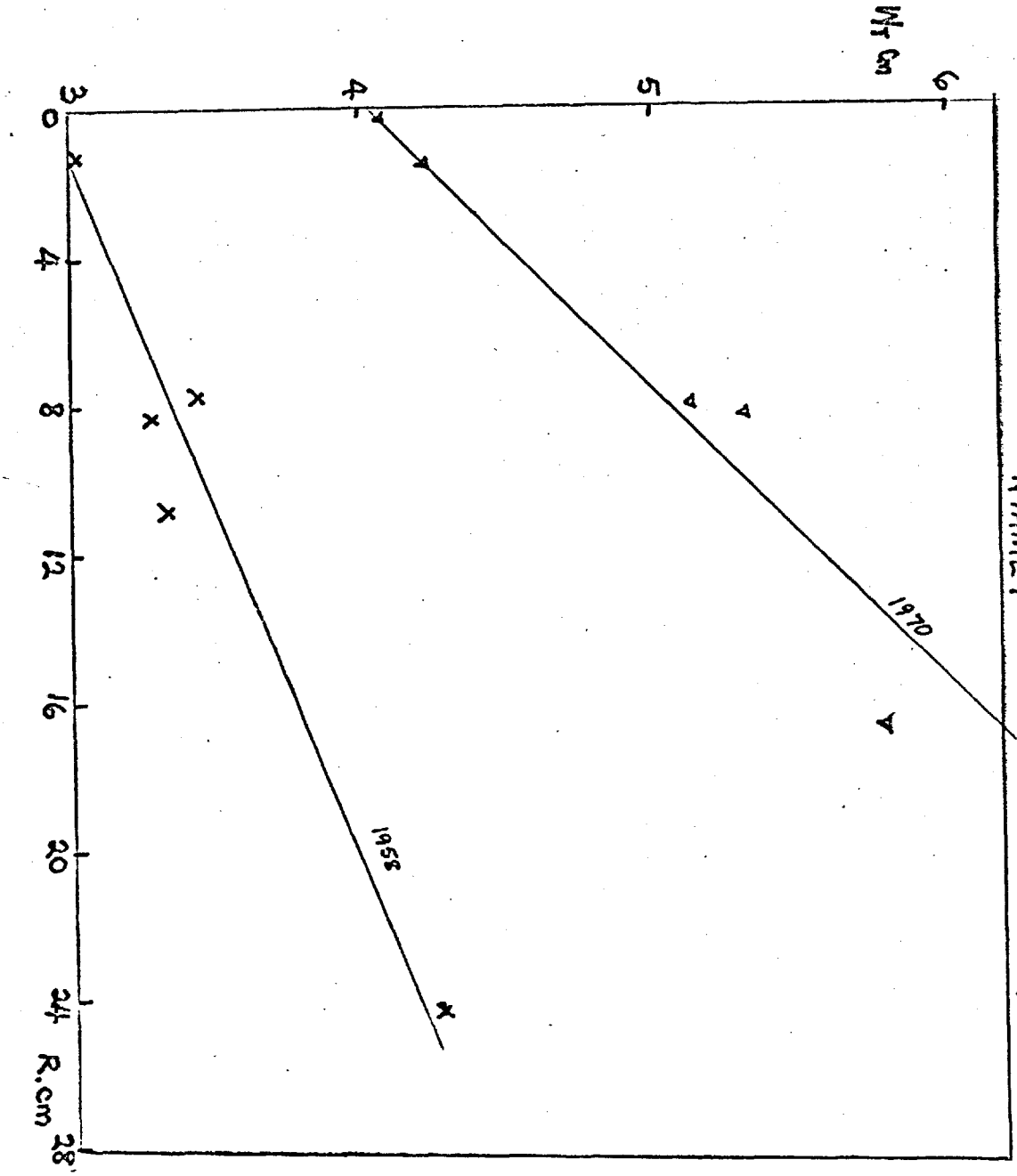

Fig. 3.15

A plot of W_T(cm) against R(cm) for 1958 (the wet) and 1970 (the dry) year respectively, indicating a rough measure of the contrast in the calibration of the two different humidity elements used.

3.(vii). THE HEAT 'BALANCE' EQUATIONS

The heat 'balance' Equation is an expression of the law of conservation of energy. It expresses the flux of heat across the atmosphere/ground interface.

a) The Net Radiation, R_N

at the earth's surface is given by

$$R_N = LE + H + G + P \quad .. \quad .. \quad .. \quad 3.17$$

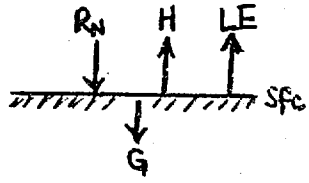

Where LE = Latent heat release
H = Sensible heat
G = Heat flux into the ground
and P = energy involved in processes of photo-synthesis by plants.

P can be neglected over the desert or semi-arid terrain like the Sahel where plant population is very thin.

Equation 3.17 implies that the Net Radiation, R_N (Radiation incident on the surface - effective out-going radiation) is partitioned into sensible and latent heat while the remainder is absorbed by the immediate layer of the soil.

The components of R_N can be expressed as:

$$R_N = \underset{(i)}{R_S\downarrow} - \underset{(ii)}{R_S\uparrow} + \underset{(iii)}{R_L\downarrow} - \underset{(iv)}{R_L\uparrow} \quad .. \quad .. \quad .. \quad 3.18$$

Where

(i) $R_S\downarrow$ is the incoming solar (short wave) radiation of wave length $(0.3\text{-}4)\mu$

$$R_S\downarrow = S(1-a)$$

S being the solar constant $= 1400\ W/m^2$

a is the albedo of the surface and is equal to the fraction of the reflected to the incident radiation.

For deserts, a $\sim$ 0.25 - 0.30.
Part of this radiation is absorbed by Ozone and other gases and atmospheric aerosols.

ii) $R_S\uparrow = aR_S\downarrow$ is the flux of solar radiation reflected back into space by the earth surface and clouds or atmospheric aerosols.

iii) $R_L\downarrow$ is the flux of long wave (Infra red) radiation of wave length 3-100μ , emitted by clouds and atmospheric aerosols which radiate approximately as black bodies in accordance with their emission spectra and rest temperature. Water vapour and CO_2 are prominent contributors to this term near the equator in particular, but in the desert and semi-arid regions, dusts are the main contributors.

iv) $R_L\uparrow = \sigma T_s^4$ where σ = Stefan-Boltzmann's Constant
and T_S = the temperature of the body

= flux of radiation emitted by the earth as a black body.

b) The Bowen Ratio

From the heat budget relationship in Equation 3.17 :

$$R_N - G = LE + H \qquad \text{(neglecting P)}$$

Introducing the Bowen ratio, $\beta = H/LE$, ... 3.19

$$R_N - G = LE(1+\beta)$$

$$\therefore LE = \frac{R_N - G}{1+\beta} \qquad \text{.. ... .. 3.20}$$

β can be obtained from the bulk aerodynamic equations of the surface fluxes of H and LE :

$$H = -\rho C_p K_H \frac{\partial \theta}{\partial z} \quad .. \quad .. \quad .. \quad 3.21$$

$$LE = -L_v \rho K_v \frac{\partial q}{\partial z} \quad .. \quad .. \quad .. \quad 3.22$$

where $K_H = k' u_* z$

and $K_v = k'' u_* z$

are assumed constant (in near neutral conditions) since heat and vapour are transferred by the same process..

Therefore,

$$\beta = H/LE = \frac{C_p}{L_v}\left(\frac{\Delta\theta}{\Delta q}\right)$$

$$= \frac{C_p}{L_v}\frac{(\theta_o - \theta_h)}{(r_o - r_h)} \quad .. \quad .. \quad .. \quad 3.23$$

Where θ_o is the screen level value of potential temperature, θ (as surface value of θ is not available)

θ_h = value of θ at some other level, h

q = specific humidity $\sim r$ = mixing ratio

r_o and r_h are mixing ratio value at screen level and level h

C_p = Specific heat at constant pressure = $1{\cdot}01 \times 10^3 \, J kg^{-1} {}^oK^{-1}$

L_v = Latent heat of vaporisation of water = $2.47 \times 10^6 \, J kg^{-1}$

Normally, these fluxes are measured near the earth's surface ie over a depth of about 10m.

However, as low-level data is hard to come by particularly as radiosonde readings only are available for the required temperature, humidity and wind profiles, this cannot be carried cut.

However, a rough estimate is here, made using the surface to 950mb profile for Niamey, August 1970 (00 GMT).

$$\Delta\theta\ (^{\circ}C)\ (950\,mb - Surface) = 2.9$$
$$\Delta r\ (g/kg) \quad " \quad = -4.6$$
$$\beta = -\frac{C_p}{L_v}\frac{\Delta\theta}{\Delta r}$$
$$= -0.26$$

This low value of β seems consistent with the fact that the flux of sensible heat is low at 00 GMT (midnight). Moreover, the data used is a monthly mean and therefore subject to errors due to effect of precipitation if and when it rains at the time of sounding. In normal cases, flux measurements should be carried out on dry convection days (with no precipitation).

c) Estimation of Latent Energy from observed precipitation

If the observed mean annual precipitation is M cm, energy required to evaporate the water completely is given by

$$LE = ML \qquad .. \quad .. \quad .. \quad 3.24$$

Where L is latent heat of vaporisation = 600 Cal gm^{-2}

Therefore,

$$LE = 600M \text{ cals}$$

The value of LE obtained for some zone 2 stations are as follows: (for 1958 annual precipitation)

	Lagos	Niamey	Kidal	Tessalit
M(cm)	114.6	52.6	1.0	13.3
LE(KCals)	68.8	31.4	0.6	8

The earth intercepts an amount of solar energy equal to $\pi r^2 S$ in unit time.

Where r = radius of the earth. If this energy is uniformly distributed all over the earth, the energy received per unit earea and time is:

$$\frac{\pi r^2 S}{4\pi r^2} = \frac{S}{4}$$

Taking account of the variation in albedo of the various regions, the amount absorbed,

$$= \frac{S(1-a)}{4} \qquad .. \quad .. \quad .. \quad 3.25$$

$$= 263(1-a) \text{ kcal/year}$$

Where a = albedo of the region

The following are typical values of a for various surfaces (derived from values given by Sellers, 1969, Budyko 1956)

Lagos :	0.15
Niamey :	0.25
Kidal :	0.27
Tessalit :	0.30 (desert type)

If the fraction of the energy absorbed (equation 3.25), used to evaporate the annual precipitation is Q , the value of Q for various stations is given by $Q = \frac{4LE}{S(1-a)}$, expressed in % as follows:

	Lagos	Niamey	Kidal	Tessalit
Q(%)	30.8	15.9	0.3	4.4

Hence, all these places and, especially Lagos, Niamey and Tessalit have got excessive energy with which any cloud formed can be easily evaporated. Mixing of dry air into clouds (entrainement) is an important factor to reckon with in this environment.

(d) Equilibrium Temperature, T_e

Assuming that the atmosphere radiates as a black body (since terrestrial radiation takes place in the long wave spectrum of the electromagnetic radiation), its energy flux will be given by Stefan-Boltzmann's law as noted above.

Since for a black body, energy absorbed = energy emitted,

$$\sigma T_e^4 = \frac{S}{4}(1-a)$$

Hence, equilibrium temperature,

$$T_e = \left[\frac{S}{4\sigma}(1-a)\right]^{1/4}, \ ^\circ K \qquad \ldots \ldots \ldots \ 3.26$$

This is found to be 270°K for Lagos and 261°K for Niamey, basing estimates on albedo values assumed.

From (equation 3.26), an increase in the albedo leads to a decrease in T_e, tending to cool the atmosphere. This cooling process gives rise to descent of air as in anti-cyclonic systems, hence, hindering convection and increasing desertification. The desert environment hence, acts as a feed back mechanism, giving rise to more desert. (Charney, 1975).

Apart from this, the large scale cooling of the Saharan region can weaken the temperature contrast existing between the North and South of the West African region. As shall be further considered in Chapter IV, this temperature contrast is crucial for the generation of Easterly waves and disturbances (squall lines, cloud clusters) over the Sahel. A decrease in the number or activities of these waves in Summer can lead to shortage of rains over the region.

Regarding the drought of 1970, here considered, there have been a general warming (rather than cooling) of the Niamey atmosphere compared with the state in the wet year, 1958. However, the said temperature contrast could still have been decreased by increased warming of the Guinea region.

3.(viii) CONCLUSION

Atmospheric thermodynamic considerations indicate that the preferred areas of convective activity are those over which low-level θ_w values exceed the θ_s minimum values aloft. A good agreement exists between the observed precipitation cross-section and the thermodynamically permitted regions of convective instability, in the Monsoon months of July, August and September, 1958, here studied. The region of convective activity and precipitation began about 1 latitude degree South of the ITD (in July) and attained a maximum $5\frac{1}{2}$ degrees South of it. However, in August, while active convection began, some 3 degrees latitude South of the ITD, precipitation commenced at 1 degree South of it as usual, attaining a maximum at about 8 degrees South of the phenomenon. Apparently due to pulses in the retreating ITD, September witnessed the commencement of precipitation and convective instability about $1\frac{1}{2}^{\circ}$N of the ITD, the precipitation maximum occurring 8 degrees South of the ITD.

The prospect of isentropic analysis is found to be rather slim in the region. However, in view of this and the fact of the region's poor data coverage, stationary (local) analysis was used and was found to indicate the stratification of the ITD atmospheric environ rather well.

This stationary analysis depicted the preferred Season of convective instability over Niamey in agreement with observed precipitation cross-sections. Occurring between the ITD Northward and Southward passage over the Station, the said season is marked by $\theta_w \geq 22^{\circ}C$ near the surface (for the IGY Year). No precipitation falls out when the bottom kilometre of the earth's surface is characterized by $\theta_w \leq 20^{\circ}C$.

The level of minimum θ_s indicates the depth of the convective systems at play. This was found to be deepest in August, the month of maximum precipitation in Niamey. It is found that at least up to 3cm precipitable water should be available in the atmosphere before any rain falls.

Considerable mid-tropospheric warming (relative to the wet year) occurred in June to September of the dry year, stabilizing the atmosphere.

In the dry year, 1970, the Monsoon precipitation commenced in May over Niamey as usual (unlike in some other areas indicated in ChapterII). As usual, the South Westerly winds ($\theta_w \sim 20 - 24^{\circ}C$ at the sub-cloud layer) replaced the drier North Easterly trade winds ($\theta_w \sim 15\text{-}19^{\circ}C$). However, the precipitation failed in June, owing to the presence of dry air (possibly advected from the Sahara) acting as a 'lid' to convection at the (650-450)mb level (fig. 3.13). The ITD was later than in the wet year and did not penetrate as far North as it did then.

Abnormally high θ_w values were obtained in the dry year (as compared to the wet) indicating a change in the humidity element used in the two years, a fact later confirmed by the French Meteorological Office Paris (private communication).

Another likely feature of the dry year is a weakening of the temperature contrast between the Sahara and Guinea regions (through an increase in the region's albedo, for instance) giving rise to a weakening of the strength of the Easterly disturbances experienced over the region - a subject to be discussed further in Chapter IV.

CHAPTER IV

SOME ASPECTS OF THE CIRCULATION PATTERNS AFFECTING THE REGION

4.(i) INTRODUCTION

In this Chapter, we shall consider some aspects of the large scale circulation of the tropical atmosphere as they influence the region and its environment.

These circulation patterns vary considerably in scales, ranging from the global scale down to that of the individual cumulus or cummulonimbus systems. Of this complex spectrum of atmospheric processes however, only important large scale features like the Inter-tropical convergence zone (ITCZ), the Walker circulation and the local anticyclonic systems associated with the Inter-tropical discontinuity (ITD) over the region, shall be discussed.

4.(ii) THE INTER-TROPICAL CONVERGENCE ZONE (ITCZ) (GLOBAL SCALE)

Tropical weather, and indeed, climate, is dominated by the disturbances originating at, or associated with, the zone of convergence of the trade winds of both hemispheres, the ITCZ. Known as "the seat of the rising branch of the Hadley cell, the ITCZ has been called various names ranging from 'Equatorial trough', 'Trade Confluence' to Inter-tropical Confluence by various authors (e.g. Riehl, 1954, Palmen et Al, 1969).

However, realistically the phenomenon is 'the statistical result of the passage of the convergent areas of many disturbances along a preferred track, but there is no doubt that the ITCZ can be prominent on daily maps.' (GATE Report No.1, 1972).

a) View from Satellites

Satellite photographs show the ITCZ as a number of cloud clusters separated by relatively clear regions of descending air, since, by continuity principle, the ascent of warm air into the clouds should be compensated by descent of dry air outside the clouds (the cloud environment). Fig (4.1) shows a typical Satellite photograph of the cloud distribution over the Western Hemisphere for September 4, 1974 chosen to illustrate the wave-like disturbances characterising the ITCZ. Various scales of motion are involved in these systems.

Kornfield et Al (1969) for example, presented the computer-produced mosaics of ESSA III and ESSAV satellite photographs which indicated, for the Northern Hemisphere Winter, two prominent strips of clouds:

i) A strip consisting of the confluence of the Northern Hemisphere (NH) trade winds and the Equatorial air, found around 5°N and

ii) a second strip consisting of the confluence of the Southern Hemisphere (SH) trade winds and the Equatorial air, found around 10°S of the geometric Equator.

In the NH Summer (SH Winter) when the Northern strip moves to about 15°N, following the solar cycle (but with about six-week lag), the Southern strip lies around 5°S.

b) Differentiating between the Oceanic and the Continental types

The fore-going applies mainly to the ocean regions where the trade winds of both NH and SH have very similar thermodynamic structures as they are both of maritime origin and equally moist. The seasonal movement of the oceanic ITCZ is not very large ($\sim 10^{\circ}$) as a result of this.

However, over the continents, owing to the considerable differential heating of the land and the sea, a larger seasonal movement of the ITCZ position (often up to 15 latitude degrees) exist. Another important

Fig 4.1

An SMS-1(GATE)4km resolution infra red Satellite photograph of the Western Hemisphere for 14.30GMT, 4 Sept 1974. The ITCZ cloud band (around 7-10°N) stretches from the W.African coast Westwards far into the Atlantic. The bright areas indicate centres of active thunderstorm activities. Though often zonally oriented, the ITCZ sometimes experiences quasi-sinusoidal (wave-like) disturbances as shown between longitudes 30°W to 50°W on this occasion.

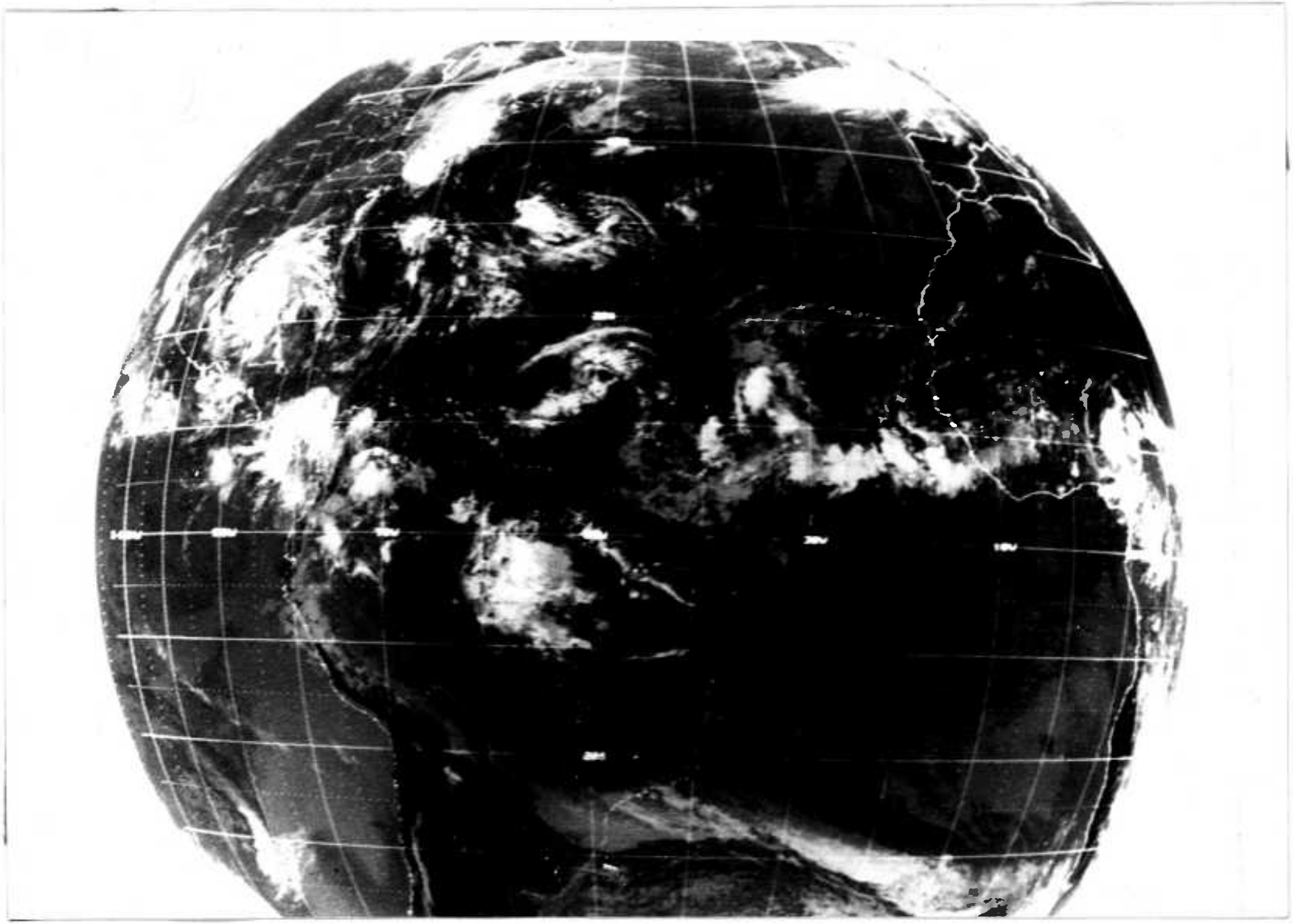

feature differentiating the oceanic from the continental ITCZ is the location of the zone of maximum cloudiness and precipitation. While over the oceans, this zone coincides with the ITCZ surface, maximum precipitation occurs some 7-10 latitude degrees south of the ITCZ surface overland (ChapterII). Fair weather Cu or complete clear sky is often found at the surface ITCZ over land.

These important differences between the oceanic and continental ITCZ patterns have led to the invention of various labels for the continental pattern. This is particularly true of West Africa where several authors have called the phenomenon names ranging from the Inter-tropical front (ITF) or 'Le front Inter-tropical' (FIT) in French to Inter-tropical Discontinuity (ITD). (e.g. Leroux 1971, Ilesanmi, 1971, Johnson, 1965).

And, although the WMO approved of the use of the title 'ITD', several authors, while recognizing that the dynamic properties and thermodynamic constitution of the phenomenon (e.g. as shown in Chapter III) are different from those of Mid-latitude frontal systems, still use the title 'ITF'.

However, as has been done in ChapterII, the title 'ITD' shall be used for this phenomenon over the West African continent.

It is recognised, however, that the ocean/land structural differences notwithstanding, a good continuity in the main ITCZ current exists round the globe.

c) Synoptic features of the ITCZ observed during the IGY

Daily weather charts of the tropical atmosphere have been computed for each day of the IGY by the German Weather Service (Deutscher Wetterdienst,1959). The main zone of tropical surface convergence are indicated on these charts and a comparison of the monthly mean ITCZ latitude obtained from these daily locations agrees remarkably well with similar local observations made by the Nigerian Meteorological service for the same year.

Some remarkable features of the ITCZ as revealed in these charts are worth considering and we shall focus attention on January - December, 1958.

i) The main ITCZ current

The main ITCZ often appears as a single zonal band running right round the globe, often, in places, parallel to the geometrical equator. Beginning from January, typified by fig 4.2a, the ITCZ fluctuates between latitude 2 and 5^{o}N from the longitude of the Americas (not shown) to the African continent, where, around longitude 30^{o}E (Central Africa) it turns sharply Southwards, from 5^{o}N to about 14^{o}S. This marked feature persisted throughout the month. The French Meteorologists call the near-meridional structure resulting from this deflection of the phenomenon, the African Equatorial Discontinuity (AED) e.g. (Dhonneur, 1971).

The AED is formed by air masses of identical characteristics:

a) A north-easterly current from the Indian Ocean and

b) A South-Westerly current from the Atlantic,

each of which has traversed similar distance overland before their meeting.

It is also likely that being a shallow phenomenon, the ITCZ can have been deflected by the East African highlands. East of this longitude, however, the ITCZ still lies South of the geometrical equator at about 10^{o}S, hence, indicating that a larger scale factor may account for this observed behaviour.

Often, shallow depressions develop around the ITCZ. Warm 'lows', stationary eddies, do inter act with it e.g. over Ethiopia area where a low pressure centre observed on the surface is replaced by a 'high' on the 500 mb chart (fig. 4.2a).

Fig 4.2a IGY surface and 500mb weather charts for January 2, 1958.

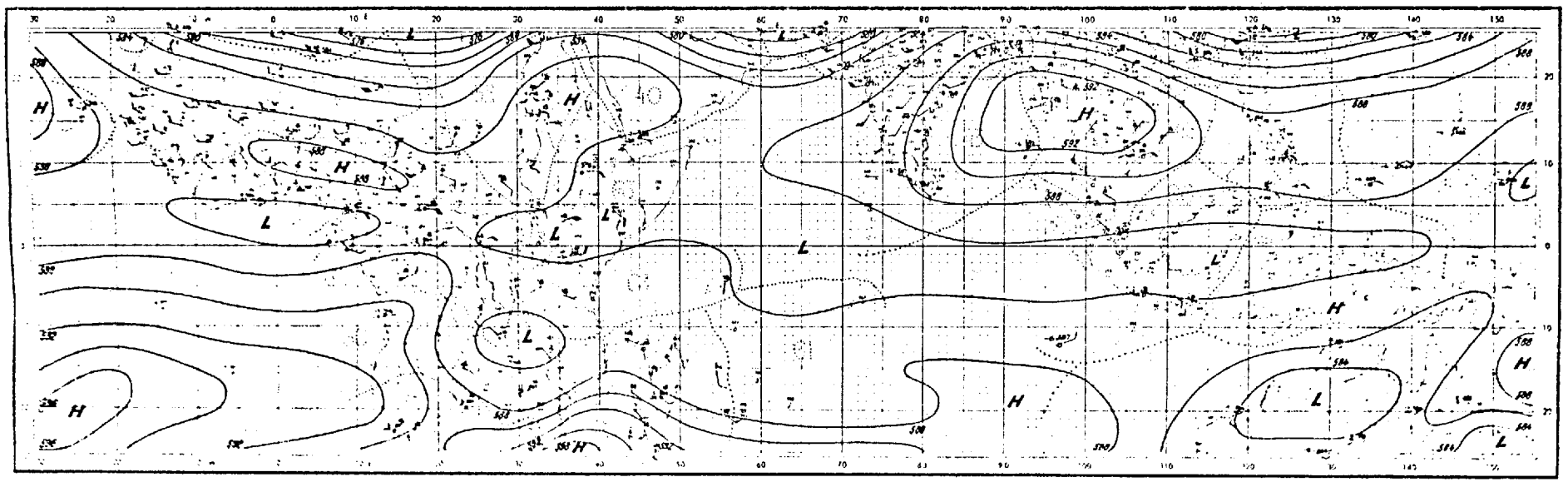

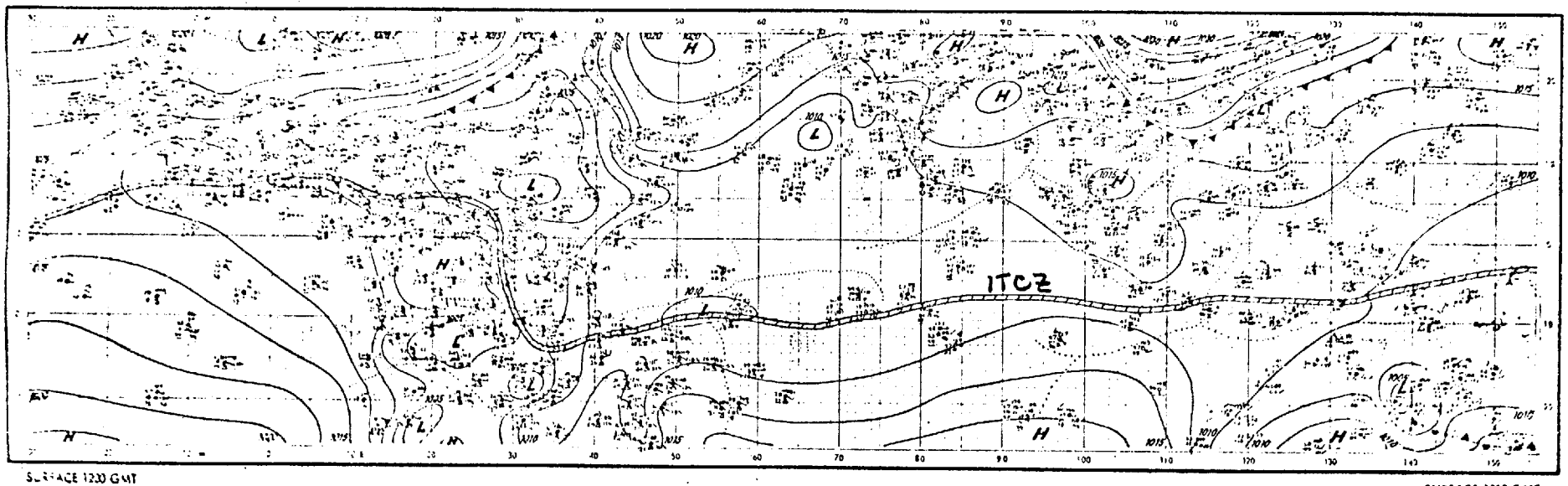

But for the development of occasional storms which broke through it in Mauritius area in February, the ITCZ pattern remained quasi-steady until April when its longitudinal gradient fell from near 90° to about 45° (around the 30°E longitude).

ii) Occurrence of the Second ITCZ Branch

In May 1958, a second branch of the ITCZ was in existence 5° South of the Equator between longitudes 60° and 140°E. It ran parallel to the equator, the prominent ITCZ zonal current then being between 5°N and 15°N. This second branch appeared for only a few days and then disappeared. The existence of the second ITCZ branch has been associated with the existence of a second type of CISK (Conditional Instability of the Second Kind) (Bates,1973). Deriving its heating from 'allobaric convergence involving falling pressure in the disturbance', this type occurs when a high moisture content exists above the cloud base level. Friction plays a significant role in retarding the allobaric convergence. Bates found a maximum growth rate of this type on the equator. This result seems quite peculiar as it is unusual to find the ITCZ on the equator.

In July, the ITCZ was situated North of the geometric equator between latitudes 0° - 5°N over the Atlantic until when it reached the West African (long 14°W) that it got pushed Northwards to 20°N. This is due to land-sea temperature contrast. The ITCZ is a heat equator and often traces the latitude of maximum sea surface temperature. Even, over land, it is marked by considerably, high temperature. As the land is warmer than the sea in this NH Summer period, it, therefore, appears at a greater latitude (fig. 4.2b).

However, from the 14°W longitude to about 130°E, it oscillated between 15° and 30°N. Tropical storms like Winnie, Alice and Tess (all in 1958) broke and sometimes deflected it Southwards to between 5-10°N during their evolution or maturity stages.

The second ITCZ branch re-appeared in late September and, though it became intense in November, it disappeared again before December.

Fig. 4.2b IGY surface and 500mb weather charts for July, 16, 1958.

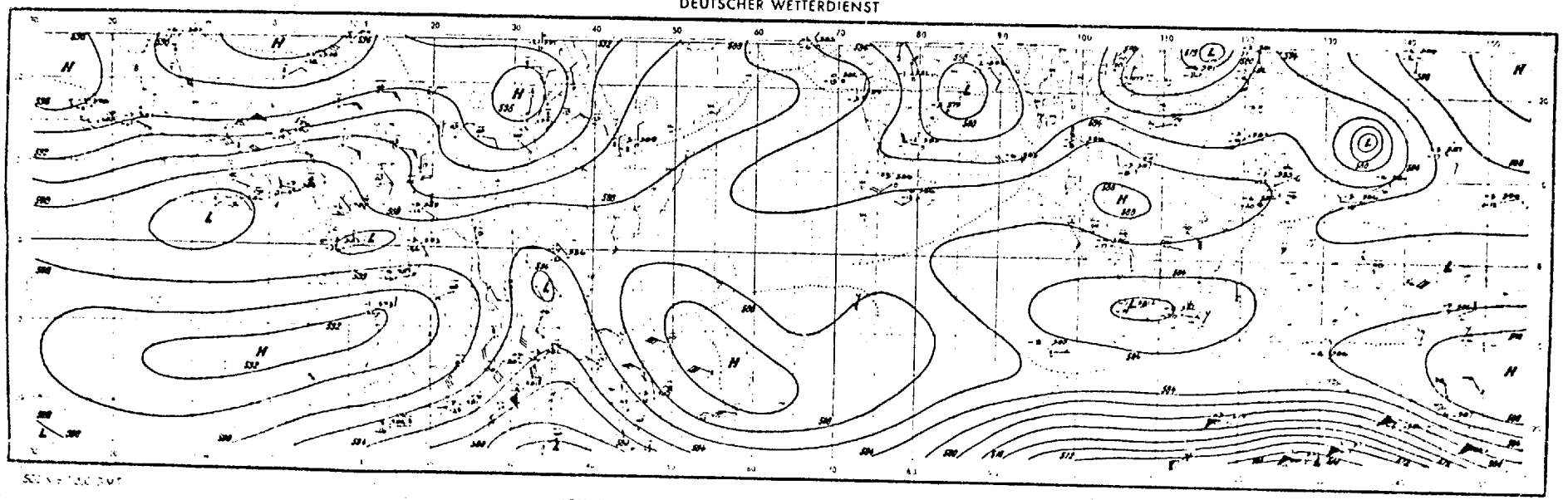

4.(iii) WALKER'S 'OSCILLATIONS'

In his series of papers on the world weather, Sir Gilbert Walker (1923, 1924, 1928, along with Bliss 1930, 1932, 1937.) isolated three prominent 'oscillations' that are embedded in the global circulation - ('Oscillation' as used here does not imply any periodicity) - namely:

1. The North Atlantic Oscillation, NAO

2. The North Pacific Oscillation, NPO and

3. The Southern Oscillation, SO

These 'Oscillations' basically express the tendency of a high pressure build up in one region of the globe to be compensated by a pressure fall in another region e.g.

1. The NAO is expressed as the tendency for sub-normal pressure in the region of the Icelandic low to be accompanied by above-Normal pressure in the Sub-tropics and vice versa.

2. The NPO, a similar oscillation to the NAO, but defined for the Pacific region, found only in Winter. These two only have slight persistence tendency and are not useful for long-range forecasting (Montgomery,1939)

3. The SO is defined as a tendency for high pressure region in the South Pacific to be accompanied by a region of low pressure in the Indian Ocean and vice versa, the rainfall varying inversely with the observed pressure.

Unlike the NAO and NPO, the SO is persistent, from Southern Winter to the following Summer (correlation coefficient, r = 0.84) thus providing a basis for season forecasting.

The Numerical definitions for the three oscillations are as shown in the Appendix (Appendix IV).

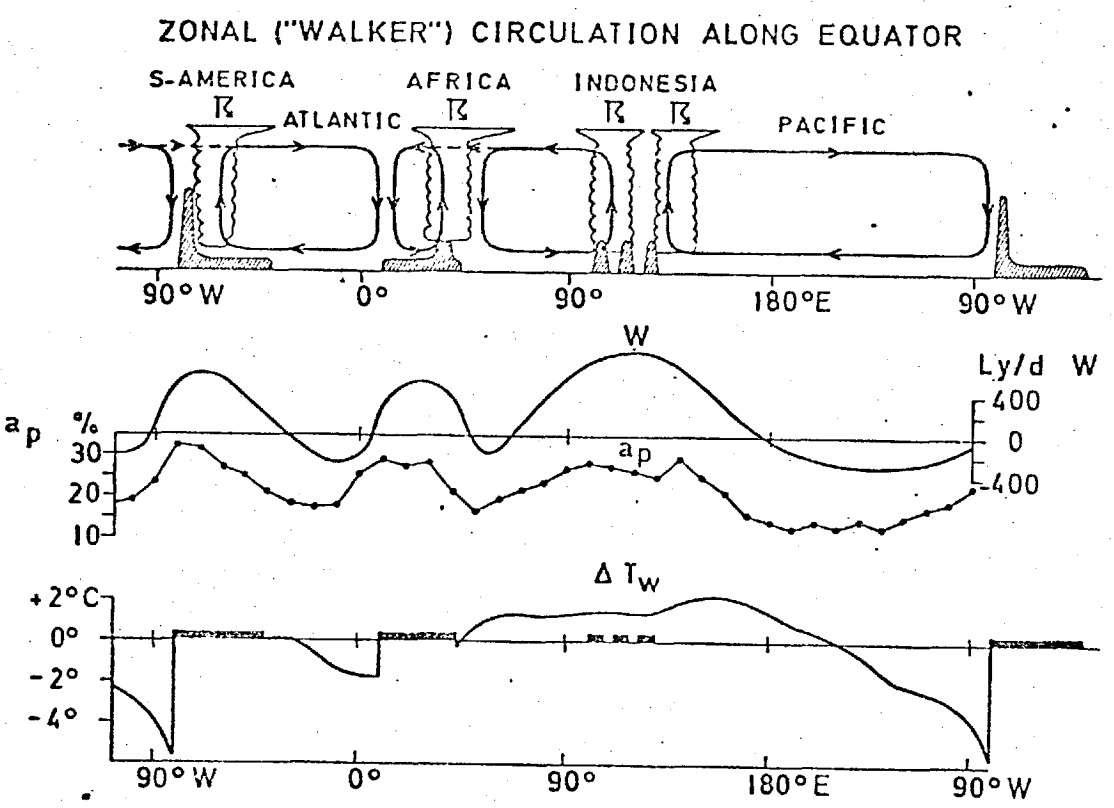

Fig 4.3a

Zonal ("Walker") circulation along the Equatorial belt. In the diagrams below, W = heat budget of an atmospheric column, a_p = planetary albedo (Krueger, 1970), ΔT_w = Water temperature anomaly (Dietrich and Kalle, 1957) - (After Flohn 1971). The descending branch of this circulation is found near the 0^o longitude (The Ghana coastal area).

a) THE ZONAL WALKER CIRCULATION

The SO influences not only the SH but certain parts of the NH as well (Troup, 1965). In particular, its role in the establishment of heat sources and sinks distributed along the equator makes it significant in the study of the thermally forced zonal circulation consisting of zones of ascending and descending motion distributed along the near-Equatorial latitude. This zonal circulation has been named the 'Walker cell' (Bjerknes, 1969). The anomalous weakening of the SH trades leads to:

i) increase in sea temperature and
ii) weakening of the equatorial upwelling

both of which closely relate to the Walker's SO as observed by (Bjerknes,1969) for the Eastern and Central equatorial Pacific.

The influence of the Walker cell is not limited to the Pacific, however, as the Atlantic coast (Gulf of Guinea, in West Africa) also experiences the effect of equatorial upwelling whose strength may be determined by the strength of the SW'ly (Monsoon) winds. Flohn (1971) mapped out the rising and descending branches of the Walker circulation styled the 'Zonal "Walker" Circulation' fig. (4.3a) along the Equatorial latitude (with due regard to the atmospheric heat sources and sinks derived from surface data and satellite albedo (cloudiness) measurements and radiation budget).

More recently, Newell et Al (1974) defined the Walker circulation as:

"those features that represent the longitudinal departures of the motions from the zonal mean" which also applies to "circulation in zonal plates at all tropical latitudes."

Defining the zonal mass flux,

$$M_z = \frac{a\Delta\varphi}{g}\int_{p}^{p_0} \overline{u}^{*}\, dp$$

.. .. .. 4.1

where a = radius of the earth,

g = acceleration due to gravity,

$\bar{u}^*$ = longitudinal departure of the motions from the zonal mean

(i.e. $\bar{u}^* = u - [\bar{u}]$)

Newell et Al (1974) obtained a model of the circulation as indicated in fig 4.3b.

b) THE WALKER CIRCULATION AND THE WEST AFRICAN PRECIPITATION

The Walker Circulation effects anomalies in tropical precipitation; for example, through 'condensation heating over a warmer-than-normal sea surface' (Bjerknes, 1969, Krueger and Winston, 1975). Numerical simulation of this heating has been carried out by Rowntree (1972).

i) Effect on the dry Ghana Coast

A descending branch of the Zonal Walker Circulation occurs over the Accra (Ghana) longitude and is, no doubt, responsible for the anomalously scanty precipitation observed in the area.

Over 90% of the Sahel region's and about 50% of the Southern Savannah/Guinea region's precipitation fall between June and September. A map of the June-September (1958) precipitation for West Africa is as shown in fig. (4.3c). It can be noticed that the Ghana coast, despite its nearness to the ocean, is as dry as the Sahel region further North.

The upwelling of cold water around this coast is possibly due to the combined effect of:

Fig 4.3b Zonal Mass Flux M (10 gm sec^{-}) along latitudes 5°N and 5°S for the NH Winter and Summer seasons respectively (from Newel et Al, 1974). These fluxes indicate the rising and descending branches of the Walker Circulation evident around the equatorial latitudes.

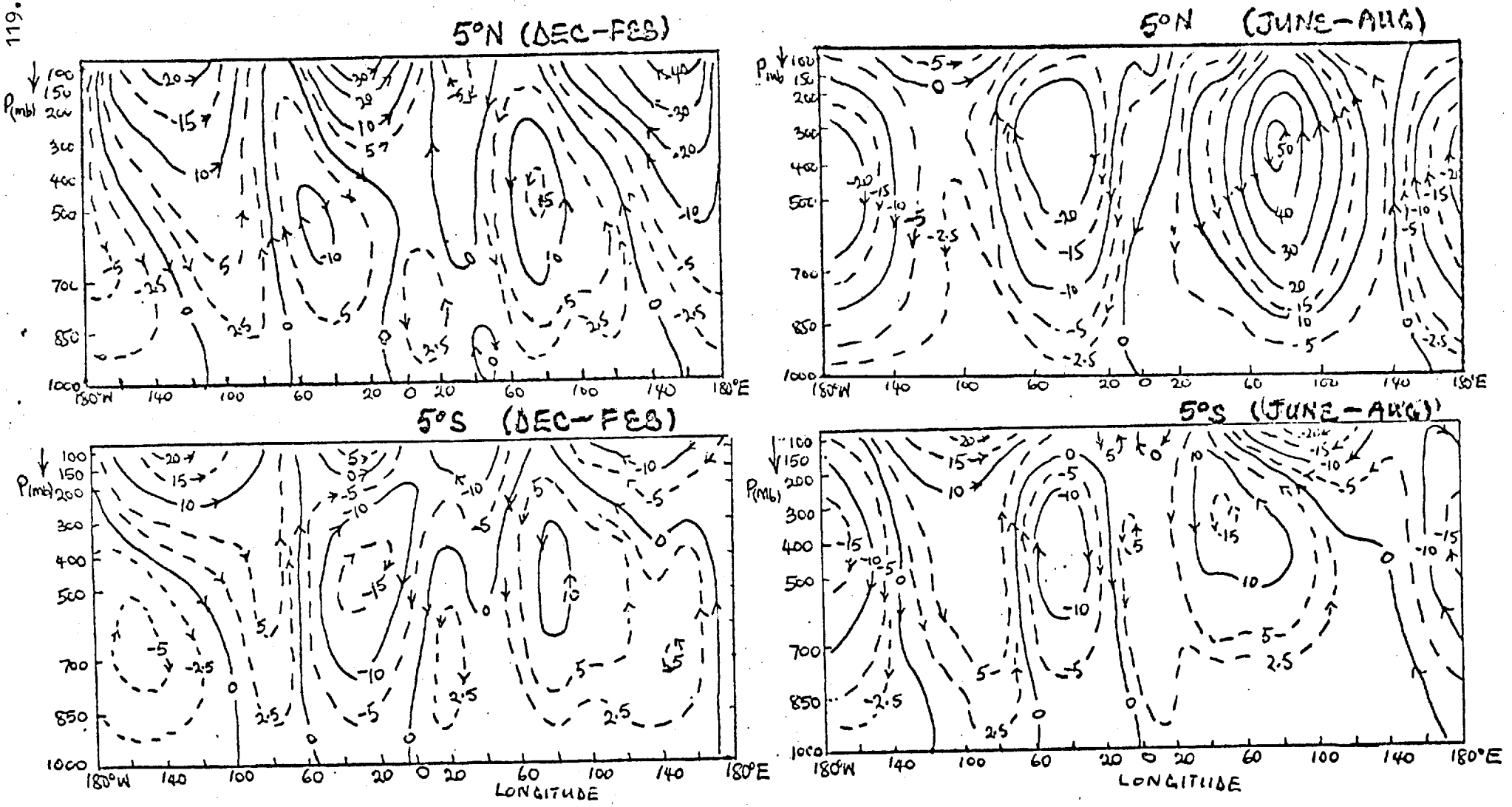

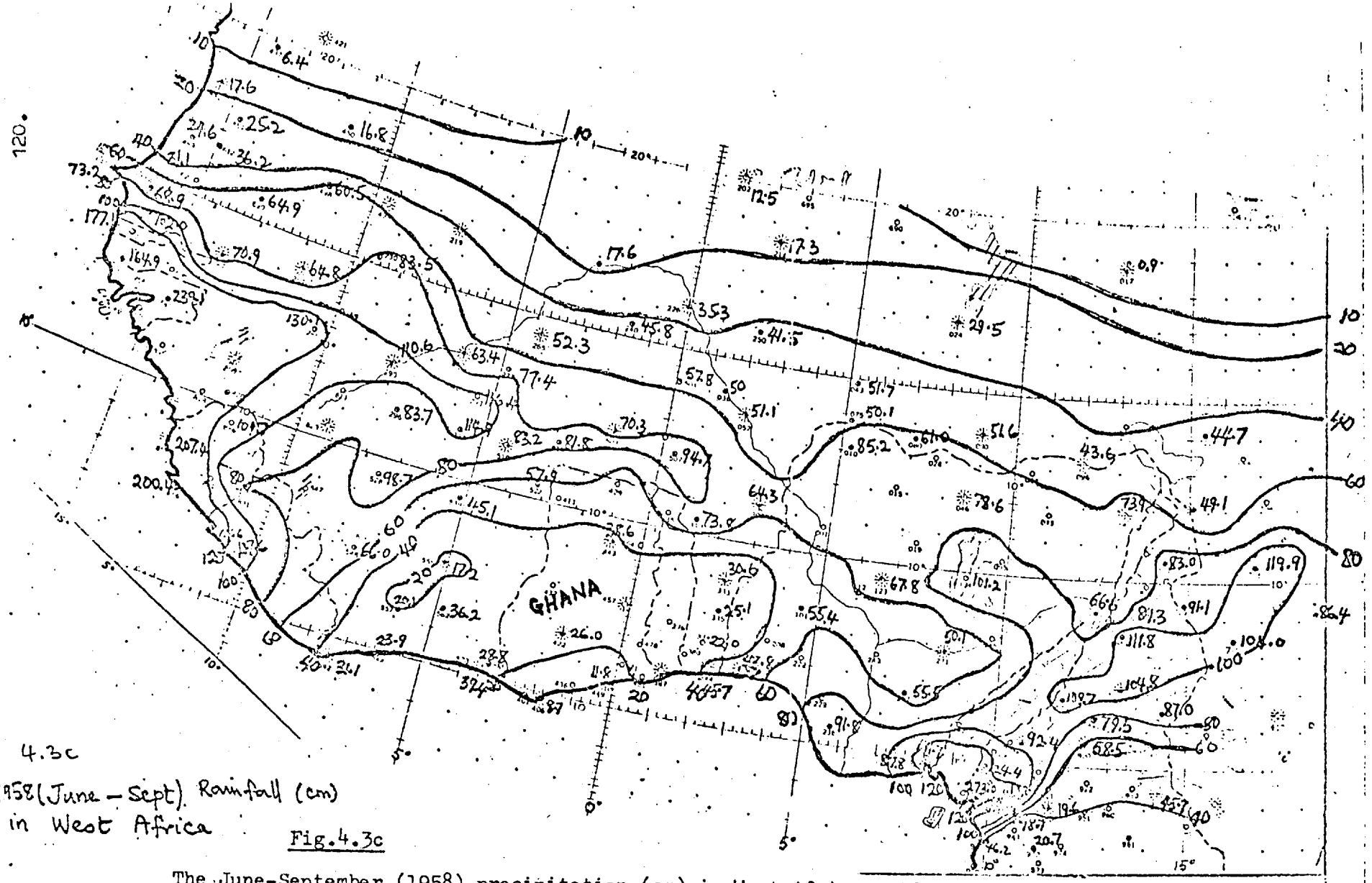

4.3c

1958 (June – Sept) Rainfall (cm) in West Africa

Fig.4.3c

The June-September (1958) precipitation (cm) in West Africa. Of particular significance is the Ghana coastal area which, as a result of the descending branch of the Walker Circulation - further enhanced by upwelling of cold water - is as dry as the Sahelian area.

1) the presence of a cold under-current (the cool Benguella current) and

2) a 'two-sided divergence of the Ekman Drift' in the Atlantic, as the Guinea Coast is approached. (Flohn, 1971)

The resulting dimunition of the upward flux of heat and water vapour stabilizes the atmosphere and prevents the occurrence of convective processes, a hinderance to cloud formation. Strong upwelling process results in the strengthening of the 'Zonal Walker' circulation - particularly as in July - August, the LDS in the Southern (Lagos) area (Chapter III) - and vice versa.

ii) Effect on the Easterly disturbances and squalls

The cooling of the Guinea coast increases the thermal contrast between the potentially hot Sahara desert to the North (θ often up to 43°C) and the cooler region to the South ($\theta \sim 21°C$) fig (3.8).

By the thermal wind relation,

$$\frac{\partial \underset{\sim}{V}}{\partial z} = \frac{g}{f\theta} \underset{\sim}{k} \wedge \nabla\theta \qquad \ldots \ldots \ldots 4$$

where $\underset{\sim}{k}$ is the unit vector in the z direction,
the flow aloft is easterly, overlying the surface westerly flow.

The strength of this flow depends on the magnitude of the potential temperature gradient. A strong easterly flow can spell increased easterly disturbances and squall occurrence. Its importance in the propagation of the African waves, some of which later develop into hurricanes in the Atlantic, has been remarked by Carlson, (1969).

In view of the fact that the easterly waves and squall frequency vary and is not the same from year to year e.g. (Obasi, 1975) so also

is the strength of the Walker Circulation (in accordance with the strength of the upwelling process) this factor can be very important in determining the variation in the region's precipitation, a bulk of which is realized from squall activity. However, although these systems come from the East and propagate Westwards, their moisture supply is mainly from the West (Obasi, 1975). The warm Dakar coast enhances this necessary moisture supply to the W/NW winds which blow towards the Sahel during the height of the Monsoon Season (July - August) e.g. Flohn, 1960a. The cyclonic nature these winds assume enables them to play the role of the SW'ly current in pushing the ITD Northwards. A situation thus arises where, in the LDS period, the dryness of the South exists simultaneously with the wetness of the Sahel. Such was the case in 1958 for instance (Chapter II)

This phenomenon is established as an important climatological feature in the region by the high negative correlation found between the Southern and the Sahel region's precipitation for August over a decade (Chapter VI.)

c) The SO Index and Precipitation

However, the role of the Walker Circulation on the region's precipitation needs to be precisely clarified. The SO depicts the fluctuation between the state of a strengthening and that of a weakening of the Walker Circulation. (Wright 1975; Berlage, 1966, Bjerknes 1969). Hence, if the precipitation is being influenced by the Walker Circulation, the SO index will be highly correlated with the precipitation. Walker's original SO index has been modified and extended to the recent era by various workers. e.g. P.B. Wright (1975), using the variation in atmospheric pressure over eight stations over the globe, estimated the SO for the period 1851 to 1974.

Troup (1965) has made a comprehensive analysis of Walker's Southern Oscillation index (WSOI) and its relevance in recent times. He correlated WSOI for standard Seasons: March-May, June-August, September - November, December-February for lag 1 and 2 'Seasons after the Season

in question'. His results are reporduced below in Table (4.1).

A comparison is made between WSOI results and that obtained from P B Wright (1975) here referred to as PWI for 1951-1973, (the period embracing the 'normal' decade of 1951-60 (Chapter VI) and the years of Sahel precipitation decline.)

The agreement between the two, (Table 4.1), is quite remarkable despite the fact that WSOI was obtained for a different time. The December - February season is the only one not in tune. What with considerable variation evident in WSOI (Troup, 1965), this agreement is not far off. In particular, both WSOI and PWI agree in indicating, as pointed out by Troup for WSOI,

a) a higher prospective 'foreshadowing' of December-February than of June - August,

b) June - August has a greater effect on the two subsequent seasons than those of other seasons e.g. December - February

Lag correlations of WSOI for Different Seasons Table (5) of Troup, (1965) compared with PWI (1975) for similar seasons but for 1951-1973.

Table (4.1)

	WSOI		PWI	
	Lag (Seasons after Seasons in question)		Lag (Seasons after Season in question	
	+1	+2	+1	+2
March-May	0.62	0.36	0.67	0.61
June-Aug.	0.82	0.84	0.75	0.62
Sept-Nov	0.90	0.60	0.81	0.51
Dec-Feb	0.68	0.20	0.57	0.06

This agreement is fair enough to make PWI applicable for testing the suspected role of the WC on the region's precipitation.

Experimentation of the Niamey and Lagos (1951-73) precipitation correlated with PWI for various seasons of the same period shows that the June-August precipitation at Lagos is negatively correlated with PWI (September-November); r=-0.41 ; SE = 0.18.

This tends to suggest that a high (June-August) Lagos precipitation spells a weak (September-November) Southern Oscillation.

However, no correlation is found between the Niamey precipitation and the index in any season. But it is found that a marked persistence exists between the Niamey precipitation in (June-August) and that of (September-November); r = 0.49; SE = 0.16.

Hence the strength of the LDS in Lagos is associated with that of the WC and while Lagos is under SO influence, Niamey is not but is ITD controlled.

4.(iv) REGIONAL (ITD) CIRCULATION

a) The Role of the Anticyclonic systems

The atmospheric circulation over West Africa is dominated by the Azores and Libyan Anticyclones in the NH and the St Helena Anticyclone in the SH. Each of these represents a maximum in the subtropical belt of high pressure.

The Azores high, often found around latitude 35°N on the longitude of the Azores Islands, is more permanent than the Libyan Anticyclone located around the same latitude but over Libya in North Africa. The St Helena Anticyclone, centred over St Helena Island, about 15°S, often oscillates Northwards in the NH Summer and Southwards in the Winter. The NH Anticyclones oscillate in reverse to this (Leroux, 1971). The Anticyclones edge in the ITD within their ridge-trough systems and carry it with them in their North-South oscillations (fig. 4.4).

The hot and dry (harmattan) NE'ly winds which have had a long trajectory over the Sahara desert, and the moist but cooler SW'ly (Monsoon) winds which have had a long trajectory over the Atlantic ocean, converge on the ITD. The NE'ly winds are a continental tropical type while the SW'ly winds are of a Tropical Maritime origin. At the surface position of the ITD, the SW'lies form a wedge pointing Northwards, under the NE'lies.

Often between 50km to 250km wide (Leroux,1971), and moving Northwards with the solar cycle (but with about six weeks' lag), the ITD attains its most Northerly position between 20-25°N in August. The Monsoon winds then penetrate far into the West/North African hinterland, bringing moisture and rain into the Sahel and Southern Sahara. Between late August and early September, the ITD starts to move Southwards again till it reaches latitude 5-7°N in the NH Winter. During this time, the NE'ly winds dominate most of the region, bringing dust and 'harmattan' as far South as Lagos on the West African coast.

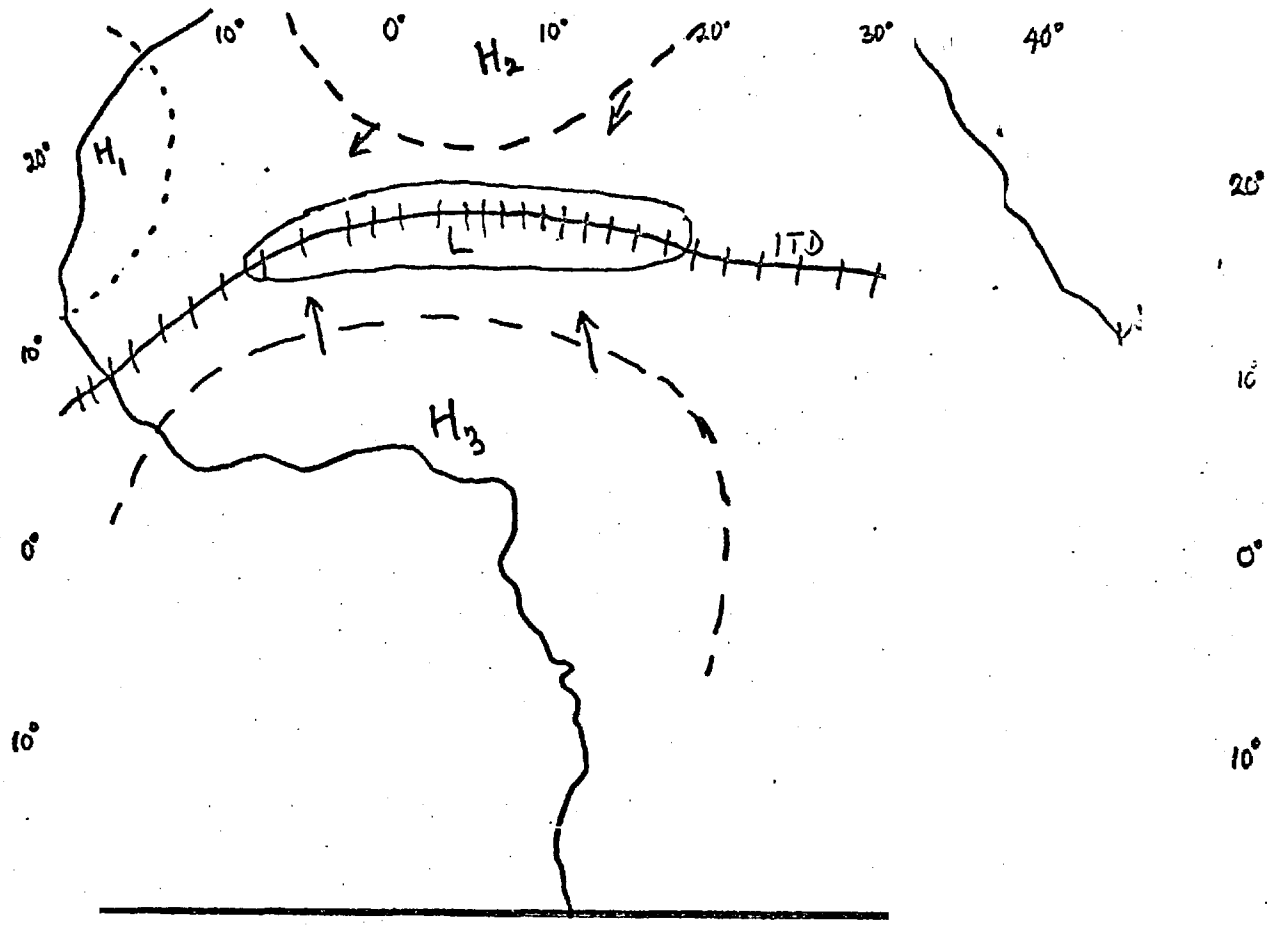

Fig 4.4

Illustrating typical cross-isobar flow in the ITD circulation pattern. H_1, H_2 and H_3 represent the Azores, the Libyan and the St Helena anticyclones respectively, while L is a heat low. H_1, H_2, H_3 shift to varying degrees North/South with the NH Summer/Winter seasons respectively. A West/East shift in H_1/H_2 is often observed also.

b) Location and Movement of the ITD

The ITD is marked by discontinuities of:

i) Wind,
ii) Dry bulb Temperature, and
iii) Dew point temperature,.

The impact of the dew-point discontinuity is such that the climatological locus of maximum dew-point gradient traces the ITD. While places North of the ITD have very low dew point temperatures (T_d ranging from $-3^{\circ}C$ to $12^{\circ}C$), places South of the phenomenon have very high T_d values (often between $18-25^{\circ}C$) Fig.4.5a shows a typical observation marking the ITD location. Considerable difficulties often arise in locating the ITD position, particularly, in areas like the Sahara desert border where observing stations are widely scattered.

Superimposed on the monthly migrations of the ITD (obtained by taking a statistical mean of the daily positions for various months) are migrations on the scale of hours and days. Three main migrations can be identified (Leroux, 1971; Pedgley, 1970; Clackson, 1957)

a) diurnal migration,
b) mesoscale migration, and,
c) annual migration.

The day-to-day (12 GMT) positions of the ITD for the IGY year show large fluctuations of up to 2, 3 or 4 degrees as indicated by the January, April and August cases shown in fig. (4.5b).

Disturbances - squall lines and Easterly waves - can give rise to perturbations which can disrupt the ITD structure. However, the monthly mean positions can be relied on as a statistical representation of the phenomenon. The North-South seasonal migration of the ITD is illustrated in fig (4.6) by the 0600 GMT positions of the phenomenon as observed in 1973. The drought which hit the region at this time witnessed about a 2 degree latitude shortage in the Normal ITD maximum Northerly (August) position. As shown in Chapter II, the ITD mean August position (along $3^{\circ}E$) was $22^{\circ}N$ for the wet year, 1958, compared with the near $20^{\circ}N$ evident here.

Fig 4.5a

Typical Temperature and pressure discontinuity associated with the ITD as obtained on January 6, 1958.

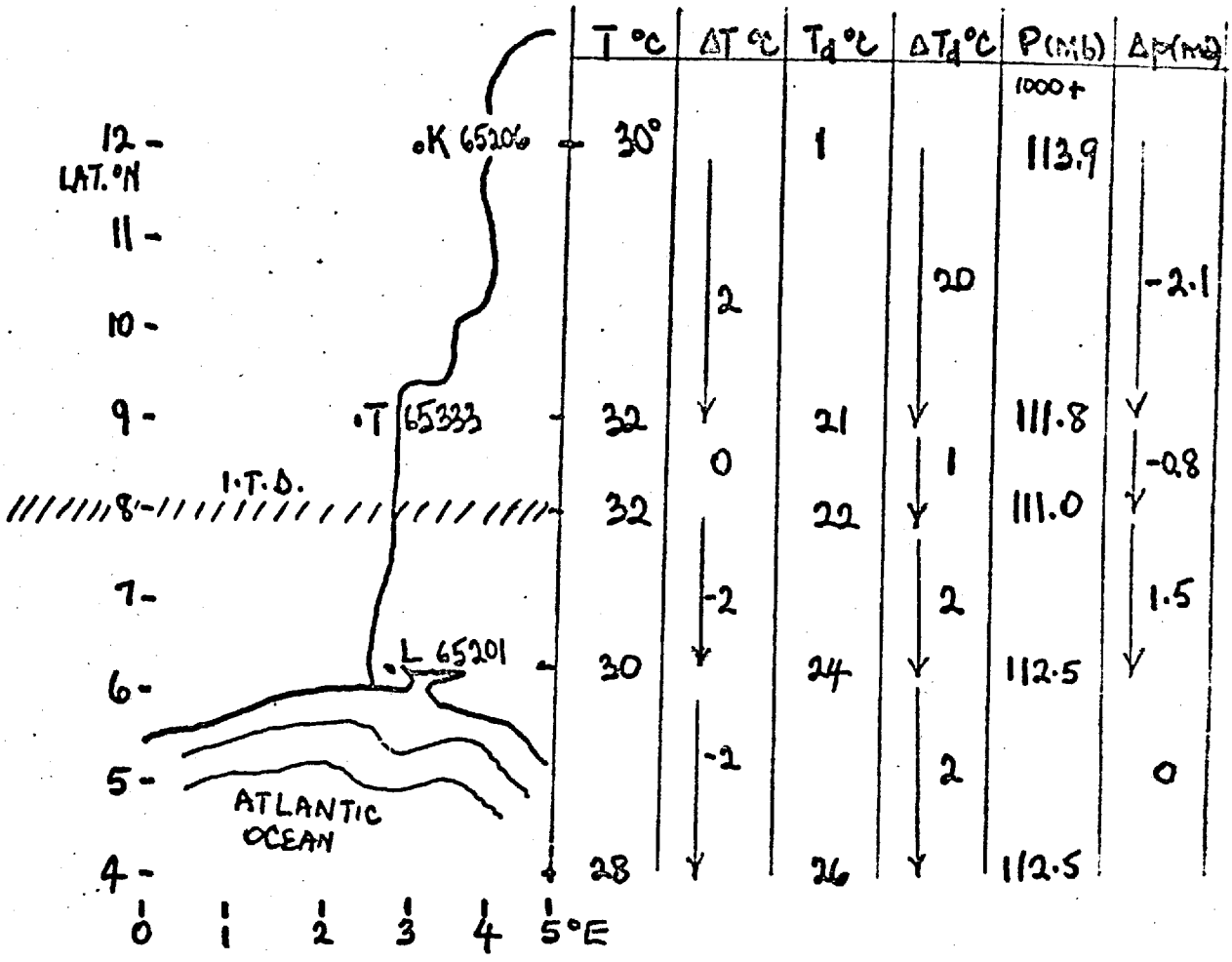

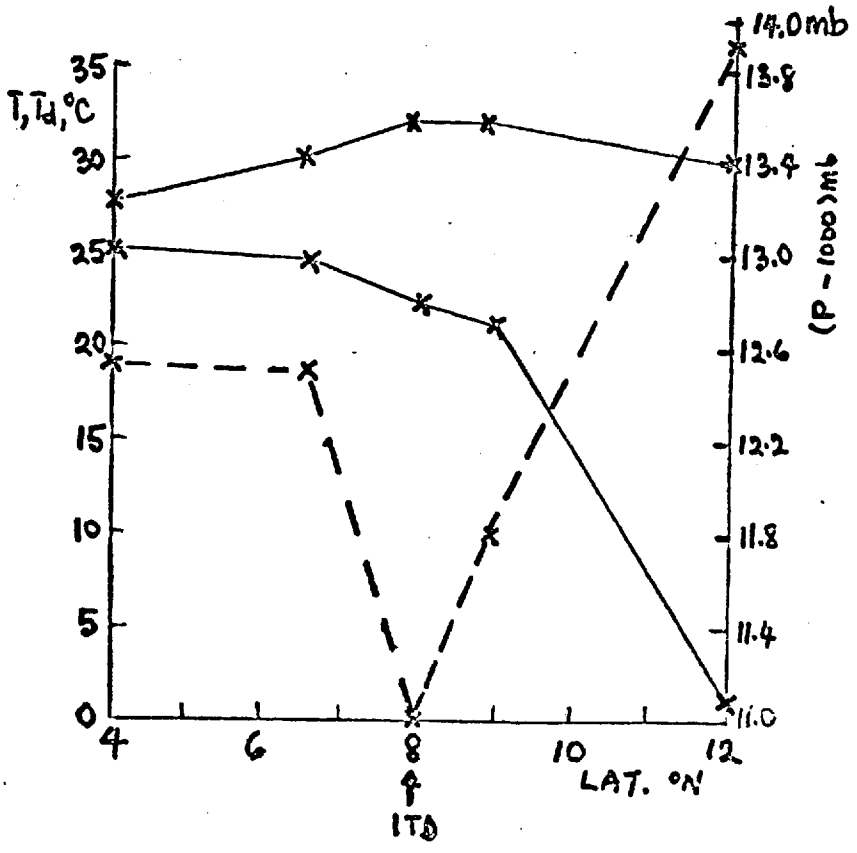

Fig 4.5b

Typical variations in the ITD latitude (along zone 2) for January, April and August 1958.

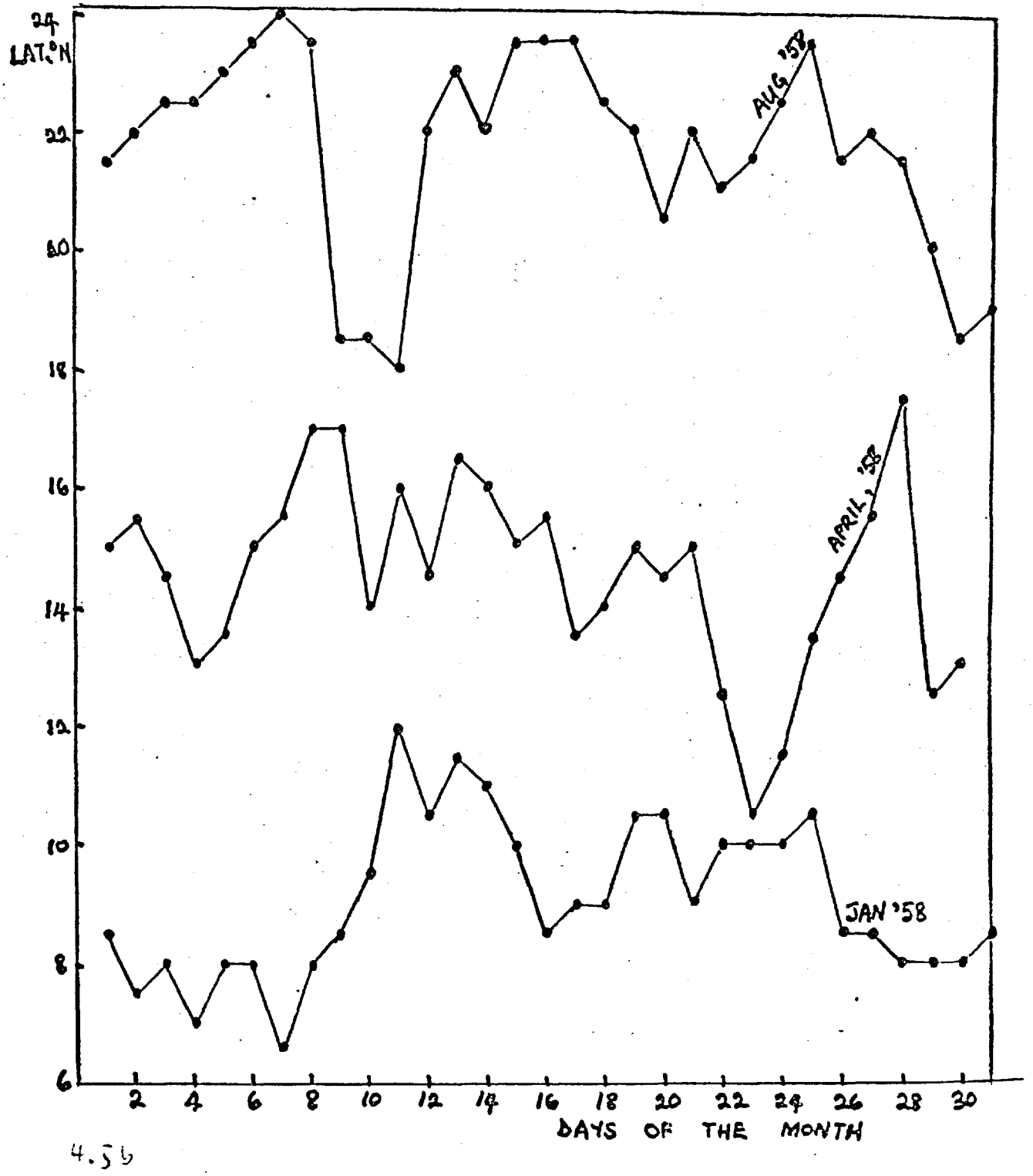

4.5b

Fig. 4.6

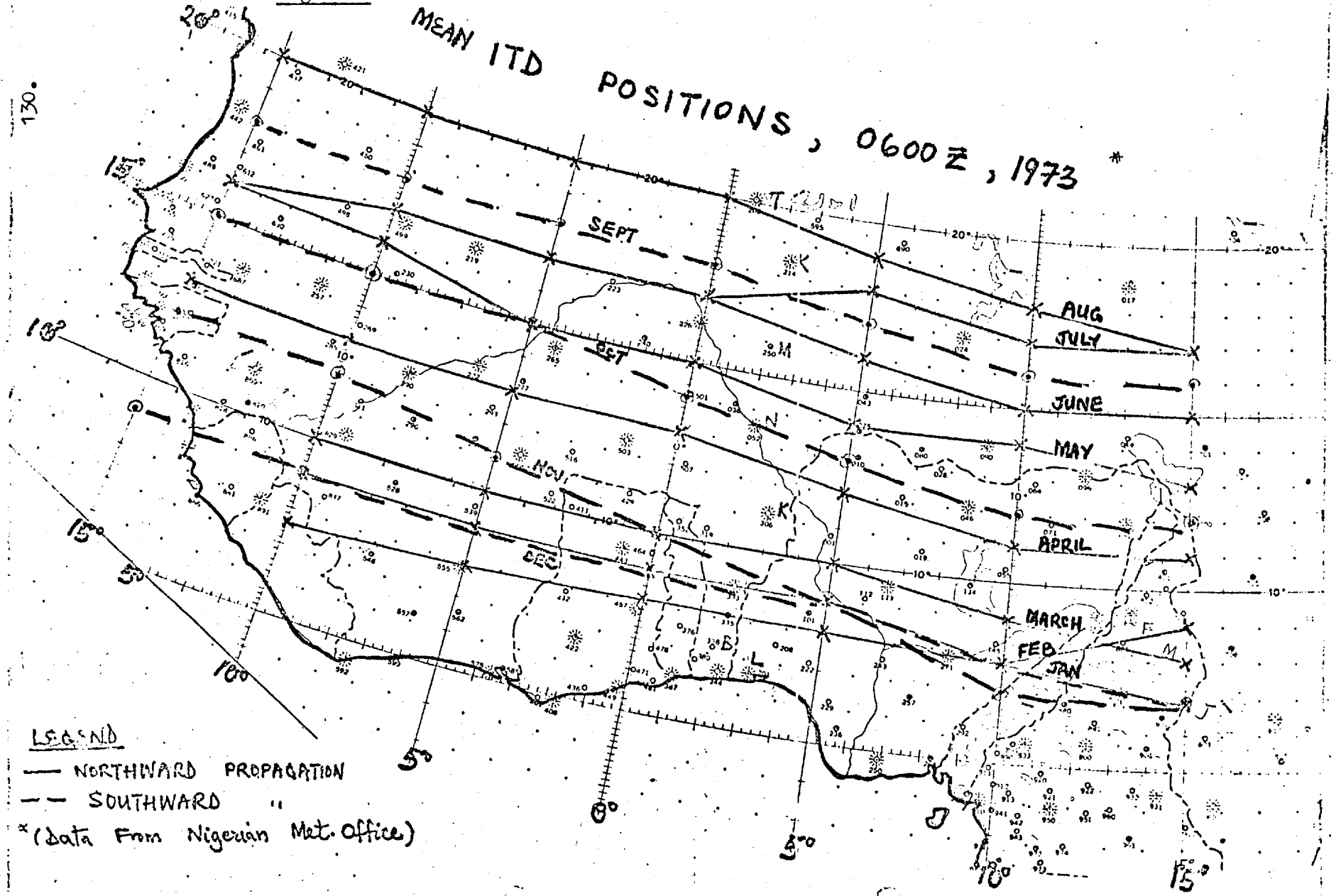
MEAN ITD POSITIONS, 0600 Z, 1973 *
SEPT
OCT
NOV
DEC
AUG
JULY
JUNE
MAY
APRIL
MARCH
FEB
JAN
LEGEND
— NORTHWARD PROPAGATION
– – SOUTHWARD "
*(Data From Nigerian Met. Office)

c) Scale analysis of the ITD Circulation

The Rossby Number, R_o, and the Ekman Number, E, typical of the ITD Circulation can be very important in considering its dynamics.

The zonal and meridional components of the momentum equation are given by:

$$\frac{Du}{Dt} + \frac{1}{\rho}\frac{\partial p}{\partial x} - fv = \frac{1}{\rho}\frac{\partial \tau_{xz}}{\partial z} = \nu\frac{\partial^2 u}{\partial z^2} \qquad \ldots\ \ldots\ \ldots\ 4.3$$

$$\frac{Dv}{Dt} + \frac{1}{\rho}\frac{\partial p}{\partial y} + fu = \frac{1}{\rho}\frac{\partial \tau_{yz}}{\partial z} = \nu\frac{\partial^2 v}{\partial z^2} \qquad \ldots\ \ldots\ \ldots\ 4.4$$

(Assuming the Ekman friction law relating the stress $\underset{\sim}{\tau}$ to the wind shear $\frac{\partial \underset{\sim}{V}}{\partial z}$,

$$\underset{\sim}{\tau} = \mu\frac{\partial \underset{\sim}{V}}{\partial z}$$

where $\nu = \mu/\rho$ is eddy viscosity (as distinct from molecular viscosity)

and $\frac{D}{Dt} = \frac{\partial}{\partial t} + u\frac{\partial}{\partial x} + v\frac{\partial}{\partial y} + w\frac{\partial}{\partial z}$ is a substantial derivative.

As indicated in Section 4.(iv) a), the ITD is often found in the trough-ridge circulation pattern set up by the NH (Libyan or Azores) Anticyclone and the SH (St Helena) Anticyclone. It is often seated in a 'heat low' centred over the region, sketched in fig (4.4).

A significant feature of this circulation is the cross-isobar flow from high towards the low pressure centre containing the ITD. Hence, this warm low is due to frictionally induced convergence at the surface or lower levels.

Over the ITD, $\partial p/\partial x$ is very small and is negligible compared with the other terms in 4.3 e.g. see fig. (4.18). However, $\partial p/\partial y$ is larger.

Scale analysis of equation 4.3 yields:

$$\frac{u^2}{L_y} - fv - \frac{\nu u}{H_f^2} = 0 \qquad .. \quad .. \quad .. \quad 4.5$$

Where the various horizonal scales L_x, l_y and L_y are as shown in the sketch below.

Assuming :

i) a steady state

ii) $\frac{u}{L_x} < \frac{v}{L_y}$ since $u \sim v$ owing to the strong cross-isobar flow and the fact that $L_y << L_x$ for the system (see below)

iii) $\frac{w}{H} < \frac{v}{L_y}$ typically ,

H_f is the height at which zero stress occurs or at which the lower Westerlies give way to the Upper Easterlies (obtainable from the wind-profile at the ITD surface).

Dividing equation 4.5 by fV , and applying the assumption $u \sim v$, we obtain,

$$\frac{u}{fL_y} - 1 - \frac{\nu}{fH_f^2} = 0 \qquad .. \quad .. \quad .. \quad 4.6$$

All the terms in 4.6 are dimensionless.

$\frac{u}{fL_y}$ = Rossby No., R_o = $\frac{\text{Inertial acceleration}}{\text{Coriolis acceleration}}$

$\frac{\nu}{fH_f^2}$ = Ekman Number, E = $\frac{\text{Viscous acceleration}}{\text{Coriolis acceleration}}$

For an occasion when the ITD is over Niamey, latitude, $\Phi = 13.5^{\circ}N$

$f = 2\Omega \sin\Phi$

$= 3.4 \times 10^{-5}\ s^{-1}$

$\sim 10^{-5}\ s^{-1}$

(Not too small compared with Mid-latitude value of $f \sim 10^{-4}\ s^{-1}$)

With $H_f \sim \frac{1}{2}$km say and eddy viscosity $\nu = 10 m^2\ s^{-1}$

Therefore $E = \nu / f H_f^2 = 1.3$

(suggesting that eddy viscosity is important in the dynamics of the system.)

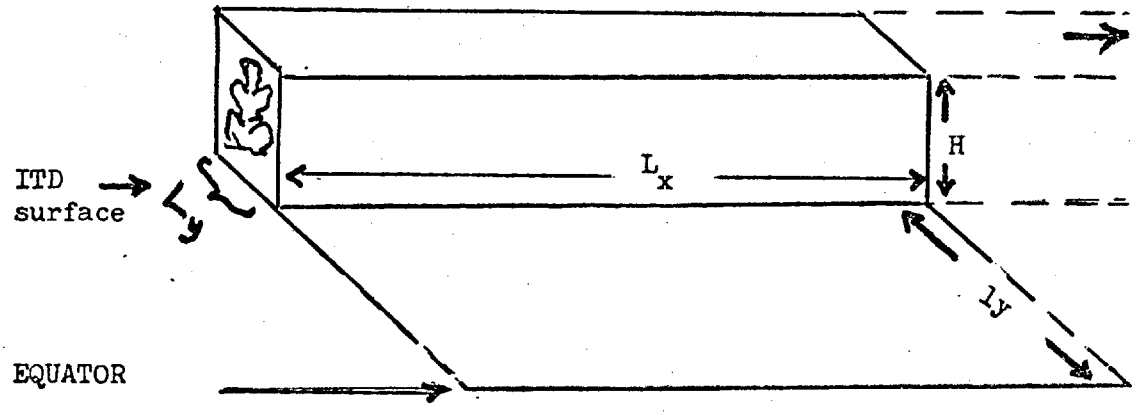

Diagramatic representation of the scale lengths in the ITD circulation.

$L_x > l_y \gg L_y$

Considering motion across the ITD,

L_y = width of the ITD $\sim$ 50km say (sometimes greater)

For L_y = 50 km

and $u \sim$ 1 m/s (calm conditions often prevail over the ITD)

$R_o = \frac{u}{f L_y}$

$= 0.8 \sim 1$

Rossby Number ∿ Unity over the ITD surface.

It need be noted that $\partial p/\partial y$ is much larger than $\partial p/\partial x$. In addition, the motion tends to be ageostrophic across the ITD, owing to frictional convergence towards the centre of the low, tending to fill it up. Ascending motion results. As the air rises up, it comes out at a higher level, moving towards a high pressure where it gets slowed down. (See the sketches below.)

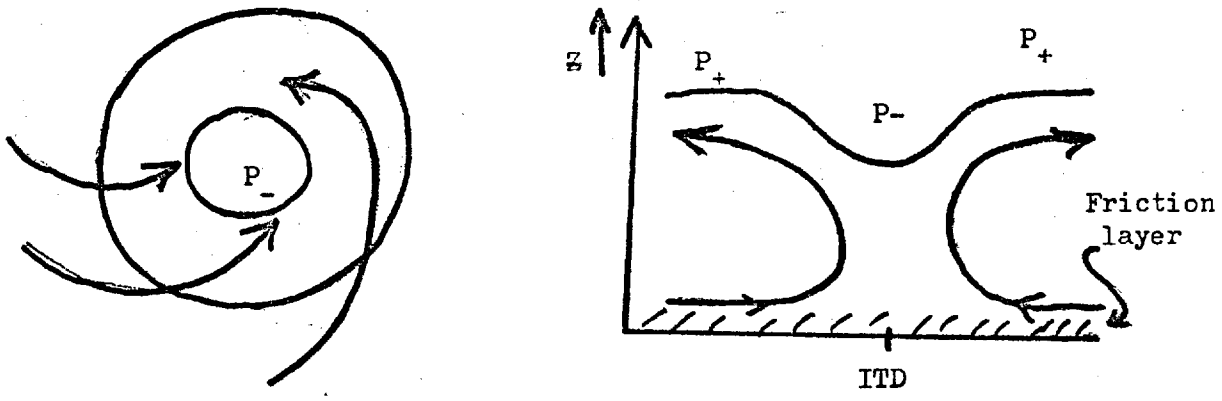

Plane view Vertical section

Sketches of typical cross-isobar flow

A similar consideration may be applied to the situation when a disturbance hits the ITD. However, a strong (Easterly) advection need be incorporated.

4.(v) THE ITD CONTROL ON THE REGION'S PRECIPITATION

a) The convective Processes within the ITD Environ:

Most of the precipitation generated within the ITD circulation actually fall out of convective systems of:

i) Cu and Cb cloud types which can be classed as 'little' and 'deep little' convection. These fall in the scale D of GATE (GATE Report No.1, 1972) and are of horizontal dimensions 1-10 km,

ii) Meso scale cloud systems of scale 10-100 km; scale C of GATE,

iii) Cloud clusters and squall lines of horizontal scales; 10^2 - 10^3 km: scale B of GATE; and,

iv) Mid-tropospheric Easterly Wave disturbances propagating Westwards across the region after originating from somewhere between Kharthoum and NDjaéma (Ex-Fort Lamy) (Burpee, 1972). These are of scale 10^3 - 10^4 km; GATE scale A.

These various scales of convection interact considerably, the smaller scale ones constituting themselves into big scale systems, the whole system giving rise to a spectral range in which each phenomenon mentioned above attain maximum amplitudes. Spectral analyses of some individual station precipitation data (e.g. Mbele Mbong, 1974) isolate some of these scales of convection.

Of very great importance are the squall lines and the Easterly waves which characterize the rainy season. The squall lines, often generated in the afternoons or evenings following a high build up of θ_w at low levels, as a result of the high input of solar radiation, owe their origin to orographic heat release from Upland areas, (Chapter II). These highly organized Cb systems appear on satellite

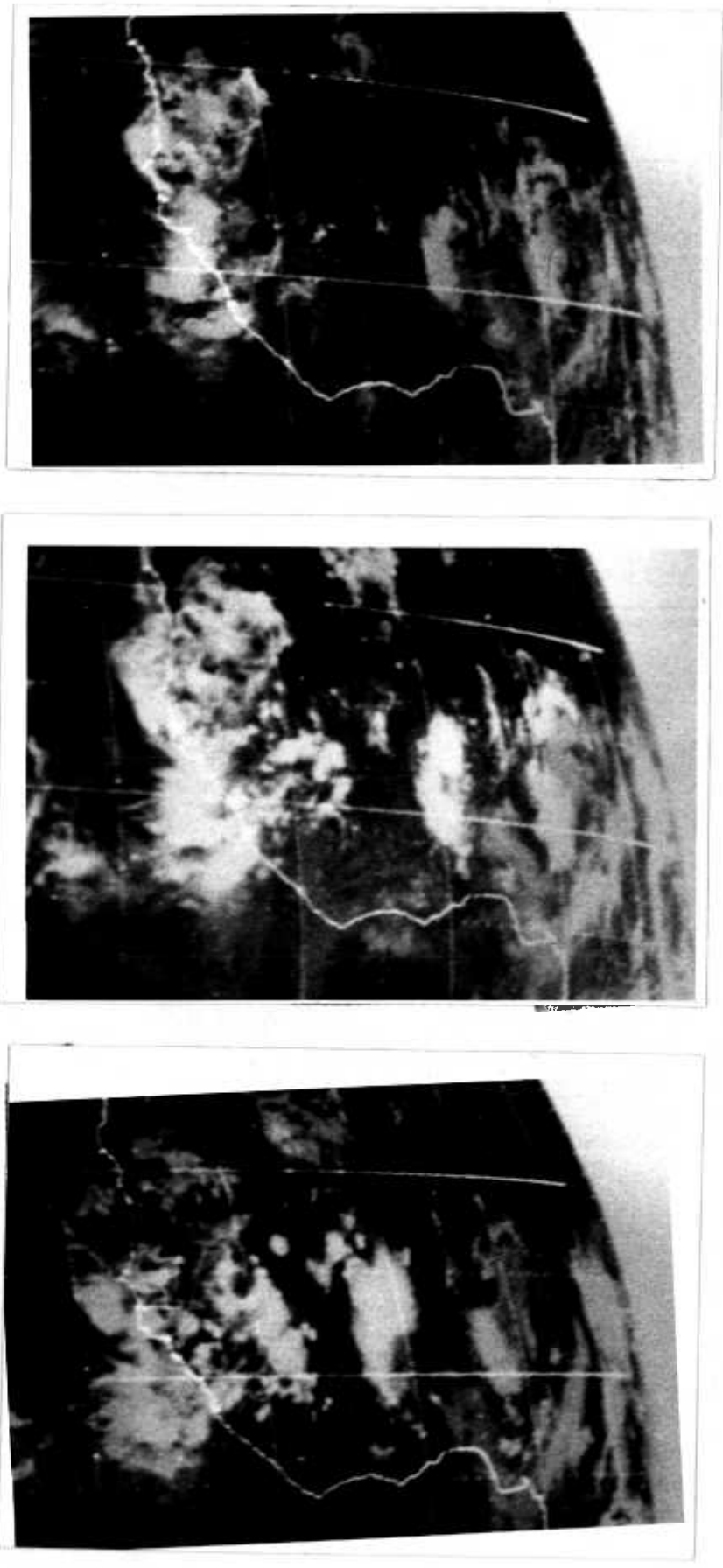

(i)

(ii)

(iii)

Fig 4.7a: SMS-1 4nm resolution (IR) Satellite photographs of the region for:

(i) 12 GMT; (ii) 15 GMT, and (iii) 18.30 GMT, 26th August 1974, briefly illustrating a typical squall line evolution.

photographs as a narrow and long stretch of clouds, often oriented between North-South to North West-South West. In pre-satellite days, Hamilton and Archbold, (1945), Eldridge, (1957) gave accounts of these systems' orientations and westward propagation.

We illustrate here, some typical view of these systems as they appear on the SMS-1 Satellite photographs. Fig 4.7a is a 4nm Infra red photograph of the cloud systems in the region, taken on 26th August 1974. At 12 GMT (fig.4.7a(i)) two narrow longitudinal squall lines could be seen located at longitudes 4 and 6°E (lat. 13-16°N). By 15GMT (fig 4.7a(ii)), further development has taken place and the lines formed a mature longer and more prominent squall line. These systems often dissipitate after some hours (owing to the heavy down pour of rains resulting from them) as they move westwards. For instance, by 18.30GMT (fig 4.7a(iii)), the line could hardly be located again.

Fig 4.7b illustrates another squall line which developed around longitude 2°E (8-13°N) some three days following those of fig 4.7a (29th August 1974). The many scales of convection evident on both photographs cannot be fully described here e.g. big cloud clusters could be seen propagating westwards as well. These systems derive their moisture from the SW'ly winds though they propagate in the direction of the 700mb flow, westwards.

As already shown in Chapter II, easterly waves often exist above the 850mb vortices prevalent over the region in the rainy season (e.g. Aina, 1964). Propagating westwards across the region, these waves, with their associated cloud clusters, account for a great percentage of the region's precipitation. The squall lines often move at about 14 m/s (faster than the waves that move at about 7 m/s e.g. Abdul, 1971).

A cross-sectional analysis of the thermodynamic structure of the atmosphere along with the fields of divergence associated with an occasion of maximum daily precipitation in our wet year case study depicts clearly, the region of pronounced activity in these systems. This shall

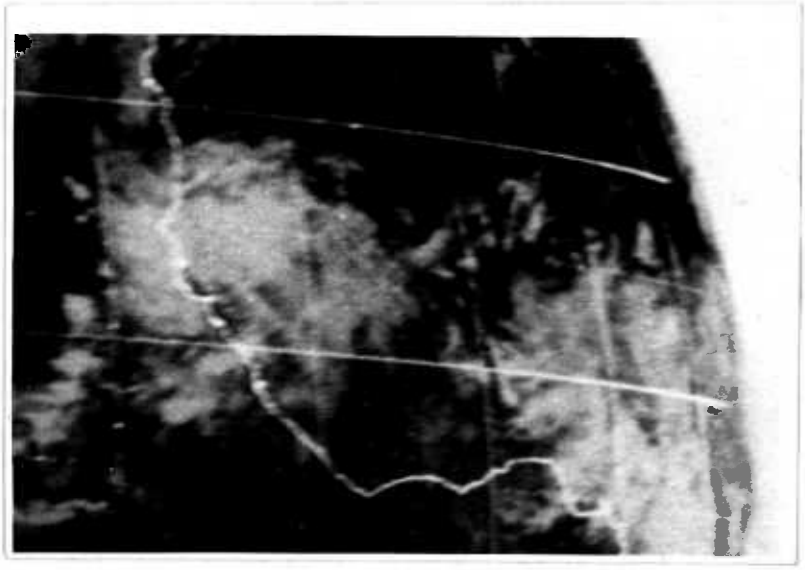

Fig 4.7b

As for fig 4.7a but for 12.30 GMT 29th August 1974. A squall line can be seen stretching between (7-13°N) at longitude (1-2)°E.

In this photograph and those of fig 4.7a, convective systems of various scales can be seen: from deep little systems (isolated Cb clouds) to squall lines and the bigger cloud cluster systems.

be considered below in section (4.vi), following a treatment of the delineation of the ITD influence (Section 4.(v) b)).

b) Delineating the ITD Region of Importance

In order to delineate the meridional extent of the ITD control on precipitation in West Africa, a consideration of the association between a station's precipitation and its position relative to the ITD is essential, i.e. $(\phi_I - \phi)$

where ϕ_I is the ITD mean monthly latitude (degrees) and

ϕ is the station's latitude.

If $(\phi_I - \phi)$ is highly correlated with a station's precipitation, R, the station is within the ITD domain of importance and vice versa.

To investigate this hypothesis, the correlation coefficient, r between $(\phi_I - \phi)$ and R (monthly means) for each station of zone 2, for the IGY, was calculated as shown in Table 4.2 below.

This result, plotted in fig (4.8) shows that except for the Southern stations of Lagos and Bohicon, significant r values exist over the various stations. The Sahel region's stations are highly ITD controlled while a decline in this control takes place as one goes further South from Kandi.

STATIONS	MEAN		STD DEVN.		r	SE	VARIANCE		COEFT OF VARN. %	
	$(\Phi_I - \Phi)^o$	R(cm)	$(\Phi_I - \Phi)^o$	R(cm)	(Corr.Coef)	(Std Error)	$(\Phi_I - \Phi)$	R	$(\Phi_I - \Phi)$	R
1. LAGOS/IKEJA	9	13	5	12	.42	.20	23.72	146.10	57.15	92.19
2. BOHICON	8	9	5	8	.51	.18	23.72	62.20	61.47	89.85
3. TCHAOUROU	6	11	5	10	.59	.16	23.72	95.20	78.27	90.86
4. KANDI	4	9	4	11	.80	.09	19.28	111.85	97.81	116.22
5. NIAMEY	2	6	5	9	.77	.10	23.22	81.35	307.59	155.21
6. MENAKA	-1	4	5	6	.79	.09	20.63	35.03	-786.05	145.93
7. KIDAL	-3	2	5	2	.83	.08	23.72	5.79	-148.58	150.35
8. TESSALIT	-5	2	5	3	.73	.11	23.72	6.81	-95.91	163.61

TABLE (4.2)

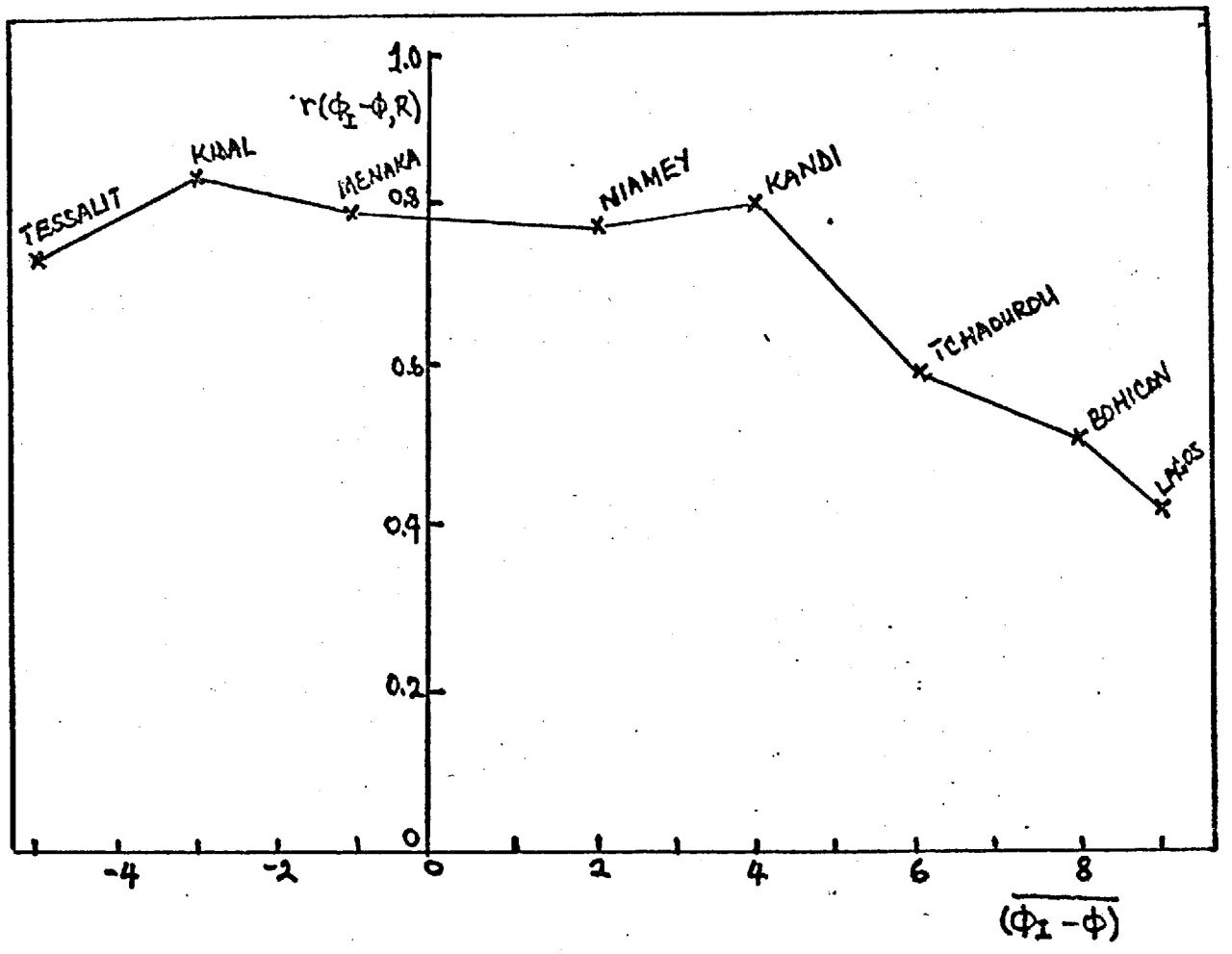

Fig 4.8

The correlation coefficient, r, between $(\emptyset_I - \emptyset)$ amd R for each station of zone 2, plotted against the mean location of the stations relative to the ITD, $(\overline{\emptyset_I - \emptyset})$ for the IGY. A threshold to the significance of r can be noted at 7°S of the ITD.

(a)

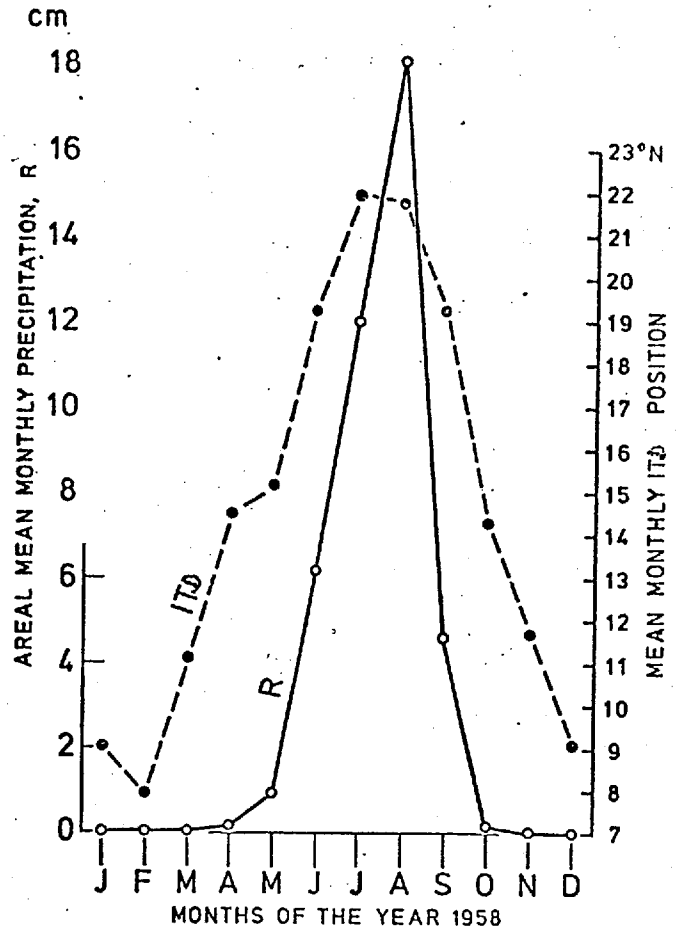

Fig 4.9 (a)

Areal mean monthly precipitation for 10 stations in the Sahel area compared with the mean monthly ITD position, 1958. Stations used are Maiduguri, Kano, Ndjaema (Ex-Fort Lamy), Maine Soroa, Niamey Aero, Zinder, Agadez, Kidal, Bilma and Tessalit (all as in Appendix II).

Fig 4.9(b)

As in fig 4.9(a) but for 1970.

(b)

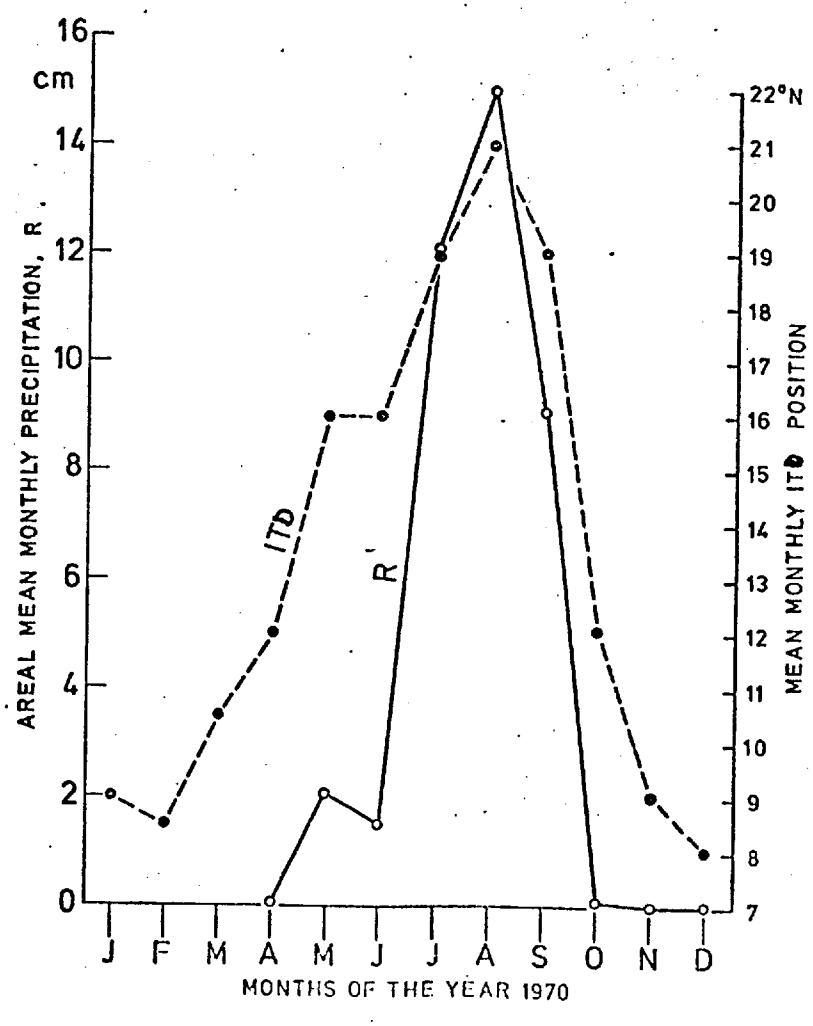

As one goes South of the ITD, the precipitation increases with latitude. However, a threshold exists to this increase as shown by fig. (4.8). This threshold of significance is about 7^{o}S of the ITD (in the mean). About this region, pronounced squall line activities give rise to strong convergence fields which are not related to the usual convergence fields associated with the ITD e.g. see 4.(vi) c) below.

The high r values obtained for stations north of the ITD (in the mean) indicate that though such stations' precipitation may be meagre, their 'lot' is still due to their position relative to the ITD.

A further investigation of the ITD-dependence of the Sahel region's precipitation has been carried out as shown in fig (4.9a) and (4.9b). These show the variations in the areal mean monthly precipitation for 8 Sahel stations and the ITD mean monthly position for the typical wet and dry years (1958 and 1970 respectively as in Chapter II). The quasi-parallel variation existing between the two parameters is indicative of an association between them.

It is, therefore, remarkable to note that while the Sahel environ is ITD controlled, Lagos area is not. Rather, as shown in section (4.(iii) b), this Southern area is influenced by the SO. Added to this, of course, is the effect of coastal convergence and divergence processes as already noted by Ilesanmi (1971) and sea breeze effects. The SO effect is, however, reckoned to be more influential than these.

4.(vi) A CASE STUDY OF AN OCCASION OF MAXIMUM PRECIPITATION IN JULY

In order to study, in more detail, the role played by these different scales of motion, we consider in detail a case study of exceptional rainfall.

Niamey recorded its highest daily precipitation in July of 1958 on the 16th of the month when 31.1mm of rain fell - about $\frac{1}{3}$ of the month's total!

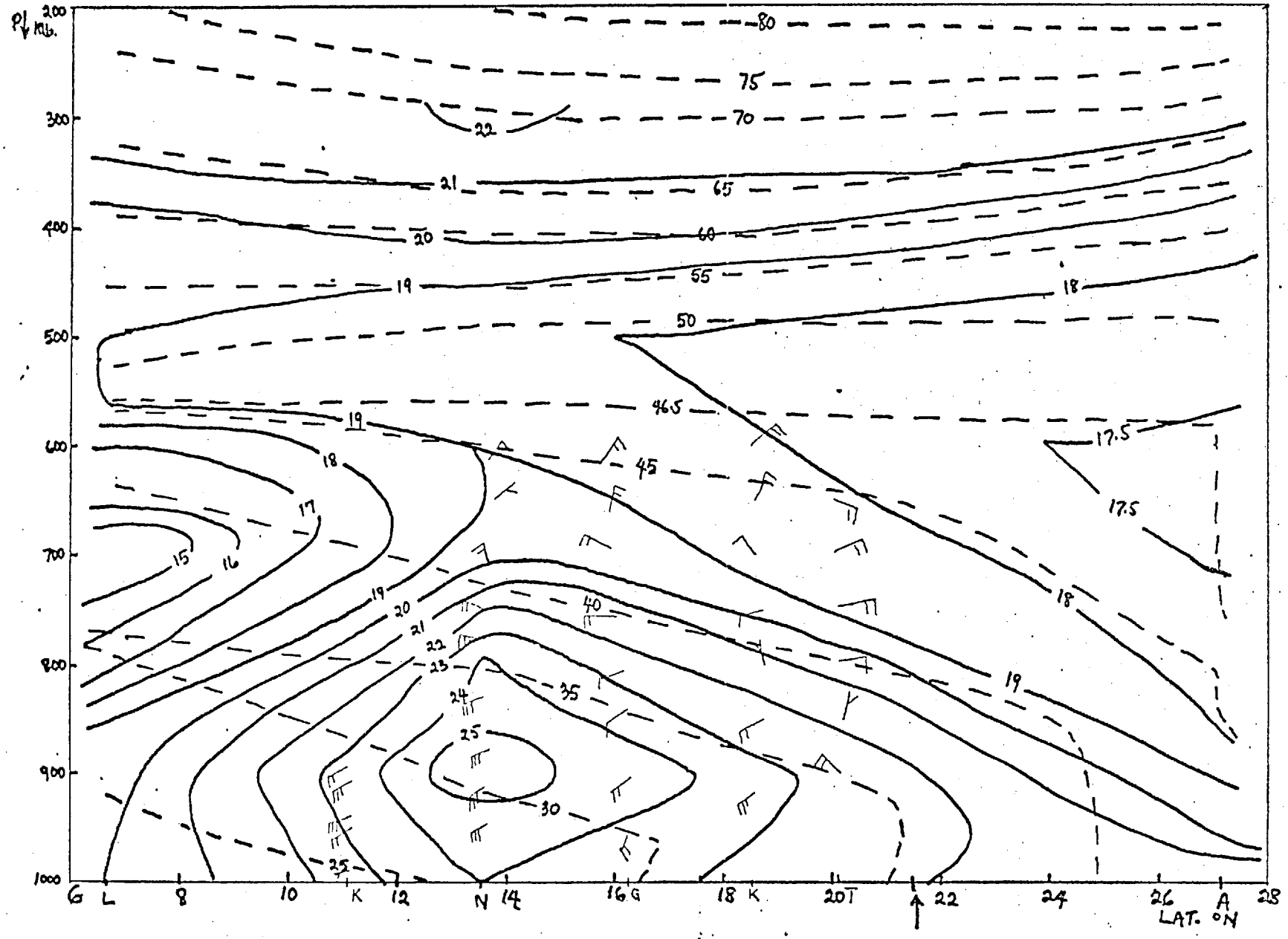

Fig 4.10

A cross-section, along zone 2, of θ_w (°C) solid lines and θ °C (pecked lines) and observed winds (indicated in the conventio al manner) for 06 GMT. (except at Aoulef where only the 11 GMT radiosonde sounding was found), 16 July 1958.

The kink in θ lines is quite remarkable.

a) Early Morning Circulation

The pilot balloon winds and radiosonde temperature and humidity soundings for 06 GMT for various stations (except for Aoulef whose published data was for 11 GMT) have been used to obtain the thermodynamic situation across zone 2 on this day fig.(4.10)

Prominent over the region is the influx of Monsoon air, typified by the high wet bulb potential temperature, $\theta_w \sim 20\text{-}25^{\circ}C$, centred over Niamey, with the winds being SW'ly from the lower levels to about 750mb.

Just to the South of this area could be seen a tongue of dry air ($\theta_w \sim 16\text{-}18^{\circ}C$) situated between 850-600mb. Although the wind observations are not dense enough to show this current, it is likely to be part of the air subjected to cold water upwelling, a typical LDS phenomenon over Lagos area.

A third air type is the hot and dry North Easterly trade winds over Aoulef with $\theta_w \sim 17.5^{\circ}C$.

The ITD is situated at the line of convergence of these three air masses. The convergence is such that the Monsoon air and the NE'ly current meet at the ITD at lower levels while at about 700mb, the three air masses are brought into juxtaposition at the ITD mid-tropospheric surface, the ITD having sloped Southwards with height.

Owing to the sparceness of surface winds, the surface position of the ITD could not be accurately located. However, the temperature and dew point temperature discontinuities can be used to locate it. Such is the nature of the problems the Meteorological analysts have to face in carrying out wind analysis over the Sahara where data are very sparse.

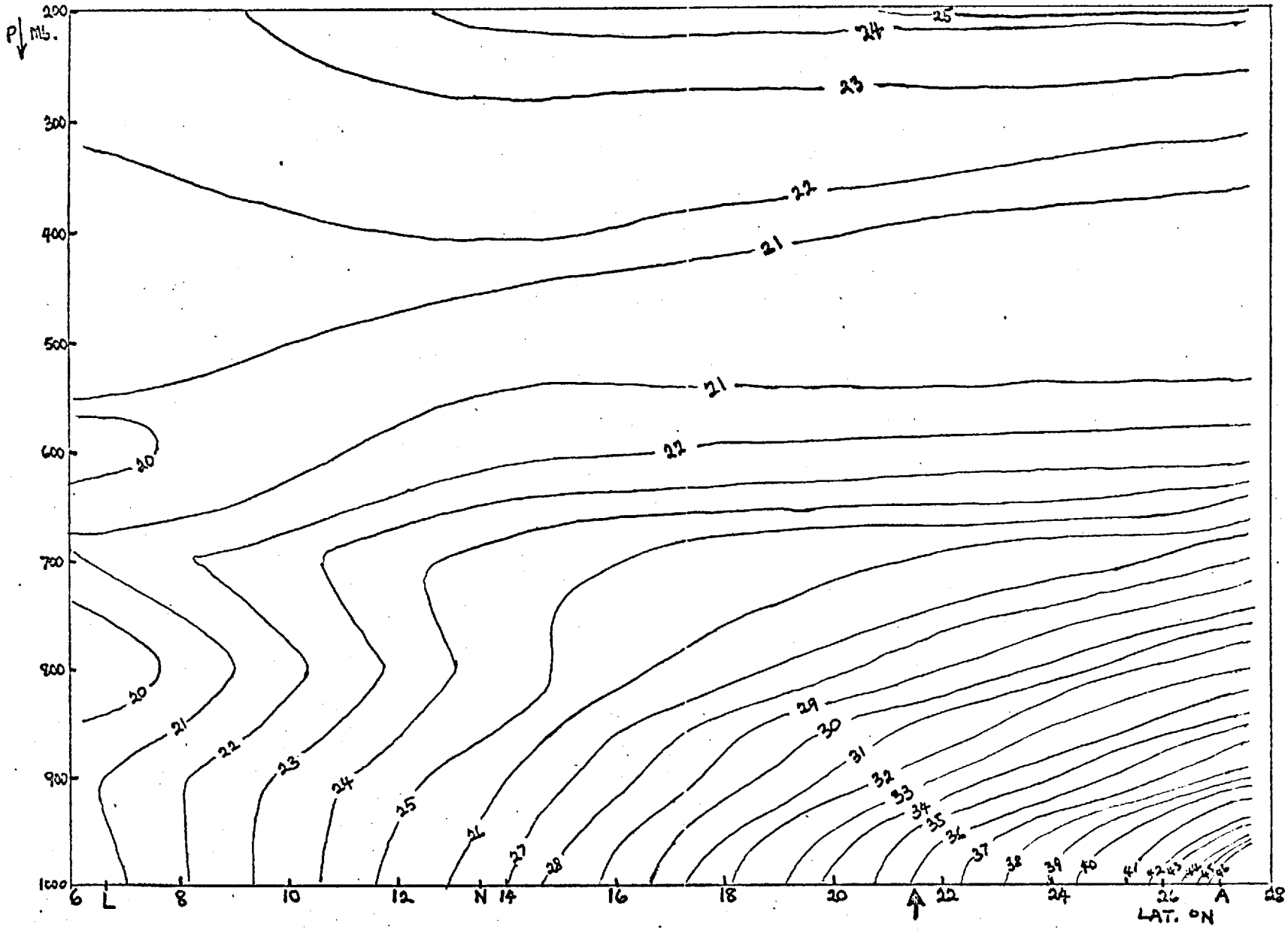

Fig 4.11

θ_s (°C) cross section, similarly obtained as in fig 4.10.

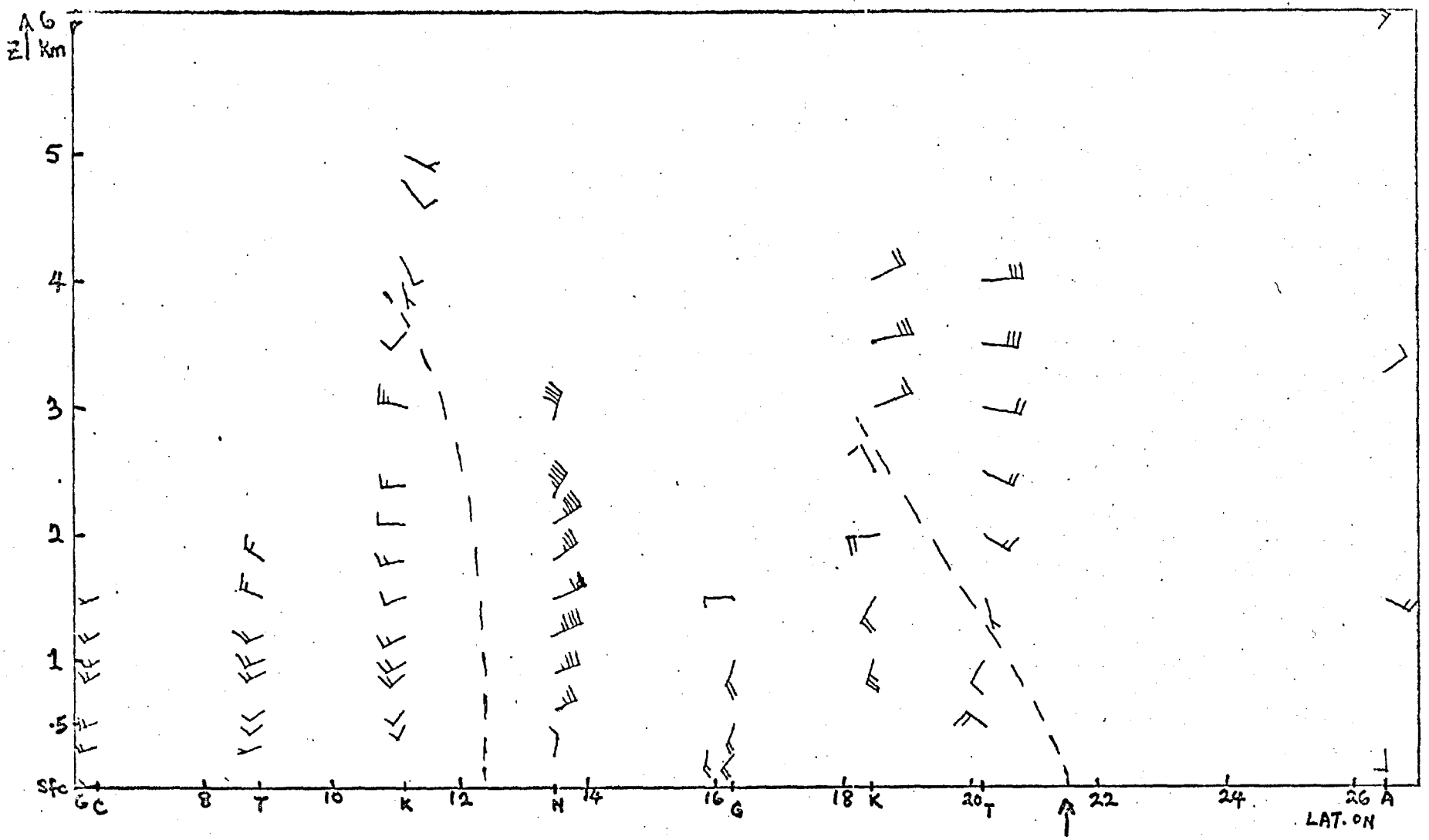

Fig 4.12

The latitude-height cross section of the wind field as observed at 12 GMT, 16 July 1958, showing the Easterly disturbance at around Lat. 12°N.

i) Region of Pronounced Convective/thermal Instability

The cross-section of saturation potential temperature, θ_s for the zone indicates a minimum mid-tropospheric (500mb) value of 21°C but for the Southern sector (Lagos) where a θ_s minimum of 20°C occurs, centred on 800mb (fig. 4.11). The area of convective instability, ACI shall therefore be typified by an averaged θ_w (over the bottom kilometre or two of the Troposphere) greater than 21°C. Encompassed under ACI, therefore, is the region from the ITD to about 10°N.

It can be seen also in fig (4.10) that the isentropes (θ lines) depict a barroclinic region centred over Niamey at lower levels (below 800mb). The thermal wind relation indicates that upper level flow should be Easterly.

b) Advent of the disturbance

By noon, 12 GMT, there has been a considerable development in the wind field as is shown in fig (4.12). Winds over Niamey veered from SW'ly to NE'ly from about 600m to 3km for which recorded data exist. The winds in the other parts of the zone remained virtually unchanged, indicating the narrow extent of this Easterly disturbance. Notice the ITD location.

An analysis of this 12 GMT wind field has been carried out in order to study the associated convergence/divergence and hence, ascending/descending air regions.

The field of zonal (U) component of winds shows an Easterly jet of speed 25m/s centred over Niamey at 1.5 km while weaker centres of Westerly wind maxima (secondary jets) could be seen at 1.2km just South and between 1.5 and 2km just North of the Easterly jet. (Fig. 4.13a)

On the other hand, the meridional cross-section fig (4.13b), shows a Northerly jet of speed 17.5 m/s at 2.75km over Niamey and

Fig 4.13(a)

The Zonal (U) component of the winds (m/s) of fig 4.12 (solid if positive pecked if negative).

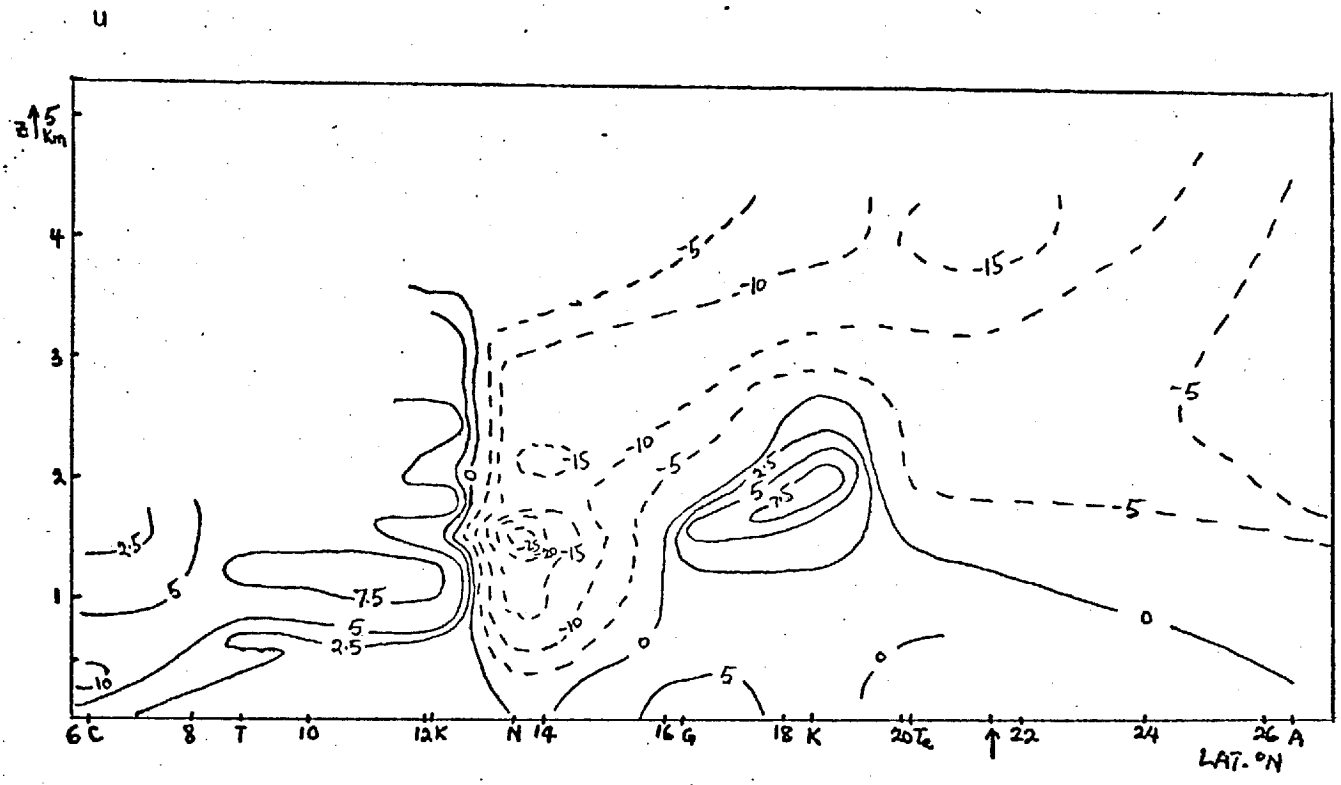

Fig 4.13(b)

The meridional (V) component of the winds (m/s) as obtained from fig 4.12.

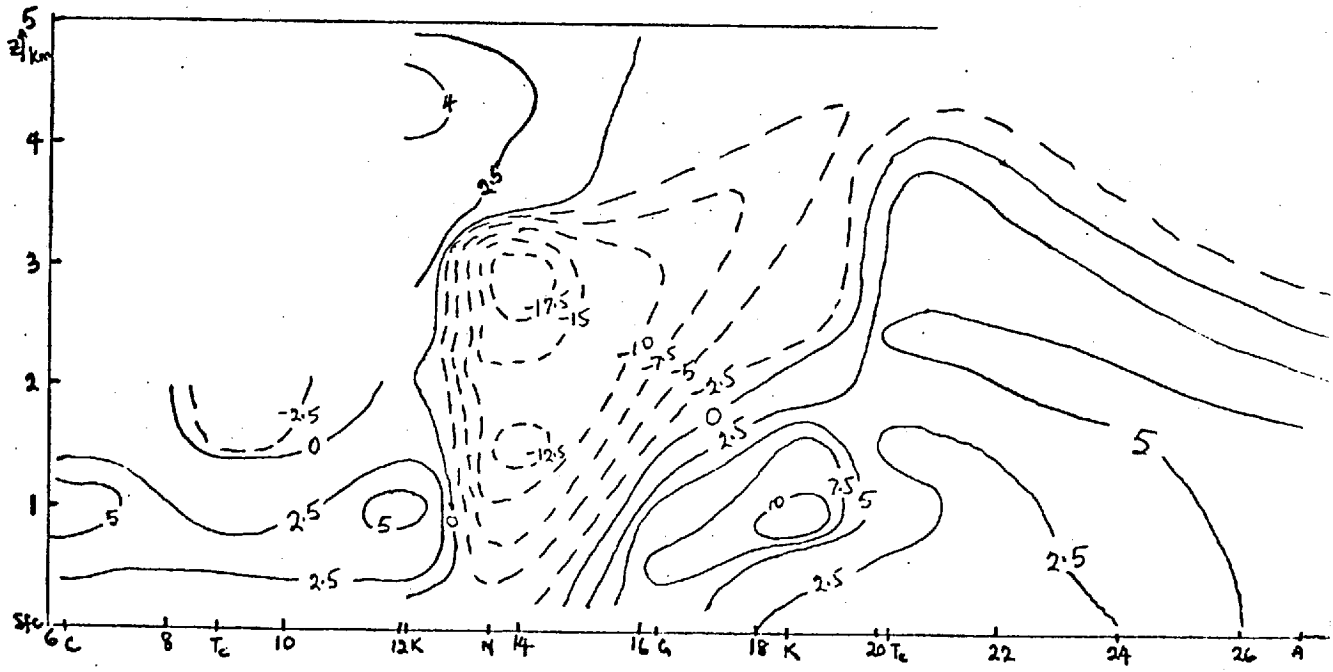

Southerly winds in nearly every where North and South of the (13-16)°N zone of disturbance, with a low-level micro jet (V~ 10 m/s) just South of the ITD.

c) <u>The Divergence Fields Associated with the disturbed ITD Environment</u>

The continuity equation is given by:

$$\frac{\delta\rho}{\delta t} + \rho \operatorname{div} \underset{\sim}{V} = 0 \qquad \ldots\ \ldots\ \ldots\ 4.7$$

For an incompressible atmosphere, the first term in equation 4.7 vanishes, leaving :

$$\operatorname{div} \underset{\sim}{V} = 0 \quad \text{after dividing through by } \rho.$$

Now,

$$\operatorname{div} \underset{\sim}{V} = \frac{\partial u}{\partial x} + \frac{\partial v}{\partial y} + \frac{\partial w}{\partial z}$$

$$\therefore \frac{\partial w}{\partial z} = -\left(\frac{\partial u}{\partial x} + \frac{\partial v}{\partial y} \right)$$

$$\ldots\ \ldots\ \ldots\ 4.8$$

after integrating, with respect to Z, equation 4.8, we obtain:

$$w = -\int_0^z \left(\frac{\partial u}{\partial x} + \frac{\partial v}{\partial y} \right) dz \qquad \ldots\ \ldots\ \ldots\ 4.9$$

From the surface weather chart of 6 GMT, 16th July 1958, (fig. 4.18) the distribution of the isobars around longitude 3°E, is such that $\partial u_g \sim .02$ m/s over 100km. (Using geostrophic approximation to estimate ∂u over the area between longitude 0° to 5°E and latitude 10°N to 15°N).

∂v_g , similarly obtained was 0.12 m/s over 100km (but for latitude 13°N - 18°N).

in equation 4.9, $\frac{\partial u_g}{\partial x}$ can, hence, be neglected compared with $\partial v_g / \partial y$

Therefore $w \sim -\int_0^z \left(\frac{\partial v}{\partial y}\right) dz$

.. .. .. 4.10

The resulting approximate divergence $\left(\frac{\partial v}{\partial y}\right)$ fields, though, rather complex, satisfies the continuity condition, as areas of divergence are separated by areas of convergence in a manner systematic with respect to the available data coverage fig. (4.14).

Just south of the ITD could be noticed an area of low-level convergence, running up to 1.9km from where divergence takes over running up to 4km level. North of the ITD, low-level divergence up to 1.9km, is topped by an area of convergence running up to 3km.

Just north of the disturbance, between Niamey and the latitude of Gao, could be seen an area of divergence, running up to 3.8km with a prominent Northward sloping axis.

Between Kandi and Niamey, the region of the disturbance is marked by a deep layer of convergence running from surface to 4km. South of this is another area of divergence, apparently balancing the coastal convergence existing around the near coastal area. A two-level integration of these divergence fields yields the vertical wind distribution shown below. Fig.(4.15).· Consistent with expectation, areas of wind convergence are typified by ascending (+ W) while those with divergence are typified by descending (-W) motion. Areas of ascending air are compensated by adjacent areas of descending air, maintaining continuity of mass.

In the atmosphere, ascending air motion leads to cloud formation, if the air reaches the condensation level where condensation of water vapour on the dust and other hygroscopic nuclei present in the air takes place. The latent heat released in the process is used to provide the cloud the energy needed to grow further into the atmosphere. Descending air motion, on the other hand, suppresses convection and gives rise to fair weather as is typical in anticyclonic situations prevailing North of the ITD.

Fig 4.14

The divergence fields given by $\frac{\partial v}{\partial y}$ (in units of 10^{-5} s^{-1}) obtained from the available wind observations. Regions of convergence have been shown(stippled), marked C. Areas of divergence have been marked D. The ITD position has been indicated as usual with an arrow.

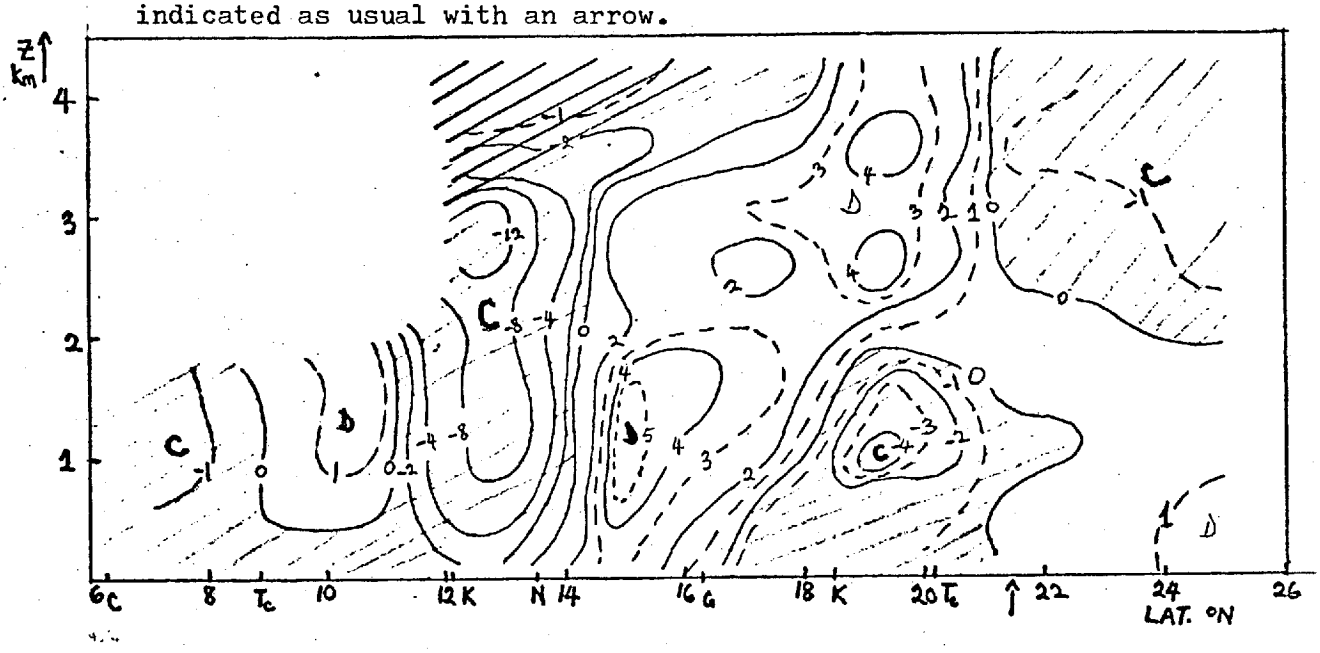

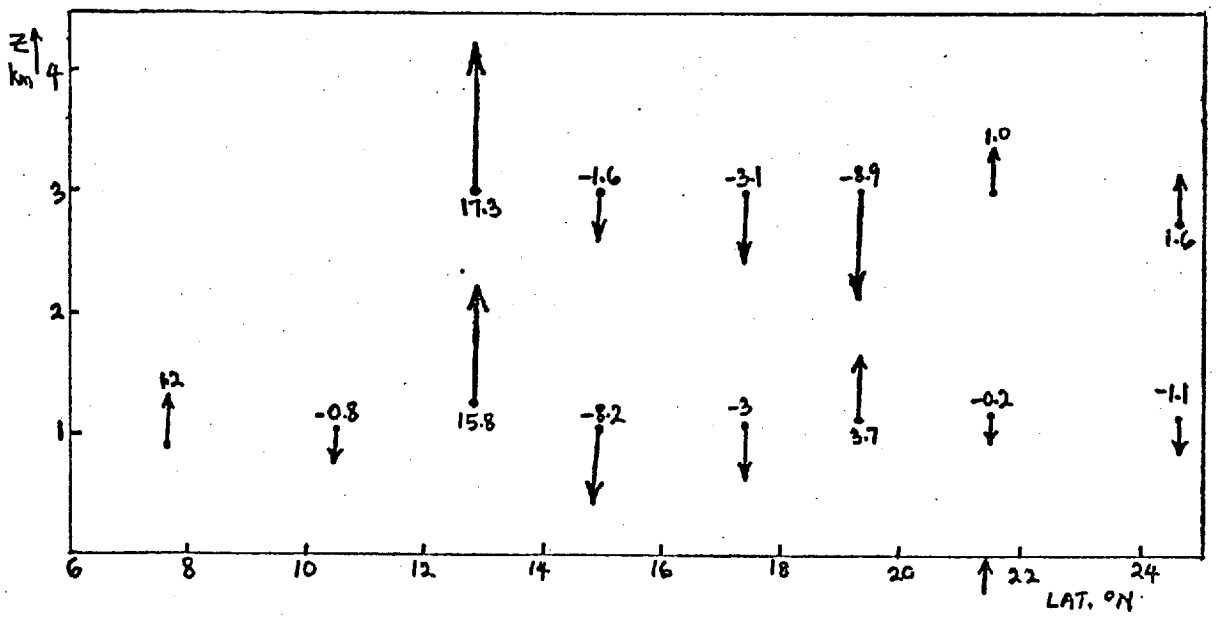

Fig 4.15

The vertical (ascending/descending) motion indicated by ω (in units of cm/sec). Rising motion occurred in areas of convergence and descending motion in areas of divergence. The strong updraft rising into the disturbance (near lat. $13^{\circ}N$) is remarkable.

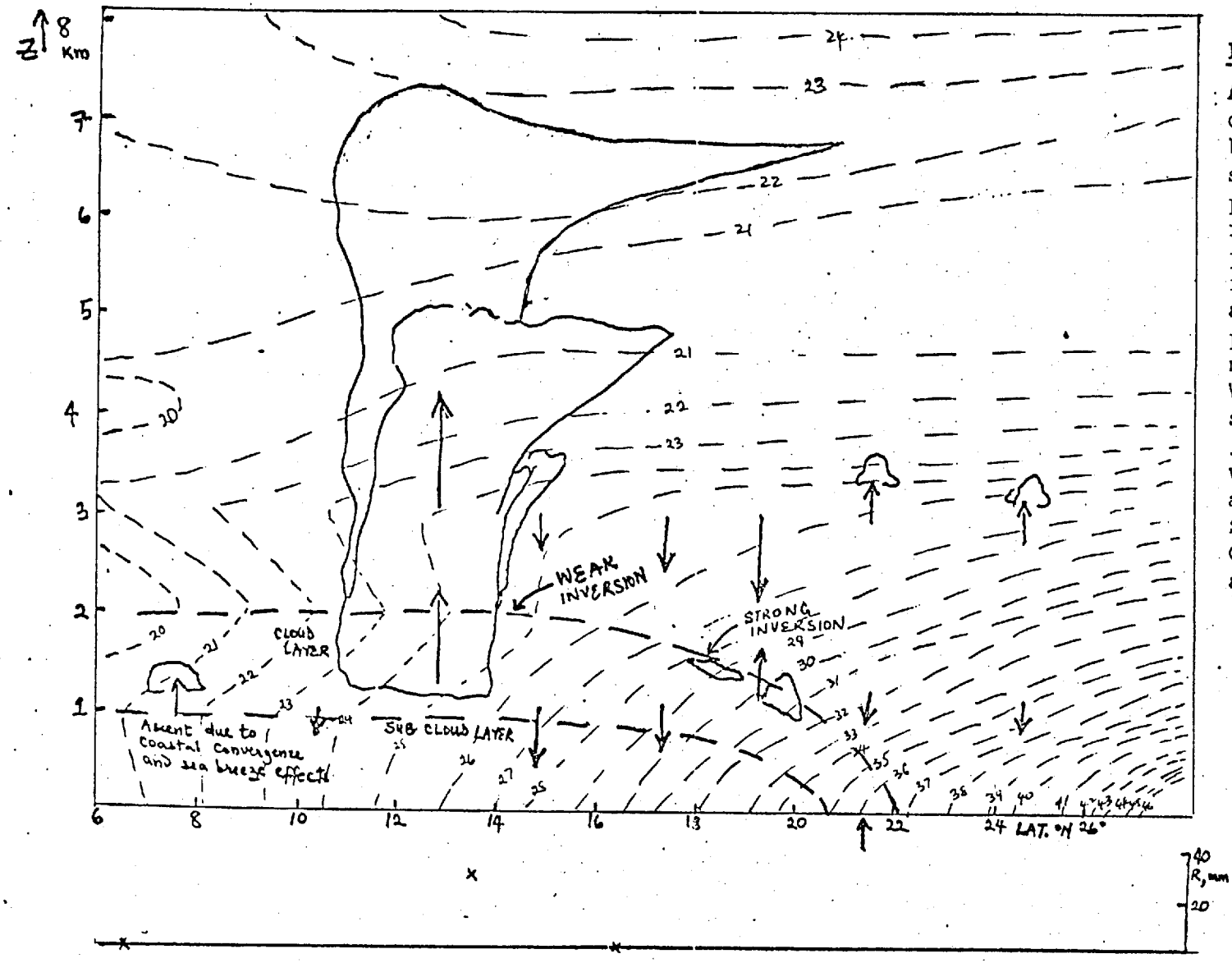

Fig 4.16

A sketch of the cloud distribution suggested by the thermodynamic structure of the atmospheric environment - indicated by θ_s °C (light pecked lines) - and the field of divergence associated with the prevailing winds for mid-day, 16th July, 1958. While strong inversion suppresses convection just south of the ITD a weak inversion prevails about (7-10)° further South, allowing strong Cb and squall activity as on this occasion.

d) The Cloud distribution suggested by the thermodynamic structure and Divergence fields

The thermodynamic structure of the atmosphere considered along with the mechanically (frictionally) induced divergence fields obtained, suggest a cloud distribution pattern shown in fig (4.16).

North of the ITD, little or no cloud exists owing to the effect of the low-level subsidence prevailing there. Just South of the ITD, a considerable ascent takes place but there is a higher level descent which suppresses whatever convection might have been generated at lower levels. At the layer above which Cu clouds resulting from this convection are contained, there is a strong inversion acting as a lid over the systems.

This so called 'trade wind inversion' (Riehl, 1954) is found over much of the region but its depth increases as one moves South of the ITD. Before Cb clouds capable of yielding substantial precipitation can be formed, the Cu Strato Cu or Cu Congestus Clouds should be strong enough to break through the inversion and rise into the Upper troposphere. The kind of strong updraught capable of effecting this is only found about 7^{o} South of the ITD. This has resulted from Easterly disturbance passing over Niamey. This area is centred in the ACI and has got the right conditions for Cb activity.

South of the Niamey area of disturbance is a subsidence region apparently compensating the ascent due to coastal convergence and sea breeze effect just South of it. As this period falls within the LDS, general large scale suppression of convection takes place in the Lagos environment then.

A calculation of the precipitable water obtainable over the three upper air stations for which data exist shows that maximum precipitable water of 5.1cm exists at Niamey. This is followed by Lagos with 3.3cm and Aoulef, 1.6 cm fig. (4. 17)

However, Niamey experienced a downpour of 31.1mm that day. That this is lower than the precipitable water is quite reasonable as all the

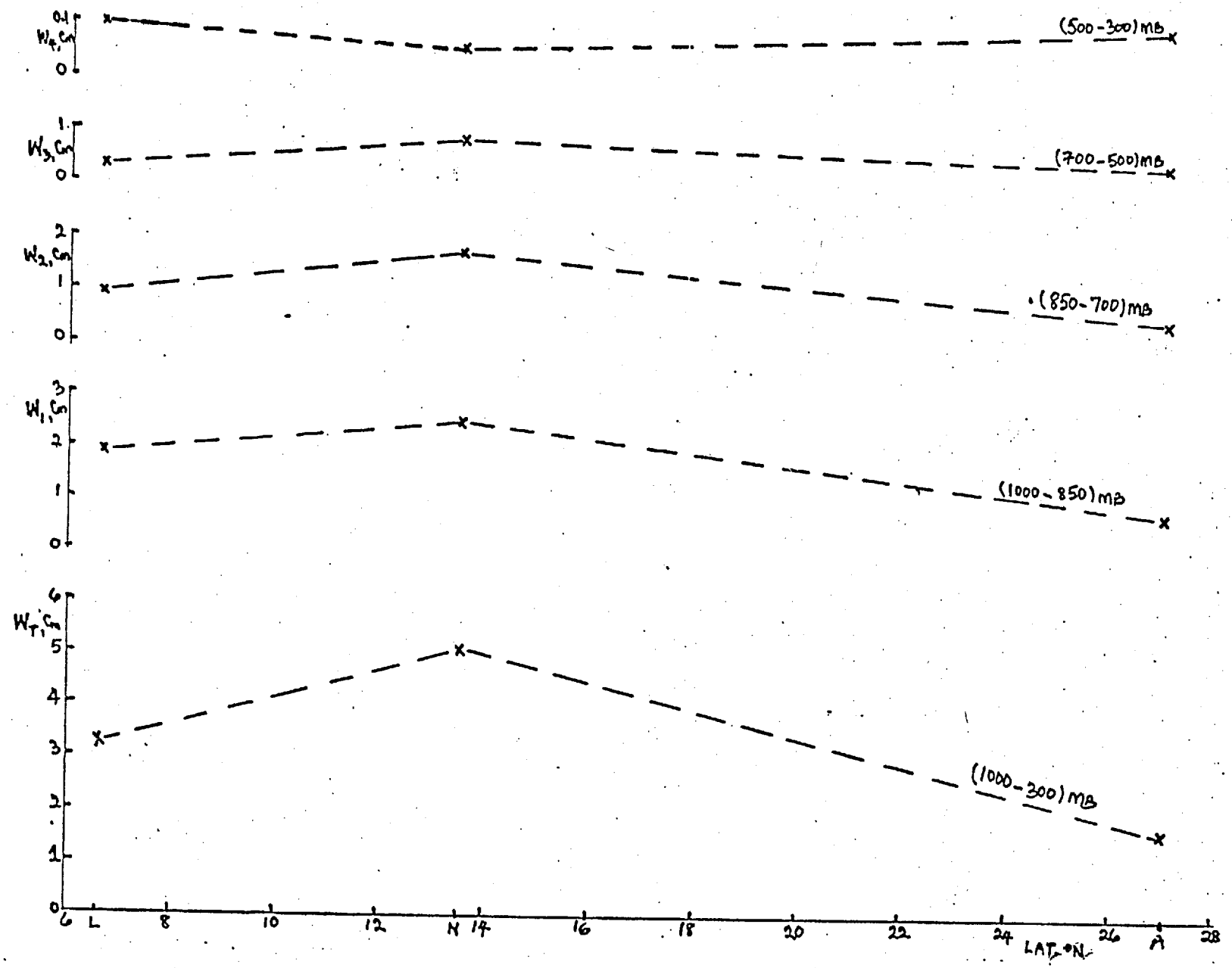

Fig 4.17

A cross-section of the precipitable water (cm) available in the atmosphere, July 16, 1958.

available water in the atmosphere cannot, normally, fall out as rain in one day. Mixing and evaporation of the cloud water within the environment, turbulence and other processes the details of which we shall not consider here, come into play, reducing the amount that fall as rain.

e) The Synoptic situation

The synoptic situation as at 6 GMT, 16th July, 1958, is as shown in fig (4.18). The ITD is seated on the warm low situated over the region with higher pressures North and South of it.

Situated between 7-10° South of the ITD (between latitudes 10 and 14°N) is a squall line, identified as L10, followed by a second one 5° East of it.

Further tracking of L10 indicated that by 18 GMT, it has moved 6° Westwards, giving it a speed of 14 m/s which agrees typically with the speed of other squall lines studied in the USA (Moncrieff and Miller, 1976). Assuming the second squall L travels at the same rate, it would arrive at Niamey by 11-12 GMT, 6 hours later. This is consistent with the mid-day wind observation plotted in fig (4.12).

The Easterly disturbance experienced over Niamey zone can, therefore, be identified as the squall L which dogs the squall L10 in their Eastward propagation across the region.

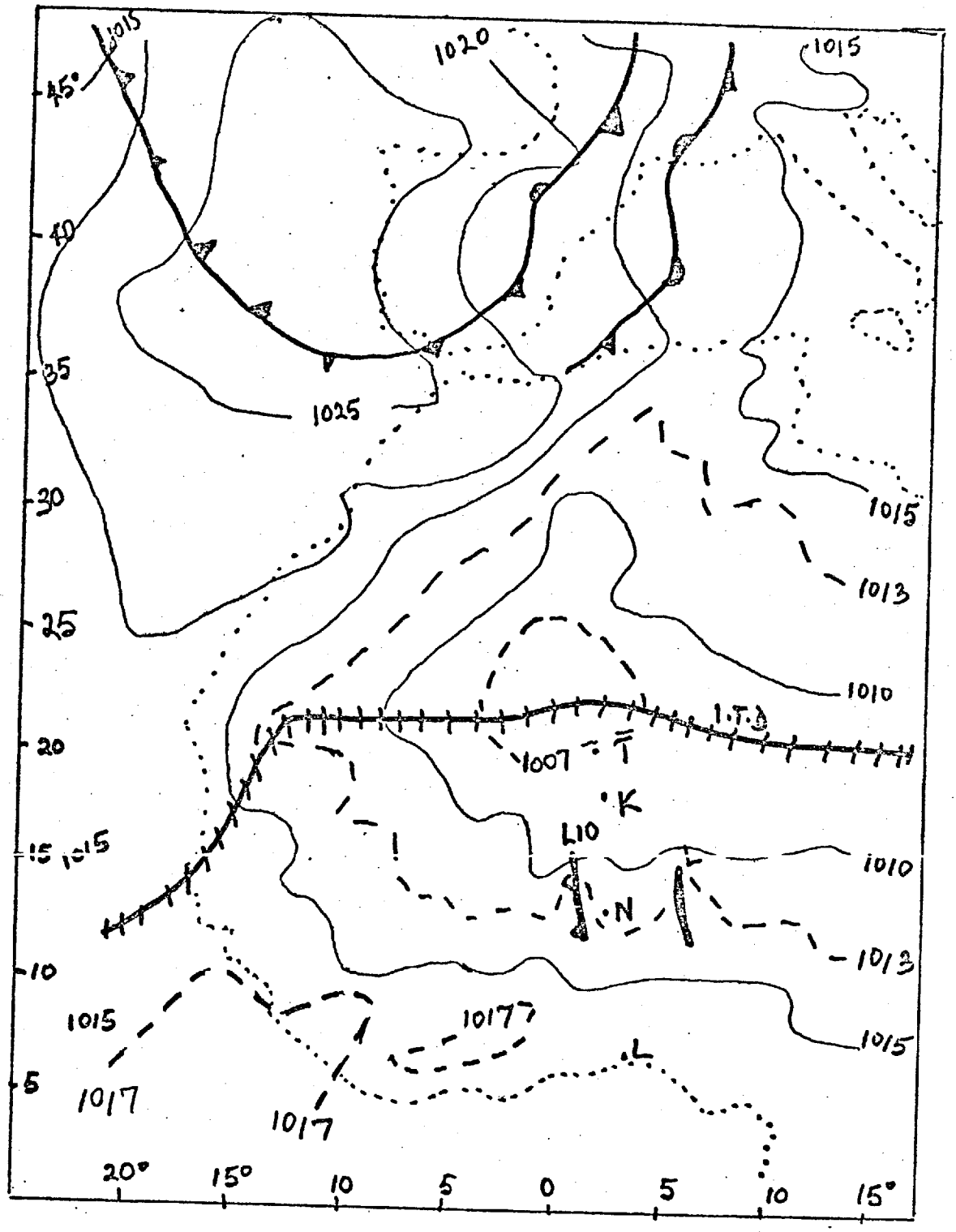

Fig 4.18

The synoptic situation existing over the region as at 6GMT 16 July 1958. The surface pressures (in mb) are indicated along with the squall line L10 and another line, L. (After Service Meteorologique de L'etat (Afrique Occid. Francaise) 'Bulletin Quotidien D'Etudes' Paris).

f) The Role of shear in the growth of the squall

The wind shear plays an important role of effecting the necessary convective over-turning required for the release of the available potential energy, APE, stored in the bottom (convective) layer of the atmosphere. This role has been considered in dynamical models of cumulonimbus systems in mid-latitudes (Moncrieff and Green, 1972) and in the tropics (Moncrieff and Miller, 1976) hereafter MM).

In MM, the fact that the tropical squall line propagates relative to the wind everywhere, unlike the mid-latitude cumulonimbus systems which propagate nearly at the speed of the mean flow and the characteristic tropical wind profile - having a mid-level easterly shear layer separating a low-level and an upper-level Westerly shear layer - make the flow field of these tropical systems different from those of the Mid-latitudes.

A perturbation, grown as a Cumulus cloud in the numerical experiment in MM, moved with the mean current in the convective layer of Easterly shear up to the layer of Westerly shear as a cumulonimbus cloud (Cb). The strong downdraught resulting from the decay of this Cb cell propagated as a density current. The low-level boundary layer convergence resulting from the outflow of this system initiated 'second generation Cb' comprising the squall line.

The observed wind profiles before, during and after the passage of the squall line under study in this work is as shown in fig (4.19), as revealed by the radiosonde and pilot balloon (PIBAL) observations carried out at 06 GMT (before), 11 GMT (during)and 17 GMT (probably after) the squall passage over Niamey on 16th July, 1958. It is worthwhile to note that:

1. Before the squall arrived at Niamey, the zonal wind component (in a direction opposite to that of the squall propagation) shows a Westerly shear at the lower levels, between the surface and 3km, reversing to an Easterly shear from 3km to 9km above which the shear goes Westerly again. The meridional component indicates a low-level Southerly shear reversing through Northerly at mid-levels to Southerly again at upper levels.

Fig 4.19

The wind profiles obtained over Niamey for 06, 11 and 17 GMT, 16th July, 1958.

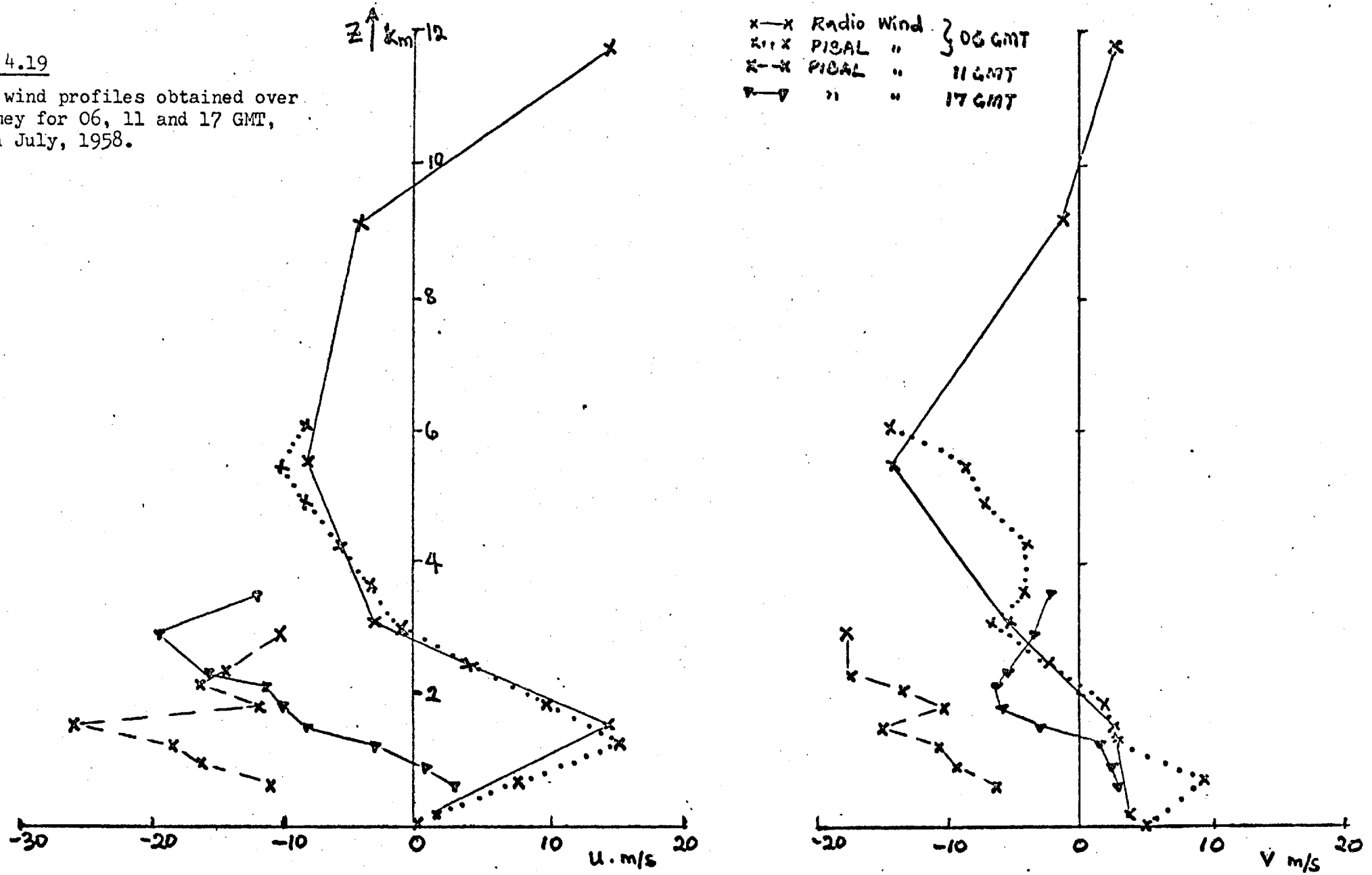

2. With the coming of the squall, a near 180° reversal in the direction of the low-level shear (from Westerly to Easterly) takes place, giving rise to increased Easterly momentum at lower levels.

A change from low-level Southerly to low-level Northerly shear is also noticed in the meridional component of winds (in a near-transverse direction to the storm propagation).

3. Conditions 6 hours after the squall passage show increasing Westerly and Northerly momentum, an effect of the modification of the environment by the squall. This agrees with the dynamic results of MM which indicates increased Westerly momentum at lower levels.

However, the mid-level and upper level winds are not available, neither are the thermodynamic (temperature and humidity) sounding during and after the squall available. This makes comparison with other aspects of MM difficult.

In addition, it is not known precisely when the squall stopped. However, the 18 GMT weather chart indicated, fig (4.20), that while squall L1O has moved 6° West of the 06 GMT position, the second squall L, behind it, has disappeared, having possibly dissipated away.

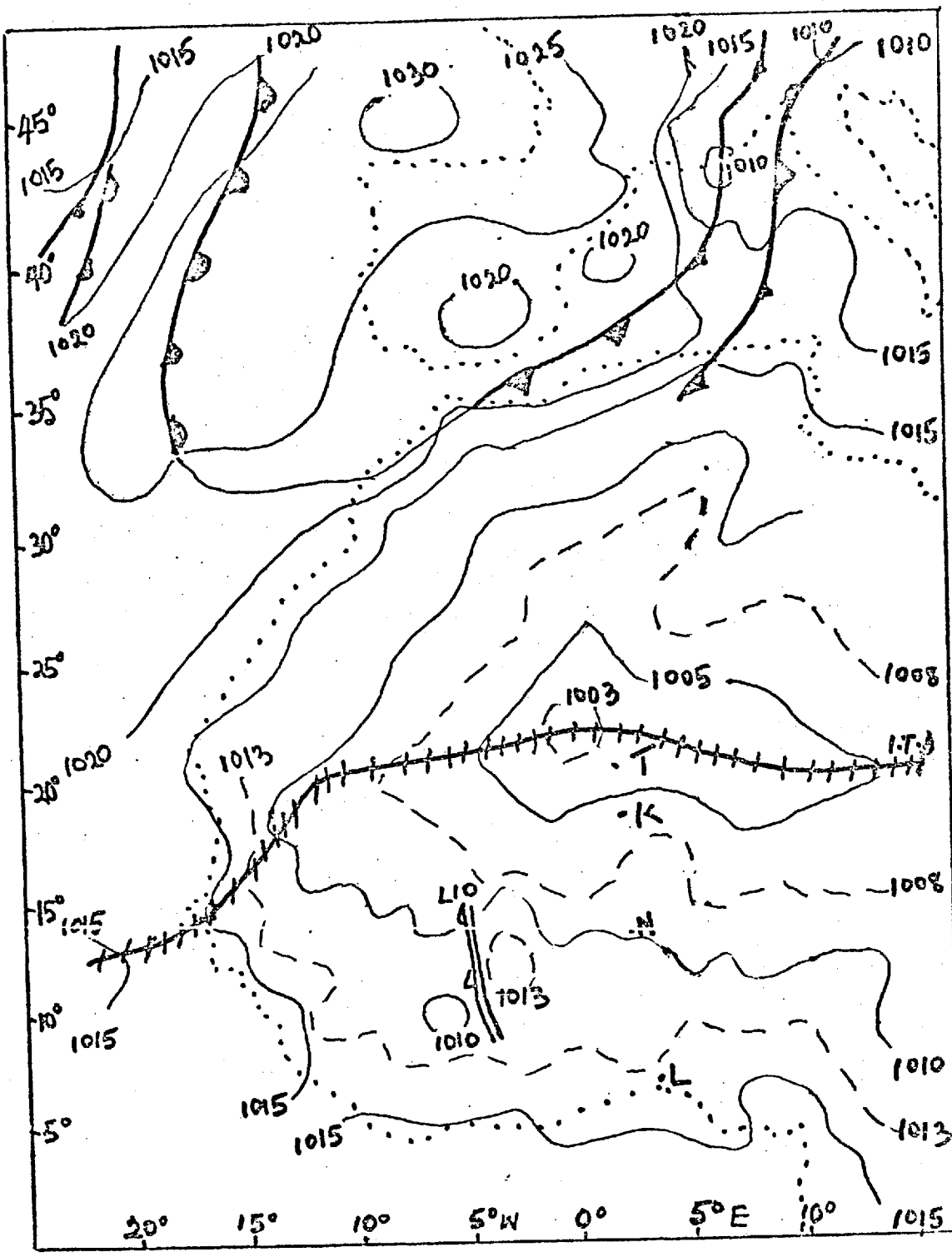

Fig 4.20

As in fig 4.18 but for 18 GMT 16th July, 1958.

(g) SUMMARY

Prior to the advent of the Esterly disturbance, three air masses met at the ITD: the Monsoon and the NE'ly current at lower levels and a third air mass (probably from the descending branch of the Walker circulation) met with them at 700mb, the ITD sloping Southwards.

At the advent of the disturbance, the wind veered from SW'ly to NE'ly over Niamey and a strong and deep zone of convergence developed there. The cloud distribution suggested by centres of convergence and divergence of air, agrees with the pattern suggested by the θ_s structure of the atmosphere: the squall, as synoptic charts portrayed the disturbance to be, occurred in the Monsoon current 7^{o}S of the ITD where the trade wind inversion (Riehl,1954) was weak enough for the strong updraught generated by the wind convergence to break through.

The Niamey wind profiles obtained before, during and after the squall passage show:

1. A low-level and an upper level Westerly shear separated by a deep layer of Easter shear.

2. A near-180^{o} reversal in the direction of the low-level shear, spelling increased Easterly momentum at lower levels at the advent of the squall and

3. An increased Westerly momentum, a modification of the environment; in agreement with the dynamic results of Moncrieff and Miller, 1976.

The maintenance of the squall wind shear (fig. 4.19) requires the establishment of a strong Easterly flow over a moist layer of Westerly flow. The squally weather is associated with the disturbances in the Easterly flow whose strength depends on the strength of the temperature contrast between the Saharan and the Guinea regions as point out in 4.(iii)b.

4.(vii) CONCLUSION

Global scale circulation systems studied include the ITCZ with due reference to its synoptic manifestation at the IGY and the Walker Circulation, the descending branch of which is responsible for the dryness of the Ghana coast. The Walker Circulation is strengthened by pronounced upwelling of cold water, a mechanism that can increase the thermal contrast between the hot Saharan region and the cooler South, thus, by thermal wind relation, increasing the Easterly flow aloft. A consequential increase in Easterly wave and squall frequency can thus be effected. The reverse holds as anomalous increase in ocean temperature (weak WC situation) can decrease this thermal contrast, giving rise to decreased Easterly wave and squall line activity and consequent drought in the Sahel.

A negative correlation, ($r \simeq -0.41$) has been obtained between the June - August precipitation at Lagos and the (September - November) SO index (as calculated by P Wright, 1975).

Some features of the regional (ITD) circulation has been studied and the scales of convective processes within its environment, discussed. The ITD control on the precipitation is high over the Sahel but this control declines as from about 7°S of the ITD down to the LDS region.

Hence, while the ITD controls precipitation in the Northern sector, the SO influences the Southern part.

A case study of an occasion of maximum daily precipitation over Niamey (16 July, 1958) has been studied. It was found that an Easterly disturbance (a squall line) occurring 7° South of the ITD gave rise to a strong low to mid-level convergence around Niamey and consequently, strong vertical motion. This resulted in strong Cb activity and heavy rain.

The wind profiles associated with the squall evolution indicated increased easterly momentum after its passage, a modification of the environment similar to that predicted by Moncrieff and Miller (1976)'s dynamical model.

OCEAN-ATMOSPHERE INTERACTION/BIOPHYSICAL FEEDBACK MECHANISMS CONTROLLING THE SAHEL PRECIPITATION

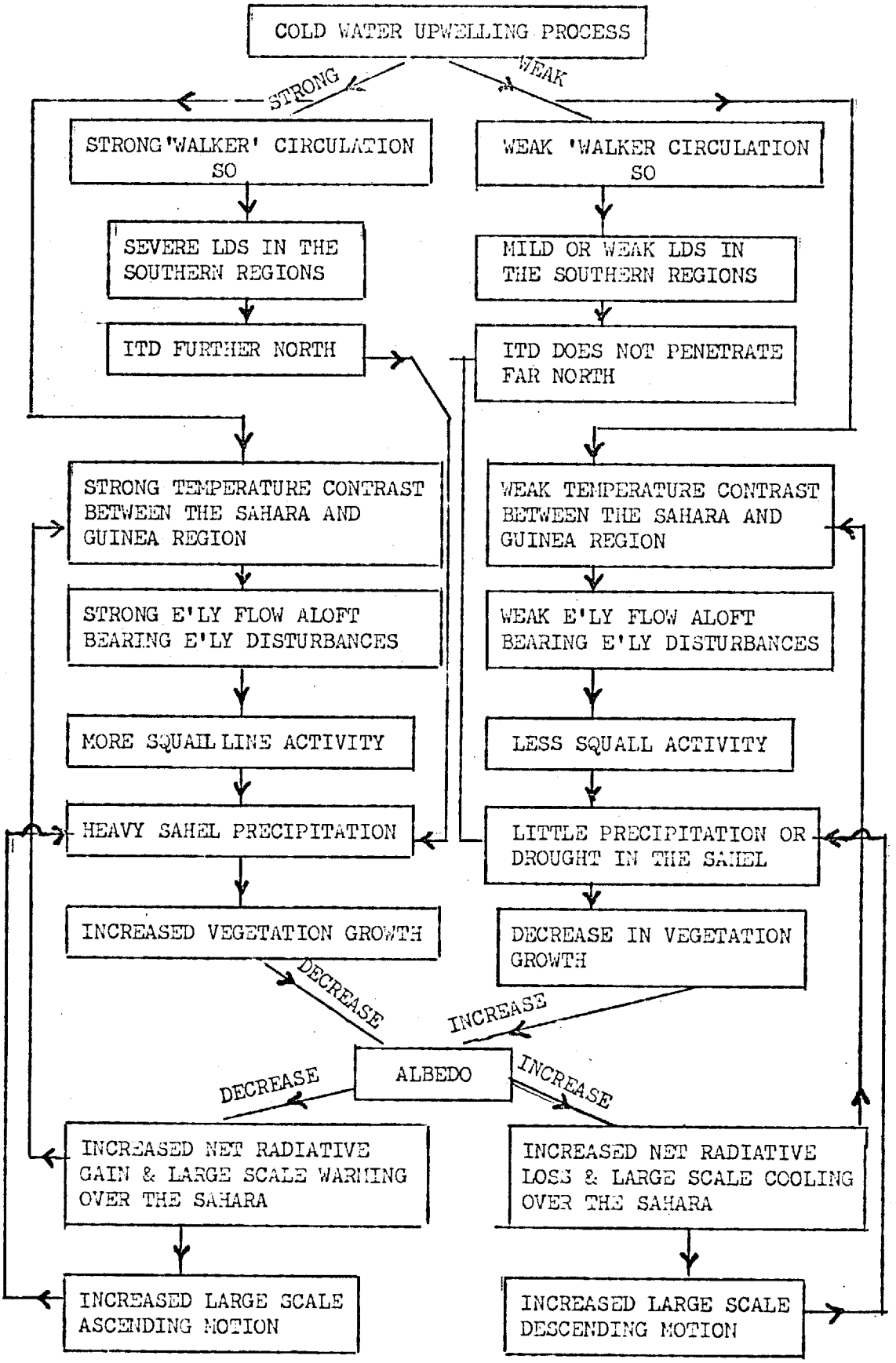

CHAPTER V

INVESTIGATION OF OCCASIONS OF CONVECTIVE INSTABILITY RELATIVE TO THE ITD

5.(i) INTRODUCTION

In Chapter IV (section 4.VI), we considered an occasion of maximum July precipitation in Niamey. That case study of squall line activity was associated with considerable convective and dynamic instability South of the ITD. In this chapter, we shall study occasions of convective instability relative to the ITD, relating them, wherever possible, to occasions and amount of precipitation on various time scales - monthly and daily (for various seasons).

To this end, an instability index, I, is defined, which takes account of two levels of the atmosphere crucial in consideration of free convection:-

a) A level at which energy if fed into the atmosphere for setting off the convection and

b) a level (mid-tropospheric environment) containing the convective systems.

This index has been evaluated over Lagos/Ikeja, Niamey and Aoulef and then plotted relative to the ITD position for each month of the year 1958 using the monthly mean radiosonde soundings. About 223 daily soundings as available for April, July, August and September 1958 have been similarly examined. The results for the daily soundings for April August and September are presented as relevant to the advancing ITD (pre-Monsoon), the Monsoon and the retreating ITD seasons respectively.

5.(ii) STRATIFICATION OF THE ATMOSPHERE

A mean thermodynamic profile of the Niamey atmosphere for May, 1958 in the wet year, is as shown in fig (5.1), featuring :

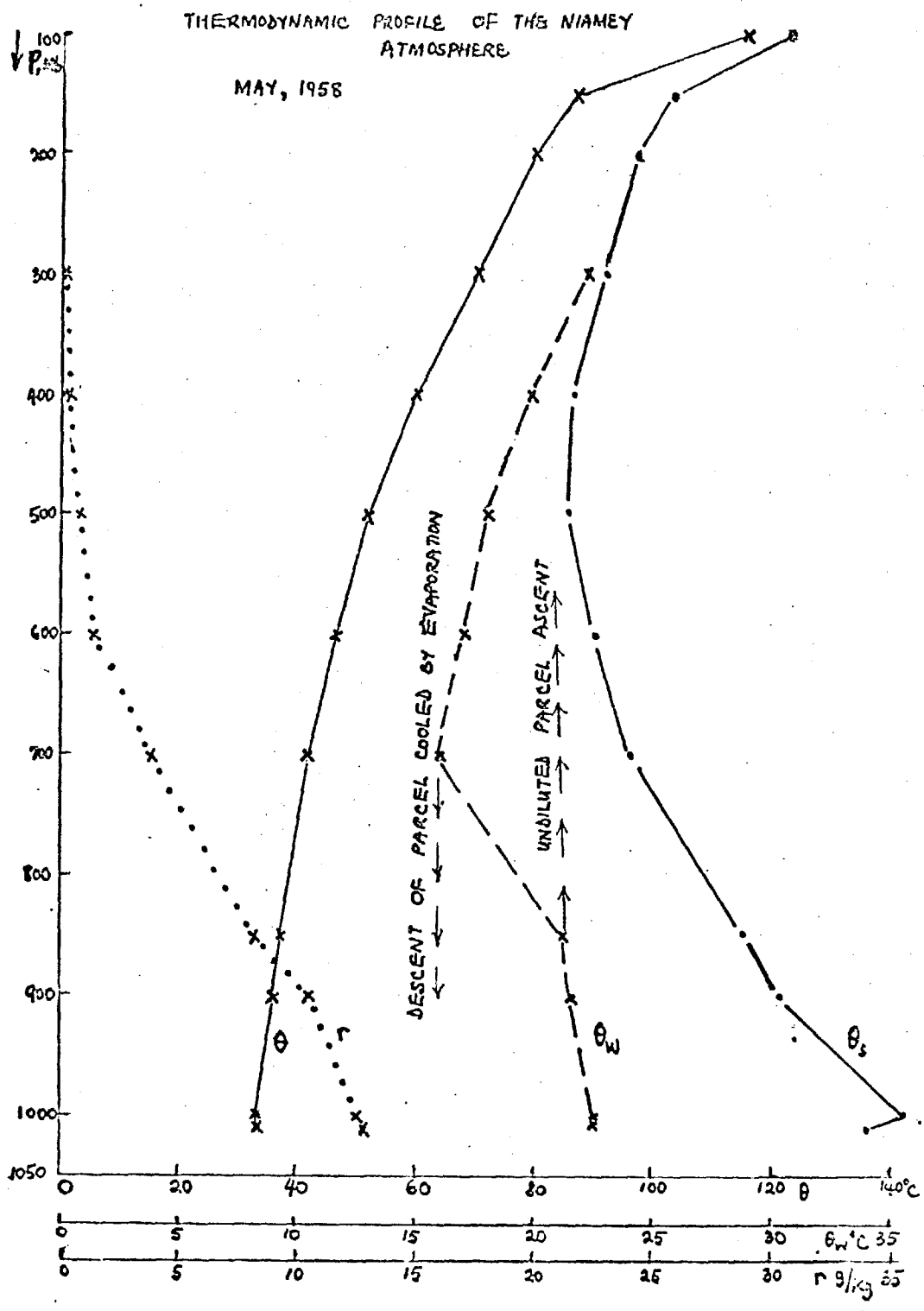

Fig. 5.1

The mean vertical thermodynamic profile of the Niamey Atmosphere, May, 1958, illustrating the interplay of entrainment and the mechanism of cooling by evaporation.

a) A quasi-super-adiabatic layer near the surface,

b) a quasi-constant θ layer (adiabatic layer) from 1000mb to 850mb from where θ_w decreases to a minimum at 700mb. θ_w rises again with height from the 700mb level.

c) A θ_s - minimum exists at the mid-troposphere ($\sim$ 500mb) level.

As shown by Darkow (1968) in his study of total energy environment of severe storms in the United States, if 'entrainment effects' are absent, a parcel rising from the surface continues up into the troposphere undiluted (θ_w constant). However, 'cooling by evaporation' gives rise to descent of the cooled parcel. This cooling by evaporation can be particularly noticed in downdrafts associated with tropical squall lines. (Zipzer, 1969).

As here shown, fig. (5.1), by the ascending and descending arrows, undiluted parcel ascent could continue from the 850mb level upwards (along constant θ_w) but because of the tropospheric adiabatic cooling evidenced in the atmosphere from the 850mb to 700mb level at this time when the Monsoon is just setting in - this could be higher up as the Monsoon current deepens (e.g. fig. 5.2) - the rising parcel tends to descend from around the 700mb level. The convective over-turning resulting from this process releases considerable available potential energy, a crucial requirement for steering the convection.

The static energy of a parcel, neglecting the small contribution due to kinetic action, is:

$$Q = C_p \theta_w \qquad \ldots\ \ldots\ \ldots \quad 5.1$$

Where C_p = specific heat of air at constant pressure.

A wide region of adiabatic cooling, Q minimum and constant, is between 700 - 600 mb (fig. 5.2) for August 1958, the month of maximum

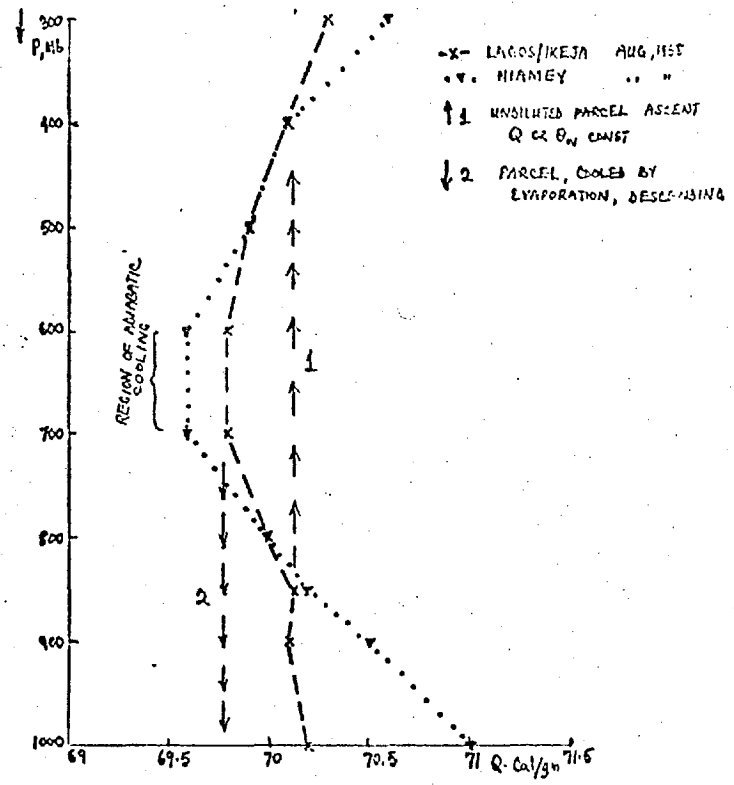

Fig. 5.2

The vertical profile of static energy Q(cal/gm) for Lagos/Ikeja, (in dashes) and Niamey, (in dots) both for August 1958.

Fig. 5.3 (below)

The vertical profile of static energy, Q(cal/gm) for Niamey, 06GMT 16th July, 1958 prior to the advent of the squall line of Chapter IV.

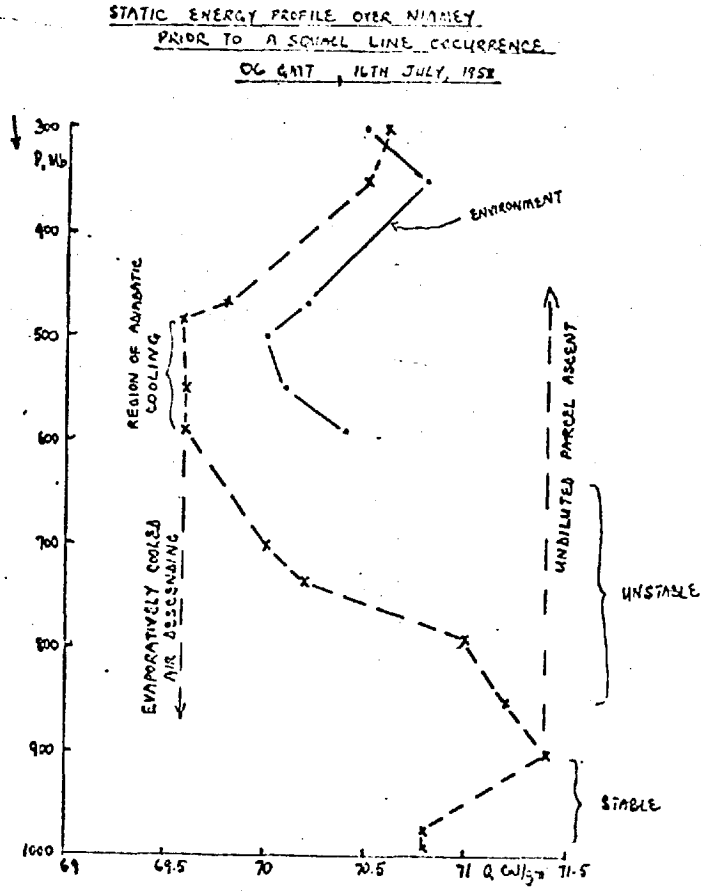

Sahel precipitation.

The high input of low-level static energy at Niamey, as compared with Lagos/Ikeja (then experiencing the LDS stabilizing effect) is remarkable. While only a shallow unstable layer (surface to 850mb) prevailed in Lagos, the Niamey atmosphere depicted a highly unstably stratified layer running up to 700mb level.

These profiles, having been obtained from monthly mean soundings, have been smoothed, owing to the averaging process and are, therefore, unable to depict the significant 'wiggles' which are of importance in explaining the (daily) weather e.g. the inversion layer is often smoothed out. Moreover, much of the weather is associated with deviations from, rather than, the mean of the meteorological variables.

It is, therefore, considered worthwhile to look at the static energy profile near to the advent of a squall line (fig. 5.3). This indicates a low-level stable layer over-lain by a much deeper unstable layer topped by the region of adiabatic cooling (600-500)mb. The environmental profile, indicated by the θ_s contribution, has been inserted, showing the 500mb level to be the likely top of the convective systems at play. In essence, the mechanism of convective over-turning occurs over a deeper layer on this occasion, giving rise to the realization of an enormous amount of energy capable of maintaining a squall line.

In the light of the foregoing, it is considered that an assessment of the degree of convective instability in any one day, must take account of:

a) a lower layer into which the energy required to set convection at play is supplied and

b) an upper layer, say, the mid-troposphere, in which the convective clouds are embedded.

Rather than take, as a measure of instability, the difference between the parcel static energy at these two levels, hence, accounting

for the environment indirectly (by the effect it has on the mid-level parcel energy) we shall, here, bring in the environmental effect more effectively by incorporating the contribution due to θ_s at the mid-troposphere as discussed below.

5.(iii) DEFINITION OF AN INSTABILITY INDEX, I

As a measure of instability, we, therefore, define an instability index, I, as the difference between the value of θ_w at 850mb and θ_s at 500mb levels. This choice of atmospheric levels similarly made by various authors previously is strengthened by the fact that being standard levels, data are routinely available over them. Moreover, the low-level (1000mb) radiosonde observations were not recorded in the 1958 data available and, although surface data exists (as used in the profiles shown in fig (5.1), it is likely to be an average of the noon screen level observation whereas the radiosonde soundings were generally for the mornings ($\sim$ 6 GCT). Hence, use of the 850mb level instead of the surface avoids this time lag in observations, a crucial factor worth taking into account as far as the convective boundary layer evolution is concerned.

Atmospheric conditions can, hence, be classified by I as follows:

$$I = \theta_w(850mb) - \theta_s(500mb) \begin{cases} >0 & \text{Unstable} \quad (a) \\ <0 & \text{Stable} \quad (b) \\ =0 & \text{Neutral} \quad (c) \end{cases} \qquad 5.2$$

However, in using the 850mb level as the level into which the energy input takes place, it need be noted that as this is within the cloud base region for most of the area , (except for the near Saharan area where the cloud base is higher) it might indicate latent energy release which accounts for further growth or towering in Cu/Cb clouds following the condensation process. In that wise, the boundaries between the I values for conditions a, b and c, shift considerably.

In particular, when very low cloud bases occur (.e.g. as in squall line situations where cloud bases are often less than 1km

in places) the 850mb θ_w value would then be more of an indicator of the energy available for further growth or up-shoot of the convective systems rather than of the low-level energy input.

However, it is reckoned that this method of estimating convective instability, taking as it were, an account of both the rising parcel and its environment, is more physically justified than that in which just the variation of the equivalent potential temperature,

$$\left(\theta_e = T + \frac{g}{C_p}z + \frac{L_o}{C_p}r \right) \quad \ldots \ldots \ldots \quad 5.3$$

Where L_o is a constant latent heat of condensation.)

for the whole depth of the atmosphere, is considered.

I, as defined above, takes account both of the parcel energetics (via $\theta_w = f(T, T_d)$) and the environment (via $\theta_s = f(T)$ only). These two, rather than just the energetics of the entire atmosphere alone (measured by θ_e above) need be precisely accounted for.

We shall, now, consider an evaluation of I for Lagos/Ikeja, Niamey and Aoulef, arrayed along the zone 2 longitude using monthly mean radiosonde data for each month of 1958 and daily soundings for April, July, August and September 1958. These are discussed with the advancing ITD, the height of the Monsoon, and the retreating ITD seasons in mind, with I plotted relative to the ITD position at the time of observation.

5.(iv) SEASONAL VARIATIONS OF MONTHLY MEAN θ_w(850mb), θ_s (500mb) AND I

Seasonal variations of θ_w (850mb), θ_s (500mb) and I for the three stations: Lagos, Niamey and Aoulef for 1958 are as follows: (Units ^{o}C)

		Pre-Monsoon (April)	Monsoon LDS (Aug.)	Retreating Season ITD (Sept.)
1. Lagos	θ_w(850Mb)	21.9	20.1	21.0
	θ_s (500Mb)	21.4	21.3	20.8
	I	0.5	- 1.2	0.2
2. Niamey	θ_w(850Mb)	18.2	20.5	18.6
	θ_s (500Mb)	21.9	21.4	21,0
	I	3.7	- 0.9	- 2.4
3. Aoulef	θ_w(850Mb)	12.7	19.2	16.6
	θ_s (500Mb)	19.4	20.7	19.6
	I	- 6.7	- 1.5	- 3.0

a) The above table shows that unlike in Lagos, the Niamey and Aoulef I values indicate a relatively higher convective state in the Monsoon period than before and after the Monsoon. The LDS is strong in Lagos at the height of the Monsoon in the Sahel.

b) In the pre-Monsoon and the post-Monsoon (or retreating ITD) season, Lagos is relatively more convective than any of the other two Northern stations. However, Niamey is the relatively most convective of these stations in the Monsoon Season even though the fact that I is still negative then suggests that advective processes (e.g. of Easterly disturbances), rather than just free convection, may account for most of the August precipitation.

c) A significant association can be noticed between θ_w (850mb) maximum and maximum I , an indication of the significant role played by solar radiation input in steering convection.

d) While mid-tropospheric cooling gradually develops between the on-set and retreat of the Monsoon in Lagos and Niamey, Aoulef typically undergoes a warming at the Monsoon season.

e) The θ_w (850mb) values label the prevailing air currents at the various seasons considered:

i.e. The SW'lies with θ_w (850mb) $\sim$ 21°C occupy the lower troposphere in Lagos throughout the pre - to the post - Monsoon season. The depth of this moist current may be very significant in the initiation of convection. (Chapter III)

These South Westerly currents feature well over Niamey in the Monsoon period while the North Easterly current predominates in the pre - and post - Monsoon seasons. Aoulef was under the influence of the NE'ly current for the entire seasons considered.

5.(v) THE ITD DEPENDENCE OF THE INSTABILITY REGION IN W.AFRICA

The observed θ_w at 850mb and θ_s at 500mb levels for each monthly sounding recorded over Lagos, Niamey and Aoulef in 1958 have been plotted as a function of each station's position relative to the ITD monthly position. fig (5.4). Maximum θ_w (850mb) of $\geq$ 22°C occurred 5-8° South of the ITD where considerable low-tropospheric moistening/heating has been experienced. This decreased across the North of the ITD, establishing a high θ_w (850mb) gradient across the phenomenon.

For the year as a whole, there was a high correlation between θ_w(850mb) and $(\phi_I - \phi)$ where ϕ_I is the ITD latitude and ϕ each station's latitude.

The correlation coefficient obtained is $r = 0.86$ with a standard error, S.E. = 0.04.

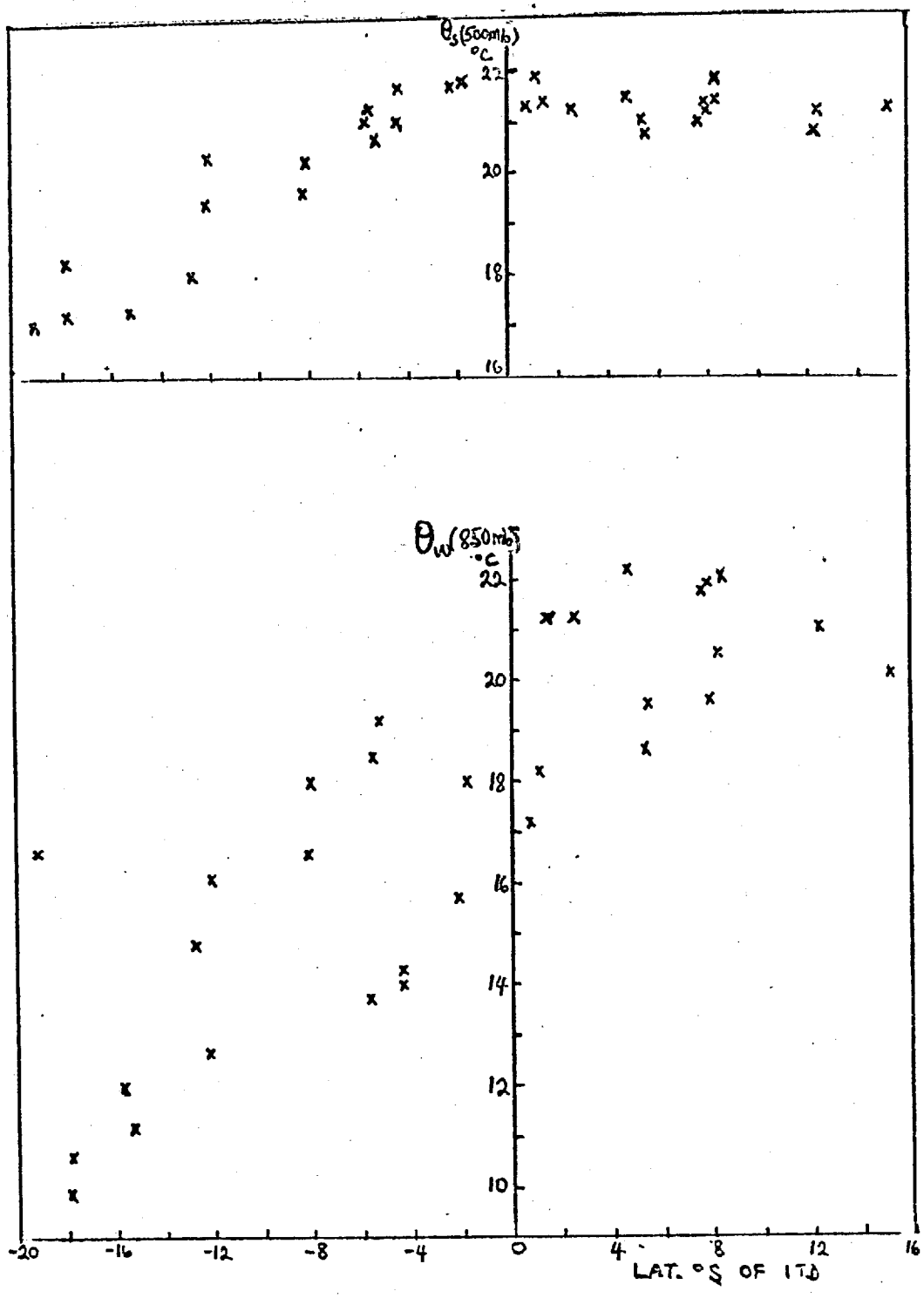

Fig. 5.4

The monthly mean θ_w (°C) obtained at the 850mb level and θ_s (°C) at the 500mb level over Lagos/Ikeja, Niamey and Aoulef for January to December 1958, plotted as a function of each station's position relative to the monthly mean ITD position ($\phi_I - \phi$). θ_w(850mb) is highly correlated with ($\phi_I - \phi$); (r = 0.86; SE = 0.04).

A regression relationship found for the two variables is:

$$\theta_w(850mb) = 18 + 0.3\ (\phi_I - \phi) \quad .. \quad .. \quad .. \quad 5.4$$

implying that at the ITD surface, θ_w (850mb) = 18°C and a region 'advected' with it will continue to have this θ_w value at the (850mb) surface. Each 1° latitude North/South of the ITD brings about an 0.3° decrease/increase in θ_w (850mb).

Similarly, the distribution of the Instability Index, I , relative to the ITD is as shown in fig.(5.5) for all the months of the year, 1958.

It is remarkable to note that occasions of convective Instability were strikingly fewer that those of stability. In actual fact, days of stable stratification far out-number those of unstable stratification, hence, yielding a net stable monthly mean.

I is well correlated with $\phi_I - \phi$; r = 0.76 and

SE = 0.07

The resulting regression relation is:

$$I = -2.6 + 0.2\ (\phi_I - \phi) \quad .. \quad .. \quad 5.5$$

I (in degrees centigrade) suggests that any station which persistently has the ITD over it will have I of - 2.6°C (stable) while for every degree latitude one moves South/North of the ITD, the Instability I increases/decreases by 0.2°C. Fig. (5.5.) also shows that I is maximum at 7.8° South of the ITD.

Finally, the correlation between the precipitation, R and $\phi_I - \phi$ was found to be r = 0.57 with S.E. = 0.11

$$\text{Therefore} \quad R(mm) = 51.5 + 4.5(mm/deg.lat.)\ (\phi_I - \phi)$$

$$.. \quad .. \quad .. \quad 5.6$$

Fig. 5.5.

The instability index, I obtained from fig. (5.4) plotted in a similar manner, relative to the ITD position. I indicates the degree of relative free convective instability North and South of the ITD. I is well correlated with ($\phi_I - \phi$); ($r = 0.76$; $SE = 0.07$). The precipitation, R(cm), hatched, similarly plotted relative to the ITD latitude, is significantly, though not very highly correlated with I; $r = 0.53$; $SE = 0.12$. Processes other than free convection - say, advective processes - are evident e.g. as in June over Lagos, indicated in the plot for R. This view is backed by the fact of a low (but significant) correlation between R and ($\phi_I - \phi$); $r = 0.57$; $SE = 0.11$.

It is worth noting, however, that the occasions of free convective instability found all occurred South of the ITD.

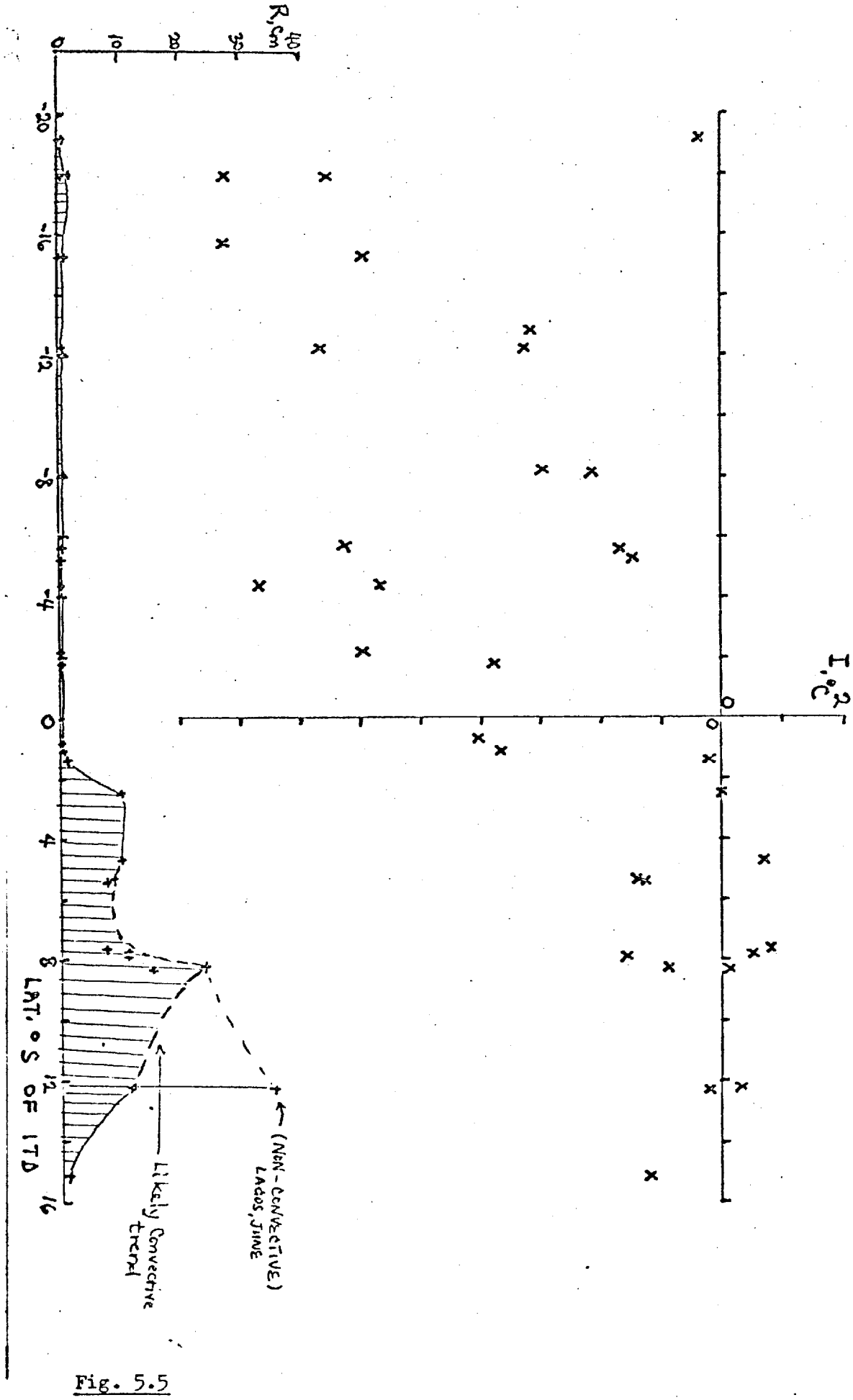

Fig. 5.5

See opposite page.

Hence, for a station which is constantly 'moving' with the ITD surface, observed precipitation would be 51.5mm/month. This agrees well with the results of the analysis of Chapter II where the ITD was often between the 0 or 5cm isohyets. For each degree South/North of the ITD, the precipitation increases/decreases by 4.5mm.

5.(vi) θ_w(850mb) AND I - RELATION WITH PRECIPITATION IN THE REGION

The relationship between the θ_w (850mb) and I variation and precipitation, R figs. (5.4 and 5.5) has been investigated for the various months of 1958.

A signifcant, though not very high, correlation exists between θ_w (850mb)(fig.5.4) and R ; ($r = 0.53$; SE = 0.12). The regression relation between the two is:

$$\theta_w\,(850\text{mb}) = 0.03\,R + 16.5 \quad .. \quad .. \quad .. \quad 5.7$$

Hence, to obtain any precipitation, θ_w (850 mb) must be greater than 16.5°C.

In fig. (5.5), the observed precipitation has been plotted along with the I distribution relative to the ITD. It is worthy of note that, in agreement with previous findings, substantial precipitation occurred only South of the ITD and so are the positive I values ($I > 0$) obtained.

Maximum I occurs around 8° South of the ITD. However, maximum R is observed around 10°S of the ITD. This, as is further considered below, may probably be due to forced convection and it is reckoned that maximum R of free convective origin occurred around 8°S of the ITD.

R and I are significantly, though not highly, correlated; ($r = 0.53$; SE = 0.12).

The regression relation between R and I is:

$$R = 72 + 8.9\,I \quad .. \quad .. \quad .. \quad 5.8$$

Hence, for I = 0, R = 72mm and for each degree rise in I, R increases by 8.9mm.

The results of fig.(5.5) show that either:

i) Occasions of forced convection when the convective systems draw their energy from the wind shear rather than the available potential energy - are many, or

ii) the boundary between I values for stable and unstable situations shift down the scale considerably as suggested above. e.g. Considerable precipitation results for $I \geq -1.0°C$ and unstable situations are not then limited to $I > 0$

a) Precipitation in the Sahel Area

A high correlation exists between the variation in the Sahel precipitation and that in I ; as typified by the Niamey (I, R) relationship :

$r = 0.61$ with S.E. = 0.19

A regression relation linking the two is:

$R_N(mm) = 112 + 18.9\ I$

Hence, over Niamey, for $I = 0$, $R = 112mm$ and for each unit degree centigrade rise in I, R increases by 18.9mm.

b) Precipitation in the Southern area

Taking the Lagos/Ikeja situation to represent the condition in the Southern area of the region, we relate I with R over Lagos/Ikeja. However, no significant correlation exists; $r = 0.33$; S.E. = 0.27. In order to explain this lack of I - dependence on R, we investigate the monthly variation in the two as shown in fig. (5.6). It can be noticed that the trend in April, May and June precipitation is not in agreement with that in I. This may contribute to the lack of correlation.

Fig.5.6 MONTHLY VARIATION OF θ_{wl}(850MB), θ_s(500MB), I AND PRECIPITATION, R, OVER LAGOS/IKEJA, 1958

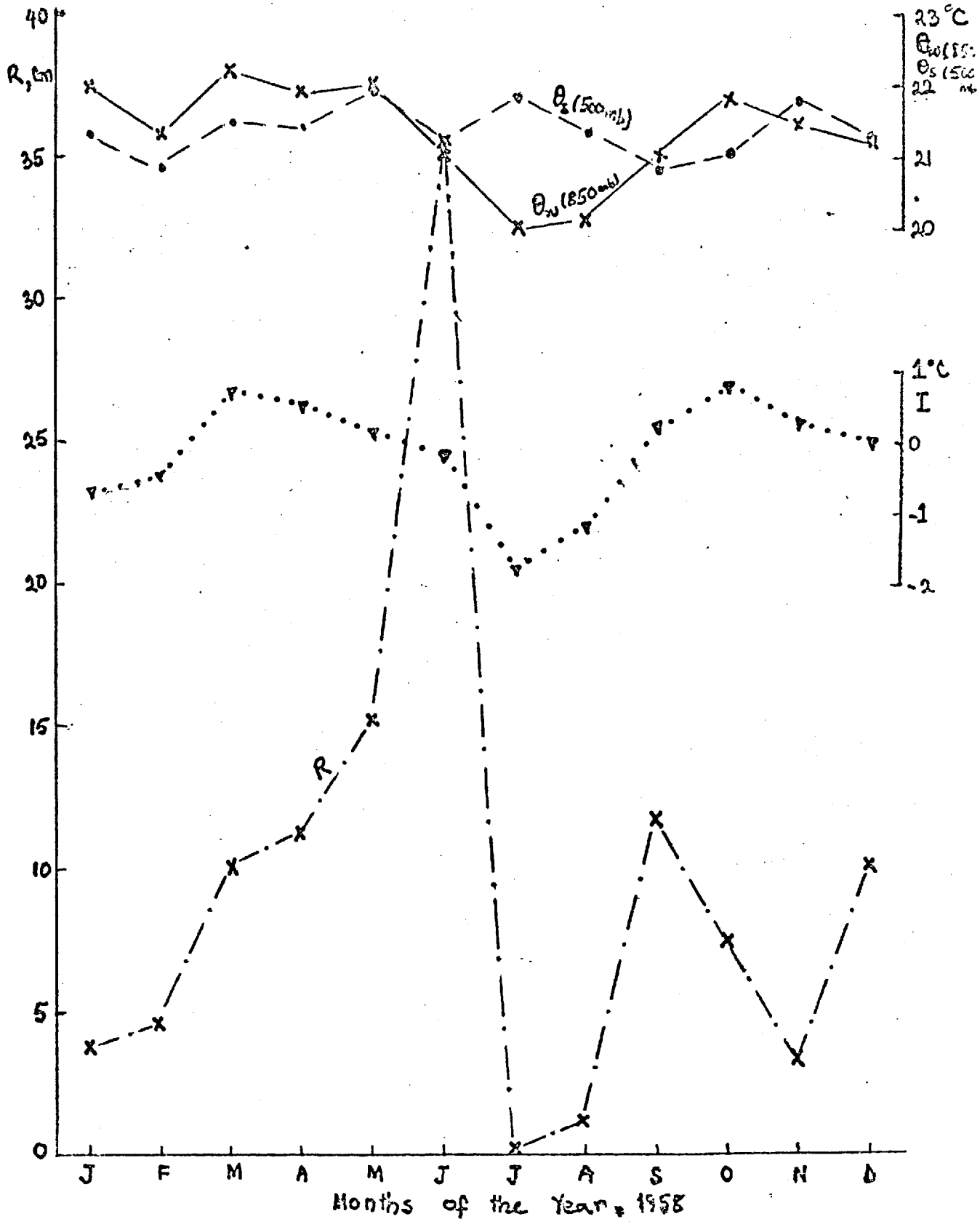

Possibly, forced convective processes may be responsible for the precipitation in these months, particularly in June. Minimum I occurred during the LDS indicating suppression of convection at this time of year.

In addition, occasions of forced convection wherein convective systems draw their energy from the available wind shear rather than from thermal stratification, cannot be ruled out.

5.(vii) DAILY VARIATIONS OF θ_w (850mb), θ_s (500mb) AND I ACROSS THE ITD

Daily upper atmosphere soundings obtained during part of the IGY for stations: Lagos, Niamey and Aoulef, all in the near-longitude of Lagos, were analysed to obtain θ_w (850mb) and θ_s (500mb) and I for each case. These were, then, plotted relative to the ITD position for the various seasons discussed below:

a) The Pre-Monsoon or Advancing ITD Season

This season is between March and May (Griffith et Al, 1972) and the April atmospheric conditions are, therefore considered to be representative of the season (Fig. 5.7(i-ii)) below showing the distribution of θ_w (850mb) and θ_s (500mb) North and South of the ITD for April 1958 indicate that:

1. Considerable low tropospheric warming and moistening takes place some 6-10° South of the ITD with θ_w (850mb) ranging from 21 to 24°C while the atmosphere dries up Northwards across the ITD to the Sahara area (Aoulef) where θ_w (850mb) $\sim$ 10-16°C.

The values of θ_w (850mb) observed North and South of the ITD typify the thermodynamic state of the NE'ly and SW'ly (Monsoon) air masses prevalent in the region.

2. In the mid-troposphere, unlike at 850mb level, the contrast in θ_s (500mb) values North and South of the ITD is not high;

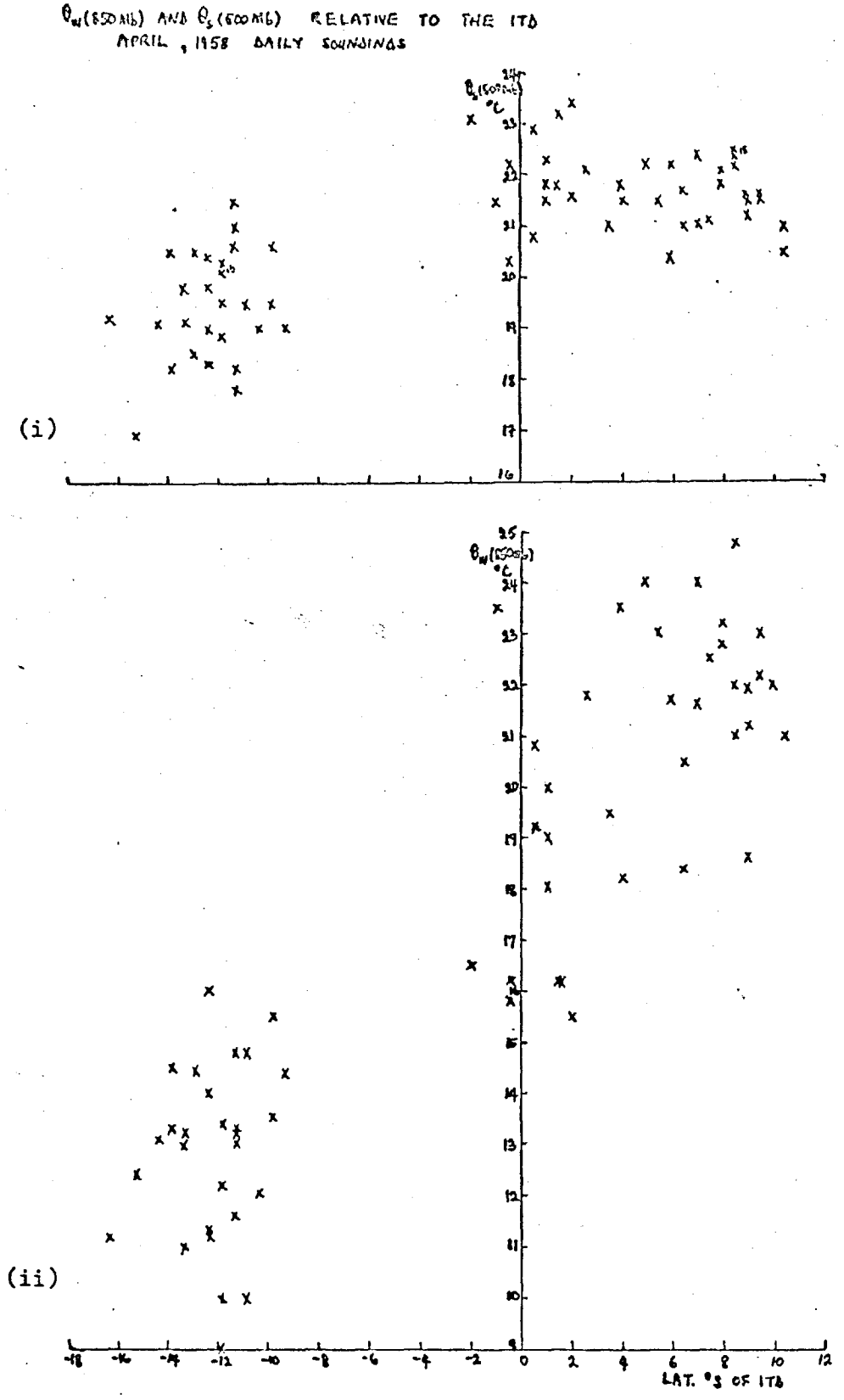

Fig. 5.7(i-ii) The daily θ_w(850mb)(°C) plotted below and θ_s(500mb)(°C) plotted above - for Lagos/Ikeja, Niamey and Aoulef - as a function of the station's latitude relative to the ITD ($\phi_I - \phi$) for the month of April, 1958. θ_w(850mb) is well correlated with ($\phi_I - \phi$); (r = 0.90; SE = 0.02).

$\Delta\theta_s$ (500mb) $\sim$ 1-2°C, the Southern area being generally higher in θ_s .

3. The correlation coefficient between θ_w(850mb) and $\phi_I - \phi$ is high; r = 0.90 with standard Error, SE = 0.02 . The regression relationship is:

$$\theta_w(850mb) = 18.1 + 0.4\ (\phi_I - \phi) \quad .. \quad .. \quad .. \quad 5.10$$

This indicates that for a station persistently under the ITD, observed θ_w(850mb) will be 18.1°C for the month and each degree South/North of the ITD increases/decreases this value by 0.4°C.

This relation is not much different from that obtained for the January-December, 1958 case (equation 5.4) above, though obtained on a different time scale.

The Instability Index, I for this month, plotted relative to the ITD latitude, fig. (5.7(iii)) shows that convective instability was at play within 4-10°S of the ITD. This, however, is interlaced with many days of considerable stability.

It is remarkable to note that of all the days of the month considered, only one occasion of convective instability could be found North of the ITD. This prevailing situation owes its existence to the large-scale subsidence resulting from the anticyclonic system found over the Sahara at this time of year.

The Instability Index, I, is well correlated with $\phi_I - \phi$, r = 0.81; SE = 0.04, with a regression relation,

$$I = -0.3 + 0.03\ (\phi_I - \phi) \quad .. \quad .. \quad .. \quad 5.11$$

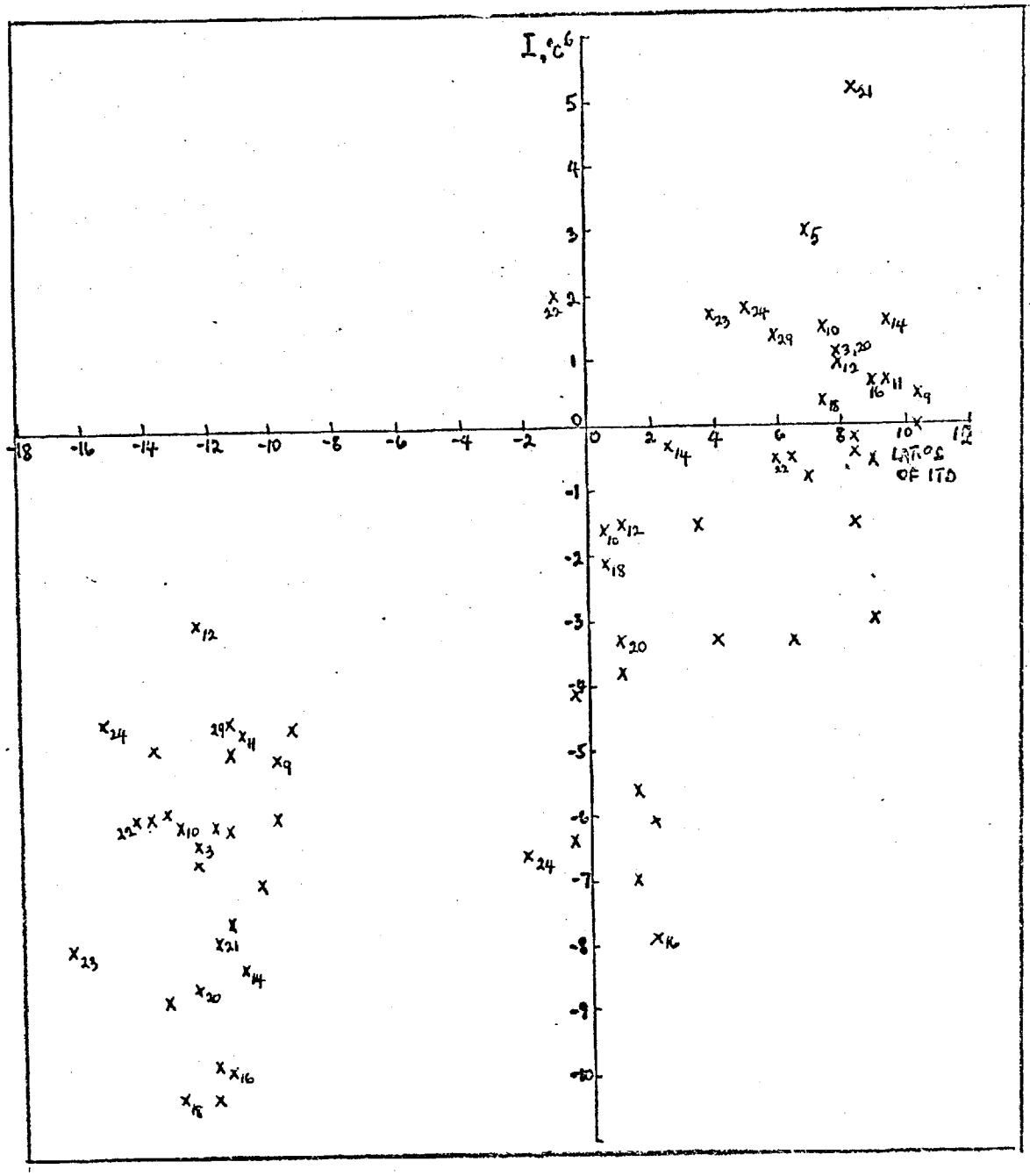

Fig. 5.7(iii)

The I values obtained from fig. 5.7(i-ii) similarly plotted relative to the ITD latitude. $r(I, (\phi_I - \phi)) = 0.81$; SE = 0.04. It is remarkable that a lot of the occasions of convective instability occurred South of the ITD.

A stable stratification is, hence, indicated on the ITD surface, $I = -0.3$, consistent in sign with the result for the annual case, equation 5.6, although the latter is an order of magnitude more stable than the April case. Similarly, as in the annual case, the I value increases/decreases South/North of the ITD (but this time, by $0.03^{\circ}C$, an order of magnitude smaller than in equation (5.5).

b) The Monsoon or (height of the ITD) Season:

The situation at the height of the ITD Season in the Sahel or the LDS in Lagos, is typified by the August conditions shown in fig. (5.8). An increase of $\sim 2^{\circ}C$ has been noted in θ_w (850mb) values South and North of the ITD relative to the Pre-Monsoon (April) case.

$\Delta\ \theta_w$ (850mb) varies in a North-South direction across the ITD and in a South-North direction South ($\sim$ 13-17°) of the ITD, converging between 7-10° South of the ITD where high $\sim 22^{\circ}C$ maximum θ_w (850mb) values can be noticed.

It has been observed that while two consecutive days of instability may occur, on occasions, days of instability are generally separated by seven to ten stable days.

Of the occasions of convective instability noticed South of the ITD in August, fig. (5.8(ii)), some were consecutive while some others (eg 20th and 30th) could be over a week apart. This shows that even at the height of the Monsoon, the tropical atmosphere is not always pouring with rain; rather, occasions of convective instability, though often associated with heavy rains, are fewer than the stable days in-between.

It is worthy of note that a lot of stable days could be observed South of the ITD itself. This is a manifestation of the LDS, a period of marked atmospheric stability due to the effect of the descending branch of the Zonal Walker Circulation. (Chapter IV)

Fig. 5.8(i-iii)

As in Figs. 5.7(i-iii) above, but for August, 1958. The sense of the $\Delta \theta_w$ (850mb) variation across the zone, as can be found on a typical day is depicted by the horizontal arrows, going by convention, from low to high θ_w (850mb).

AUG 1958 : θ_w(850 mb), θ_s(500 mb) AND I , RELATIVE TO THE ITD

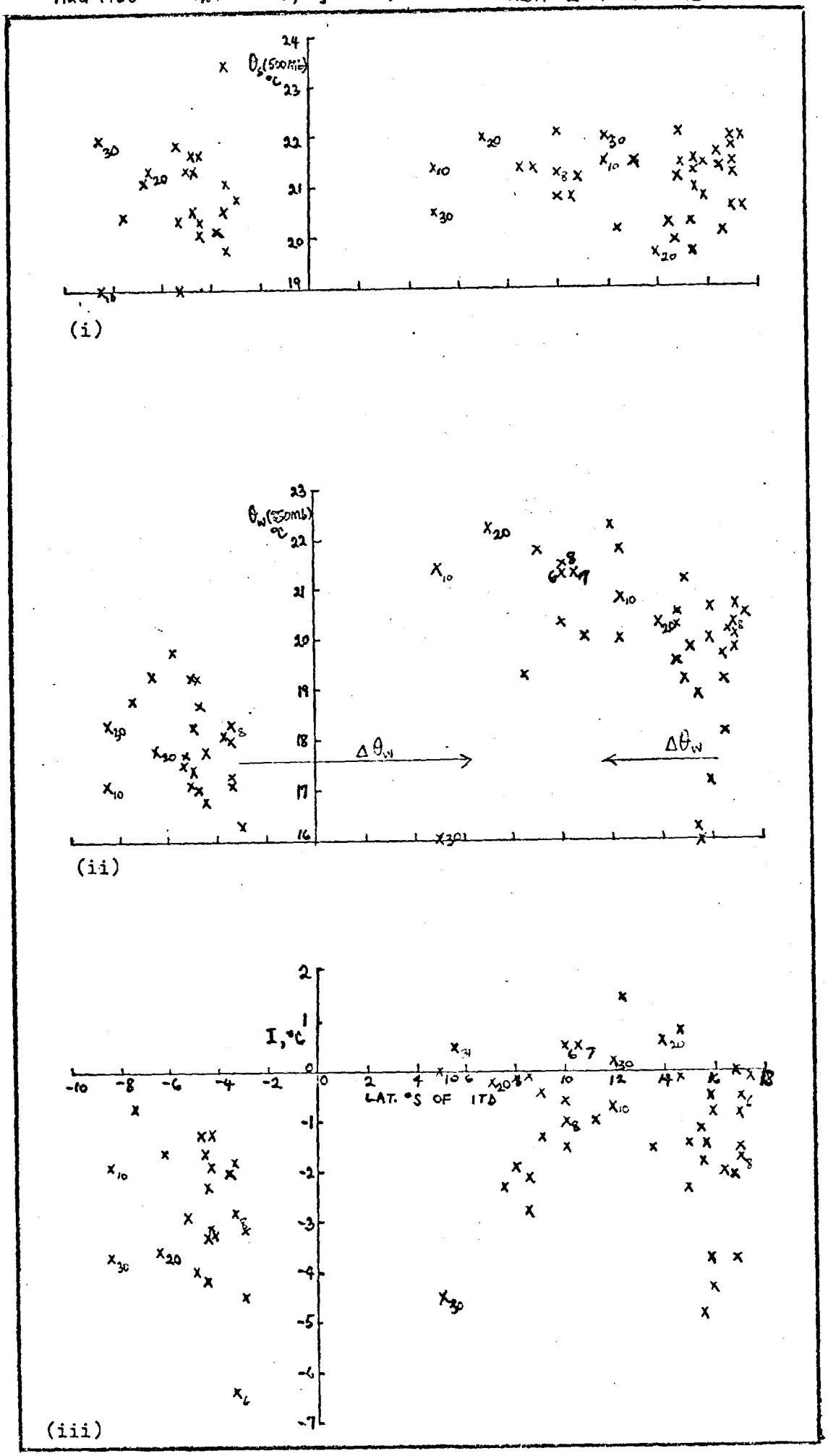

Fig. 5.8(i-iii) - see opposite page

c) The Retreating ITD Season

The ITD attains its most Northerly penetration into West Africa in August, but starts moving Southwards again towards the end of the same month, often with Northward fluctuations perturbing the trend. However, by September, the Southward movement is clearly marked and for this reason, the September situation has been chosen as typical of the retreating ITD Season as shown in fig. (5.9) below.

1. Although only Niamey and Aoulef data were available (Lagos data not found for this month), the θ_w (850mb) values destributed North and South of the ITD were such as to uphold the sense of the $\Delta\theta_w$(850mb) variation already observed in the August case. No such $\Delta\theta_s$ (500mb) variation could be seen however.

2. Relative to the August situation, an increase of $\sim \frac{1}{2}^{\circ}$C in θ_w (850mb) and a decrease of $\sim 1^{\circ}$C in θ_w(850mb) have been noted in Niamey and Aoulef respectively.

3. The I plot indicates the existence of convective instability at about 3-6° South of the ITD, each occasion often occurring at about one week interval to the next one.

4. During this season, the zone of convective instability South of the ITD was quite narrow, (3-6)° South; and the region (8-9)° South of the ITD was quite stable.

5.(viii) $\Delta\theta_w$(850mb) VARIATION AND THE ITD

The foregoing has shown that θ_w (850mb) increases from the North to the immediate Southern part of the ITD and then falls as one progresses further Southwards. We shall investigate the relationship between the change in θ_w (850mb) and the ITD latitude in this section.

The change in θ_w at the 850mb surface between Aoulef and Lagos is:

$$\Delta\theta_w(850mb)(A-L) = \Delta\theta_w(850mb)(N-L) + \Delta\theta_w(850mb)(A-N) \quad .. \quad .. \quad .. \quad 5.12$$

SEPT. 1958

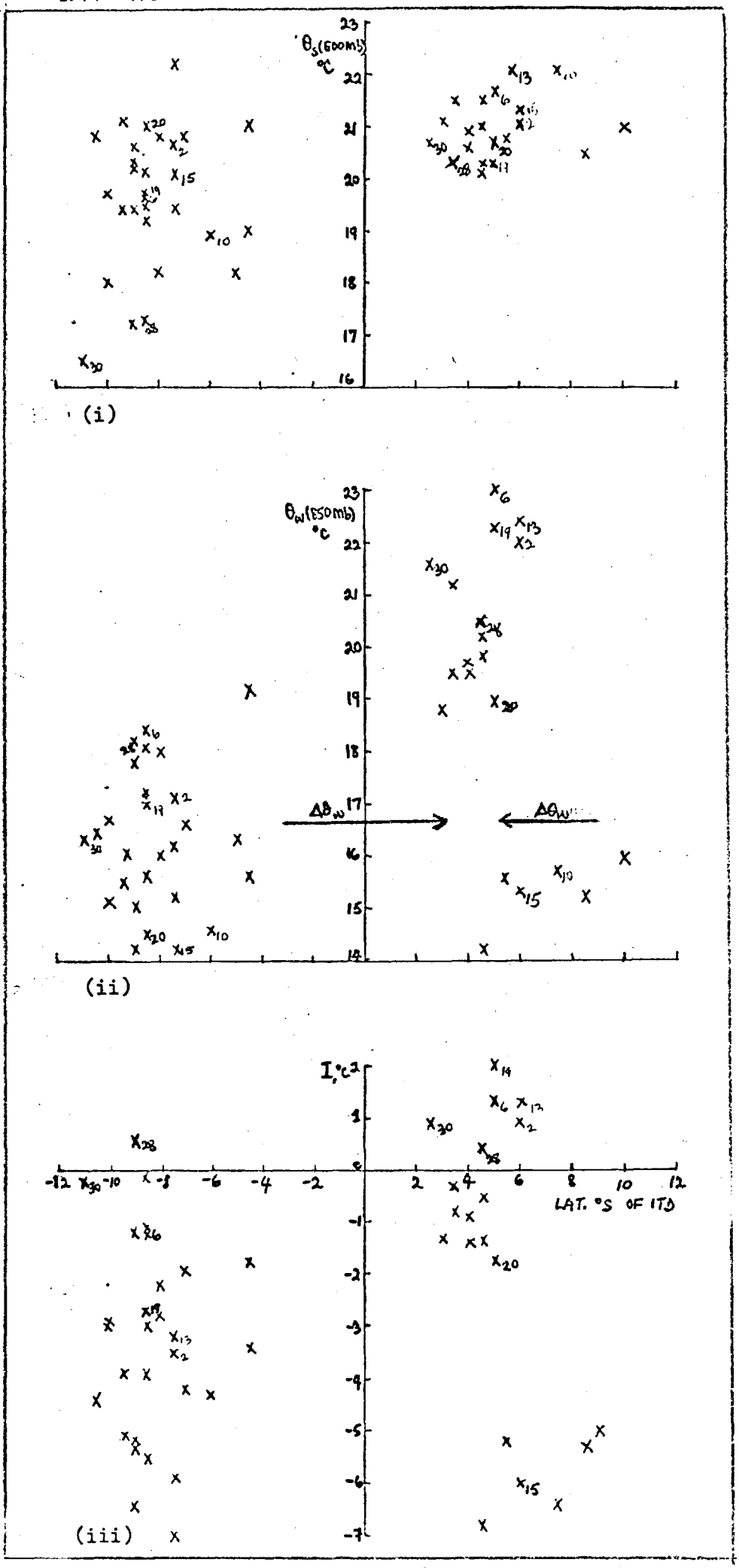

Fig 5.9

As in figs 5.7(i-iii) but for September, 1958.

where $\Delta\theta_w$(850mb)(N-L) gives the change in θ_w at the 850mb surface between Niamey and Lagos and the $\Delta\theta_w$ (850mb(A-N) term, an equivalent change between Aoulef and Niamey.

Each of the three terms in equation (5.12) has been plotted to show how they vary between January and Dcember of the year 1958 in fig. (5.10).

The variation in the ITD latitude has been plotted along with $\Delta\theta_w$ (850mb)(A-L) for comparison.

It can be seen that a high correlation exists between $\Delta\theta_w$(850mb(A-L) and the ITD; r = 0.941; SE = 0.04.

The regression relation between the two is:

$$\Delta\theta_w \text{ (850mb(A-L)} + 7 = 0.75\ (\phi_I - 14) \qquad \text{.. .. .. 5.13}$$

Therefore

$$\Delta\theta_w \text{ (850mb)(A-L)} = 0.75\ \phi_I - 17.5$$

This shows that the variation in θ_w at the 850mb between Aoulef and Lagos can be used to track the ITD.

The ITD essentially partitions the θ_w (850mb) variation across the region. Fig. (5.10) shows that $\Delta\theta_w$ (850mb) between Lagos and Niamey relates more to the ITD variation than $\Delta\theta_w$ 850mb between Niamey and Aoulef.

The correlation coefficient between $\Delta\theta_w$ 850mb(N-L) and the ITD is 0.93 with SE = 0.04.

The regression relation resulting is:

$$\Delta\theta_w \text{ (850mb)(N-L)} + 4 = 0.56\ (\phi_I - 14) \qquad \text{.. .. .. 5.14}$$

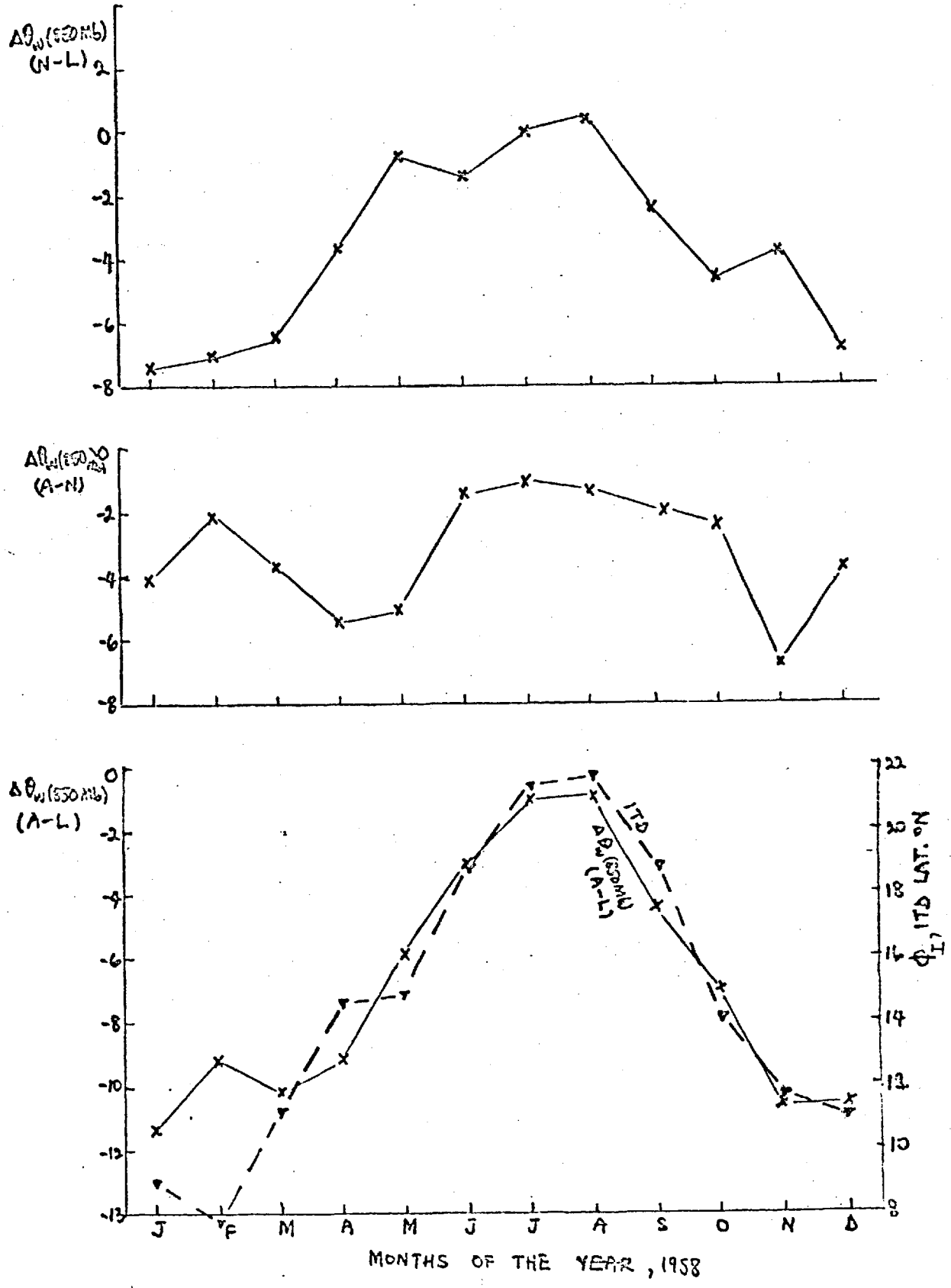

Fig. 5.10

The climatological variation in $\Delta\theta_w$ (850mb)(N-L), $\Delta\theta_w$ (850mb)(A-N) and $\Delta\theta_w$ (850mb)(A-L) compared with the ITD latitude variation (pecked) for zone 2, 1958. The high correlation between $\Delta\theta_w$ (850mb)(A-L) and the ITD latitude, ϕ_I; (r = 0.94; SE = 0.04) and $\Delta\theta_w$ (850mb)(N-L) and ϕ_I; (r = 0.93 SE = 0.04) are remarkable.

while on the other hand, $\Delta\theta_w$ (850 mb) (A-N) and ϕ_I are not as well correlated; r = 0.52 ; SE = 0.22 with a regression relation:

$$\Delta\theta_w \text{ (850mb) (A - N)} + 3 = 0.42 \ (\phi_I - 14) \qquad \text{.. .. .. 5.15}$$

However, as shown below, fig (5.11), although $\Delta\theta_w$ (850mb) (A - N) is not well correlated with the ITD, θ_w (850mb) (Aoulef) and θ_w (850mb) (Niamey) each correlates well with the ITD:

i.e.

a) for Niamey, r = 0.85 ; SE = 0.08 with a regression relation:

$$\theta_{w(850mb)(Niamey)} - 18 = 0.51 \ (\phi_I - 14) \qquad \text{.. .. .. 5.16}$$

b) for Aoulef, r = 0.95 ; SE = 0.03 with a regression relation:

$$\theta_{w(850mb)(Aoulef)} - 14 = 0.57 \ (\phi_I - 14) \qquad \text{.. .. .. 5.17}$$

For Lagos, on the other hand, the 850mb θ_w is negatively correlated with the ITD ; r = 0.55 ; SE = 0.21 with a regression relation:

$$\theta_{w(850mb)(Lagos)} - 21 = -0.11 \ (\phi_I - 14) \qquad \text{.. .. .. 5.18}$$

We also note in fig.(5.11) that θ_w (850mb) are higher over Lagos than those over Niamey which are also higher than those over Aoulef; except

in July and August (the LDS Season in Lagos).

The foregoing is an effective indication of the characteristics of the regimes of the prevailing winds over the region.

While the Lagos - Niamey area is more under the influence of the moist South Westerlies (particularly in the Monsoon Season) with θ_w (850mb) $\geq 20^{\circ}C$, the Niamey-Aoulef area is more under the influence of the drier and hotter North Easterlies; θ_w (850mb), typically $\leq$ 16-18°C.

It seems paradoxical to note that the 850mb θ_w over Aoulef has a parallel variation with the ITD latitude (shown above) although the ITD never passes over the station. However, the paradox is resolved when it is noted that while Aoulef is constantly under the influence of the North Easterlies, the moistening of the atmosphere effected by the Northward penetration with the ITD, of the moist South Westerly current, affects the atmosphere there to some degree. We also note that Aoulef often experiences some precipitation in NH winter, from extra-tropical frontal systems.

A survey of the 850mb θ_w and 500mb θ_s for the months of the year 1958 shows the maximum, minimum and range values for these thermodynamic variables (table 5.1).

We can also notice that the range in θ_w (850mb) increases from 2.6°C at Lagos to 7.5°C at Niamey and 9.3°C at Aoulef.

Similarly, the range in the 500mb θ_s decreases from 1.2°C in Lagos to 1.1°C in Niamey but rises to 4.2°C in Aoulef. Hence, the moisture contrast at lower levels is higher than the saturation potential temperature contrast at the mid-troposphere over the region.

The yearly range of monthly precipitation, surprisingly, decreases Northwards. This is due to the over-whelming effect of the LDS in Lagos and the sharp contrast between the Monsoon precipitation peak and the dry season in Niamey. Aoulef, on the other hand, is mainly arid for most of the year and hence has a smaller precipitation range. The range is not as good an indicator of precipitation variability as the coefficient

TABLE 5.1

STATIONS	MAX θ_w(850mb)		MIN θ_w(850mb)		θ_w(850mb) RANGE °C	MAX θ_s (500mb)		MIN θ_s (500mb)		θ_s (500mb) RANGE °C	MAX PRECIPITATION, R_{max}		MIN PRECIPITATION, R_{min}		PRECIPITATION RANGE (mm)
	Value °C	Month	Value °C	Month		Value °C	Month	Value °C	Month		Value (mm)	Month	Value (mm)	Month	
1. LAGOS	22.2	March	19.6	July	2.6	22.0	Jan	20.8	Sept	1.2	355	June	2	July	353
2. NIAMEY	21.2	May	13.7	Feb.	7.5	21.9	April	20.8	June	1.1	243	Aug.	0	Jan-March, Nov.	243
3. AOULEF	19.2	Aug.	9.9	Jan.	9.3	21.2	July	17.0	Feb.	4.2	8	Jan.	0	F-O	8

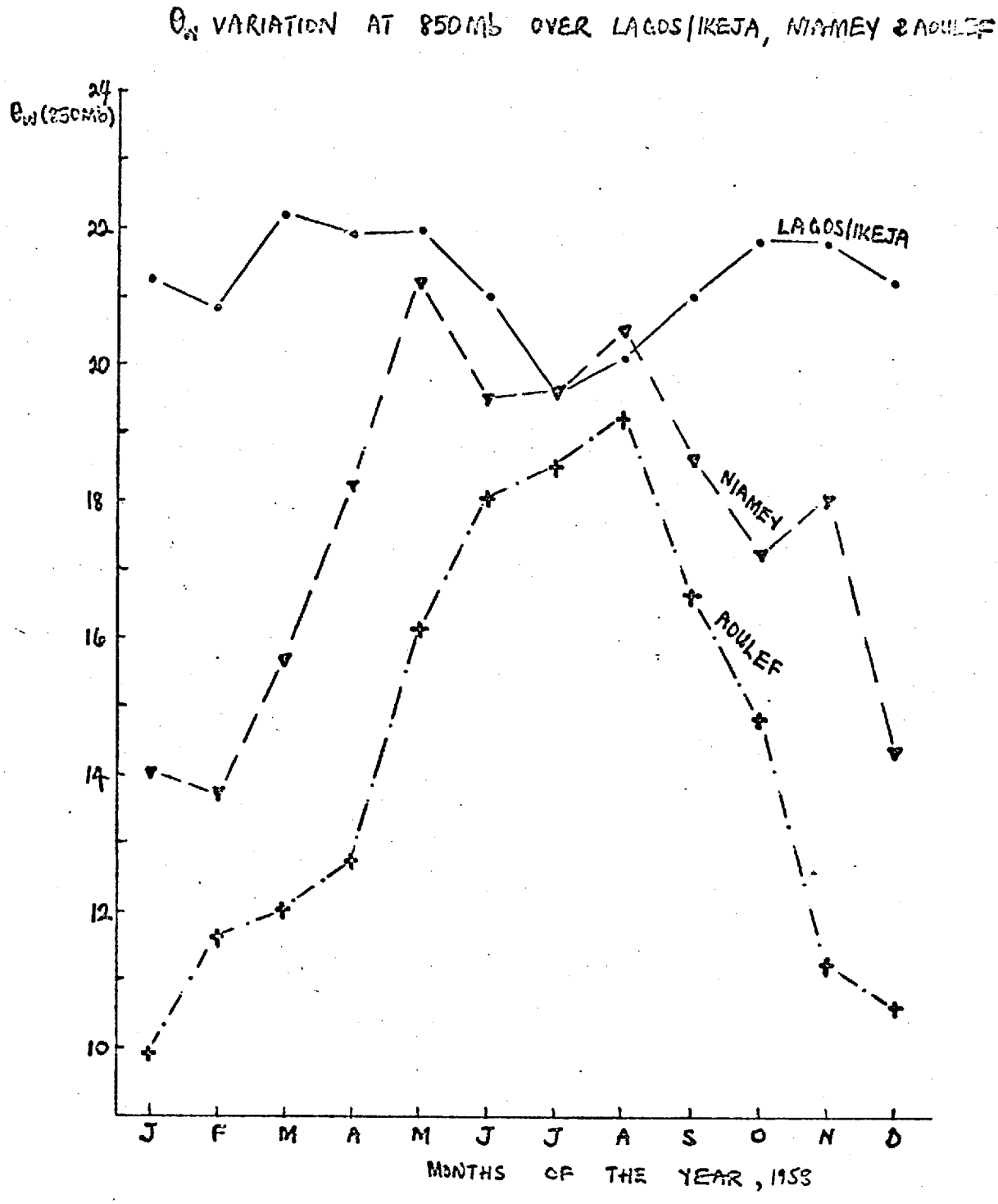

Fig. 5.11

The Climatological variation in θ_w (850mb) over Lagos/Ikeja, Niamey and Aoulef for various months of the year, 1958.

of variation, considered in chapter II.

5.(ix) PREDICTORS OF THE SAHEL PRECIPITATION

For the Sahel rainy season months of May-September 1958, the Niamey precipitation was highly correlated with each of the following

1. The 850mb θ_w at Aoulef, $\theta_w(850mb)_A$

with r = 0.85 ; SE = 0.14 and regression relation:

$$R_N - 105 = 72 \quad (\theta_w(850mb)_A - 18) \qquad .. \quad .. \quad .. \quad 5.19$$

2. The latitude of the ITD (3°E longitude)

r = 0.83 ; SE = 0.16 with a regression relation:

$$R_N - 105 = 23.4\ (\phi_I - 19) \qquad .. \quad .. \quad .. \quad 5.20$$

3. $\Delta\theta_w(850mb)(A-L)$

r = 0.82 ; SE = 0.17 with a regression relation:

$$R_N - 105 = 34.7 \sum \Delta\theta_w(850mb)(A-L) + 37$$

$$.. \quad .. \quad .. \quad 5.21$$

4. $\Delta\theta_w(850mb)(A-L)$

r = 0.66 ; SE = 0.28 with a regression relation:

$$R_N - 105 = 28.2 \quad \Delta\theta_w 850mb) \quad (A - N) + 2$$

.. .. .. 5.22

5. Lagos θ_w(850mb), with a negative but significant correlation coefficient, $r = -0.70$; SE = 0.25 and regression relation:

$$R_N - 105 = -59.8 \quad \theta_w(850)L - 21$$

.. .. .. 5.23

Where, in equations 5.19 to 5.23, R_N is in mm
θ_w(850mb) in ^oC and
Φ_I , in degrees of latitude.

5.(x) CONCLUSION

A qualitative consideration of convective instability, taking account of atmospheric stratification relative to the ITD position has been undertaken, using an instability index, I, defined as the difference between θ_w (850mb) and θ_s (500mb).

Generally, on a monthly mean basis, I increases/decreases South/North of the ITD by about 0.2°C/degree. So does the precipitation, but by about 8.9mm/degree. The two are significantly correlated; $r = 0.53$, SE = 0.12.

From numerous daily soundings considered, the variation of I for three seasons - the advancing ITD, the Monsoon and the retreating ITD seasons - has been studied. I is, essentially, an indicator of relative free convective instability around the ITD. It is found that, generally, days of convective instability are very few and interlaced by many days of stability. While two or three consecutive unstable days may some times occur, unstable days are often interlaced by about a week of stable days. Even during the Monsoon Season, the region is not always 'pouring with rain' rather, the few convectively unstable days may be associated with heavy squally weather, accounting for most of the precipitation experienced.

Regression relations have been established between the region's precipitation and likely predictors like I and θ_w (850mb). The latitudinal change in θ_w (850mb) across the region (Zone 2) parallels the ITD.

These results were obtained along zone 2 using the Lagos/Ikeja, Niamey and Aoulef radisonde data on monthly mean and daily bases. Its generalization for the entire region is reasonable, in view of the good zonal symmetry in precipitation there, but not necessarily imperative, in view of the effects of orographic and other local features.

In addition, occasions of forced convection, particularly in the presence of strong wind shear, are considerable, due to the strong Easterly disturbances advected westwards over the region in NH Summer.

CHAPTER VI

INTER-STATION CORRELATION OF PRECIPITATION ACROSS THE REGION

6.(i) INTRODUCTION

In this chapter, we shall study the correlation of monthly precipitation totals in a South-North direction across the region, from the Atlantic coast, through the Sahel region, to the Saharan border.

This exercise, suggested by the latitude-time cross-section of precipitation studied in Chapter II, rather than as a problem in statistical significance, is aimed at examining a possible lag relation in precipitation between the Sahel and Southern parts of West Africa.

It is also useful as a method of indicating the nature of the precipitation zones resulting from the action of the atmospheric mechanisms influencing the region. Prominent among these are the ITD, the Walker Circulation, the squall lines and the Easterly waves, as discussed in Chapter IV, and the often sporadic, orographically induced thunderstorms, all of which, acting severally or jointly in various parts of the region, leave their marks on the distribution and duration of precipitation.

6.(ii) A LINEAR REGRESSION MODEL

If the monthly precipitation observed over a station A is x_i and that over a station B is Y_i , $i = 1, 2 \ldots\ldots N$, The least square regression line of Y on x is

$$E(Y) = a + bx \quad \text{(e.g. Spiegel, 1961)} \quad .. \quad .. \quad 6.1$$

where E(Y) is the expected variable.

We want to determine the values of the constants a and b such that the discrepancy between the observed Yi and the

corresponding $f(xi) = a + bxi$ given by Eqtn. (6.1), is a minimum.

The deviations ε_i between each of the observed Y_i and the corresponding f(xi) is:

$$\varepsilon_i = Y_i - a - bxi$$

Hence, $$Y_i = a + bx_i + \varepsilon_i \quad .. \quad .. \quad .. \quad 6.2$$

is the equation of a linear regression model,

where (i) the expected value of ε's = 0, ie. $E(\varepsilon_i) = 0$

(ii) its variance $E(\varepsilon_i^2) = \sigma^2$

(iii) the covariance between any two pairs of εs is zero.

ie. $\text{Cov}(\varepsilon_1 \varepsilon_2) = E(\varepsilon_1 \varepsilon_2) = 0$

(Searle, 1971, Kendal, et Al. 1960)

The method of least squares requires that χ^2, the measure of the goodness of fit, be minimized.

The function

$$\chi^2 = \sum_{i=1}^{N} \left(\frac{\varepsilon_i}{\sigma_i^2}\right)^2 \quad .. \quad .. \quad .. \quad 6.3$$

To obtain the values of a and b for which χ^2 is minimum, we differentiate χ^2 with respect to a and b respectively and equate each to zero.

$$\frac{\partial}{\partial a}\chi^2 = \frac{\partial}{\partial a}\left[\frac{1}{\sigma^2}\sum_{i=1}^{N}(Y_i - a - bx_i)^2\right] = 0$$

$$= -\left[\frac{1}{\sigma^2}\sum_{i=1}^{N}(Y_i - a - bx_i)2\right] = 0$$

$$\therefore \sum_{i=1}^{N} Y_i = \sum_{i=1}^{N} a + \sum_{i=1}^{N} bx_i = Na + b\sum_{i=1}^{N} x_i \quad .. \quad .. \quad .. \quad 6.4$$

Similarly,

$$\frac{\partial}{\partial b}\chi^2 = \frac{\partial}{\partial b}\left[\frac{1}{\sigma^2}\sum_{i=1}^{N}(Y_i - a - bx_i)^2\right] = 0$$

$$= -\sum_{i=1}^{N} 2(Y_i - a - bx_i)\sum_{i=1}^{N} x_i = 0$$

$$\therefore \sum_{i=1}^{N} x_i Y_i = a\sum_{i=1}^{N} x_i + b\sum_{i=1}^{N} x_i^2 \qquad \ldots\ \ldots\ \ldots \quad 6.5$$

The solutions of equations 6.4 and 6.5 yield the required values of a and b.

$$a = \frac{1}{\Delta}\begin{vmatrix} \sum_{i=1}^{N} Y_i & \sum_{i=1}^{N} x_i \\ \sum_{i=1}^{N} x_i Y_i & \sum_{i=1}^{N} x_i^2 \end{vmatrix} = \frac{1}{\Delta}\left(\sum_{i=1}^{N} Y_i \sum_{i=1}^{N} x_i^2 - \sum_{i=1}^{N} x_i \sum_{i=1}^{N} x_i Y_i\right)$$

$$\ldots\ \ldots\ \ldots \quad 6.6$$

$$b = \frac{1}{\Delta}\begin{vmatrix} N & \sum_{i=1}^{N} Y_i \\ \sum_{i=1}^{N} x_i & \sum_{i=1}^{N} x_i Y_i \end{vmatrix} = \frac{1}{\Delta}\left(N\sum_{i=1}^{N} x_i Y_i - \sum_{i=1}^{N} x_i \sum_{i=1}^{N} Y_i\right)$$

$$\ldots\ \ldots\ \ldots \quad 6.7$$

where $$\Delta = \begin{vmatrix} N & \sum_{i=1}^{N} x_i \\ \sum_{i=1}^{N} x_i & \sum_{i=1}^{N} x_i^2 \end{vmatrix} = N\sum_{i=1}^{N} x_i^2 - \left(\sum_{i=1}^{N} x_i\right)^2$$

$$\ldots\ \ldots\ \ldots \quad 6.8$$

Putting 6.8 in 6.6 and 6.7, we obtain

$$a = \frac{\sum_{i=1}^{N} x_i^2 \sum_{i=1}^{N} Y_i - \sum_{i=1}^{N} x_i \sum_{i=1}^{N} x_i Y_i}{N\sum_{i=1}^{N} x_i^2 - \left(\sum_{i=1}^{N} x_i\right)^2} \qquad \ldots\ \ldots\ \ldots \quad 6.9$$

$$b = \frac{N\sum_{i=1}^{N} x_i Y_i - \sum_{i=1}^{N} x_i \sum_{i=1}^{N} Y_i}{N\sum_{i=1}^{N} x_i^2 - \left(\sum_{i=1}^{N} x_i\right)^2} \qquad .. \quad .. \quad .. \quad 6.10$$

If x and Y are not correlated, the least square fit yields a horizontal straight line (of slope b = 0). However, the regression of x on Y need be considered also.

$$x = a^1 + b^1 Y \qquad .. \quad .. \quad .. \quad 6.11$$

where $a^1 \neq a$ and $b^1 \neq b$ but are related if x and Y are correlated.

A similar process applied to equation 6.11 yields:

$$a^1 = \frac{\sum_{i=1}^{N} Y_i^2 \sum_{i=1}^{N} x_i - \sum_{i=1}^{N} Y_i \sum_{i=1}^{N} x_i Y_i}{N\sum_{i=1}^{N} Y_i^2 - \left(\sum_{i=1}^{N} Y_i\right)^2} \qquad .. \quad .. \quad .. \quad 6.12$$

$$b^1 = \frac{N\sum_{i=1}^{N} x_i Y_i - \sum_{i=1}^{N} x_i \sum_{i=1}^{N} Y_i}{N\sum_{i=1}^{N} Y_i^2 - \left(\sum_{i=1}^{N} Y_i\right)^2} \qquad .. \quad .. \quad .. \quad 6.13$$

Given that x and Y are not correlated, least square fit yields a horizontal straight line with slope $b^1 = 0$

However, if x and Y are correlated, a and b and a^1 and b^1 are related.

$$Y = a + bx = -a^1/b^1 + x/b^1$$

$$\Rightarrow a = -a^1/b^1 \quad \text{and} \quad b = 1/b^1$$

For perfect correlation between x and Y, $bb^1 = 1$
and for no correlation between x and Y, $b = b^1 = 0$

Hence, a measure of linear correlation is the correlation coefficient, $r = \sqrt{bb^1}$

From 6.10 and 6.13,

$$r = \frac{N\sum_{i=1}^{N} x_i Y_i - \sum_{i=1}^{N} x_i \sum_{i=1}^{N} Y_i}{\left[N\sum_{i=1}^{N} x_i^2 - \left(\sum_{i=1}^{N} x_i\right)^2\right]^{1/2}\left[N\sum_{i=1}^{N} Y_i^2 - \left(\sum_{i=1}^{N} Y_i\right)^2\right]^{1/2}} \quad \ldots\ \ldots\ \ldots \quad 6.14$$

The value of r ranges from 0 (when there is no correlation between x and Y) to ± 1 (when a complete correlation exists between x and Y .

Equation 6.14 can be re-expressed as:

$$r = \frac{\frac{1}{N}\sum_{i=1}^{N} x_i Y_i - \bar{x}\bar{Y}}{\sigma_x \sigma_y} \quad \ldots\ \ldots\ \ldots \quad 6.15$$

where

$$\left.\begin{aligned} \bar{x} &= \frac{1}{N}\sum_{i=1}^{N} x_i \\ \bar{Y} &= \frac{1}{N}\sum_{i=1}^{N} Y_i \end{aligned}\right\}$$ are the means of x_i and Y_i distributions

and

$$\left.\begin{aligned} \sigma_x &= \left[\frac{\sum_{i=1}^{N} x_i^2}{N} - (\bar{x})^2\right]^{1/2} \\ \sigma_Y &= \left[\frac{1}{N}\sum_{i=1}^{N} Y_i^2 - (\bar{Y})^2\right]^{1/2} \end{aligned}\right\}$$ are the standard deviations

$\ldots\ \ldots\ \ldots \quad 6.16$

The standard Error SE $= (1 - r^2)/\sqrt{N-1}$

For use in computing the inter-station correlation coefficients between M stations alligned in a N-S direction across the region, the regression model was generalized thus: (Kendall et Al, 1960):

$$\underline{Y} = \underline{x}\underline{\beta} + \underline{\varepsilon} \qquad \ldots\ \ldots\ \ldots\ 6.17$$

where $\underline{Y}$ is an $N \times 1$ vector of observations, (N being the number of observations)

$\underline{x}$ is an N X M matrix of known coefficients

$\underline{\beta}$ is an M X 1 vector of regression coefficients

$\underline{\varepsilon}$ is an N X 1 vector of "error" random variables.

A standard soub-routine of this model was used in carrying out computer estimates of the correlation coefficients resulting from the observed precipitation. (Appendix V).

6.(iii) a) Normal Monthly precipitation

The correlation coefficients between every pair of the stations in zones 1, 2 and 3 have been calculated for the Normal (long term, 1931-60 wherever possible) mean monthly precipitation as cyclic data. The resulting spatial distribution of correlation coefficients, r, is as shown in figs. 6.1, 6.2 and 6.3. below.

Each of these figs. shows the correlation coefficients between each station (in j = 1 to M) and every other one in the North-South zone being considered. By definition, r is unity over the station itself.

(i) Zone 1

The stations precipitation in this zone are generally highly correlated, $r \geqslant 0.7$, one with another. However, it can be seen that stations in the South e.g. Daru and Kabala; while highly correlated with one another, $r \geqslant 0.9$, were not as highly correlated with stations further inland (r falls to 0.7). Similarly, stations to the North were

SPATIAL DISTRIBUTION OF CORRELATION COEFFICIENTS, ZONE 1 : NORMAL PRECIPITATION

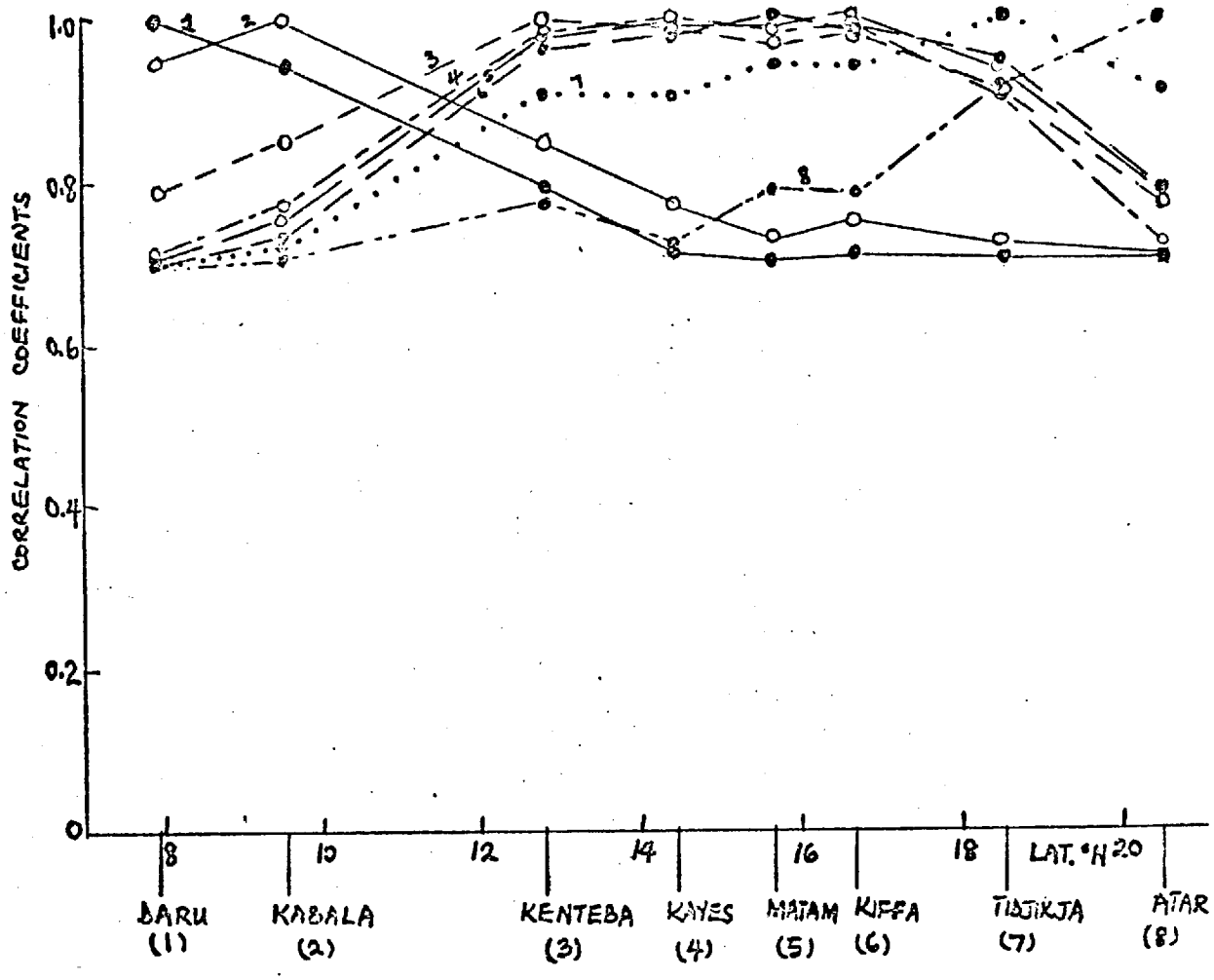

Fig 6.1

The spatial distribution of the correlation coefficients between the monthly precipitation observed over a station and those of every other station in the zone (indicated by each curve (1----8); maximum (unity) over the station itself) for zone 1, Normal precipitation.

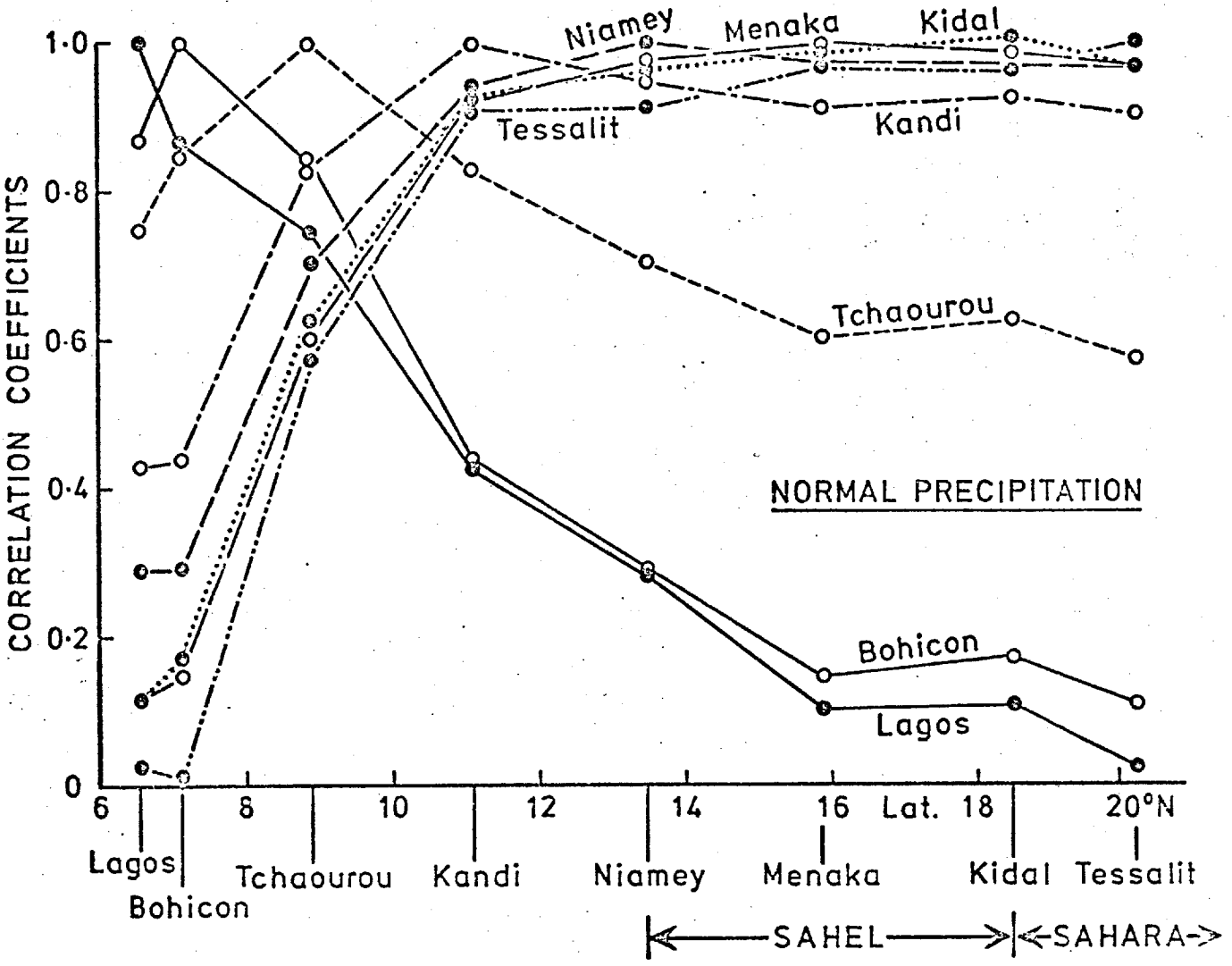

Fig 6.2

Same as in fig 6.1 but for zone 2.

more highly correlated with one another than with the Southern stations, while for stations in the Central region, r fell off at extreme North and South but they are highly correlated with stations near them.

ii) Zones 2 and 3

The results obtained for zone 3, fig. (6.3) are not much different from those of Zone 1 but for the fact that r's are generally between 0.5 and 1. The variation in r with latitude is similar to the case in zone 1.

However, for zone 2, a remarkable three-class regime could be observed; fig. (6.2):

a) The Southern, near-coastal stations of Lagos and Bohicon are well correlated in precipitation, one with another and with Tchaourou, the nearby station, but are poorly correlated with stations inland.

b) The Sahel stations of Niamey, Menaka and Kidal, along with Tessalit in the Sahara, are also highly correlated with one another, but poorly correlated with the Southern stations in a) above.

c) Tchaourou is fairly well correlated with all the stations, though more highly correlated with the nearby stations in a).

A transition is noticed in the region of importance of the various regimes occurring around latitude 9.5°N with an r threshold of 0.7.

For convenience, we shall call the regimes in a), b) and c) regimes A, B and C respectively.

Regime A typifies a good inter-station correlation in the coastal/southern region and poor or no correlation in the hinterland.

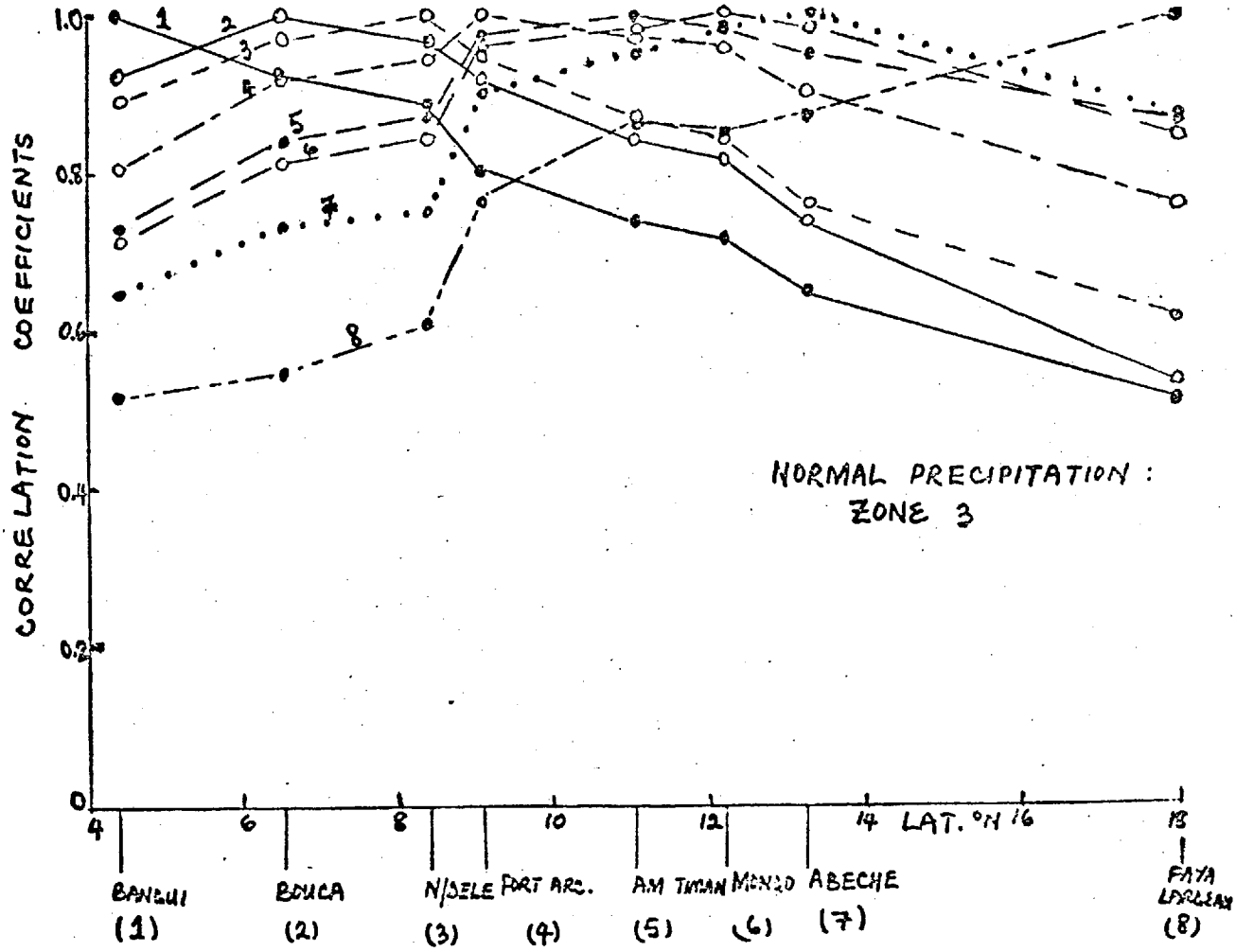

Fig 6.3

Same as in fig 6.1 but for zone 3.

Regime B exhibits a good inter-station correlation in the Sahel/hinterland region but poor or no correlation in the coastal/southern region, while,

Regime C, intermediate between A and B, typifies a good inter-station correlation in most of the zone as a whole.

We shall examine these regimes of r distribution in case studies of the wet and the dry year considered in the earlier chapters along with the associated weather.

6.(iii) b) Case studies of a wet and a dry year

i) Wet Year

These calculations were similarly carried out for the typical wet Sahel year, 1958 (Chapter II) and the results shown in figs. 6.4, 6.5, and 6.6 were obtained for zones 1, 2 and 3 respectively.

Zone 1

The spatial distribution of the correlation coefficients, between station pairs in this zone (fig. 6.4) is akin to that in zone 2 of the Normal case fig. (6.2). It can be seen that the Regime B type dominates inland while Daru and Kabala in the South tend towards regimes A and C types respectively. This suggests that much of the region (mainly inland) are under the same or similar atmospheric mechanism which differs from that at play in the Southern part.

Zone 2

Notable features in zone 2 (fig. 6.5) are:

a) The existence of two prominent regimes: A and B. The ex-Regime C station, Tchaourou, now behaves as a typical A type.

SPATIAL DISTRIBUTION OF CORRELATION COEFFICIENTS
ZONE 1, 1958

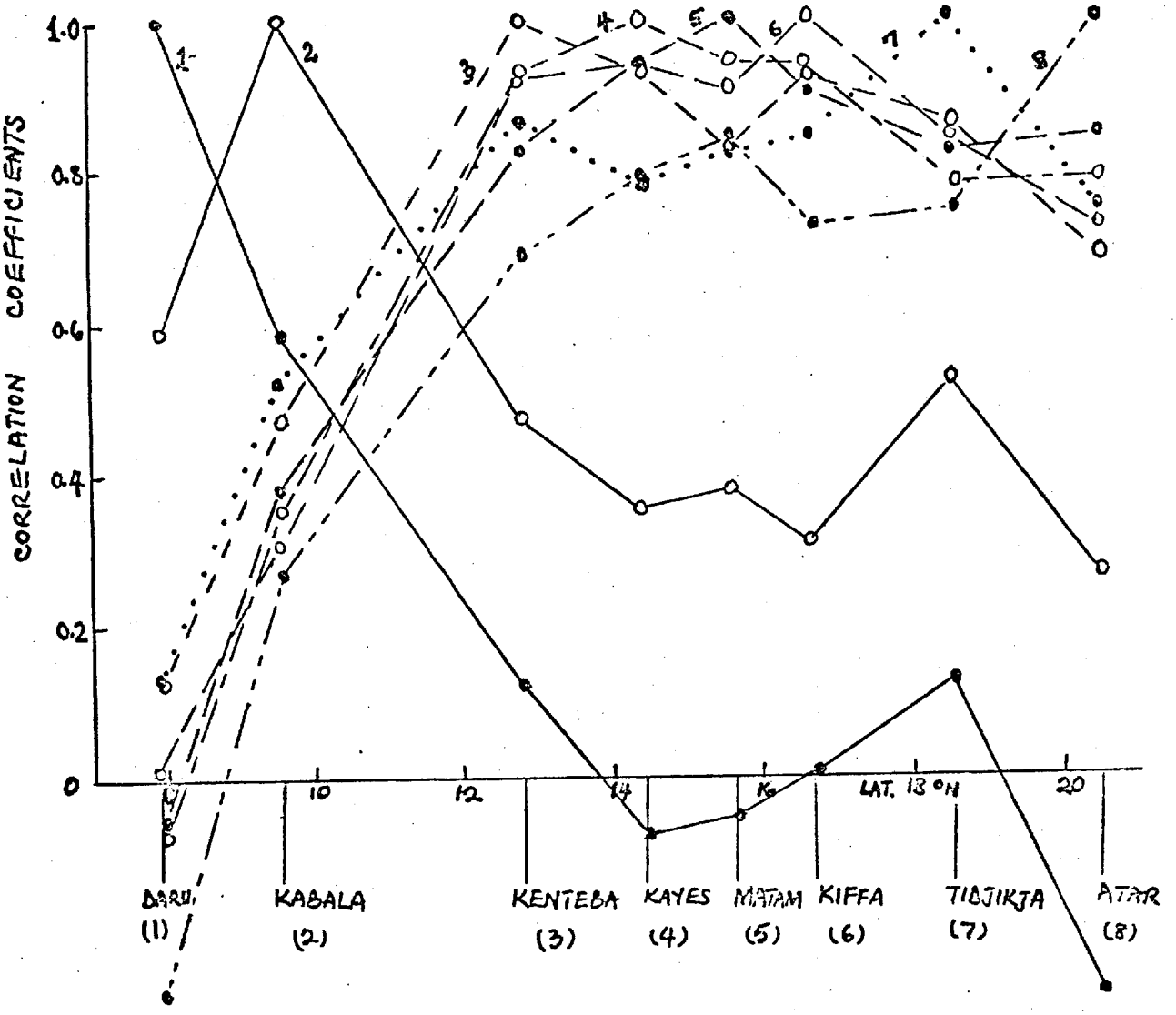

Fig 6.4

Same as in fig 6.1 but for the wet Sahel year, 1958 and zone 1.

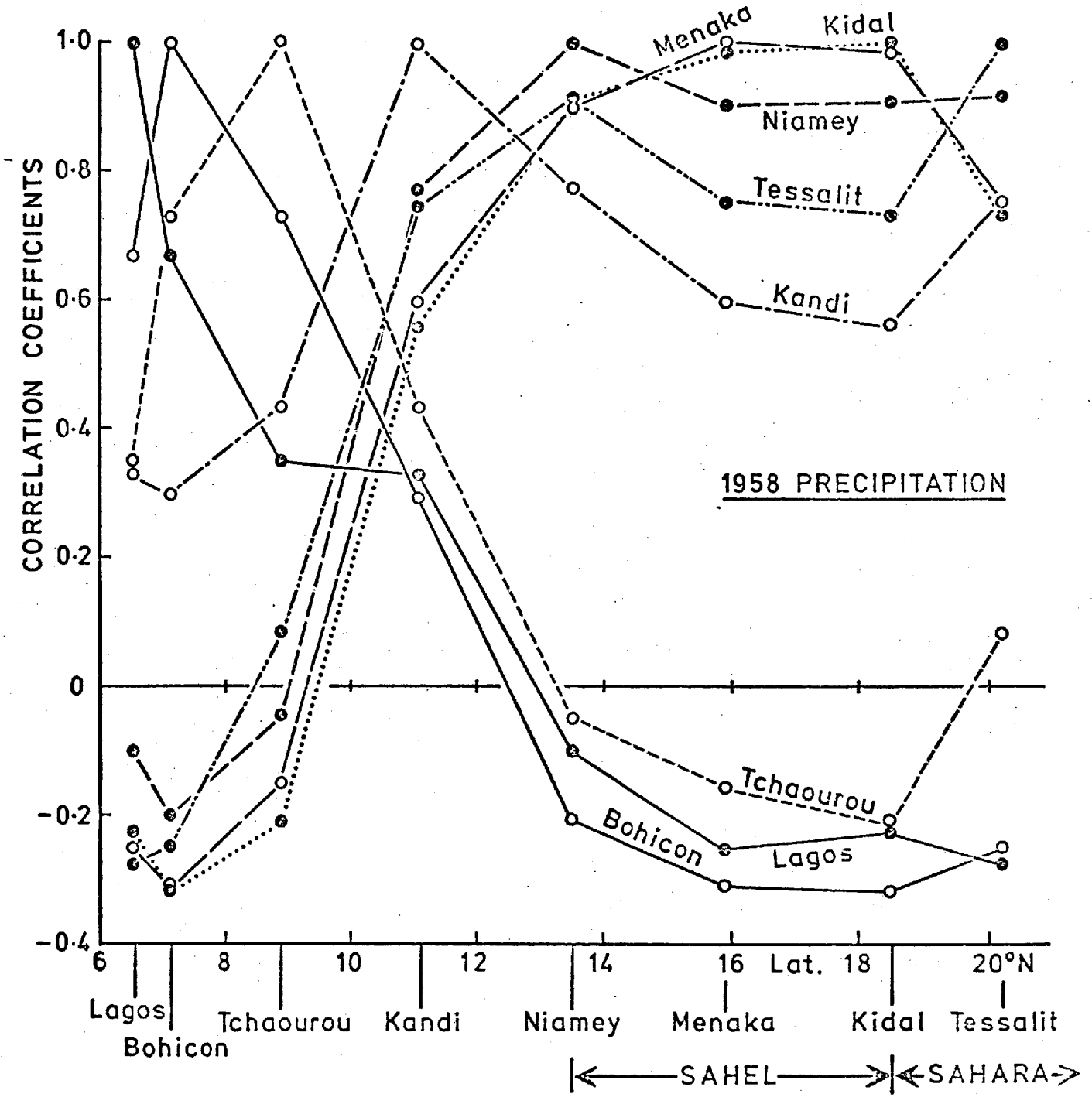

Fig 6.5

Same as in fig 6.1 but for the wet Sahel year, 1958 and zone 2.

b) The regime A type dominates over the region about 400km inland from the coast, an increase of 100km over the Normal value while Regime B type also decreases by a similar value in its extent inland.

c) The transition in the region of importance of the regimes now occurs at $10\frac{1}{2}^{o}$N, corresponding to a 1^{o} shift Northwards from the Normal position. (The threshold r value is now 0.4.) This suggests a Northward shift in precipitation zones consequent on the atmospheric mechanisms responsible for the precipitation.

Zone 3

Unlike in the Normal case, the precipitation in this zone depict a predominantly regime B correlation type. Only Bangui at the South depicts a typical Regime A correlation type fig. (6.6). Again, this behaviour suggests that the stations North of Bangui are predominantly influenced by the same or similar weather type different, of course, from that at Bangui. It is also worthy of note that between 7^{o} and 13^{o}N, a greater homogeniety in correlation relations exist than at Faya Largeau, further North. This delimits the Saharan from the Sahel type of weather.

ii) Dry Year

The dry year under consideration is 1970 (Chapter II), notable as one of the drought years in the Sahel region.

Zone 1

As shown in fig (6.7), Daru to Matam (latitude 8^{o} to 16^{o}N) from the distribution of the correlation coefficients, are under the influence of a similar weather or precipitation type.

Places to the North of this region (16^{o} to 19^{o}N in particular) seem to be different from the Southern region. The Southern region, during this period, has become drier than usual, while the hitherto

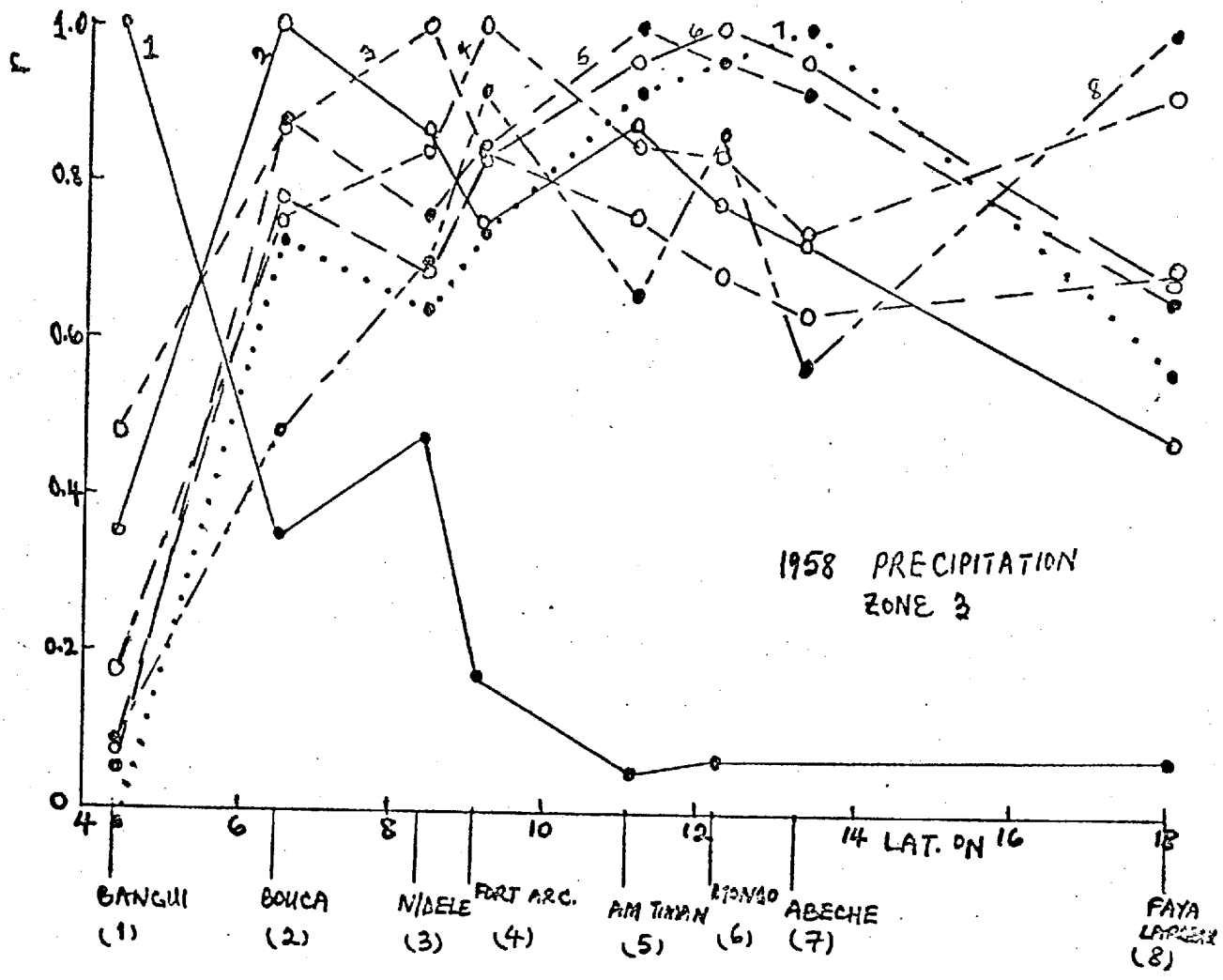

Fig 6.6

Same as in fig 6.1 but for the wet Sahel year, 1958, and zone 3.

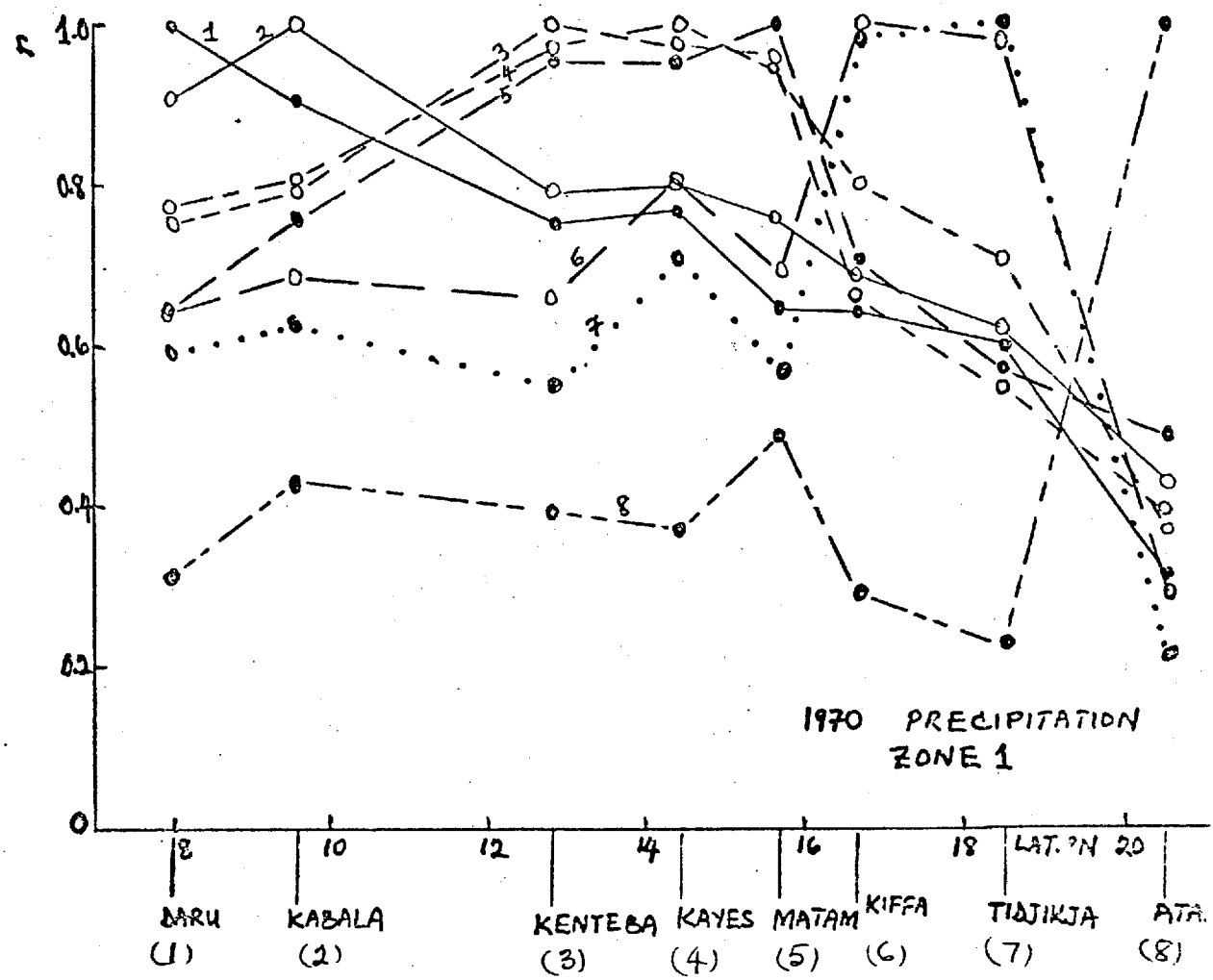

Fig 6.7

Same as in fig 6.1 but for the dry Sahel year, 1970, and zone 1.

Sahel type was tending towards the arid (desert) precipitation type owing to the drought.

The dominant correlation regime in the region is the regime C type although there is a regime A tendency which is not clearly demarcated.

Zone 2

Fig. 6.8 shows the results of the correlation relations obtained between station pairs in zone 2 for 1970. Owing to the fact that some vital months' data were missing over Tchaourou, that station could not be incorporated into the calculations.

a) The three regimes A, B, C could be identified in fig.(6.8) though there has been a re-adjustment in some stations' patterns. e.g. Bohicon, formerly in Regime A and Tessalit, formerly in B, now fall into the C regime. Hence, while Bohicon is now better correlated with the Sahel stations, Tessalit is more poorly correlated with them. Lagos, still in Regime A, is now better correlated with Tessalit than with the Sahel stations.

   Along with Lagos, Tessalit had an above-normal precipitation in the dry Sahel year, 1970, apparently due to occurrence of isolated thunderstorms resulting from forced convection.

b) Though the Sahel stations retained their usual Regime B behaviour, they were not as highly correlated with one another as in the Normal or Wet year.

c) The regime A spatial domain of importance is now drastically reduced (to about 100km from the coast). While there has been a Southward increase in the domain of the regime B type, it also suffers an equivalent limitation Northwards (in the Tessalit area).

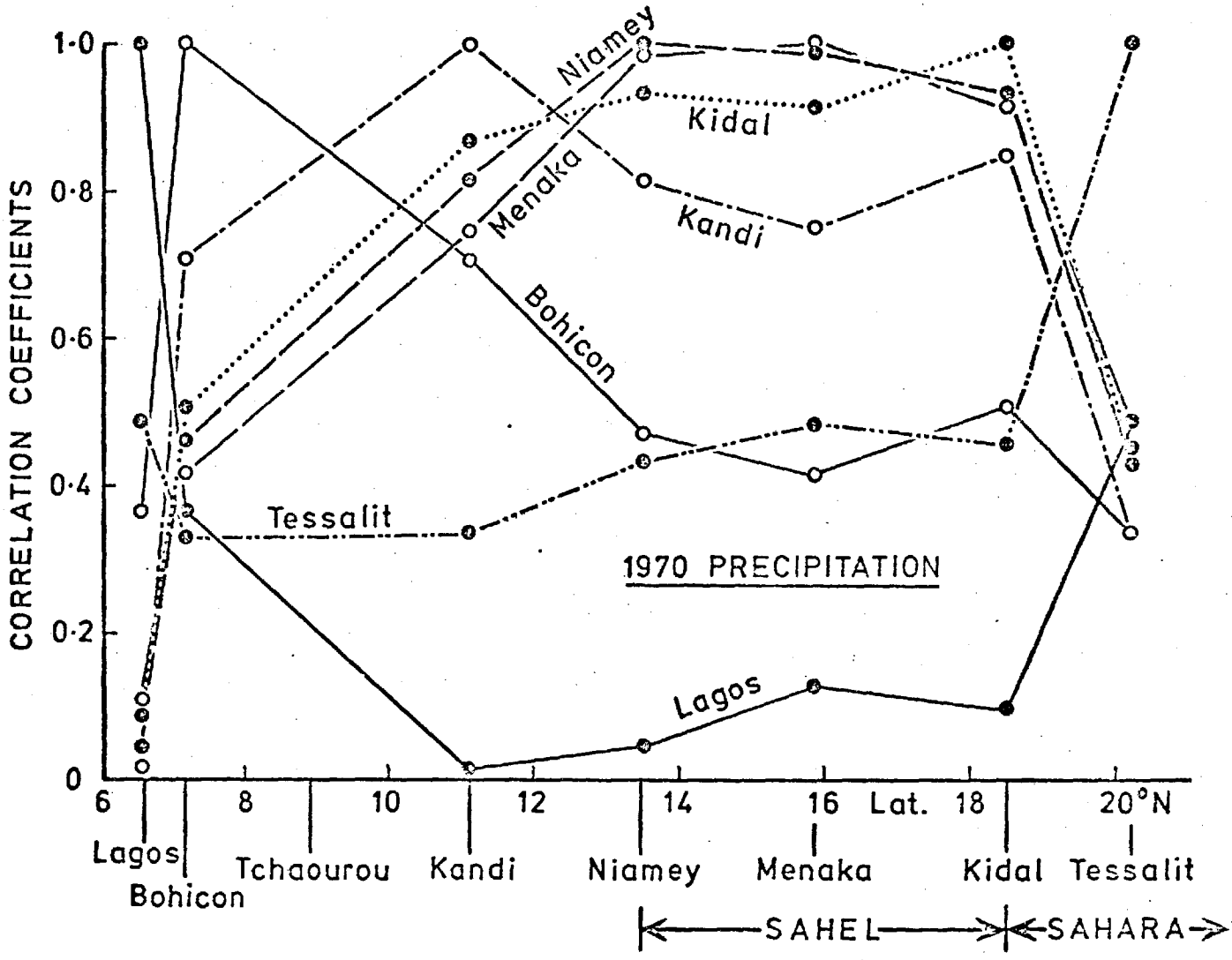

Fig 6.8

Same as in fig 6.1 but for the dry Sahel year, 1970, and zone 2.

d) The region of transition between the regimes A and B domain of importance has now shifted Southwards by about $2\frac{1}{2}^{o}$ from the Normal position of $9\frac{1}{2}^{o}$N. (the r threshold value is 0.4.) However, the absence of Tchaourou makes the pattern structure less well defined in that region.

Zone 3

A complete analysis of the correlation relations for the zone 3 stations was hindered by the fact that the data for two stations (Boende and Faya Largeau) were missing.

However, the spatial distribution of inter-station precipitation correlation made up from the other stations' data, though unrepresentative of the entire zone, is as shown in fig. 6.9.

Regime C tendency could be seen in the array of r depicted. Generally, the inter-station correlation coefficients were high $r \geq 0.5$, not much different from the Normal case in fig. (6.3).

6.(iii) c) Significance of the Correlations

In accordance with a rule of thumb criterion in use in Meteorological and climatological literature, J.E. McDonald (1957), a coefficient must be equal to or exceed thrice its standard error it it is to be evident of the existence of correlation in the parent population.

The standard error, SE is given by

$$SE = (1 - r^2)/(N-1)^{1/2}$$

where r is the correlation coefficient and
N is the number of observations made.

McDonald showed that the same threshold values are employed in this criterion as in t-test for r applied at the 95 per cent significance level.

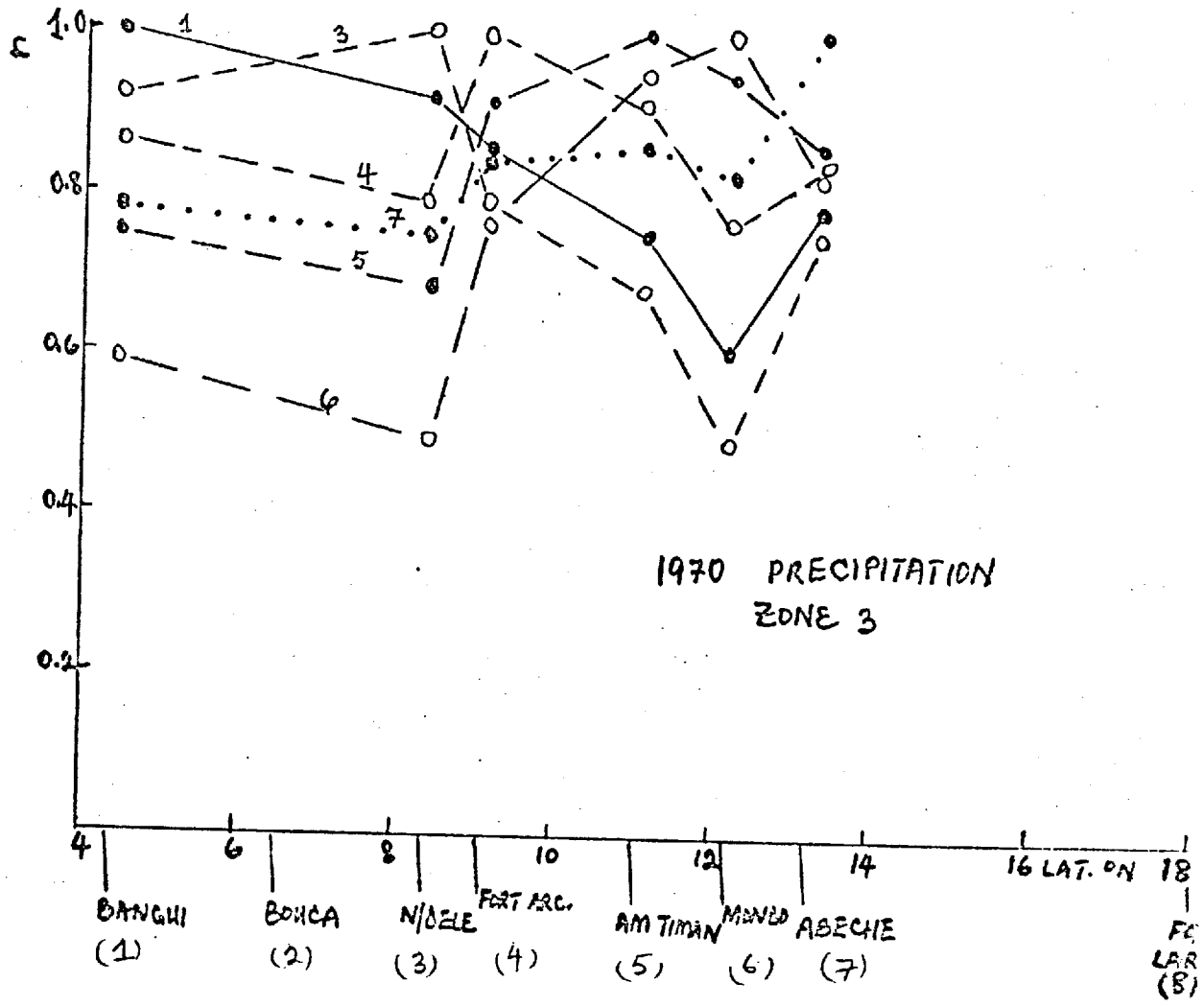

Fig 6.9

Same as in fig 6.1 but for the dry Sahel year, 1970, and zone 3. (Data for Faya Largeau and Bouca not found.)

Hence, the criterion $r \geq 3$ SE has been used to assess the domain over which regimes A, B and C are significant in this study as shown below:

TABLE 6.1 - ZONE 1

Year	Regime	Domain of Significance
1. Normal	C	8° to 20.5°N
2. 1958 (A wet Sahel year)	A	8° to 10° N
	B	11° to 21° N
	C	-
3. 1970 (A dry Sahel year)	A	8° to 18° N
	B	-
	C	8° to 18° N

ZONE 2

1. Normal	A	Coast to 10°N
	B	9° to 20° N
	C	Coast to 19°N
2. 1958 (A wet Sahel year)	A	Coast to 10°N
	B	10° to 18½°N
	C	-
3. 1970 (A dry Sahel year)	A	Coast to 7°N
	B	8° to 18°N
	C	Coast to 12°N;19-20°N

ZONE 3

1. Normal	C	4° to 18°N
2. 1958 (A wet Sahel year)	A	4.5° to 5.5°N
	B	6° to 18°N
	C	-
3. 1970 (A dry Sahel year)	C	4° to 13°N)

6.(iii) d) A Model of the Regimes* of Precipitation Correlations

From the foregoing, a schematic pattern of the regimes of correlation of precipitation across West Africa for a typical year is proposed fig. (6.10).

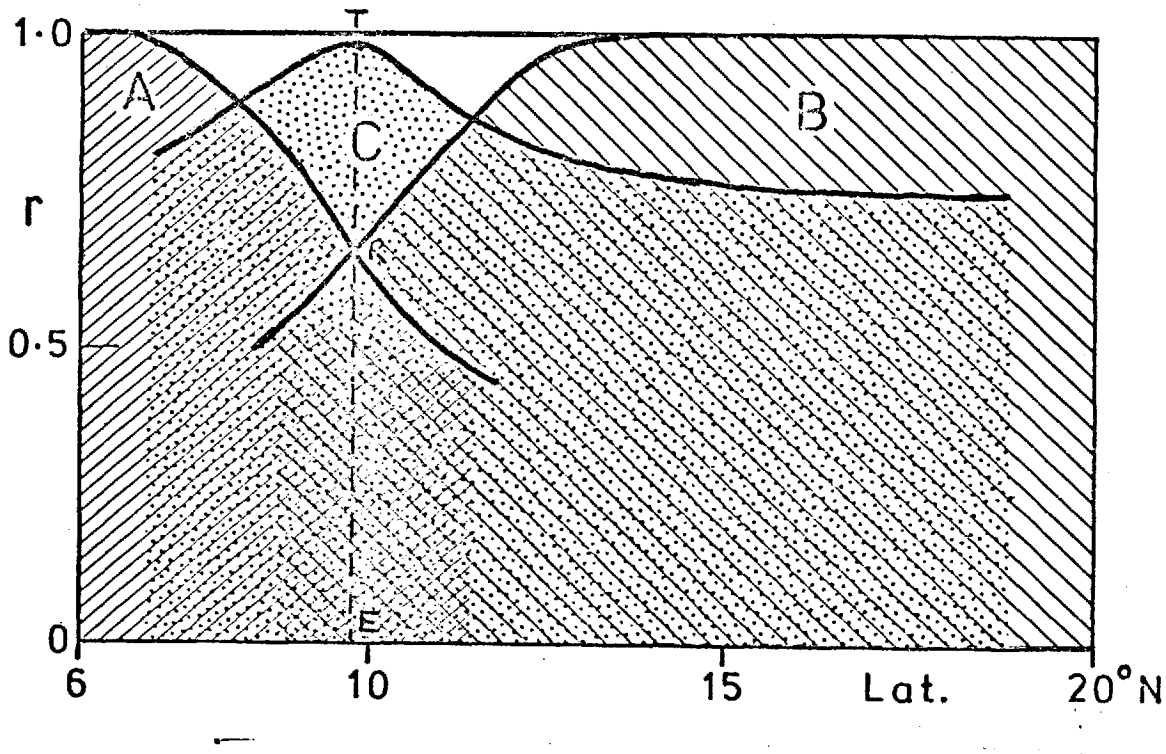

Fig.(6.10)

TRE indicates the axis of the 'threshold of significance' of regimes A and B. In the wet Sahel year, the regime A domain expands Northwards while that of B retreats Northwards also, giving a Northward displacement of TRE. A Southward displacement similarly results in a dry year, assuming a homogeneous distribution. The Sahel region is under the regimes B and C domain.

* Regime A A regime which exhibits a good inter-station correlation with the coastal region and poor or no correlation with the hinterland.

Regime B A regime exhibiting a good correlation with the Sahel and Saharan region and poor correlation with the coastal region.

Regime C A regime, intermediate between A and B, which exhibits a fairly good inter-station correlation with most of the regions.

6.(iii) e) Weather types Associated with the Regimes

Regime A

The regime A type is dominant over the Southern part of the region, particularly in zone 2. Sea breeze effect is important along the coastal strip extending within 200 to 300km inland. Convection occurs overland mainly during the day while it occurs both night and day over the sea. This area experiences early morning cloud advected from the sea (owing to the night time convection which occurred there). Precipitation resulting from this source and from coastal convergence/ divergence of the Monsoon winds approaching the Concave/Convex coast line could contribute a significant amount to the areas annual total rain. Monsoon rain, resulting from layer clouds, often of a widespread nature, is predominant in this area. The SO effect on the Lagos precipitation (Chapter IV) suggests a dominating effect of the Walker circulation in this area.

The regime A area of prominence was drastically reduced during the drought period (as shown in the 1970 results). A double peak precipitation type characterizes this area (the LDS region).

Regime B

Centred over the Sahel region, the Regime B domain of significance is characterized by a single (August) precipitation peak. Over 90% of the annual precipitation falls in June-September and about 40% of this in August when the ITD is in its maximum Northerly position. At this time, the ITD is located sufficiently North of the area to enhance the existence of a sufficiently deep convective layer capable of giving rise to thunderstorms and squall lines. The existence of orography in this area aids in triggering mechanically induced convection, resulting in

sporadic and isolated thunderstorms in places.

Easterly wave activity, fuelled by the 850mb vortices, occur aloft (700-500mb) over the region, often associated with cloud clusters evident on satellite pictures advected Westwards at 13-25kts. An analysis of these waves show that they have wave length 15-20° of longitude and are centred at about 15°N. (Obasi (1965) , Balogun E.E. (private communication, Riehl et Al, (1974)).

The domain of significance of the correlation of Regime B was shortened by about 100km in the dry year, 1970, as compared with the wet year, 1958 (particularly in zone 2). In 1970, the Sahel stations were poorly correlated with Tessalit in the Sahara, contrary to the Normal and 1958 cases. This behaviour agrees with the relative shift in the ITD position Southwards in 1970 compared with 1958 (Chapter II).

Regime C

This regime is intermediate between the Regime A and B types and the stations involved are characterized by being averagely correlated with other stations North and South of the zone. It is influenced by the interaction between the Easterly wave and squall activities to the North, and the Monsoon and sea breeze effects to the South. The area lies in the switch-over zone between the action of 'warm lows' located over the ITD in the North and the SO influence to the South (particularly at the coastal strip's LDS period). Unlike the regimes A and B, this regime is not quite stable and is sometimes non-existent.

6.(iv) THE CROSS-EQUATORIAL INTER-STATION (PRECIPITATION) CORRELATIONS

Using the data obtained from an extension of zone 3 across the Equator to latitude 16°S (Chapter II) a cross-equatorial pattern of correlations is established as shown in fig. (6.11) for the Normal case.

Each curve, as in similar diagrams of inter-relation correlation coefficients, represents the correlation relation between the precipitation over a station and that over each of the other stations in the zone. A first glance at this figure would rightly suggest a

Fig 6.11 SPATIAL DISTRIBUTION OF r : NORMAL PRECIPITATION : ZONE 8 EXTENDED ACROSS THE EQUATOR

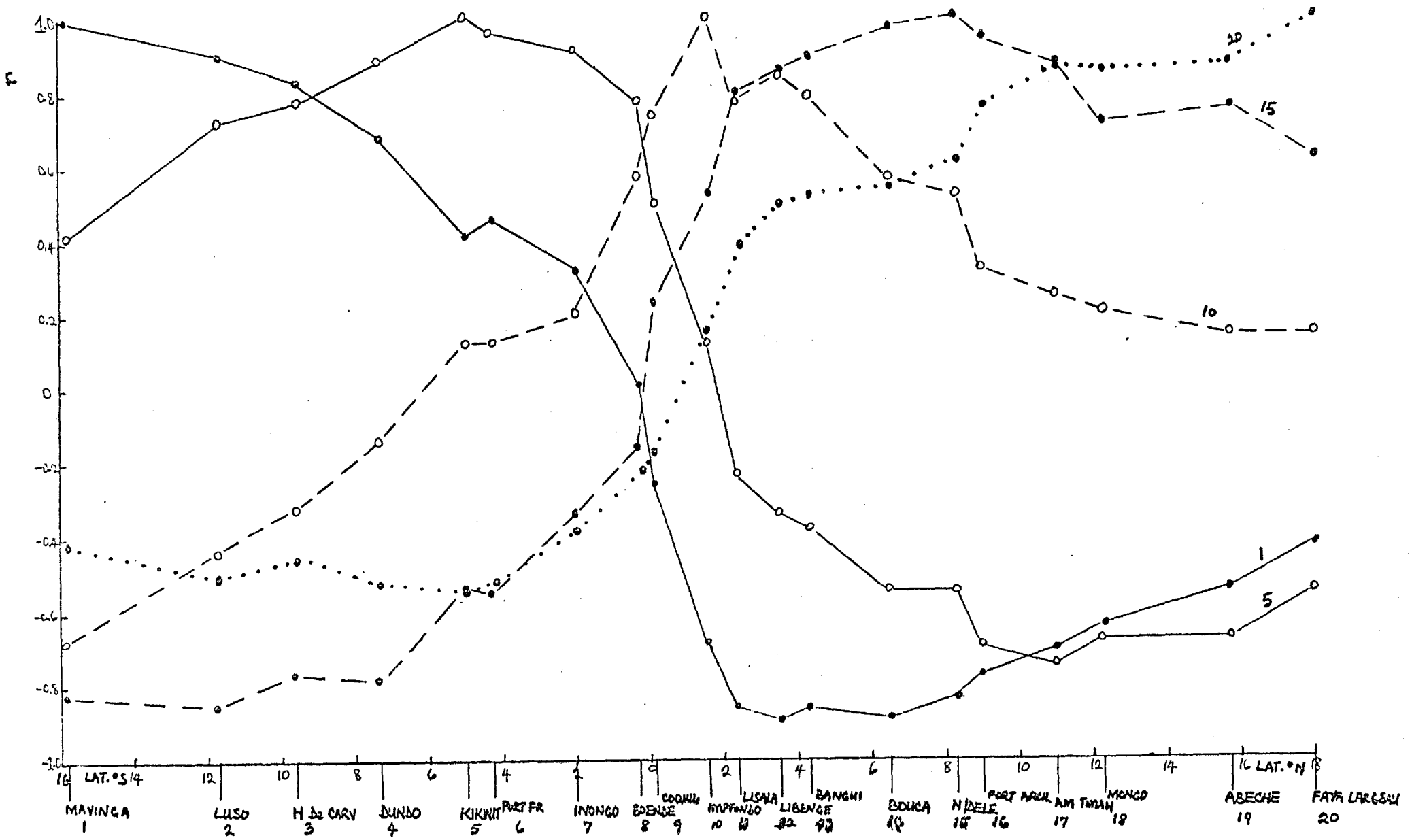

negative correlation between the NH and SH precipitation input. This is in agreement with the fact that during the Monsoon (rainy) season in West Africa (Mainly NH Summer) the SH is in the Southern Winter period and is, hence, dry. The converse holds for both regions.

To illustrate this clearly, two stations in the North: Faya Largeau (18^{o}N) and N/Dele (8.5^{o}N) and two to the South: Mavinga (16.2^{o}S) and Kikwit (5^{o}S) were plotted, each with its correlation with every other station along the zone. It can be seen that the Northern stations are highly (positively) correlated with the stations to the North but negatively correlated with the stations to the South. The converse holds for the Southern stations as well.

As an illustration of the behaviour of stations near the Equator, Impfondo (1.5^{o}N) has been chosen. This station is highly correlated with stations between 0.5^{o}S and 8.5^{o}N and negatively correlated with stations between 13^{o}S - 16^{o}S but not (significantly) correlated with other stations in the region. This tends to indicate that areas around the stations are influenced by similar atmospheric convective systems which are bounded in their latitudinal extent.

In this cross-Equatorial scale, the Southern stations display a Regime A characteristic while the Northern stations, a regime B type. The near-Equatorial station tended towards a quasi-regime C type behaviour.

6.(v) THE CROSS-CORRELATION OF PRECIPITATION IN THE REGION

The cross correlation coefficient, r_c between two stations can be defined as

$$r_c = \sum_{t=1}^{N-Lag} (X_{t+Lag} - \bar{x})(y_t - \bar{y}) / \sigma_x \sigma_y N \qquad \ldots\ \ldots\ \ldots\ 6.18$$

where $\bar{x}$ and $\bar{y}$ are the mean precipitation in the two stations respectively.

σ_x and σ_y are their standard deviations

N = Number of observations used (here, number of months)

t = the time in months.

The cycle of precipitation in the region (Chapter II) indicates that an investigation of the cross-correlations between station pairs might be suggestive of prediction over some lag period. We shall, therefore, investigate the cross-correlations between the various station pairs in zone 2, along the longitude of Lagos for lag periods 1-11 months.

Results obtained from this exercise, using the Normal long term (1931-60, wherever possible) precipitation treated as cyclic data, indicate a symmetric r_t matrix at the 6 month lag (Appendix VI(i)). For all the other lags, reciprocal correlation results i.e. if a station x is highly correlated with another station, y, at lag α month, y will be highly correlated with x at lag $(12 - \alpha)$ month.

Lag period 1 month indicated a demarcation of regimes already observed in the lag 1 month treated in the last section. However, at lag 2 month, inter-regime correlations could be seen. This trend manifests itself also in lag 3 month but declines in significance for higher lag periods. The 2 month lag cross-correlation coefficients are spatially distributed as shown below in fig (6.12). It is remarkable to note that a Southern station like Lagos in regime A is now well-correlated with the Sahel station which are typical regime B type.

a) The 2 month lag maximum

To highlight this properly, a cross-correlation between Lagos and all the other stations in the zone has been carried out for lags 0-12 months, fig (6.13).

Remarkable features of fig (6.13) are:

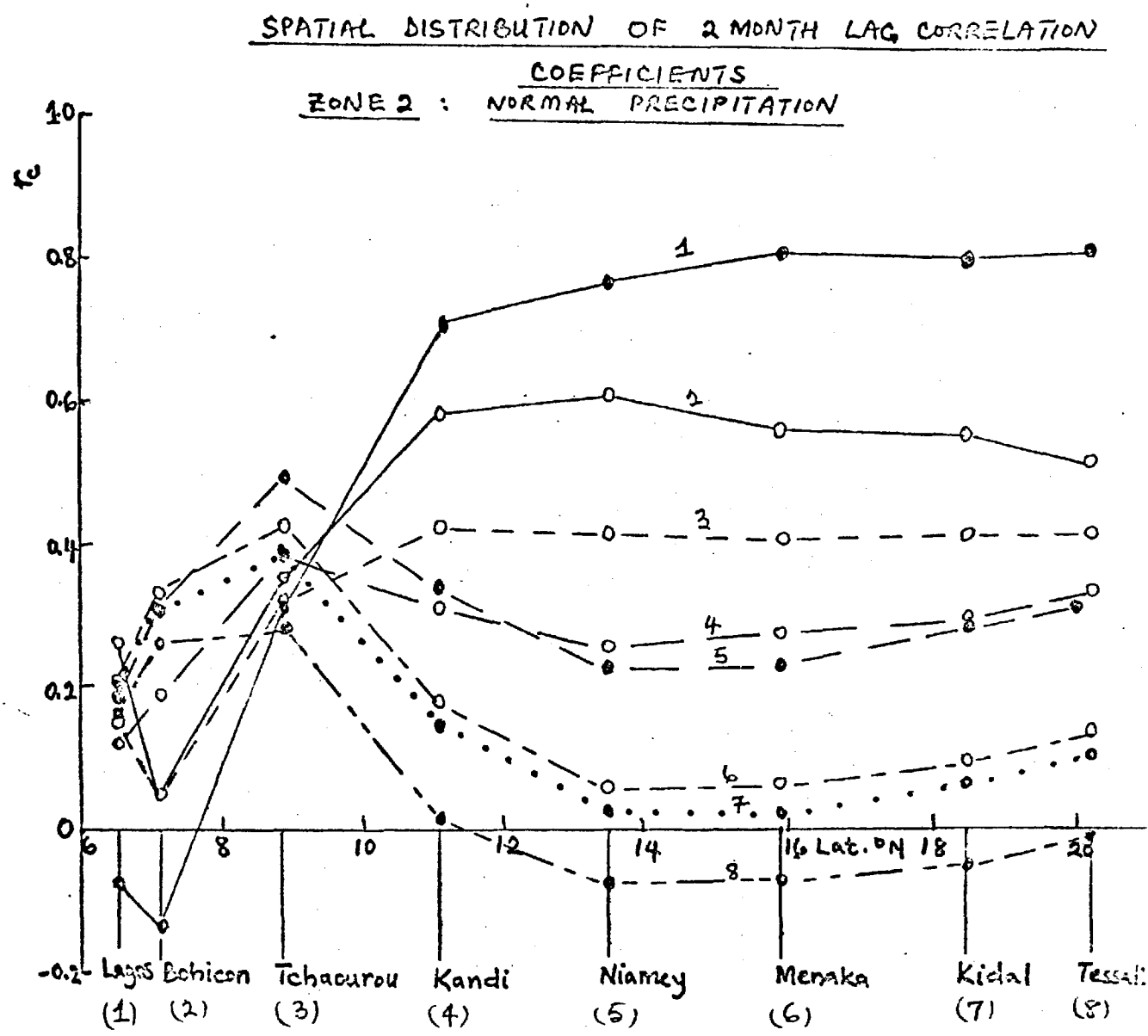

Fig 6.12

The spatial distribution of the cross-correlation coefficient, r_c at lag 2 months between each station and every other one in the zone (zone 2); Normal precipitation. Lagos and Bohicon in the South are well correlated with the inland (Sahelian) stations of Niamey, Menaka Kidal and Tessalit. ($r_c \sim 0.8$ and 0.6 respectively)

Fig 6.13:

The cross-correlation coefficients, r_c at lag 0 to 12 months between Lagos and each of the other stations in zone 2: Normal precipitation. A maximum can be noticed at lag 2 months between Lagos and the Sahel stations. This is clearly depicted in fig. 6.13b where Niamey typifies the Sahel stations' behaviour and Bohicon and Tchaourou are stations further South. The negative correlations existing at the 6-8 month lags result from the Seasonal contrast between the wet and the dry seasons.

Fig 6.13 a)

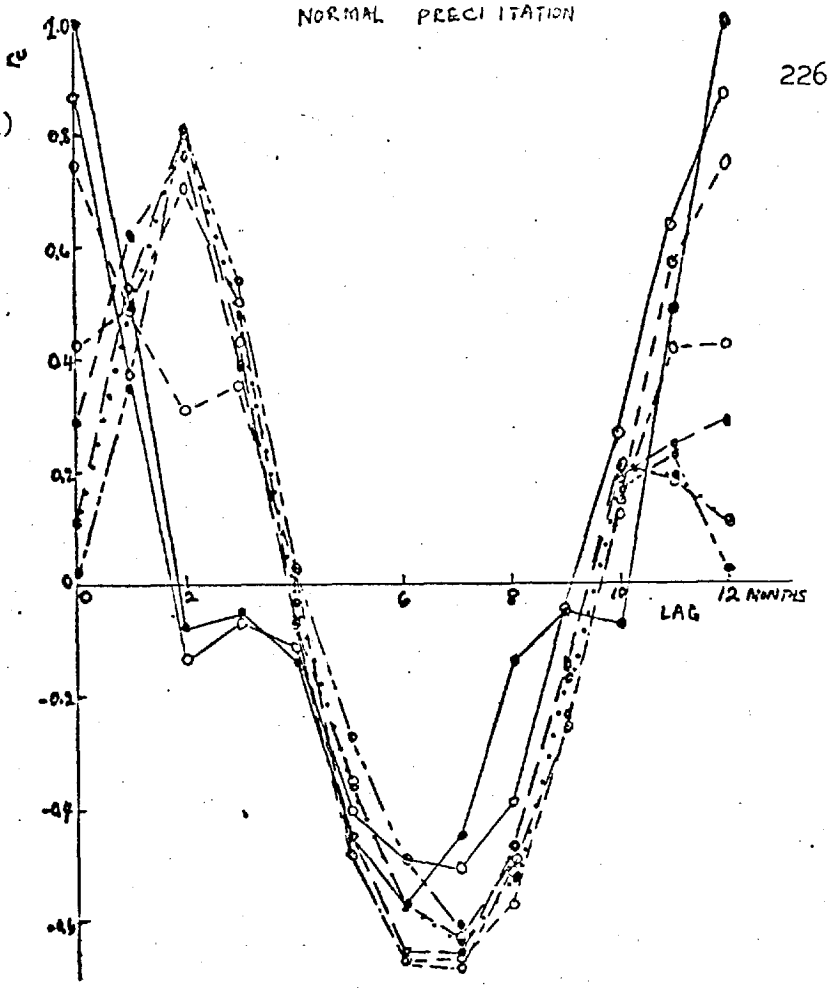

Fig 6.13 b)

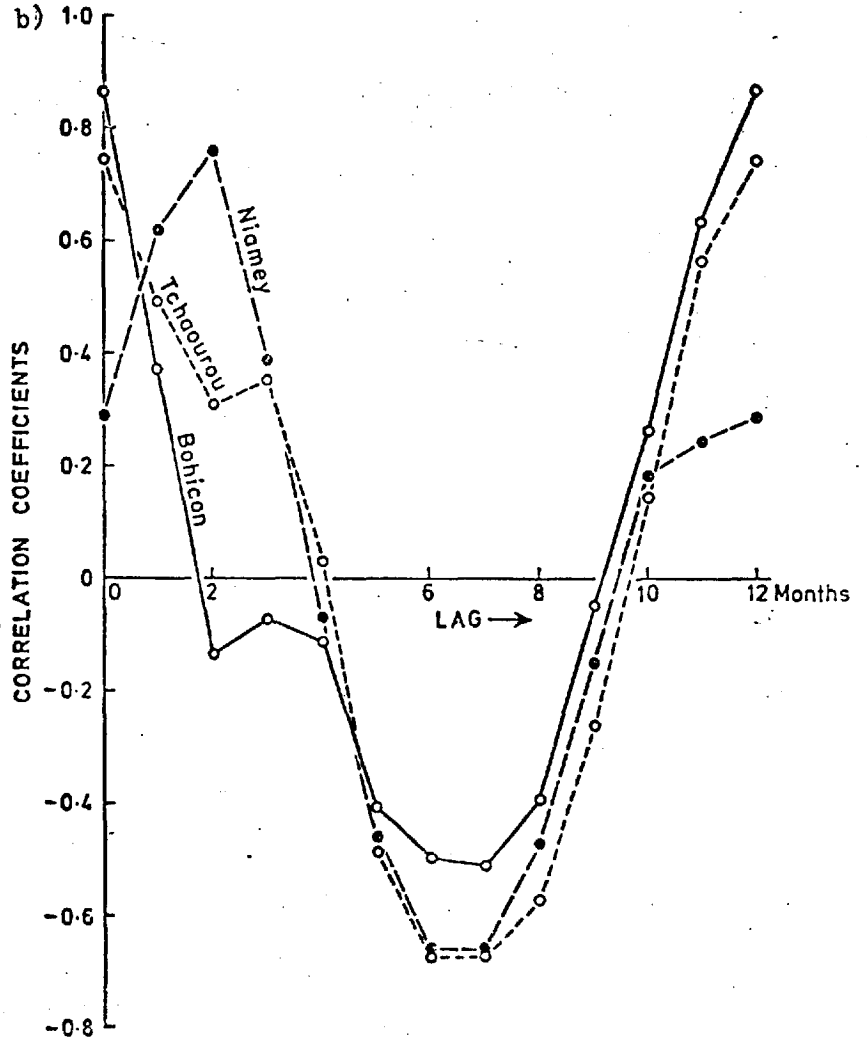

(i) the two-month lag maximum between Lagos and the inland (Sahel/Saharan) stations: $r_c > 0.7$

(ii) the minimum (and negative) lag correlations at lag 6-8 months, which are indicative of the switch over between the dry season and the rainy season in the region.

These calculations were repeated using the data for the wet Sahel year (1958) and the dry year (1970) and the results obtained were similar to those of figs 6.12 and 6.13, exhibiting the two features (i) and (ii) remarked above.

In view of the advantage, to agriculture in the Sahel, of knowing two months ahead what the Monsoon rains would spell, the two month lag maximum here obtained, was further investigated.

b) Significance of the two month lag correlations:

A graphical representation of the significance of the two-month lag correlation between Lagos and the other stations in zone 2 is as shown in fig (6.14), for both the Normal and the wet and dry years considered.

Both the normal, the wet and dry years' results indicate that Lagos is highly correlated (and significantly) with the Sahel stations: $r \geq 3SE$.

The stations not satisfying this condition for significance shown in fig (6.14), are:

a) Normal case: i) Lagos (auto-correlation) } $r < -SE$
ii) Bohicon
iii) Tchaourou $2SE > r > SE$

all in the Southern part.

b) 1958 i) Lagos (auto-correlation) $2SE > -r > SE$
ii) Kandi $2SE > r > SE$
iii) Bohicon $r = -SE$

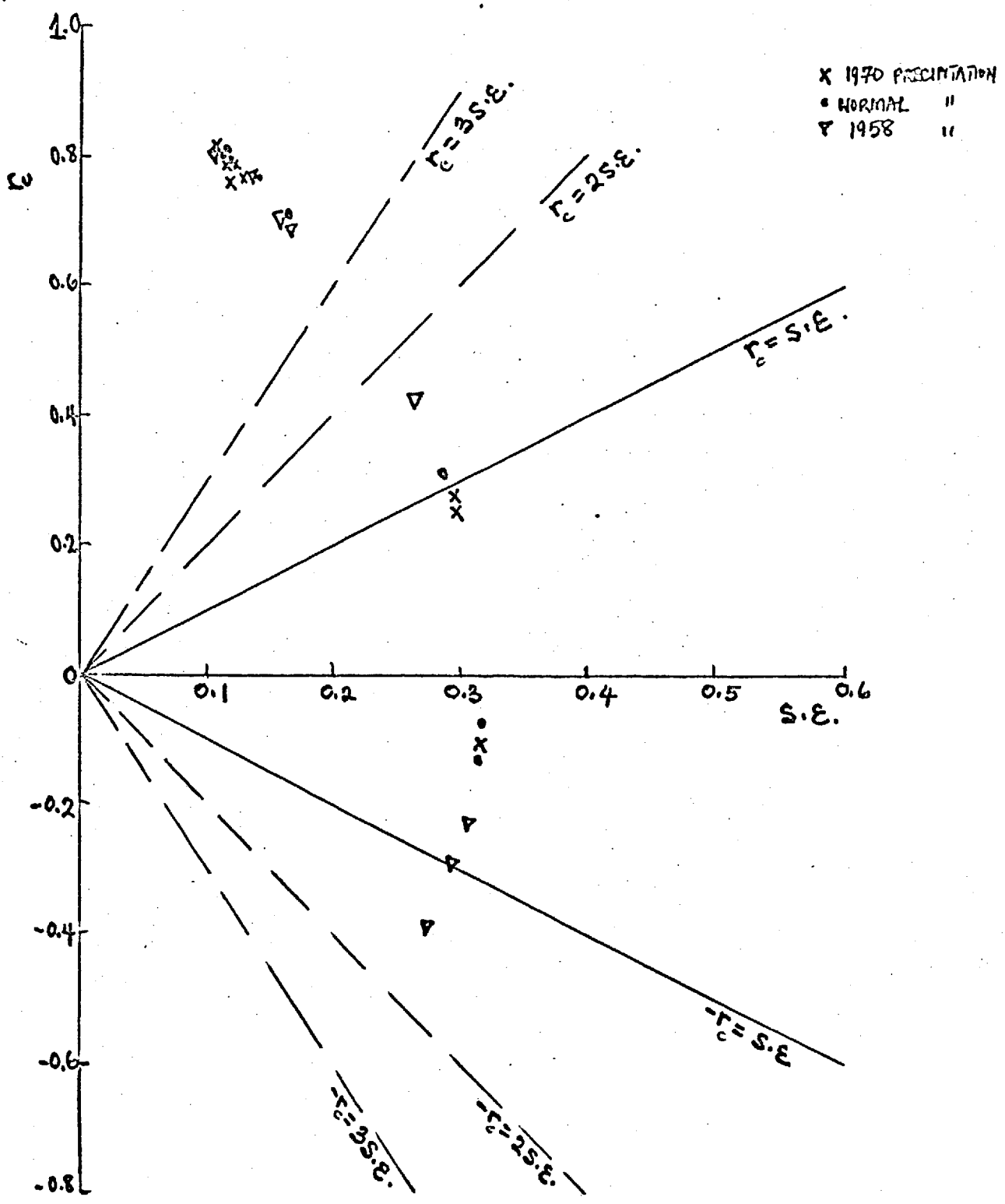

Fig 6.14

A graphical representation of the significance of the 2 month lag correlation between Lagos and the Sahel stations. The cross correlation, r_c has been plotted against the standard error, SE and the stations over which r_c is significant satisfy the condition $r_c \geq 3SE$ and hence, lie to the left of the $r_c = 3SE$ demarcation line. Except Lagos (auto correlation), Bohicon and Tchaourou in the Normal case and along with Kandi in the wet year case, but Tessalit in the dry year case, the other (mainly Sahel) stations are significantly correlated with Lagos at the 2 month lag.

c) 1970

i) Bohicon
ii) Tessalit } $0 < r < SE$
iii) Lagos (auto-correlation) $0 < r < -SE$

The regression relations for the two-month lag are as shown in table 6.2.

TABLE 6.2

REGRESSIONS OF THE LAGOS PRECIPITATION (X)(mm) ON SAHEL STATIONS (Y (mm) IN EACH CASE), AT LAG 2 MONTHS

1. NORMAL PRECIPITATION (This is the 1931-60 mean, wherever possible).

a) Lagos (X) and Niamey (Y) :

$X = 75.3 + .88Y$ $r_c = .76$ SE = .13

b) Lagos (X) and Menaka (Y) :

$X = 79.4 + 1.9Y$ $r_c = .81$ SE = .11

c) Lagos (X) and Kidal (Y) :

$X = 80.2 + 3.8Y$ $r_c = 0.80$ SE = .12

d) Lagos (X) and Tessalit (Y) (Saharan station) :

$X = 81.3 + 4.07Y$ $r_c = .80$ SE = .11

2, 1958

a) Lagos (X) and Niamey (Y) :

$X = 50.9 + 1.05Y$ $r_c = .82$ SE = .11

b) Lagos (X) and Menaka (Y) :

$X = 57.5 + 1.1Y$ $r_c = .71$ SE = .16

c) Lagos (X) and Kidal (Y) :

$X = 2.82Y + 56.6$ $r_c = .77$ SE = .13

d) Lagos (X) and Tessalit (Y) :

$X = 62.16 + 3.08Y$ $r_c = .70$ SE = .17

3. 1970

a) Lagos (X) and Niamey (Y) :

$X = 78 + 1.64Y \qquad r_c = .82 \qquad SE = .11$

b) Lagos (X) and Menaka (Y) :

$X = 88 + 3.76Y \qquad r_c = .78 \qquad SE = .12$

c) Lagos (X) and Kidal (Y) :

$X = 88.5 + 6.35Y \qquad r_c = .76 \qquad SE = .14$

* d) Lagos (X) and Tessalit (Y)

$X = 131.8 + 1.34Y \qquad r_c = .25 \qquad SE = .30$

* Not significant

c) Cross-correlation between Lagos and Niamey over a 20-year period

An extensive cross-correlation of the Lagos and Niamey monthly precipitation for January 1951 to December 1970 has been carried out for 0 to 60 month lags, an extension of the (0 - 11) month lag scheme.

As shown plotted in fig (6.15), a maximum (and significant) correlation is obtained at the 2 month-lag while a cyclic recurrence of this happens at every (12n + 2) month lag (where n represents the annual cycle). An exception to this occurred at the 13th lag (with $r_c = 0.49$) which is higher than the 14th lag value ($r_c = 0.47$).

The significant negative correlations observed at the 6-8 month (centred on 7 month) lag, also recurred after n annual cycles, indicating the seasonal contrast in precipitation between Lagos and Niamey wet and dry months. This seasonal contrast apart, no particular importance need be attached to this negative correlation maxima. The correlations, after elimination of the seasonal contrast, are investigated in the following section (6.V.d)

Table 6.3 (Appendix (vi.2) shows the results of the cross-correlation exercise, indicating the values of r_c and the standard error, SE, obtained for various lags, l.

The regression relation for the 2 month lag correlation between Lagos and Niamey, for the 20 years of running monthly precipitation here considered:

($r_c = 0.6$; SE = 0.04) is:

$$R_L \text{ (mm)} = 1.01\, R_N + 96 \qquad \text{.. .. .. 6.19}$$

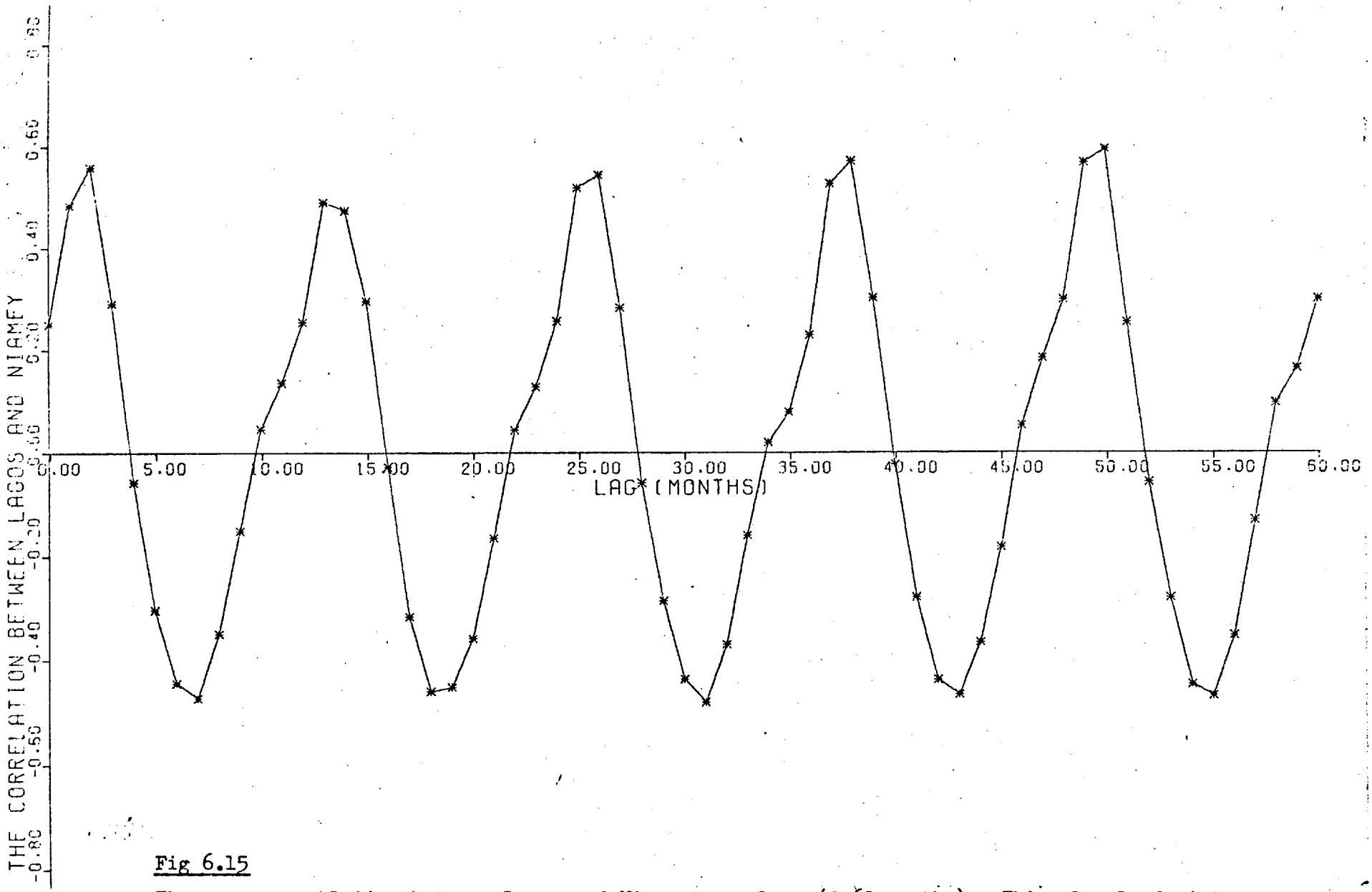

Fig 6.15

The cross-correlation between Lagos and Niamey over lags (0-60 months). This clearly depicts a maximum at lag 2 months and its annual recurrence at lag (12n + 2) months, where n = no of years. The negative correlations at lag 7 months etc are due to the seasonal contrast in precipitation trend.

d) Elimination of the effect of the Seasonal contrast

In order to remove the effect of the Seasonal contrast between Lagos and Niamey, which featured in the cross-correlation of the two stations' precipitation for January 1951 - December 1970, a consideration of the Sahel rainy season (May to October) along with March to August of the Lagos rainy season was made.

Hence, a correlation of Lagos, March-August and Niamey, May-October, mapping out the two-month lag for each year of 1951 to 1970, was carried out, as shown in fig (6.16). The detailed results showing r_c, SE, variance, coefficient of variation, along with the regression relations are shown in Appendix (VII). Highlights of the results are that:

i) higher r_c values than obtained earlier in Table 6.2 resulted for:

	r_c (modified)		r_c table (6.2)
1958	0.871	compared with	0.816
1970	0.935	compared with	0.819

ii) Poor correlations were obtained in 1954-7 and 1968. This may be due to the fluctuation in the strength of the Walker Circulation which, as discussed in Chapter IV, influences the temperature contrast between the South and the Sahel region. The higher this temperature contrast is, the stronger the Easterly flow aloft, and consequently, the action of the Easterly disturbances in whose wake squall lines develop.

The variation in θ_w (850mb) and θ_s (500mb) determines the instability index I relative to the ITD position (Chapter V).

Using the July 1957 and 1958 upper air soundings for Lagos/Ikeja, Niamey, Tamanrasset and Aoulef, it is found (fig (6.17) that:

i) both places were more convectively unstable in 1957 than in 1958;

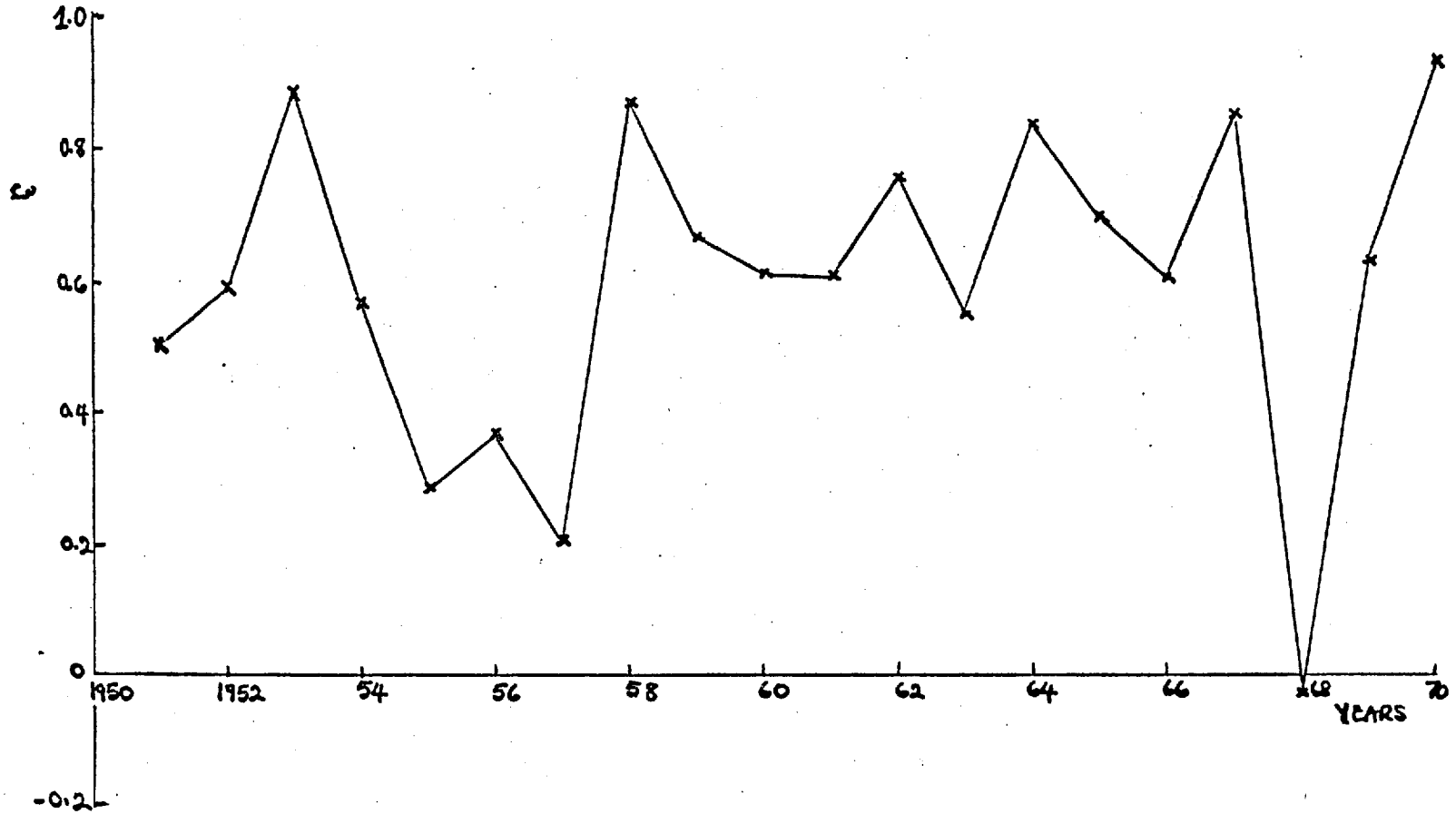

Fig 6.16

The two month-lag correlation as computed for each year 1950-1970. The poor correlation noted in 1955-1957 and 1968 are remarkable.

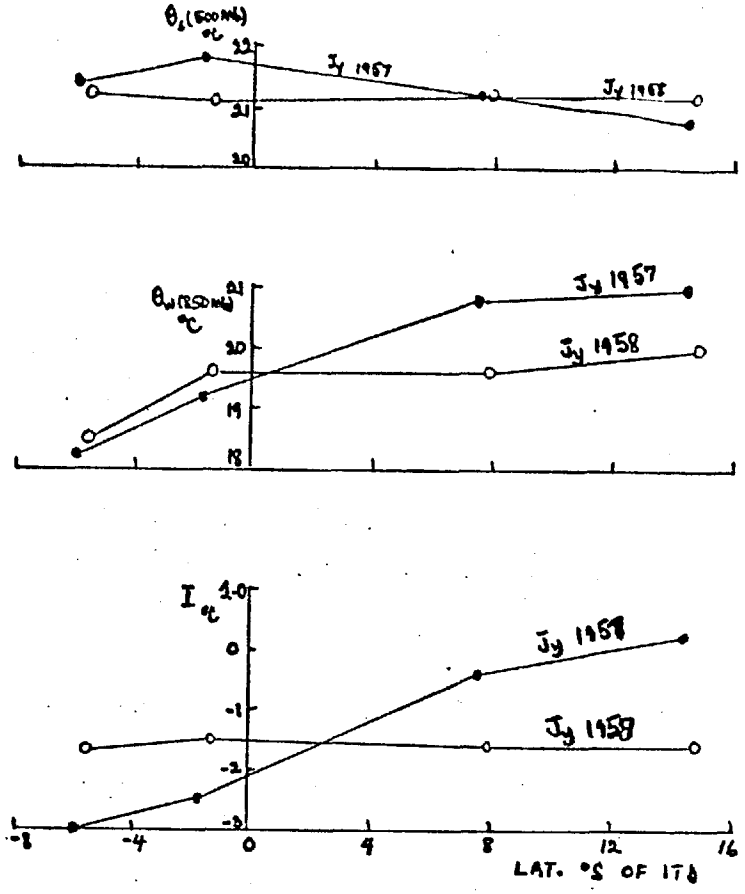

Fig 6.17

The variation, across the ITD, of θ_s (500mb), θ_w(850mb) and I($^{\circ}$C) for July 1957 and July 1958 compared. More convective instability typified the former than the latter.

Fig 6.18 The variation in the correlation coefficient $r(\phi_I-\phi,R)$, for each station in zone 2 based on July-Dec. of 1957, 1958 and 1970. The ITD-control on R declines Southwards and is poor in the LDS (eg Lagos) area e.g. 1958,1970. When this improved in 1957, spelling an ITD control over the Lagos precipitation the 2 month Lag correlation between Lagos and Niamey broke down.

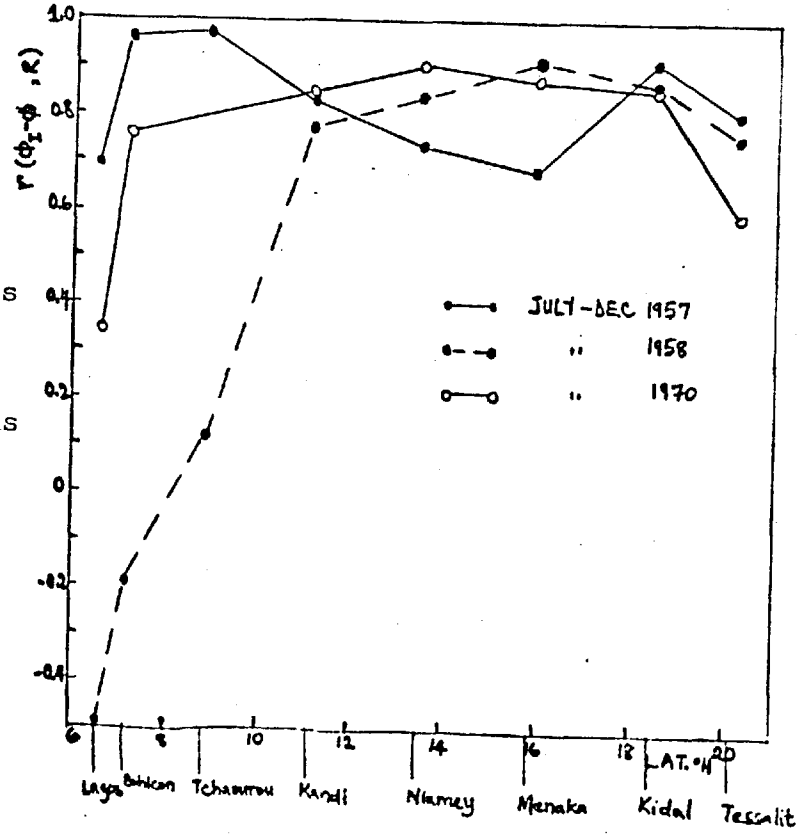

ii) Lagos was more convectively unstable than Niamey in 1957, while both were equally stable in 1958.

The two-month lag correlation was high in 1958 but poor in 1957. Hence, sharp contrasts in the degree of convective instability between the two places may be decisive in this.

e) Other conditions under which the two-month lag correlation does not hold:

1. The dependence of the stations' precipitation on their positions relative to the ITD may play a part in determining whether or not the two-month lag between the two stations' precipitation holds.

The Niamey precipitation is highly correlated with $(\phi_I - \phi)$, its position relative to the ITD. That at Lagos is usually poorly or negatively correlated with its position relative to the ITD as shown by the correlation between $(\phi_I - \phi)$ and R for (July - December) 1958 and 1970 fig (6.18). When, however, in 1957 (July - December) Lagos $(\phi_I - \phi)$ was well correlated with R, an anomalous behaviour, Niamey $(\phi_I - \phi)$ and R were still well correlated as usual.

However, unlike in 1958 and 1970 when high two-month lag correlation existed between Lagos and Niamey, the 1957 case proved contrary.

The relevant regression equations are:

LAGOS

July-December 1958: $R(mm) = 10.9 - 0.49(\phi_I - \phi)$; $r = -0.49$, $SE = 0.34$

July-December 1970: $R(mm) = 7.50 + 0.69(\phi_I - \phi)$; $r = 0.34$, $SE = 0.39$

July-December 1957: $R(mm) = -0.9 + 2.09(\phi_I - \phi)$; $r = 0.7$, $SE = .23$

NIAMEY

July-December 1958: $R(mm) = 1.94 + 1.69(\phi_I - \phi)$; $r = 0.84$; $SE = .13$

July-December 1970: $R(mm) = 5.64 + 1.36(\phi_I - \phi)$; $r = .91$ $SE = .08$

July-December 1957: $R(mm) = 3.84 + 1.75(\phi_I - \phi)$; $r = .73$; $SE = .21$

2. Another criterion may be the variation in the intensity of the LDS in the Lagos area. The LDS, a well marked climatic phenomenon is Lagos environ is observed in late July - August under Normal circumstances. Below is an indication of the Occurrence of the phenomenon shown by the July and August precipitation for 1958, 1970 and 1957 expressed as % Normal :

LAGOS PRECIPITATION AS % NORMAL

YEAR	JULY	AUGUST
1958	0.01	0.02
1970	146	0.2
1957	169	244

Unlike in the other two years, the LDS did not show up in 1957. It is, therefore, probable that :

The LDS occurs when a break-down exists in the dependence of the Lagos precipitation on the ITD position. This enhances the establishment of the two-month lag correlation between the Lagos and the Sahel (e.g. Niamey) precipitation (noted for its single peak in August). A deviation from this state weakens the two-month lag correlation relationship but promotes the dependence of Lagos precipitation on the ITD position.

As already shown in Chapter IV, the SO affects the Lagos precipitation while the ITD control does not hold there as manifest for various seasons of 1951-1973.

6.(vi) INTER-STATION CORRELATION OF DECADAL MONTHLY PRECIPITATION

Recent series studies of the Sahelian precipitation (Wrights, 1974: Bunting et Al., 1976) have shown that in the 1905 to 1974 period, the decade 1951-60 had less fluctuation in precipitation than any other decade. While large variations exist in other decades in this series (a likely indication of existence of 'noise' in the series) the 1951-60 decade was devoid of such variations and was relatively better behaved. For this reason, it is considered appropriate to use this decade for investigating the decadal inter-station correlation behaviour.

The decadal correlations for the month of August, at which time the Sahel stations have their highest precipitation and the Southern (Lagos etc) area experience the LDS are shown in fig (6.19). Important features of the climatological nature of the region indicated in these results are:

1. The mapping out of the LDS region as distinct from the maximum precipitation (Sahel) region. The Lagos and Bohicon inter-correlation curve clearly indicate the zone over which the LDS was at play by means of the high correlations they have with stations between 6 and 11°N. As normally expected, they indicated a negative correlation with the Sahel area.

2. Similarly, the Menaka and Kidal curves, indicate the region of the Sahel precipitation maxima, by virtue of their good correlation with these stations, as contrasted with the LDS stations in the South, with which they are negatively correlated. Menaka's low correlation with Tessalit may be due to the fact of the latter's aridity, relative to the former.

3. A region of transition exists between these two areas of distinct climatological characteristics.

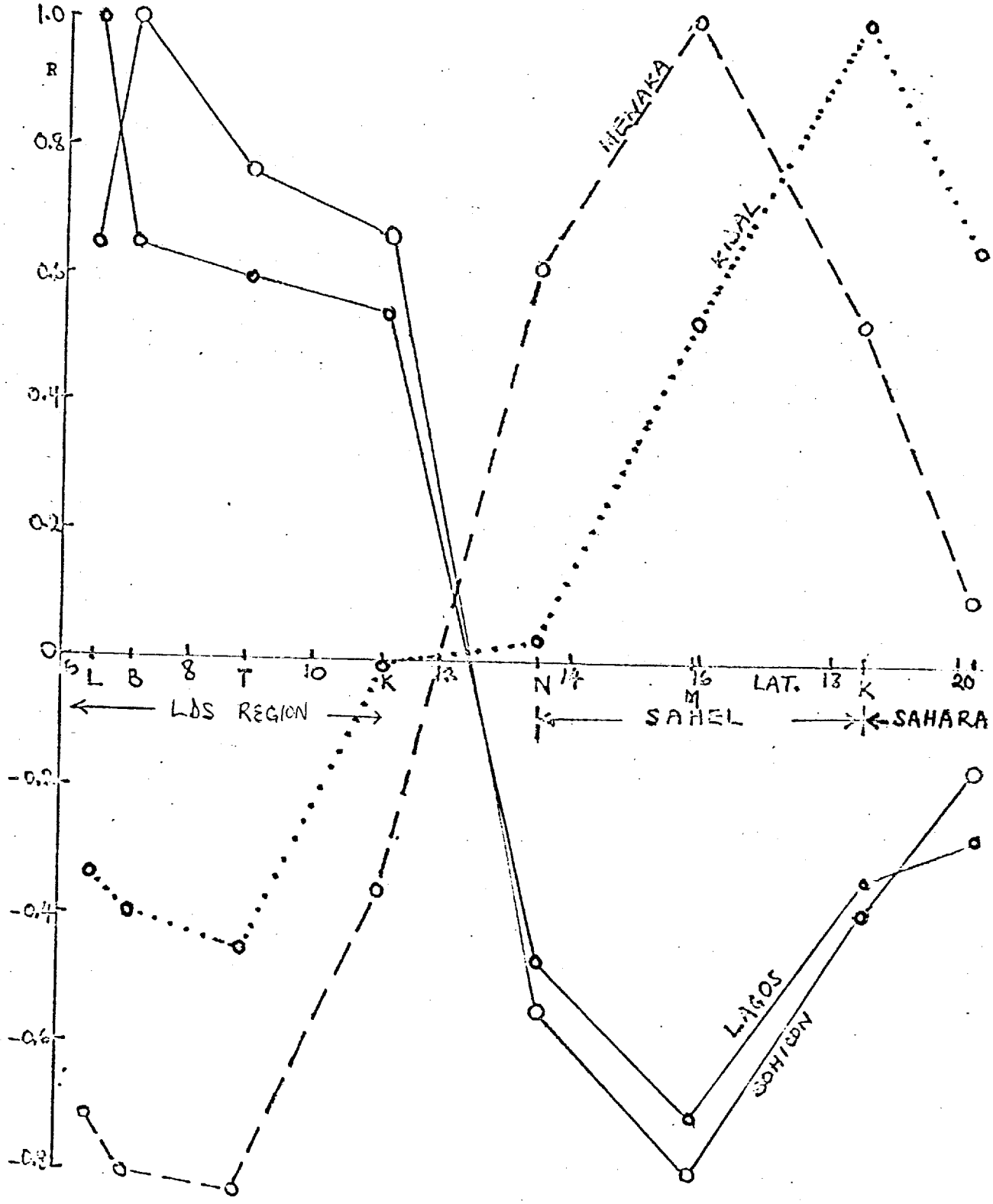

Fig 6.10

The spatial distribution of the correlation relation existing between various stations' precipitation in zone 2 for the month of August in the decade 1951-1960.

Compared with the previous sections' results, the Lagos and Bohicon results indicate a Regime A correlation type while the Menaka and Kidal results are a Regime B type.

The runs carried out for other months in the May - October (Monsoon) season depict a variation in the position of the prominent Sahel precipitation maximum region which may be related to the seasonal oscillation of the ITD.

Furthermore, apart from its manifestation in July and August, the LDS region of negative correlations (with the Sahelion stations) became obscurred in the other months.

The prevailing circulation features experienced in the region at this time of year are the 'warm low' pressure region centred on the ITD (then situated about 22°N) and the Northward push of the St Helena anticyclone region which extends its influence to the Southern areas (Lagos etc). Considerable upwelling of cold water results at the Guinea coast, giving rise to a stable stratification of the atmosphere in the Southern part of the region and a consequent hinderance to convective processes. This strengthens the Walker circulation whose fluctuation, as shown in Chapter IV, is monitored by SO index.

As frictionally induced ascent gives rise to occasions of rainfall in the Sahel region at this time, in addition to the strong activity of the rain-bearing Easterly disturbances experienced by the area, considerable precipitation input is experienced there. The Southern part, on the other hand, experiences prevailing fair weather Cu systems and little rain. (Chapters III and IV)

The results obtained here agree with the analysis of the weather zones in a North-South section along longitude 5°E across the region, made by Adejokun (1964) [reviewed by Obasi (1965)] in depicting the LDS region (Zone 4 of Adejokun). However, the region of single precipitation maximum, here shown as lat.(13-18)°N, is narrower than Adejokun's zone 3 (lat 9-18.5°N).

It need be remembered that our analysis is for 3°E longitude while Adejokun's is for 5°E longitude. Though both zones are very near, the slight WNW - ESE slope in the ITD across Nigeria may play a part in effecting a slight variability in the zones.

6.(vii) AUTO- CORRELATION OF STATIONS' PRECIPITATION

The auto-correlation of a station's data is a process of lagging the station's data with itself. This can prove useful in forecasting the station's precipitation over the lag period considered. Moreover, the coefficient at lag = 1 month is a measure of persistence in the station's precipitation.

Auto-correlation coefficient, R_a can be expressed as:

$$R_a = \sum_{t=1}^{N-lag} (X_t - \bar{X})(X_{t+lag} - \bar{X}) / \sigma_x^2 N \qquad .. \quad .. \quad .. \quad 6.20$$

where $\bar{X}$ is the mean of the monthly precipitation

σ_x is the standard deviation

N is the number of months used in the calculation of the lag and

t is the time in months.

The results of the auto-correlation of the decade (1951-60) August precipitation, carried out over various stations in the zone, for various lags, show that generally, poor auto-correlations are obtained. Except for some stations with significant negative auto-correlation; e.g. Kandi $R_a = -0.62$ at lag = 1, indicating negative or no persistence, the stations' data do not exhibit significant auto-correlation.

Below, fig (6.20), is a plot of the values of R_a for Lagos and Niamey, where, by definition, R_a for lag = 0 is 1.

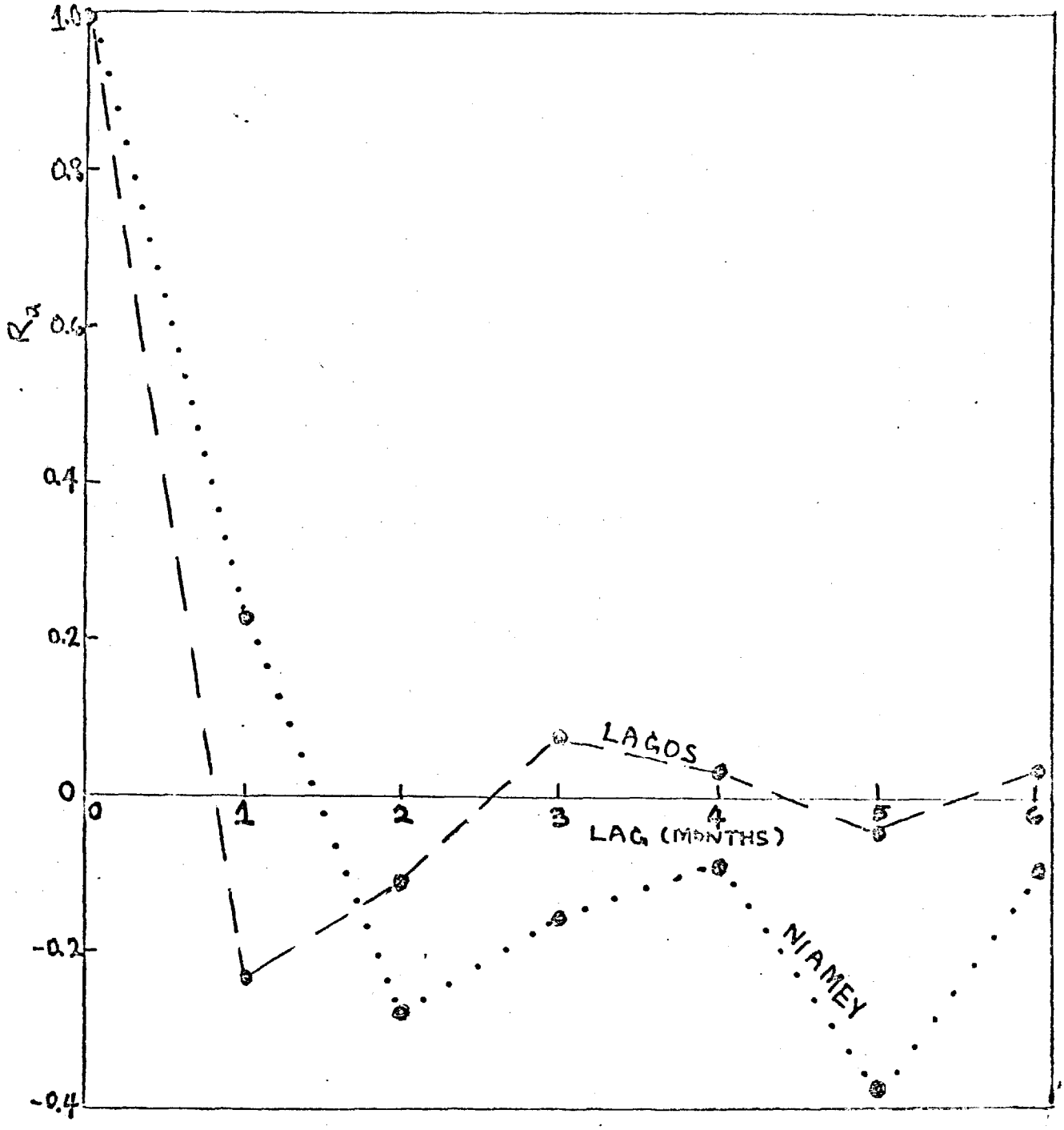

Fig 6.20

The Auto-correlation coefficients, R_a, plotted as a function of the lag (in months) for Lagos and Niamey (Decade 1951-60: Aug.)

Although generally poor, the lag = 1 result shows that, to some extent, the Niamey precipitation has a higher persistence than that of Lagos. However, as these R_a values are not significant, it can be concluded that there is no persistence in the region's precipitation.

The generally poor auto-correlation results suggest that a forecast of a station's precipitation, using the station's past data, may not be fruitful. The lack of persistence here depicted, agrees with the findings of Bunting et Al (1976).

However, as indicated in Chapter IV, the Niamey precipitation shows a seasonal persistence from (June - August) to (September - November; r = .49 and SE = 0.16, as found for 1951-1973.

6.(viii) CONCLUSION

By means of a linear standard regression model, an inter-station correlation of precipitation has been made over zones 1, 2 and 3 for the Normal and the case studies of a wet and a dry year. Three main correlation regimes A, B and C were isolated over the region and a model depicting the region of significance of this postulated.

The contrast in the NH/SH precipitation correlation relations were examined along the cross-equatorial extension of zone 3.

A cross-correlation of stations' precipitation for various lags in zone 2 shows a 2-month lag maximum between Lagos and the Sahel stations. This relationship was further examined using a 20-year running precipitation data for Lagos and Niamey and was found to hold.

This 2-month lag relationship is found to break down occasionally and its association with the variation in the strength of the Walker Circulation is highly likely. Unlike the Niamey precipitation, Lagos precipitation is not, normally, ITD-controlled - but an SO control has been previously found in Chapter IV. As long as this holds, the two-month lag between the two stations' precipitation holds. However, when the Lagos precipitation is subjected to an anomalous ITD-control, the 2 month lag relation breaks down. Occurring with a breakdown in the LDS, this 2 month lag correlation break down may be associated with the fluctuation in the strength of the Walker Circulation.

Inter-station correlation of precipitation carried out over the 1951-60 decade (August) indicates regimes A and B types and has an association with the prevailing weather systems over the region.

Except for a seasonal persistence from June - August to September--November, found in the Niamey precipitation, (1951-1973), the region's precipitation exhibits little or no persistence. This result is in agreement with that of Bunting et Al, (1976).

CHAPTER VII

SUMMARY AND CONCLUSIONS

In as much as we have included at the end of each chapter of the thesis a conclusion, we shall avoid unnecessary repetition of most of what has been said but will stress important outcomes of the work along with essential recommendations for further research.

This study shows that the degree of penetration, inland, of the moist SW'ly (Monsoon) winds, (typified by $\theta_w \sim$ 20-24°C) indicated by the ITD position determines largely the amount and duration of precipitation over West Africa, barring orographic and coastal influences - in agreement with Bryson, (1973), Ilesanmi (1971) and Leroux, (1971). While little or no precipitation is observed at the ITD surface position - where the drier and hotter NE'ly (trade) winds ($\theta_w \sim$ 15-19°C) meet the SW'lies-the precipitation increases Southwards with latitude, attaining a maximum around 7-10 degrees of latitude South of the phenomenon.

As shown by climatological cross-sectional analyses, the regions belt of high precipitation moves North and South with the ITD. A strong relation exists between the May to September cycle of precipitation in the Northern (Sahel) part of the region and the January to December cycle in the South. This provides a basis for a useful within-the-season forecast of the Sahel precipitation.

Cross-sectional (latitude-height) analyses of the thermodynamic state of the region's atmosphere indicate the preferred areas of strong convective activities. However, such analyses are somewhat limited by lack of an adequate aerological data coverage. And, as isentropic analysis holds out no prospect in this region, stationary (local) analysis is carried out. Over Niamey, this depicts, in agreement with the observed precipitation, the preferred seasons of convective instability (typified by surface $\theta_w \geq 22$°C and occurring in-between the Northward and Southward passage of the ITD).

However, this work shows that while the ITD is a major control on the region's precipitation, its effect declines after a threshold of about 7 latitude degrees Southwards. A negative correlation (r = -0.41; SE = 0.18) exists between the June-August precipitation at Lagos and the SO index for September - November over 1951-1973. This suggests an SO control over the precipitation in the Southern part of the region, the LDS area.

The SO is a measure of the fluctuation between the weak and strong states of the Walker circulation, which zonal circulation is set up by the presence of heat sources and sinks along the equatorial latitudes and is reputed to be responsible for precipitation anomalies in the tropics. The Walker circulation's effect on the coastal areas of Ghana has been discussed along with the role of the upwelling of cold water whose strength depends on that of the maritime (Monsoon) winds from the SH.

An increased upwelling process gives rise to increased cooling of the Southern part of the region, increasing the temperature contrast between the hot Saharan region to the North and the Southern (Guinea) region. The effect of this contrast is to increase the easterly flow aloft, hence setting up the necessary shear required to generate convective over-turning and intense squall line activity within the sufficiently deep moist layer existing South of the ITD. This mechanism, occurring in the summer over the region, accounts for most of the region's precipitation. On the other hand, an increased weakening of the upwelling process gives rise to increased warming of the Southern area and a consequent decrease of the thermal contrast over the region, spelling a decrease in the strength of the Easterly flow and, consequently of squall activity. A similar decrease in thermal contrast can be brought about by an increased cooling of the Saharan region e.g. by increasing the albedo over the Sahara desert. This, in addition to causing increased large scale descent of air over the Saharan region (Charney, 1975) can also effect drought by decreasing the squall frequency over the Sahel.

The structure of the wind shear associated with the squall line case study considered in this work confirms the dynamical model

prediction of Moncrieff and Miller (1976) which work particularly stresses the importance of the characteristic wind shear to the growth of the squall lines.

The tropical atmosphere is conditionally unstable and cooling by evaporation is very important in the consideration of convective instability in the atmosphere. Adiabatic cooling occurs in the mid-troposphere and as shown in the case study of a wet and a dry year considered, a warming of this region of the atmosphere occurred in the dry year, giving rise to stable conditions.

An instability index, I, defined to take account of θ_w over the bottom 1 or 2km of the earth's surface and θ_s at the mid-troposphere, is used to investigate occasions of convecitve instability relative to the ITD. Generally, I increases/decreases South/North of the ITD as does the precipitation, R, and the two are significantly correlated ($r = 0.53$; $SE = 0.12$, for the 1958 monthly mean data considered). Occasions of forced convection, giving rise to considerable precipitation, even for I negative, often arise. Generally, days of free convection are separated by several days, sometimes up to a week, of stable conditions. This, as the precipitation distribution also shows, indicates that even in the Monsoon season, the region is not always 'pouring with rain'. Rather, occasions of intense convection may be few but associated with high downpours e.g. as is typical of squall lines.

Inter-station correlation of precipitation indicates the existence of three regimes: A, B and C of distribution of correlation coefficient r, each of which can be associated with important atmospheric mechanisms prevailing in the region. Regime A region is influenced by the Walker circulation and sea breeze effects, regime B region is ITD-controlled while C experiences the interaction of both, along with Easterly disturbances and squall lines advected Westwards across the region. The Monsoon winds supply the needed moisture for the convection. Various scales of motion are involved and considerable interaction takes place among them.

A two-month lag maximum is found in the cross correlation of the

precipitation at Lagos and at stations, e.g. Niamey, in the Sahel, suggesting some relation between the latter and the former some months previously. An association between this 2-month-lag correlation and the fluctuation in the strength of the Walker circulation, is highly suspected.

Except for a seasonal persistence from June - August to September - November found in the Niamey precipitation (1951-1973), little or no persistence generally exists in the region's precipitation. This agrees with the earlier finding of Bunting et Al, (1976).

Finally, a moral to be drawn from this study by meteorological analysts or climatic (Numerical) modellers who may require upper air initial data in comparing the state of the atmosphere over various years in the region:

Our thermodynamic analyses show that the Niamey radiosonde humidity element has been changed between the late fifties and the early seventies. This change, confirmed by the French Meteorological Office, Paris (private communication) may well affect the varicus francophone radiosonde/rawinsonde stations. This warning should be heeded in case of any compilation of the mean specific humidity over these periods particularly for the francophone countries of West Africa.

RECOMMENDATIONS

1. The Walker Circulation in the South and the ITD in the North of the region feature prominently in their control on the region's precipitation. While the latter has been given some attention, the former's role needs to be recognised as important also. To this end, necessary meteorological observations need be carried out over the Guinea coast in order to promote a better understanding of the air-sea interaction along the region's equatorial areas. An ocean weather ship to be jointly manned by the West African nations can meet this need.

2. Much of what is known, to date, on Disturbance lines (squall lines) observed in West Africa is obtained from the account of Hamilton et al (1945) and Eldridge (1957). A keener study of these system, with a view to understanding their energetics and detailed structure, is still needed.

From a climatological standpoint, the association between the squall line frequency and the Sahel precipitation needs to be established. The said frequency is going to be a function of the temperature contrast between the Sahara and the Guinea coast, which, in turn, can be varied by the action of the Walker circulation and the albedo variation over the region.

To prevent an increase in the region's albedo, a stringent control on the vegetation cover need be applied e.g.

a) by a joint inter-West African national promulgation of a government ban on burning of bush (a usual NH winter phenomenon in parts of Nigeria, despite recent state government's order) and deforestation.

b) Active steps towards aforestation e.g. by planting trees, or vegetable cover, particularly by the arid borders.

3. The Easterly disturbances and cloud clusters advected Westwards across the region are excellent atmospheric 'reservoirs' whose water need be more effectively tapped. To this end, cloud seeding experiments, if well planned, can be of good use, particularly as the arid region can benefit from the resulting run-off. Such experiments should be backed by a proper tracking of the disturbances e.g. via the Satellites and the excellent upper air stations zonally arrayed along their path like: Ndjaema (Ex-Fort Lamy), Kano, Niamey, Gao, Bamako and Dakar.

Meanwhile, the recent GATE (1974) atmospheric research programme is expected to turn out adequate data to promote a further understanding of these systems. The relationship between the Easterly waves and the squall lines needs be clearly defined and the systems' energetics and dynamics properly understood, for instance.

4. Finally, the climatological association between the cycle of

precipitation across the region need be appreciated and harnessed for within-the-season forecast of precipitation in the hinterland. This will, no doubt, benefit agricultural concerns in their planning against any likely drought occurrence. A step towards this, incorporating the ITD movement, is illustrated in Appendix VIII .

REFERENCES

Abdul M O, 1971 — 'A case study of a disturbance line'. Nigerian Met. Serv. Quart. Met. Mag. Vol 1, No 4, pp 17-43.

Adejokun J A, 1964 — The three dimensional structure of the Inter-Tropical Discontinuity. Nig. Met. Serv. Techn. Note.

Aina J O, 1964 — Wind flow and associated weather in the Lower Troposphere over West Africa. Nig. Met. Serv. Techn. Note No 30, pp 23.

Bates J R, 1973 — A generalisation of the CISK theory, J Atmos, Sciences, Vol 30, No 8, pp 1509-1519.

Betts A K, 1973 — Non-precipitating Cumulus convection and its parameterization. Quart J. Roy. Met. Soc. 99, 178-196.

Berlage H P, 1966 — 'The Southern Oscillation and World Weather' KNMI, Med. en Verh., N88.

Bjerknes J, 1969 — Atmospheric teleconnections from the equatorial Pacific. Monthly Weather Review 97, 1969, 163-172.

Brunt D, 1934 — "Physical and Dynamical Meteorology" Cambridge University Press, New York.

Budyko, 1956 — Teplovoi Zemnoi Poverkhnosti Gidrometeorologicheskoe Izdatel'stvo, Leningrad. (English Transl. : Stepanova, J A, 1958, "The Heat Balance of the Earth's Surface." Office of Techn. Services, U.S. Dept. of Commerce Washington).

Bunting et Al, 1974 — Weather and climate in the Sahel: An initial study. Dept. of Agricultural botany. University of Reading.

Bunting et Al, 1976 — 'Rainfall trends in the West African Sahel'. Q J Roy. Met. Soc. 102. Pg 59-64.

Burpee R W, 1972 — 'The origin and structure of Easterly Waves in the Lower Troposphere of North Africa.' J Atmos. Sciences, Vol 29, No.1, pp77-90.

Carlson T N, 1965 — Ph.D Thesis: University of London, Unpublished

Carlson T N, 1969 — Some remarks on African disturbances and their progress over the Tropical Atlantic: Mon. Wea. Rev. Vol 97, No 10, pp 716-726.

Charney J G, 1969 — The ITCZ and the Hadley Circulation of the Atmosphere. Proceedings of the WMO/IUGG Symposium on NWP, Tokyo, 1968.

Charney J G, 1975 — 'Dynamics of deserts and drought in the Sahel (Symons Memorial Lecture): Q J Roy Met. Soc. 101 Pg 193-202.

Clackson J R, 1957 — 'The Seasonal Movement of Boundary of Northern Air' Nig. Met. Serv. Techn. Note No.5.

Darkow G L, 1968 — The total energy environment of severe storms. J. Appl. Meteor 7, 199-205.

Dhonneur G, 1971 — General Circulation and Types of Weather over Western and Central Africa. GATE, Experimental Design Proposal. Annex IV.

Dietrich G and Kalle K, 1957 — Allgemeine Meereskunde. Borntraeger Berlin, 1957, 492 p.

Eldridge R H, 1957 — A synoptic study of West African disturbance lines. Quart. J Roy. Met. Soc. Vol 83, 1957 pp 303-314.

Flohn, H, 1960a) — 'Equatorial Westerlies over Africa, their extension and significance': Tropical Meteorology in Africa: Symposium, Nairobi, 1960 WMO/Munitalp Foundation).

Flohn H, 1960b) — 'on the structure of the ITCZ', Ibid.

Flohn H, 1971 — "Tropical circulation pattern" Bonner Meteorologische Abhandlunger Heft 15(1971) pp 55.

GATE Report No.1, 1972 — Experiment Design Proposal for the GARP Atlantic Tropical Expt.
International Council of Scientific Unions.
WMO

Report No 7, 1974 — The Convection sub-programme for GATE. Ibid.

Green J S A, Ludlam F H and McIlveen JFR 1966 — 'Isentropic relative-flow analysis and the parcel theory' Quart J Roy. Met. Soc. Vol 92; No 392 pp 210-219.

Griffith J F et Al, 1972 — 'The Northern desert (Sahara): climate of Africa: World survey of climatology, Vol 10, edited by J F Griffith (Elsevier Publishing Co.), p.604(75-111).

Hamilton R A and Archbold, 1945 — Meteorology of Q J Roy. Met. Soc. 1945 pp 231.

Ilesanmi O O, 1971 — 'An Empirical Formulation' of an ITD Rainfall model for the Tropics: A case study of Nigeria'. Journal of Applied Meteorology 10, pg 882-890.

Ireland A W, 1962 — "The little dry season of Southern Nigeria". Nigerian Meteorological Service. Techn Note 24.

Jenkinson A F,1973 ' A Note on variations in May to September Rainfall in West African Marginal Rainfall areas.' pg 31 of 'Drought in Africa': Report of the 1973 Symposium, Edited by D Dalby and R J Harrison Church. Centre for African studies School of Oriental and African Studies, University of London.

Johnson D H, 1965 African tropical Meteorology WMO, Techn. Note No 69, Geneva, Switzerland, pg 48-90.

Kendal et Al, 1922 'The Advanced theory of statistics,' Vol II, London, Griffin 1963-67.

Kornfield, J et Al, 1969 'A photographic summary of the Earth's cloud cover for the year 1967.' Jour. App. Meteor. Vol. 8, 1969 pp 687.

Krueger A F, 1970 The zonal variation of cloudiness and convection over the Tropics. Proceedings of the symposium on Tropical Meteorology. Honolulu (Hawaii, 1970,

Krueger A F and Winston J S, 1975 Large-scale circulation Anomalies over the Tropics during 1971-72. Monthly Weather Review Vol 103, No.6 p.465-473.

Leroux M, 1971 'La Dynamique des precipitations en Afrique Occidental' ASECNA No 39. La D E M Dakar. (Eng. Transl. by D E Parker: 'The Dynamics of precipitation in West Africa' Unpublished.

Ludlam F H, 1963 'Severe local thunderstorms - A Review', Meteor. Monographs, Vol 5, No.27 Sept 1963 pp 1-30.

Mason B J, 1976 Towards the understanding and prediction of Climatic variations (Symons Memorial Lecture). Q J Roy Met Soc Vol 102 433 pp473-498.

Mbele-Mbong S, 1974 — Rainfall in West Central Africa: Progress Report. Atmospheric Science Paper No 222, Colorado State University, Fort Collins, Colorado.

McDonald J E, 1956 — Variability of precipitation in arid region: A survey of characteristics for Arizona. Techn Reports on the Meteorology and Climatology of Arid Regions. No.1 University of Arizona Institute of Atmospheric Physics pp88

McDonald J E, 1957 — 'A critical evaluation of correlation methods in climatology and Hydrology' Ibid. Report No.4 36pp

Moncrieff M W and Green J S A,. 1972 — 'The propagation of steady convective overturning in shear'. Quart. J Roy. Met. Soc. 98, 336-352.

Moncrieff M W and Miller M J, 1976 — The dynamics and simulation of tropical cumulonibus and squall lines. Q J R Met. Soc. Vol.102 pp 373-394.

Montgomery R B,1939 — Report on the work of Sir G T Walker. M.W.R.Supp.39 pp 1-22.

Mooley and Crutchers, 1968 — (See Atkinson, G D "Forecasters Guide to Tropical Meteorology". Air weather Service (MAC) US AIR FORCE. 1971 pg 6-24.)

Monthly Climatic Data for the World,1958 — U.S. Department of Commerce, Asheville, N.C. U.S.A.

Obasi G O P, 1963 — Thermodynamic and Dynamic Transformation over Ikeja. Nig. Met. Serv. Tech. Note No.33, Lagos.

Obasi G O P, 1965 — Atmospheric, Synoptic and Climatological Features of the West African Region. Nigerian Met. Service Techn Note No 28, Lagos pp 43.

Palmen E et Al, 1969 'Atmospheric Circulation Systems'. Academic Press, New York.

Pedgley D E, 1972 'Monsoon Weather of North Africa', Unpublished.

Riehl H, 1954 'Tropical Meteorology' McGraw-Hill, New York, 392pp.

Riehl H and Malkus J, 1958 On the heat balance of the euqatorial trough zone. Geophysica 6, 503-538.

Riehl H and D Rossignol W, Luckefedt, 1974 'On the structure and Maintenance of West African Squall lines'. Direction de L'Exploitation Meteorologigue. ASECNA B.P. 3144 - Dakar.

Rossby C G et Al, 1937 "Isentropic Analysis", Bulletin of the Amer. Met. Soc. XVIII (1937); 201-9.

Rowntree P R, 1972 The influence of tropical east Pacific Ocean temperatures on the atmosphere. Q J Roy. Met. Soc. 98, April 1972 pp 290-321.

Searle S R, 1971 Linear Models. N.Y. Wiley

Sellers W D, 1969 'Physical Climatology'. University of Chicago Press, Chicago and London pp 272.

Shaw, Sir Napier, 1926 "Manual of Meteorology": (Vols 1-4) Cambridge University Press, 1926-32) Vo.III, 259-266.

Spiegel M R, 1961 Schaum's outline of theory and problems of statistics - New York. Schaum Pub. Co. 1961. (Schaum's Outline Series)

Troup A J, 1965 The 'Southern Oscillation': Quart.Jour. Roy. Met. Soc. 91, 1965 pp 490-506.

Walker, Sir G T, 1923 Correlation in Seasonal variations of weather, VIII. A preliminary study of world weather (World Weather 1). Mem. India Met. Dept. 24, 75-131 (1923)

Walker, Sir G T, 1924 Correlation in seasonal variations of weather IX. A further study of world weather (World Weather II). Mem. India Met. Dept. 24, 275-332 (1924).

Walker, Sir G T, 1928 World Weather. Q.J.R.M.S. 54, 79-87.

Walker, Sir G T, and Bliss E W 1930 World Weather IV. Some applications to Seasonal foreshadowing. Mem. R.M.S. 3, 81-95 (1930).

Walker, Sir G T, and Bliss E W, 1932 World Weather V. Mem. R.M.S.4, 53-84. (1932).

Walker, Sir G T, and Bliss E W, 1937 World Weather VI. Mem. of the Royal Met. Soc 4: 119-139(1937).

Willett H C and Bodwitha F T, 1952 'An abbreviated Southern Oscillation': Bull Amer. Met. Soc. Vol 33, No.10, 1952.

Winstanley P, 1973a) Nature 243: 464-465. Recent rainfall trends in Africa, the Middle East and India.

Winstanley P, 1973b) Nature 245: 190-194. Rainfall patterns and general atmospheric circulation.

WMO, 1953 World Thunderstorm Days

Wright P B, 1975 'An Index of the Southern Oscillation'. Climatic Research Unit, School of Environmental Science University of East Anglia, Norwich, CRORP4 pp20.

Zipzer E J, 1969 The role of organized unsaturated convection downdrafts in the structure and rapid decay of an equatorial disturbance. J. Appl. Meteor. 8, 799-814.

APPENDIX I : SOURCES OF DATA

The data used in this study were obtained from a wide range of sources within and outside the United Kingdom. As gaps do exist in some of the records locally available here, the various regional Meteorological headquarters were contacted to make up for many of the missing datam.

I a) PRECIPITATION DATA :

Precipitation data were obtained from:

1. World Weather Records, U.S. Department of Commerce, Washington D.C. (1967)
2. Records of the British Meteorological Office, Bracknell, courtesy of Mr R A H Taylor; and Mrs Cowlard and other library staff.
3. The Nigerian Agrometeorological Bulletins, Lagos. (1970)
4. Nigerian Monthly Weather Report: 1958-66, Lagos.
5. Private communication with:

   i) Sierra Leone Meteorological Service, Freetown.
   ii) Niger Republic Meteorological Service, Niamey.
   iii) Mali Republic Meteorological Service, Bamako.
   iv) Chad Republic Meteorological Service, Ndjaéma (Ex-Fort Lamy).
   v) Ex-Dahomey Republic (Now Republic of Benin) Porto Novo.
   vi) Agence Pour La Securite de la Navigation Aerienne en Afrique et A Madagascar (ASECNA), Dakar.
   vii) Nigerian Meteorological Service, Lagos
   viii) Prof Bunting's Group, Department of Agricultural Botany, University of Reading, U.K.

b) RADIOSONDE/RAWINSONDE AND PILOT BALLOON DATA:

i) Monthly Climatic Data for the World (Weather Bureau, Department of Commerce, Washington D.C., U.S.A.), 1958

ii) Nigerian Meteorological Office Notes No.5, Lagos, 1960

iii) 'Radiosondages': ASECNA, Dakar, 1970

iv) Private communications as in I.a) 5.(ii)-(iii),(v) above.

c) OTHER SYNOPTIC DATA

i) World Weather Maps, IGY Year 1957-1958, Tropical Zone Part II. Deutscher Wetterdienst, Seewetteramt, Hamburg.

ii) Nigerian Agrometeorological Bulletins, Lagos.

iii) 'Bulletin Quotidien D'etudes: Establi par la section de prévision de Dakar-Y off, 1958. Direction de la Meteorologie Nationale, Paris, France.

APPENDIX II: STATIONS USED IN THE ANALYSIS

STATION	WMO NO	COUNTRY	LATITUDE	LONGITUDE	ELEVATION (M)
1. Daru	61891	Sierra Leone	07 59N	10 52W	90
2. Kabala	61886	" "	09 35N	11 33W	464
3. Kenteba	61285	Mali	12 48N	11 21W	135
4. Kayes	61257	"	14 26N	11 26W	47
5. Matam	61630	Senegal	15 38N	13 15W	17
6. Kiffa	61498	Mauritania	16 38N	11 24W	115
7. Tidjikja	61450	"	18 33N	11 26W	396
8. Atar	61421	"	20 31N	13 04W	226
II.2					
ZONE 2					
≠ 9. Lagos/Ikeja	65201	Nigeria	06 35N	03 20E	38
10. Bohicon	65338	Dahomey	07 10N	02 04E	167
11. Tchaourou	65333	"	08 52N	02 36E	327
12. Kandi	65306	"	11 08N	02 56E	292
≠*13. Niamey	61052	Niger	13 29N	02 10E	222
14. Menaka	61250	Mali	15 52N	02 13E	280
*15. Kidal	61214	"	18 26N	01 21E	464
*16. Tessalit	61202	"	20 12N	00 59E	494
II.3 STATIONS IN AND AROUND THE SAHEL ZONE					
17.Maiduguri	65082	Nigeria	11 51N	13 05E	354
18. Kano	65046	"	12 03N	08 32E	476
19. Ndjaema (Ex-Fort Lamy)	64700	Chad	12 08N	15 02E	300
20. Maine Soroa	61096	Niger	13 14N	11 59E	339
21. Zinder	61090	"	13 48N	09 00E	489
22. Agadez	61024	"	16 59N	07 59E	507
23. Bilma	61017	"	18 41N	12 55E	359

APPENDIX II.4: ZONE 3 (Extended Across the Equator)

STATION	WMO NO	COUNTRY	LATITUDE	LONGITUDE	ELEVATION
24. Faya Largeau	61753	Chad	18 00N	19 10E	234
25. Abeche	64756	"	13 51N	20 51E	549
26. Mongo	64758	"	12 12N	18 47E	430
27. Am Timan	64754	"	11 02N	20 17E	436
28. Fort Archambault	64750	"	09 08N	18 23E	365
29. N/Dele	64654	Central Africa Republic	08 24N	20 39E	510
30. Bouca	64603	"	06 30N	18 16E	458
31. Bangui	64650	"	04 23N	18 34E	381
32. Libenge	64015	Congo/ Kinshasha	03 38N	18 38E	365
33. Lisala	64014	"	02 19N	21 34E	460
34. Impfondo	64459	Congo/ Brazzaville	01 37N	18 04E	326
35. Coquilhatville	64005	Congo/ Kinshasha	00 03N	18 16E	345
36. Boende	64126	"	00 13S	20 51E	370
37. InOngo	64115	"	01 58S	18 16E	310
38. Port Francqui	64224	"	04 20S	20 35E	435
39. Kikwit	64222	"	05 02S	18 48E	485
40. Dundo	66152	Angola	07 22S	20 50E	727
41. Henrique de Carvalho	66226	"	09 39S	20 24E	1082
42. Luso	66285	"	11 47S	19 55E	1328
43. Mavinga	66447	"	15 50S	20 21E	1190

II.5 RADIOSONDE/RAWINSONDE STATIONS: (FOR ZONE 2, Extended Northwards)

44. Tamanrasset	60680	Algeria	22 47N	05 31E	1378
45. Aoulef	60625	Algeria	26 58N	01 05E	290

* Also within the zone in II.3

≠ Also radiosonde/rawinsonde stations

APPENDIX III : Precipitation Variability (tables)

Table (2.1b): Variability in the (Jan - Dec) Precipitation: Zone 2

STATIONS	NORMAL			1958			1970		
	MEAN (mm)	S.D. (mm)	C.V. (%)	MEAN (mm)	S.D. (mm)	C.V. (%)	MEAN (mm)	S.D. (mm)	C.V. (%)
1. Lagos	122	86	70	96	94	98	152	144	95
2. Bohicon	91	56	62	60	62	103	103	78	76
3. Tchaourou	101	76	75	72	68	94			
4. Kandi	86	100	116	71	82	115	91	148	163
5. Niamey	53	74	140	44	74	168	37	68	184
6. Menaka	22	36	164	35	61	174	17	30	176
7. Kidal	11	18	164	14	26	186	10	17	170
8. Tessalit	10	17	170	11	22	200	15	27	180

Table (2.1c): Variability in the Jan - Dec Precipitation: Zone 3 (Extended across the Equator)

STATIONS	NORMAL			1958			1970		
	R(mm)	S.D. (mm)	C.V. (%)	MEAN R(mm)	S.D. (mm)	C.V. (%)	R(mm)	S.D. (mm)	C.V. (%)
1. Faya Largeau	1	3	300	4	7	175	-	-	-
2. Abeche	42	73	174	39	73	187	35	61	174
3. Mongo	72	104	144	75	120	160	70	145	207
4. Am Timan	77	98	127	69	99	147	61	98	160
5. Fort Archambault	95	108	114	86	109	127	87	115	132
6. N/Dele	105	100	95	95	92	97	96	97	101
7. Bouca	117	97	83	96	91	95	-	-	-
8. Bangui	130	68	52	122	83	68	122	97	79
9. Libenge	128	59	46	158	119	75	73	75	103
10. Lisala	136	50	37	110	64	58	66	123	187
11. Impfondo	149	44	30	139	86	62	82	70	86
12. Coquilhat-ville	140	44	31	125	58	46	106	129	122
13. Boende	174	40	23	164	74	45	98	85	87

(Continued overleaf)

(Table (2.1c) continued)

STATIONS	NORMAL			1958			1970		
	R(mm)	S.D. (mm)	C.V. (%)	MEAN R(mm)	S.D. (mm)	C.V. (%)	R(mm)	S.D. (mm)	C.V. (%)
14. Inongo	144	68	47	127	101	80	77	84	109
15. Port Francqui	143	83	58	131	80	61	-	-	-
16. Kikwit	137	86	63	110	88	80	79	86	109
17. Dundo	138	97	70	137	100	73	-	-	-
18. H de Henrique	121	96	79	113	118	104	81	107	132
19. Luso	99	88	89	80	85	106	93	89	96
20. Mavinga	73	82	112	81	103	127	25	46	184

APPENDIX IV

'THE WALKER CIRCULATION': SIR G T WALKER'S 3 OSCILLATIONS

1. The North Atlantic Oscillation: (NAO) : (Dec.-Feb.)

The NAO arises as a result of opposition in pressure between Iceland and the Azores, with correlation coefficients varying from

-0.54 (December - February)
-0.60 March - May
-0.48 June - August to
-0.40 September - November all for 1875-1921

The numerical definition for the NAO (December to February) is:
(Vienna Pressure) + (Bodo temperature) + (Stornoway temperature) + 0.7 (Bermuda pressure) - (Stykkisholm Pressure) - (Ivigtut Pressure) -0.7 (Godthaab temperature) + 0.7 (Hatteras + Washington temperature)/2

(1)

Where the quantities in brackets are departures from Normal in limits such that the standard deviation is $\sqrt{20}$ in each case.

Walker correlated the observed quantities in each station with the NAO as defined in (1) for each year of 1875-1930 and observed the following correlation coefficients:

Station	r	Period
Vienna Pressure	0.76	1875-1930
Stornoway temperature	0.84	1875-1919, 1921-30
Bodo temperature	0.86	1875-1930
Stykkisholm pressure	-0.80	1875-1930
Ivigtut Pressure	-0.84	1879-1918, 1920-26
Bermuda pressure	0.72	1875-86, 1888-1929
½ (Hatteras + Washington temp)	0.72	1875-1930
Godthaab temperature	-0.70	1875-84, 1886-1928

The NAO generally indicates an increase in the general circulation over the North Atlantic Ocean.

2. The North Pacific Oscillation (NPO)

An opposition in pressure variations between Hawaii and the region around Alaska and Alberta. High pressure in Alaska meant a more Southerly track of the lows and consequently, rain in parts of the United States, observed Walker.

The NPO was numerically defined as:

(Honolulu Pressure) + $\frac{1}{3}$ (Qu'Appelle + Calgary + Prince Albert temperature) - $\frac{2}{3}$ (Sitka, Fort Simpson, or Juneau Pressure) + (Dawson Pressure) + (Nome Pressure) - (Dutch Harbour temperature)

.. .. .. (2)

where the fractions $\frac{2}{3}$ and $\frac{1}{3}$ were used because quantities multiplied by them related to places not as far from one another as to be independent.

The various factors were each correlated with the NPO as in the NA O case.

3. The Southern Oscillation: (SO)

Walker defined the SO as "the tendency of pressure at Stations in the Pacific (San Francisco, Tokyo, Honolulu, Samoa, and South America) and of rainfall in India and Java (presumably, also in Australia and Abyssinia) to increase, while pressure in the region of the Indian Ocean (Cairo, Northwest India, Fort Darwin, Mauritius, South East Australia, and the Cape) decreases."

A high pressure in the Pacific Ocean tends to be compensated for by a low in the Indian Ocean from Africa to Australia, with the rainfall varying inversely with the pressure. These conditions differ from

Winter to Summer and the Numerical definition for June - August, Southern Winter is:

(Santiago Pressure) + (Honolulu Pressure) + (India rain) + (Nile flood) + 0.7 (Manila Pressure) - (Batavia Pressure) - (Cairo Pressure) - (Madras temperature) - 0.7 (Darwin Pressure) - 0.7 (Chile rain). (3)

Here, 'India rain' refers to the Peninsula and North West India and 'Chile rain' is the mean rainfall in nine stations between $30^{\circ}S$ and $42^{\circ}S$. The SO was similarly defined for some centres during the Southern Summer.

Unlike the two Northern Oscillations whose persistence from Winter to Summer was found to be very small, the SO indicated a high persistence.

December-February	correlated with	March-May	0.68
March - May	"	" June-August	0.62
June - August	"	" Sept.-Nov.	0.82
Sept.-November	"	" Dec.-Feb.	0.92

It needs be noted that the numerical definitions can be waived in such a way as to preserve the principle of pressure variation compensation, even though leaving out some terms in the definition.

Such a modification has been carried out by some workers (e.g. H.C. Willett and Frank T Bodurtha Jr, 1952) who left out India rain + Nile flood - 0.7 (Chile rain) in their SO definition and yet obtained higher correlations than Walker did.

In recent years, it is considered appropriate to use only pressure variations (since of course, pressure and precipitation vary inversely, this seems a good substitute for both). This method is being used, for instance, by P B Wright (1975) to define a SO index which he estimated for every quarter of the years 1851-1974.

The applicability of these modified indices to observed climatic variations is yet to be well demonstrated.

Both Walker's original SO 1875-1930 June-August and P Wright's Indices for the same season agreed in depicting negative SO during 1911-1913 at which time the Sahel region had a drought which was worse but not as long as the current 1968-73 case. However, the latter is yet to be conclusively depicted by the second investigator's indices.

From the variation in Zonal Walker Circulation, it is expected that a low SO corresponds to little rain or drought in the Sahel while a high SO would spell heavy rain. (Since a low SO effects a weak Zonal Walker Circulation and hence, weak upwelling of cold water, consequently there is a decrease in the North-South temperature gradient across the region. This spells a weak Easterly flow aloft and hence, decreased squall activity, Chapter IV.)

APPENDIX V: Information on computer Programming

Method of calculation of Correlation Coefficients using a standard sub routine GO2AAF (ICCU LIB Manual) in which N precipitation observations (monthly in this instance), taken over M stations, can be set up as an array.

$$[X_{ij}], \quad i = 1, 2, \ldots, N \qquad N \geq 2$$
$$j = 1, 2, \ldots, M \qquad \text{(stations)}$$

The means for each station are given by

$$\bar{X}_j = \sum_{i=1}^{N} X_{ij}/N \quad , \quad j = 1, 2, \ldots, M .$$

The Standard deviations:

$$S_j = \sqrt{S_{jj}/(N-1)} \qquad j = 1, 2, \ldots, M$$

The correlation coefficients:

$$R_{jk} = S_{jk} / \sqrt{S_{jj} \cdot S_{kk}} \quad , \quad j, k = 1, 2, \ldots, M$$

For S_{jj} or $S_{kk} = 0$, R_{jk} is set to zero.

We show, below, a typical programme used to call this sub-routine.

```
      PROGRAM STAT(INPUT,OUTPUT)
      DIMENSION Y(21,8)
      COMMON X(1Ø,9),XBAR(9),STD(9),RX(9,9),R(9,9),STN(8),SE(9)
      DATA N,M/1Ø,8/
      DATA IFAIL/Ø/
      MP1=M+1
      READ 1,(STN(J),(Y(I,J),I=1,N),J=1,M)
1     FORMAT(A1Ø,1ØF3·Ø)
      PRINT 1Ø,(STN(J),(Y(I,J),I=1,N),J=1,M)
1Ø    FORMAT('1ORIGINAL DATA'//(1X,A1Ø,3X,1ØF6·Ø))
      DO1ØØ1  J=1,8 £DO 1ØØ1 I=1,1Ø
1ØØ1  Y(I+N,J)=Y(I,J)
      DO 3ØØØ LAG=Ø,5
      DO 3ØØØ L=1,M £ DO 15ØØ J=1,M
      IF(J·EQ·L)GO TO 15ØØ
      DO 14ØØ I=1,N
14ØØ  X(I,J)=Y(I+LAG,J)
15ØØ  CONTINUE
      DO 16ØØ I=1,N
      X(I,MP1)=Y(I+LAG,L)
16ØØ  X(I,L)=Y(I,L)
      CALL GØ2AAF(N,MP1,X,XBAR,STD,RX,R,IFAIL)
      PRINT 11,STN,(XBAR(K),K=1,M),(STD(K),K=1,M)
11    FORMAT('MEANS AND STANDARD DEVIATIONS'//15X,8A1Ø/(11X,8F1Ø·Ø))
      PRINT 12,STN(L),(RX(K,L),K=1,MP1)
12    FORMAT('-SUM OF CROSS-PRODUCTS OF DEVIATIONS FROM MEAN'//
     -      (1X,A1Ø,9F1Ø·1))
      PRINT13,STN(L),(R(K,L),K=1,MP1)
13    FORMAT('-CORRELATION COEFFICIENTS'//(1X,A1Ø,9F1Ø·3))
      DO 2ØØØ K=1,MP1
      RR=1·Ø-R(K,L)*R(K,L)
      IF (RR·LT·Ø·Ø)RR-Ø·Ø
2ØØØ  SE(K)=RR/SQRT(FLOAT(N-1))
```

```
3ØØØ    PRINT 3Ø,STN(L),SE
3Ø      FORMAT('-STANDARD-ERROR'//(1X,A1Ø,9F1Ø•3))
        DO 3 K=1,M £DO 4 J=1,M
4       CV=STD(J)/XBAR(J)
3       VCE+STD(K)*STD(K)
        PRINT 31,VCE,CV
31      FORMAT('-VARIANCE'//11X,8F1Ø•3//'-COEFFICIENT OF VARIATION'//11X,8
        1F1Ø.3)
        STOP
        END
```

APPENDIX VI.

TABLES OF CORRELATION COEFFICIENTS

NORMAL PRECIPITATION: CORRELATION COEFFICIENTS : (ZONE 2)

	LAGOS	BOHICON	TCHAOUROU	KANDI	NIAMEY	MENAKA	KIDAL	TESSALIT
1. LAGOS	1.00	0.87	0.75	.45	.29	.11	.11	.02
Standard Error	0	0.08	.14	.26	.29	.31	.31	.32
2. BOHICON	.87	1.00	.84	.44	.29	.15	.17	.11
Standard Error	.08	0	.09	.26	.29	.31	.31	.32
3. TCHAOUROU	.75	.84	1.00	.83	.70	.60	.63	.58
Standard Error	.14	.09	0	.10	.16	.20	.19	.21
4. KANDI	.43	.44	.83	1.00	.95	.92	.93	.91
Standard Error	.26	.26	.10	0	.03	.05	.05	.06
5. NIAMEY	.29	.26	.70	.95	1.00	.98	.97	.91
Standard Error	.29	.29	.16	.03	0	.02	.02	.05
6. MENAKA	.11	.15	.60	.92	.98	1.00	.99	.97
Standard Error	.31	.31	.20	.05	.02	0	.01	.02
7. KIDAL	.11	.17	.63	.93	.97	.99	1.00	.97
Standard Error	.31	.31	.19	.05	.02	.01	0	.02
8. TESSALIT	.02	.11	.58	.91	.91	.97	.97	1.00
Standard Error	.32	.32	.21	.06	.05	.02	.02	0
LAG = 1 MONTH								
1. LAGOS	.49	.38	.49	.50	.62	.52	.49	.35
Standard Error	.24	.27	.24	.24	.20	.23	.24	.28
2. BOHICON	.64	.59	.59	.45	.45	.35	.31	.24
Standard Error	.19	.21	.21	.25	.25	.28	.29	.30
3. TCHAOUROU	.57	.57	.75	.63	.58	.51	.51	.48
Standard Error	.22	.21	.14	.19	.21	.24	.24	.24
4. KANDI	.42	.49	.82	.77	.66	.63	.67	.66
Standard Error	.26	.24	.11	.13	.18	.19	.18	.18
5. NIAMEY	.24	.34	.75	.85	.74	.76	.80	.83
Standard Error	.30	.28	.14	.09	.15	.14	.12	.10
6. MENAKA	.18	.32	.70	.76	.61	.63	.69	.75
Standard Error	.31	.29	.16	.14	.20	.19	.17	.14
7. KIDAL	.19	.34	.70	.73	.58	.61	.66	.73
Standard Error	.31	.29	.16	.15	.21	.20	.18	.20
8. TESSALIT	.22	.37	.67	.61	.43	.44	.52	.56
Standard Error	.30	.27	.17	.20	.26	.26	.23	.22

	LAGOS	BOHICON	TCHAOUROU	KANDI	NIAMEY	MENAKA	KIDAL	TESSALIT
LAG = 2 MONTHS								
1. LAGOS	-0.08	-.14	.31	.70	.76	.81	.80	.80
Standard Error	.32	.31	.29	.16	.13	.11	.12	.11
2. BOHICON	.26	.05	.35	.58	.60	.56	.55	.51
Standard Error	.30	.32	.28	.21	.20	.22	.22	.24
3. TCHAOUROU	.15	.05	.32	.42	.41	.40	.41	.41
Standard Error	.31	.32	.29	.26	.27	.27	.26	.26
4. KANDI	.12	.19	.38	.31	.26	.28	.30	.33
Standard Error	.31	.31	.27	.29	.30	.29	.29	.28
5. NIAMEY	.18	.30	.49	.34	.23	.23	.28	.31
Standard Error	.31	.29	.24	.28	.30	.30	.29	.29
6. MENAKA	.21	.33	.42	.18	.06	.06	.10	.14
Standard Error	.30	.28	.26	.31	.32	.32	.32	.31
7. KIDAL	.20	.31	.38	.15	.02	.02	.07	.10
Standard Error	.31	.29	.27	.31	.32	.32	.32	.32
8. TESSALIT	.17	.26	.28	.02	-.07	-.06	-.05	-.01
Standard Error	.31	.30	.29	.32	.32	.32	.32	.32
LAG = 3 MONTHS								
1. LAGOS	-.05	-.07	.36	.50	.39	.43	.48	.54
Standard Error	.32	.32	.28	.24	.27	.26	.24	.23
2. BOHICON	-.04	-.21	.24	.48	.50	.52	.53	.53
Standard Error	.32	.30	.30	.24	.24	.23	.23	.23
3. TCHAOUROU	-.26	-.37	-.05	.13	.14	.19	.21	.25
Standard Error	.30	.28	.32	.31	.31	.31	.31	.30
4. KANDI	-.25	-.29	-.16	-.11	-.13	-.07	-.05	.01
Standard Error	.30	.29	.31	.32	.31	.32	.32	.32
5. NIAMEY	-.14	-.14	-.10	-.17	-.20	-.15	-.15	-.08
Standard Error	.31	.31	.32	.31	.31	.31	.31	.32
6. MENAKA	-.15	-.18	-.21	-.28	-.29	-.25	-.25	-.20
Standard Error	.31	.31	.30	.29	.29	.30	.30	.31
7. KIDAL	-.17	-.20	-.24	-.31	-.30	-.26	-.27	-.23
Standard Error	.31	.31	.30	.29	.29	.30	.29	.30
8. TESSALIT	-.24	-.31	-.35	-.35	-.33	-.29	-.29	-.24
Standard Error	.30	.29	.28	.28	.28	.29	.29	.30

	LAGOS	BOHICON	TCHAOUROU	KANDI	NIAMEY	MENAKA	KIDAL	TESSALIT
LAG = 4 MONTHS								
1. LAGOS	-.14	-.11	.03	-.06	-.10	-.06	-.03	..01
Standard Error	.31	.31	.32	.32	.32	.32	.32	.32
2. BOHICON	-.39	-.40	-.04	.15	.17	.26	.30	.34
Standard Error	.27	.27	.32	.31	.31	.30	.29	.28
3. TCHAOUROU	-.57	-.67	-.42	-.24	-.22	-.12	-.09	-.03
Standard Error	.22	.17	.26	.30	.30	.31	.32	.32
4. KANDI	-.51	-.64	-.55	-.45	-.43	-.35	-.34	-.28
Standard Error	.24	.19	.22	.26	.26	.28	.28	.29
5. NIAMEY	-.47	-.61	-.58	-.48	-.45	-.38	-.38	-.32
Standard Error	.25	.20	.21	.25	.26	.27	.27	.30
6. MENAKA	-.49	-.64	-.62	-.48	-.42	-.36	-.37	-.33
Standard Error	.24	.19	.20	.25	.26	.28	.28	.28
7. KIDAL	-.52	-.68	-.65	-.48	-.43	-.36	-.37	-.32
Standard Error	.23	.17	.18	.24	.26	.28	.28	.29
8. TESSALIT	-.51	-.67	-.64	-.48	-.41	-.35	-.36	-.32
Standard Error	.23	.18	.19	.25	.26	.28	.28	.29
LAG = 5 MONTHS								
1. LAGOS	-.45	-.40	-.48	-.48	-.46	-.35	-.36	-.27
Standard Error	.25	.27	.24	.24	.25	.28	.28	.29
2. BOHICON	-.51	-.39	-.33	-.29	-.33	-.19	-.17	-.05
Standard Error	.24	.27	.28	.29	.28	.31	.31	.32
3. TCHAOUROU	-.67	-.70	-.70	-.60	-.57	-.45	-.43	-.34
Standard Error	.18	.16	.16	.20	.22	.26	.26	.28
4. KANDI	-.68	-.84	-.82	-.66	-.59	-.50	-.50	.-44
Standard Error	.17	.09	.10	.18	.21	.24	.24	.26
5. NIAMEY	-.66	-.84	.80	-.62	-.54	-.46	-.47	.42
Standard Error	.18	.10	.12	.20	.23	.25	.25	.26
6. MENAKA	-.63	-.81	-.74	-.54	-.46	-.39	-.39	-.35
Standard Error	.19	.11	.14	.23	.25	.27	.27	.28
7. KIDAL	-.64	-.82	-.75	-.54	-.46	-.39	.39	-.36
Standard Error	.19	.11	.14	.23	.25	.27	.27	.28
8. TESSALIT	-.61	-.77	-.71	-.51	-.43	-.36	-.36	-.33
Standard Error	.20	. 13	.16	.24	.26	.28	.28	.28

	LAGOS	BOHICON	TCHAOUROU	KANDI	NIAMEY	MENAKA	KIDAL	TESSALIT
LAG = 6 MONTHS								
1. LAGOS	-.57	-.49	-.67	-.68	-.66	-.57	-.59	-.49
Standard Error	.22	.24	.18	.17	.18	.21	.22	.24
2. BOHICON	-.49	-.28	-.53	-.71	-.76	-.66	-.63	-.55
Standard Error	.24	.29	.23	.16	.14	.18	.19	.22
3. TCHAOUROU	-.67	-.53	-.79	-.84	-.81	-.69	-.68	-.61
Standard Error	.18	.23	.12	.09	.11	.17	.17	.20
4. KANDI	-.68	-.71	-.84	-.72	-.64	-.54	-.54	-.50
Standard Error	.17	.16	.09	.15	.19	.23	.22	.24
5. NIAMEY	-.66	-.76	-.81	-.64	-.56	-.47	-.47	-.43
Standard Error	.18	.14	.11	.19	.22	.25	.25	.26
6. MENAKA	-.57	-.66	-.69	-.54	-.47	-.39	-.39	-.36
Standard Error	.21	.18	.17	.23	.25	.27	.27	.28
7. KIDAL	-.57	-.63	-.68	-.54	-.47	-.39	-.39	-.35
Standard Error	.22	.19	.17	.22	.25	.27	.27	.28
8. TESSALIT	-.49	-.55	-.61	-.50	-.43	-.36	-.35	-.33
Standard Error	.24	.22	.20	.24	.26	.28	.28	.28

APPENDIX VI.2

Table (6.3): Cross-correlation of Lagos & Niamey Precipitations
January 1951 - December 1970

	LAGOS	NIAMEY
Mean (mm)	148	52
Standard deviation	136	81
Variance	18625	6495
Coeft. of variation	92%	154%

LAG(Month), l	0	1	2	3	4	5	6	7	8	9	10
Correlation Coeft, r	0.25	.48	.56	.29	-.06	-.30	-.44	-.47	-.35	-.15	.05
Standard Error SE	.06	.05	.04	.06	.06	.06	.05	.05	.06	.06	.07

LAG, l	11	12	13	14	15	16	17	18	19	20
r	.14	.25	.49	.47	.30	-.03	-.32	-.46	-.45	-.36
SE	.06	.06	.05	.05	.06	.07	.06	.05	.05	.06

LAG, l	21	22	23	24	25	26	27	28	29	30
r	-.16	.05	.13	.26	.52	.54	.28	-.06	-.28	-.44
SE	.06	.07	.06	.06	.05	.05	.06	.06	.06	.05

LAG, l	31	32	33	34	35	36	37	38	39	40
r	-.48	-.37	-.16	.02	.08	.23	.53	.57	.30	-.02
SE	.05	.06	.06	.07	.06	.06	.05	.04	.06	.07

LAG, l	41	42	43	44	45	46	47	48	49	50
r	-.28	-.44	-.47	-.36	-.18	.05	.18	.30	.57	.59
SE	.06	.05	.05	.06	.06	.06	.06	.06	.04	.04

LAG, l	51	52	53	54	55	56	57	58	59	60
r	.25	-.06	-.28	-.45	-.47	-.35	-.13	.10	.16	.30
SE	.06	.06	.06	.05	.05	.06	.06	.06	.06	.06

APPENDIX VII

On the 2 month-lag Correlation of Precipitation:

Lagos (March-August) Vs Niamey: (May-October) 1951-1970

YEAR	MEAN (mm)	STD DEV (mm)	r	S.E.	VARIANCE, V	C.V. %	REGRESSION EQNS
1951	L 160 N 90	125 58	.05	.34	15564.67 3362.97	78.14 64.55	L = 62.8 + 1.08N
1952	L 151 N 163	121 162	.59	.29	14588.40 26275.37	79.99 99.34	L = 79.6 + .44N
1953	L 160 N 127	159 92	.88	.10	25273.90 8459.07	99.67 72.23	L =-33.8 + 1.53N
1954	L 191 N 73	191 62	.56	.31	36495.07 3902.17	99.85 85.77	L = 64 + 1.74N
1955	L 158 N 106	115 75	.29	.41	13258.70 5675.20	73.11 71.07	L = 111.7 + .44N
1956	L 112 N 89	73 85	.36	.39	5266.27 7230.17	64.99 95.36	L = 84.3 + .31N
1957	L 225 N 121	110 101	.20	.43	12096.00 10273.87	48.88 83.54	L = 198.4 + .22N
1958	L 122 N 87	128 87	.87	.11	16454.57 7617.37	105.00 100.13	L = 9 + 1.28N
1959	L 174 N 88	115 81	.66	.25	13210.67 6616.67	65.93 92.09	L = 91.3 + .94N
1960	L 174 N 84	110 71	.62	.28	12161.37 500.67	63.32 84.52	L = 94 + .96N
1961	L 226 N 105	176 89	.62	.28	30801.50 7870.00	77.83 84.49	L = 98 + 1.22N
1962	L 284 N 120	187 139	.76	.19	35075.47 19200.00	65.87 115.47	L = 161.5 + 1.02N
1963	L 242 N 62	117 56	.55	.31	13603.20 3176.67	48.20 91.40	L = 171.2 + 1.14N
1964	L 218 N 142	182 106	.84	.13	33047.47 11136.67	83.52 74.49	L = 16 + 1.44N
1965	L 261 N 122	119 86	.70	.23	14128.17 7376.67	45.51 70.59	L = 143.2 + .97N
1966	L 188 N 83	130 55	.60	.28	16867.47 3066.67	68.96 66.45	L = 69.5 + 1.43N

(APPENDIX VII continued)

YEAR	MEAN (mm)	STD DEV (mm)	r	S.E.	VARIANCE, V	C.V. %	REGRESSION EQNS
1967	L 199 N 140	185 110	.86	.12	34350.17 12040.00	93.06 78.38	L = -1.5 + 1.44N
1968	L 363 N 92	280 68	-.03	.45	78678.27 4672.17	77.20 74.16	L = 372.8 -.11N
1969	L 240 N 102	127 92	.62	.27	16242.97 8491.10	53.14 90.79	L = 152.5 + .86N
1970	L 204 N 74	168 83	.94	.06	28245.60 6817.87	82.38 111.08	L = 64 + 1.9N

APPENDIX VIII : TOWARDS FORECASTING THE MAY-AUGUST PRECIPITATION OVER WEST AFRICA

The knowledge of:

(1) the climatological association between the cycle of precipitation in the North and South of the region and

(2) the displacement of the ITD along with which precipitation zones are advected Northwards and Southwards with seasons,

can be utlised in formulating a simple forecast model for the region's precipitation, given the January to March precipitation in the Southern (near-Coastal) area. A step towards this end is here discussed.

i) Forecasting the 5cm- isohyet

Suppose the Normal latitude/time slope of the 5cm isohyet as obtained for February-August is

$$\alpha = \partial\phi/\partial t \qquad \ldots\ \ldots\ \ldots\ 1$$

where $\partial\phi$ is the latitudinal displacement and
∂t is the time (month)

For any given year for which the forecast is required, we obtain the January to March precipitation at a Southern (near-coastal) station and locate the 5cm point P(to, Øst) on the t- axis for the station's latitude (Øst). Fig 1.

Using the relation in equation (1), we proceed in time steps of $t = 1$ month to obtain consecutive

$$\phi_n (t) = \phi_{n-1} + \alpha\delta t$$

points on the ϕ - t plane whose loci define the 5cm isohyet e.g. PS in Fig. 1.

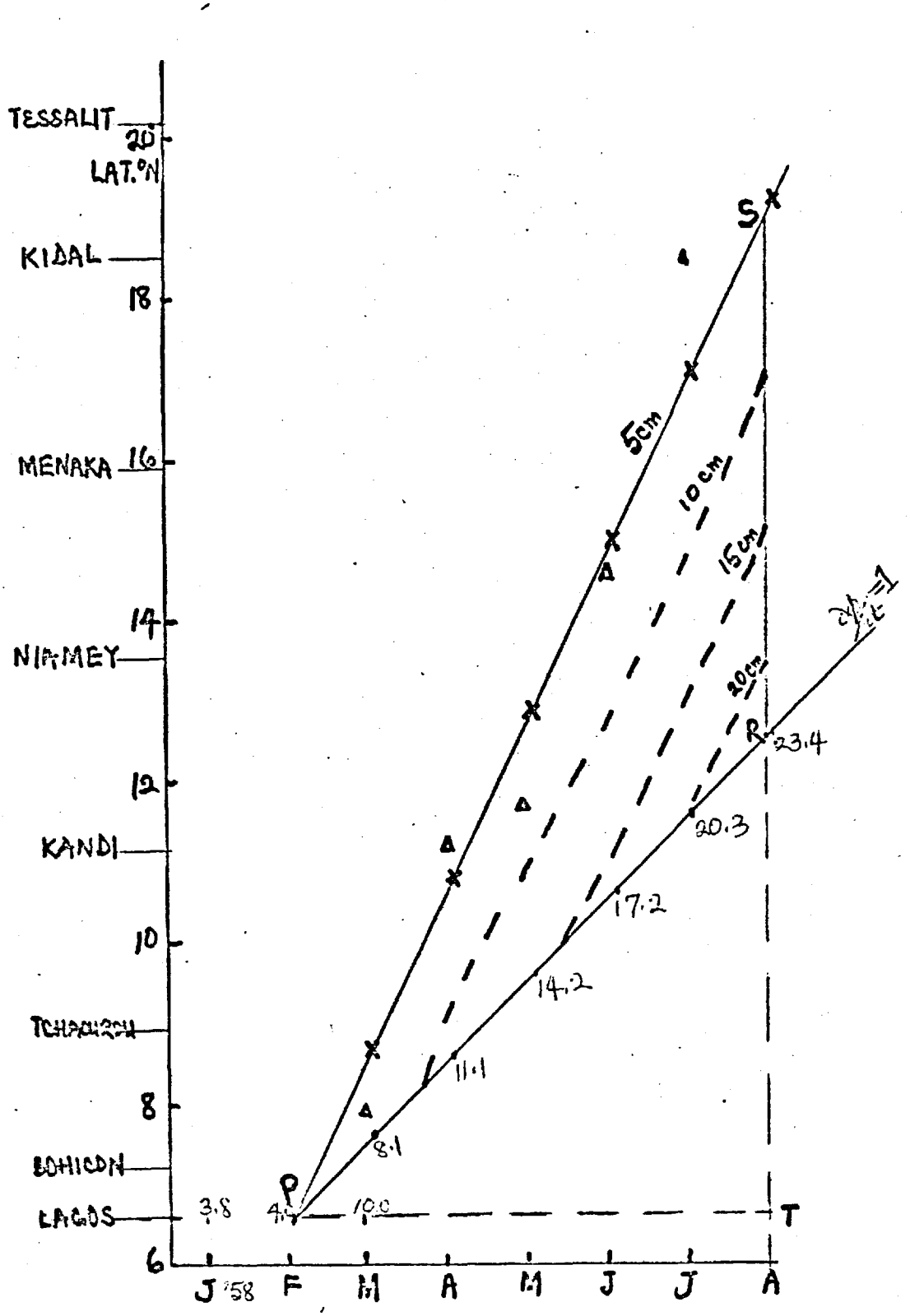

Fig 1:

The latitude-time section of precipitation forecast for Zone 2, May-Aug. 1958 after March. Δ PRS is the characteristic triangle of the forecast precipitation. PS is the 5cm line and PR, the line along which $\partial\Phi/\partial t = 1$. The calculated R(cm) values have been inscribed on appropriate points along PR.

This line (PS) indicates when an area is expected to have up to 5cm of rain. Generally, till August, any month t after the month of the 5cm minimum ushers in a prospect of more rain. The agreement between the forecast and observation carried out for 1958 (Fig.(1)) and 1970 (Fig.2) has been very encouraging. The 10cm isohyet can be similarly forecast a month later.

However, we shall use the ITD precipitation control in deriving the 10cm and higher isohyets given the January to March precipitation.

ii) ITD Control

Suppose $\partial\phi/\partial t = 1$, for convenience.

This has a locus, PR (Fig.1).

Using (1) the ITD Normal latitude/time slope determined in (Chapter II, Fig 2.3), (for zone 2) to be

$$\frac{\partial \phi_I}{\partial t} = 2.03 \text{ deg./month}$$

And (2) the fact that over many Nigerian stations, an increase of 7.15 inches in annual rainfall is experienced for every degree latitude the ITD is further North of the station (Ilesanmi, 1971), we can calculate the precipitation, R, expected/month along PR. Assuming the precipitation increase is ΔR.

A consistent ITD monthly increase of R along PR yields:

$$\frac{\partial}{\partial \phi_I}(\Delta R) = 1.5\text{cm/degree}$$

If: $$\frac{\partial(\Delta R)}{\partial t} = \frac{\partial(\Delta R)}{\partial \phi_I}\frac{\partial \phi_I}{\partial t} \quad .. \quad .. \quad .. \quad 2.$$

$$\partial(\Delta R) = (1.5 \times 2.03)\delta t = 3.05\delta t$$

Fig 2:

Legend as in fig 1 above, but for 1970.

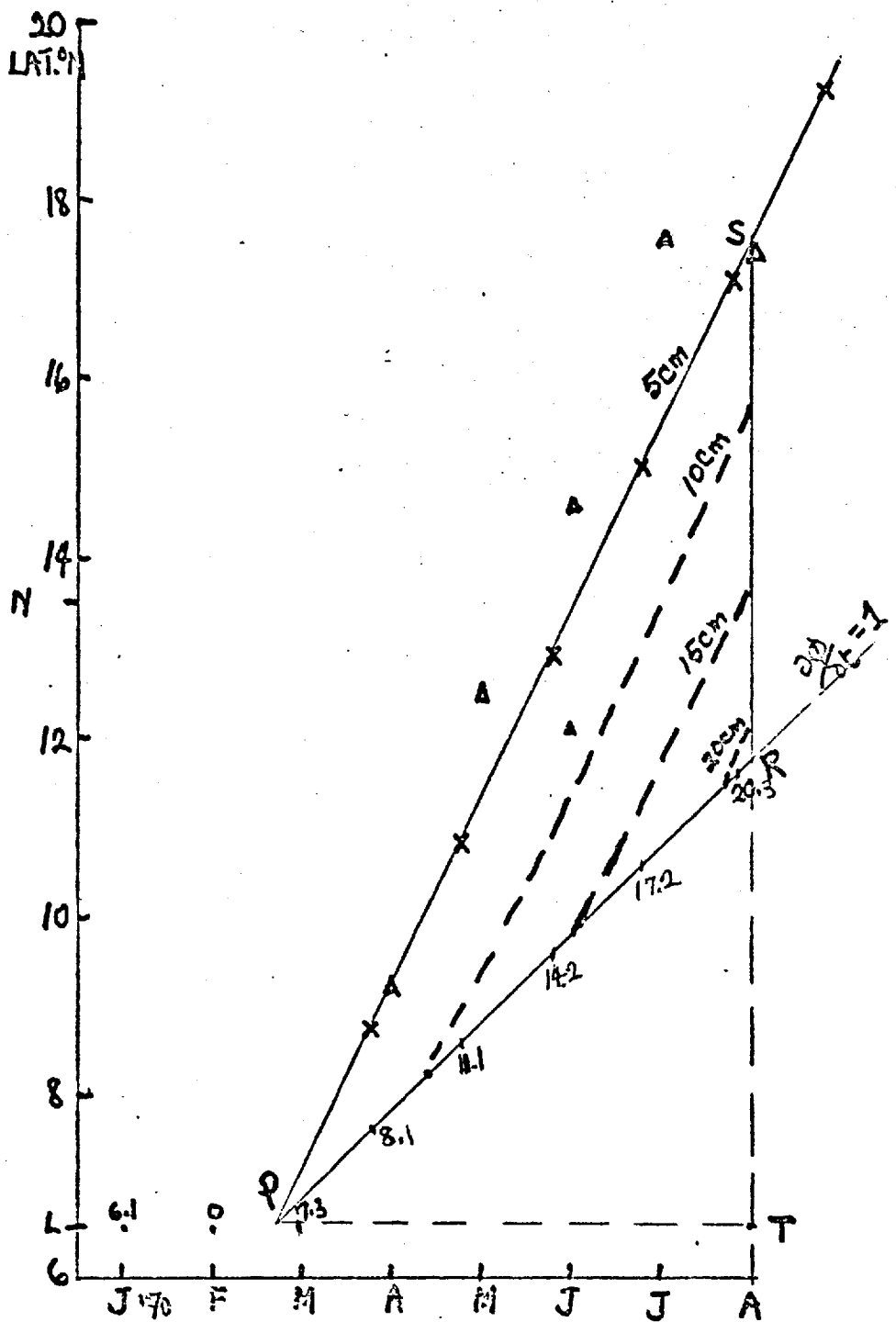

The precipitation obtained along PR for each month after the 5cm isohyet R(to) might have been fixed, is then given by:

$$R = R(to) + \delta(\Delta R)$$

$$R(cm) = 5 + 3.05\,\delta t \qquad .. \quad .. \quad .. \quad 3$$

iii) Trial Forecasts

Using the relation is (3), we obtain values of R for each month along PR.

Joining RS, we have a characteristic triangle, PRS, within which model forecasts of R for various times and latitudes can be made, subject to some atmospheric circulation constraints which will be mentioned below.

Meanwhile, the forecasts made for 1958 are as shown below (Tables 1 and 2).

TABLE 1: Areal Forecast for 1958

Latitude	Month	R_f (Forecast) (cm)	R_o (Observed) (cm)	ΔR (cm)	$\frac{\Delta R}{R_f} \times 100\%$
7.5	March	7.9	4.5	3.4	43.
8.5	April	10.8	13	-2.2	20
9.5	May	13.9	12	1.9	13.6
10.5	June	16.9	15	1.9	11
11.5	July	19.9	7	12.9	65
12.5	August	23	22.5	0.5	1.4
				Mean	26%

The 10cm-, 15cm- and 20cm- isohyets are then inserted into their appropriate positions within the characteristic triangle PSR using the 5cm line and the R values obtained along PR.

On the basis of this, a forecast for Niamey precipitation, 1958 is hereby made:

TABLE 2: Forecast for Niamey, 1958:

Month	R_f(Forecast) (cm)	R_o(Observed) (cm)	ΔR (cm)	$\frac{\Delta R}{R_f}$ x 100%
Between May and June	5.5	4.6	0.9	16
June & July	10.5	10	0.5	4.8
July & Aug.	16	15	1	6
Aug.	20	23.4	-3.4	17
			Mean =	11%

A similar procedure was used for 1970 as shown in Fig.(2) and tables (3-4).

TABLE 3: Areal forecast for 1970

Lat.(^{o}N)	Month	R_f(Forecast) (cm)	R_o(Observed) (cm)	ΔR (cm)	$\frac{\Delta R}{R_f}$ x 100%
6.8	March	5.5	7.2	-1.7	31
7.8	April	8.6	8.5	0.1	1
8.8	May	11.6	12.4	-0.8	7
9.8	June	15.2	10	5.2	30
10.8	July	18.2	16	2.2	10
11.8	August	>20	40		
				mean =	16%

TABLE 4: Forecast for Niamey, 1970

Month	R_f(Forecast) (cm)	R_o(Observed) (cm)	ΔR (cm)	$\frac{\Delta R}{R_f} \times 100\%$
Between May and June	$\angle$ 5cm	0.7		
June & July	7.5	4	3.5	46
July & Aug.	13.5	12	1.5	11
August	> 15	16.7		
			mean =	29%

iv) Constraint on the Normal Isohyet behaviour

In locating the 5cm-isohyet, we have assumed that given the initial (January to March) precipitation for a given year, the Normal climatological behaviour holds for the remaining months till August. However, as we have discussed in Chapter IV, atmospheric constraints exist on the year-to-year precipitation, effecting considerable fluctuations.

Taking the decade 1951-60, noted for its quasi-normal behaviour (Chapter VI) for instance:

If Lagos March precipitation is $R_L(\text{Mar}) = x_i$

and Lagos February precipitation is $R_L(\text{Feb})$ and

$R_L(\text{Mar}) - R_L(\text{Feb}) = x_2$

Suppose Niamey (May) precipitation is $R_N(\text{May}) = y$ then,

$$y = f(x_1, x_2)$$

$$= f_2 \left\{ R_L(\text{Mar}), R_L(\text{Feb}) \right\}$$

Hence, if we plot R_L(Mar) against R_L(Feb), we should obtain a family of curves for corresponding R_N(May).

This was tried for 1951-55 and a well-behaved concentric family of curves was obtained (Fig.3).

However, a similar trial carried out for 1956-60 behaved abnormally. Fig(4).

This change in behaviour may be due to the fluctuation in the Walker circulation as manifest by the SO which, as shown in Chapter IV, exercises some control on the Lagos precipitation.

A detailed investigation of the period involved in this fluctuation is beyond the scope of this presentation. However, Berlage has been quoted to have stated (Newell, 1974):

"the air pressure fluctuations (associated with the SO) show a 2-to-3 year rhythm" and, again by the same author that:

"there is no strict periodicity in the SO, the length of its pressure waves varying between 1 and 5 years roughly."

We feel the SO control is a likely constraint on this forecast, particularly, as far as the LDS months, not well depicted in the forecast, are concerned.

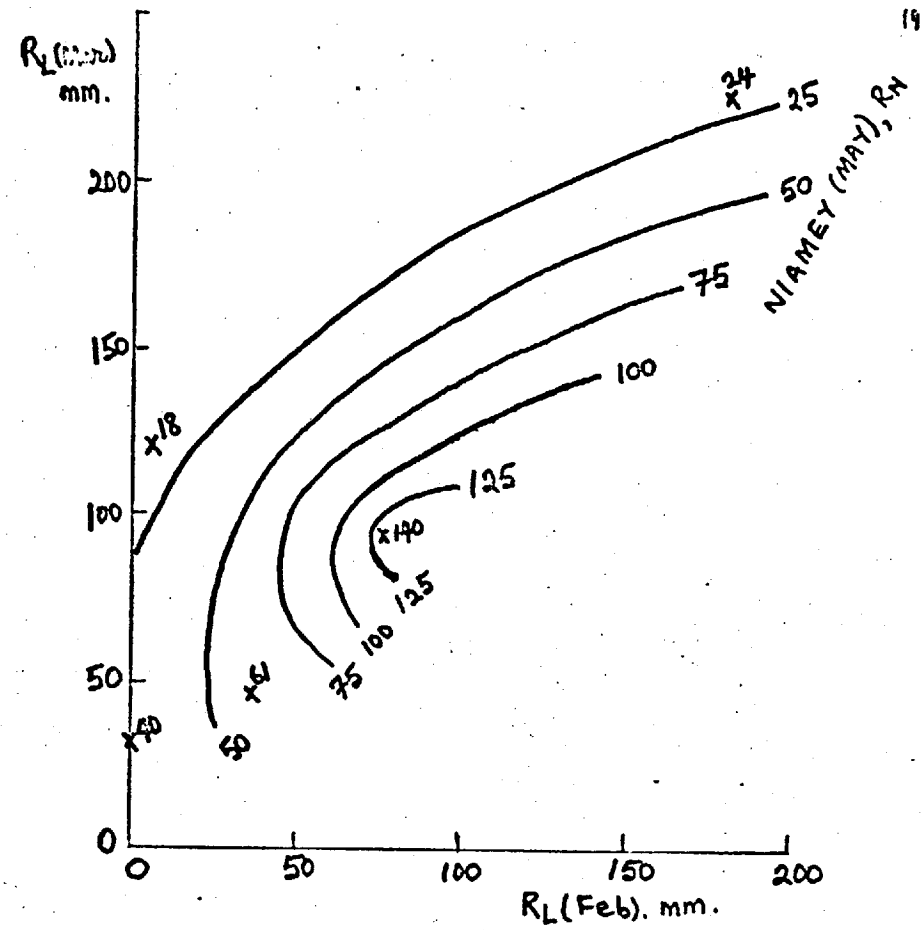

Fig 3.

Isopleths of R_N(May) in mm, corresponding to various R_L(Mar)(mm) and R_L(Feb)(mm) as obtained in 1951-1955.

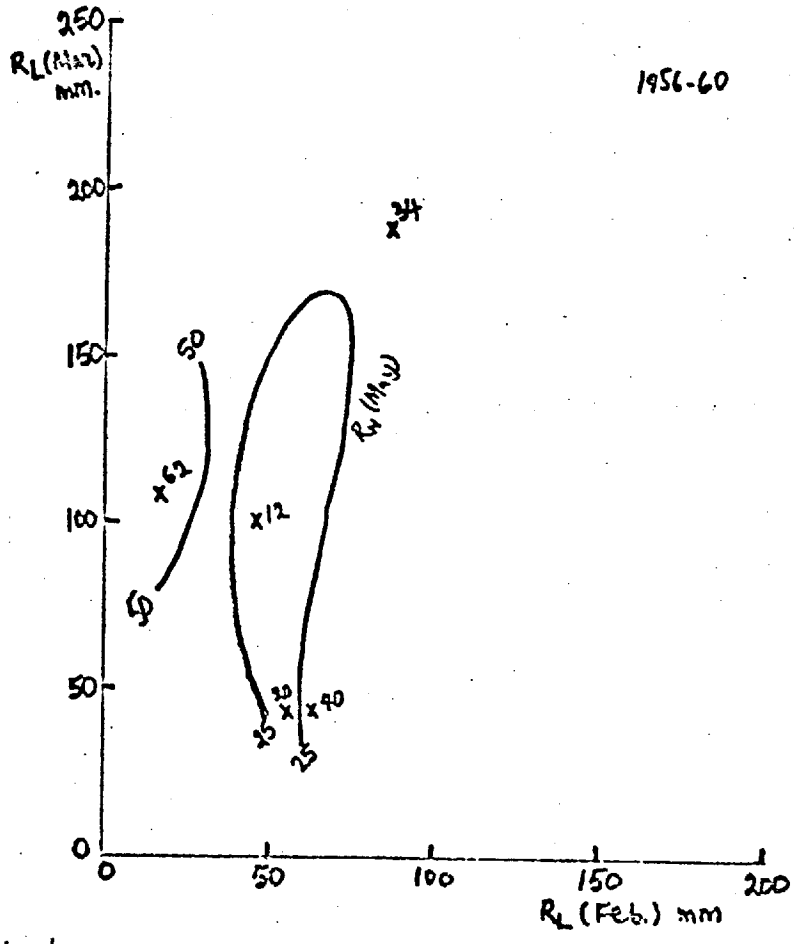

Fig 4.

Legend as in fig 3, but for 1956-1960.

v) Concluding remarks

A simple climatological forecast model of the March to August precipitation in the West African region is developed which can be used to forecast the April to July precipitation to within 20%.

This method does not work well for the August precipitation. This month of active LDS activity in the South is outside the normal ITD rain band but is SO controlled. However, trial forecasts carried out for 1958 and 1970 show a fair degree of agreement ($\sim$ 25% in the mean), fig (5), with observation.

Considerable challenge is posed to further investigations on this problem whose solution holds good promise not only for warning the Sahel of the approach of drought but also of boosting the cocoa output. (Cocoa being an 'LDS' region crop.)

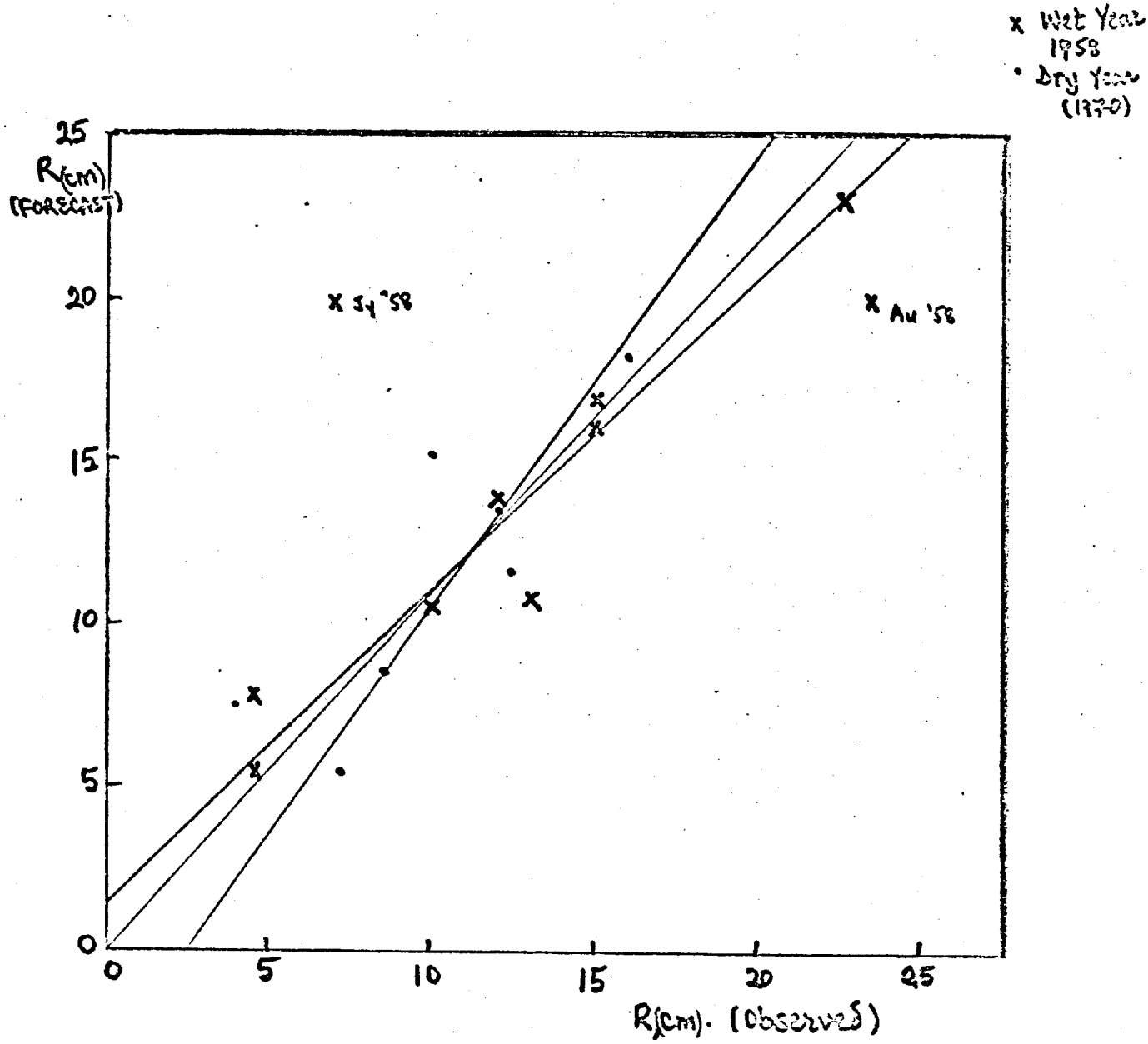

Fig 5:

Diagramatic comparison of R(cm) forecast with R(cm) observed for both the wet and the dry years considered. July and August, 1958 both LDS months (hence, SO controlled) do not fall in line, an indication of a limitation in the ITD control.

ACKNOWLEDGEMENTS

The author wishes to express his deep gratitude to the Almighty Hand that designed the giant atmospheric 'heat engine' and the complexity of the environ thereof, even the Almighty God, whose grace has been keeping him all along.

Many thanks to my supervisor, Mr J R Probert-Jones for his kind supervision and enthusiastic encouragement, to Prof. F H Ludlam and Dr J S A Green for many helpful and stimulating discussions, and Dr H T Bull for starting me thinking on the Sahel drought problem.

The help of Mr A G Seaton in computer assistance, Dr K J Bignell in the development of the Satellite photographs used and of Miss Marion Street in the preparation of figs 4.9(a) and (b) and 6.10 are gratefully acknowledged.

To all those who helped in data collection as mentioned in Appendix I(a), and the entire members of the Atmospheric Physics Group, Imperial College whose interaction has been of good help, I say thank you.

I wish to thank Miss Pauline Bunday for her patience and help in typing the thesis and the entire brethren both in Twynholm Baptist Church, Fulham, the Africa Fellowship and the Overseas Fellowship of Nigerian Christians for their fellowship and prayerful support. God bless you all.

Finally, the author gratefully acknowledges the University of Ife's Sponsorship for his stay and studies in Imperial College.